Functional Analysis and Genetic Mapping of Mouse Centromere Protein Genes

Kerry J. Fowler
Grad Dip Ed, Deakin University, 1994
MSc, University of Melbourne, 1991
M App Sc, RMIT University, 1989
B App Sc, RMIT University, 1982
Dip App Sc, RMIT University, 1978

Submitted in fulfilment of the requirements for the Degree of
Doctor of Philosophy by previous publication.

University of Tasmania (November, 2000)

Declaration of originality and Statement of authority of access

This thesis contains no material which has been accepted for a degree or diploma by the University or any other institution, except by way of background information and duly acknowledged in the thesis, and to the best of my knowledge and belief no material previously published or written by another person except where due acknowledgment is made in the text of the thesis.

This thesis maybe available for loan and limited copying in accordance with *Copyright Act 1968.*

Signed

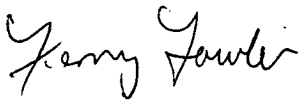

Kerry J Fowler

Acknowledgments

I wish to thank The Murdoch Childrens Research Institute, University of Tasmania, Prof Andy Choo and Dr Adrian West for providing an excellent working environment and being most supportive of my PhD application. I thank all my co-authors and collaborators for their enthusiasm and valuable contributions which have been previously documented. I would like to especially acknowledge Dr Christine Kozak who generously included her earlier unpublished localisation of the mouse gene *Yes1* in the *Cenpa* chromosomal mapping paper; Dr Peter Mountford for IRES constructs; Dr Steve Delaney, Dr Jeff Mann, Dr Graham Kay and Dr Liz Robertson for mouse cell lines; Dr CW Chow for histopathology and Sophie Gazeas, Anick Sylvain and Jodi Ladhams for their dedicated care of mice. A special vote of thanks to my two acadaemic referees Prof Jim Camakaris and Prof Dick Cotton for written references.

List of Abbreviations

A	A/J mouse strain
AXB	recombinant inbred set derived by crossing A/J with C57BL/6J
AK	AKR/J mouse strain
AKXL	recombinant inbred set derived by crossing AKR/J with C57L/J
A+T	adenosine and thymidine
α-satellite	alphoid satellite DNA
APC	anaphase promoting complex
Api4	apoptosis inhibitor 4 protein or survivin
B	C57BL/6J mouse strain
BAC	Bacterial Artificial Chromosome
BIR	baculoviral IAP repeat
bp	basepair
BSB Panel	(C57BL/6J x *Mus Spretus*)F_1 x C57BL/6J
BSS Panel	(C57BL/6JEi x SPRET/Ei)F_1 x SPRET/Ei
BUB	budding uninhibited by benzimidazole
BUdR	5-bromo-2′-deoxyuridine
C57	C57BL/6 mouse strain
cDNA	complementary DNA
cM	centiMorgan
CENP	centromere protein
Cenp	mouse centromere protein
CF	cystic fibrosis
CGH	comparative genome hybridisation
Cre	Cre recombinase
CREST	calcinosis, Raynaud phenomenon, esophageal dismotility, sclerodactyly, telangiectasia
C-terminus	carboxyl terminus
DAPI	4′, 6-diamidino-2-phenylindole

DNA	deoxyribonucleic acid
ES cells	mouse embryonic stem cells
FACS	fluorescence-activated cell sorter
FISH	fluorescence *in situ* hybridisation
Flp	Flp recombinase
Frt	Flp Recombine Target sites
G_2 phase	gap 2 phase of cell cycle
GDB	Genome Database
GFP	green fluorescent protein
IAP	inhibitor of apoptosis
ICM	inner cell mass
INCENP	INner CENtromere Protein
IRES	internal ribosomal entry site
IVF	*in vitro* fertilisation
kDa	kiloDalton
L	C57L/J mouse strain
lacZ	*lacZ* β-galactosidase
Lox P	Locus Of crossover X in bacteriophage P1
MAC	mammalian artificial chromosome
MAD	mitotic arrest deficient
Mb	megabase
MGD	Mouse Genome Database
M-phase	mitotic phase of cell cycle
mRNA	messenger RNA
N-terminus	amino terminus
p	probability value determined by Student's t-Test
pc	post conceptus; day 0.5 pc, time of observing vaginal plug after mating
PCR	polymerase chain reaction
QIMR	Queensland Institute of Medical Research
QTL	quantitative trait loci

RCH	Royal Children's Hospital
RCH AEC	RCH Animal Ethics Committee
RFLP	restriction fragment length polymorphism
RH panel	radiation hybrid panel
RI strains	recombinant inbred mouse strains
RNA	ribonucleic acid
SDP	strain distribution pattern
S-phase	synthetic phase of cell cycle
TD-60	Telophase Disc 60 protein
TGFα	transforming growth factor alpha
TUNEL	terminal deoxynucleotidyl transferase-mediated UTP nick end-labeling
WD	repeating amino acid unit ending with a tryptophan (Trp or W) and aspartate (Asp or D) sequence
WEHI	Walter and Eliza Hall Institute of Medical Research

Page

List of Figures

Abstract

This study focuses on the functional analysis and genetic mapping of a number of the centromere-associated protein genes.

The mammalian centromere is the pinched region on metaphase chromosomes and is made up of an inner heterochromatin core coated with a protein complex known as the kinetochore. Numerous constitutive and transient proteins assemble at the centromere-kinetochore complex during mitosis and meiosis facilitating microtubule attachment and accurate separation of sister chromatids. Aberrations in cell division may lead to chromosome missegregation and a range of pathologies including cancer and miscarriage. The function of many centromere-associated proteins has been studied in yeasts, fungi, invertebrates and mammalian cell culture systems however their roles are undefined in whole animals.

To determine the requirement for six centromere-associated proteins during mitosis, meiosis and development, gene targeting experiments in mice were undertaken. Heterozygous mice carrying disrupted *Cenpa*, *Cenpb*, *Cenpc*, *Incenp*, *survivin* (*Api4*) and *Bub3* genes were healthy and fertile however, with the exception of *Cenpb*, their null offspring were embryonic lethal. The *Cenpc*-, *Incenp*- and *Api4*-deficient embryos failed to hatch from their zona pellucida and implant, whereas the *Cenpa* and *Bub3* knockout embryos were able to hatch and form trophectoderm and inner cell mass outgrowths before mitosis halted at day-5.5 to -6.5 post conceptus.

Morphological examination revealed affected embryos with severe mitotic problems including formation of micro- and macronuclei, nuclear bridging and lagging chromosomes. Surprisingly the *Incenp*- and *Api4*- disrupted embryos displayed bundling of microtubules and giant nuclei suggesting that these proteins act in concert in the regulation of microtubule dynamics and/or cell cleavage. In contrast, Cenpc appears to be essential at the metaphase stage of mitosis; and in an absence of Cenpa, immunofluorescence stainings demonstrated that Cenpb and Cenpc DNA-binding proteins were unable to form functional kinetochores. Finally *Bub3*-disrupted embryos failed to arrest following treatment with the microtubule-poison nocadazole indicating a vital role in the mitotic spindle checkpoint pathway.

In comparison, assessment of *Cenpb*-null mice demonstrated that Cenpb is not required for mitosis and meiosis. However *Cenpb*-null mice are smaller in size and display significantly smaller testis (>14 %) and uteri (>30%) in adulthood. The observed body-weight reduction is dependent on the genetic background (R1, W9.5 and C57) as well as the sex of the mice. Likewise *Cenpb*-deficient female mice exhibit age-related uterine dysfunction that is more severe in the C57 background. Histological analysis of the uterus points to defective luminal and glandular epithelium as the likely primary cause.

In a complementary study the chromosomal position of six of the centromere-associated protein genes was determined with a view to identifying possible candidate mouse mutants in the mouse database. The genetic mapping of the *Cenpa*, *Cenph*, *Cenpe*, *Cenpf*, *Incenp* and *Bub3* loci to chromosomes 5, 13, 6, 1, 19 and 7 respectively, was achieved by linkage analysis using specific probes to analyse sets of recombinant inbred mouse strains and *Mus spretus*-based interspecific backcross panels. The mapping of these loci failed to reveal any pre-existing mouse mutants for further study however the mapping of *Cenpa* and *Cenpe* did extend or identify novel regions of mouse-human homology.

Overall, the discoveries made in these studies have provided new insight into the functional intricacy of the centromere-kinetochore complex. Furthermore the observed phenotypes in mice bearing disrupted centromere protein genes provide fresh genetic clues to understanding the pathogenesis of mammalian pregnancy disorders such as miscarriage and pyometra.

Aims of Studies and Structure of Thesis

a) Setting the scene

My research on the 'Functional Analysis and Genetic Mapping of Mouse Centromere Protein Genes' started in late 1994 when I returned to The Murdoch Childrens Research Institute to Head the Disease Model Unit and began working with a number of groups including Prof Andy Choo's Chromosome Research Group. One of the major interests of Prof Choo's group is to understand the structural and functional properties of the centromere. In this study I have used my skills in cell biology, transgenesis, functional mouse genomics and genetic mapping to complement and broaden the field of knowledge of the mammalian centromere-associated proteins and genes that encode them.

The cloning and sequencing the DNA of the human centromere to find the minimal sequence that is required for centromere function, has been achieved by Prof Choo's group (du Sart et al, 1997; Barry et al, 1999). To compliment these studies members of Prof Choo's group and I have undertaken the functional analysis of six mouse centromere-associated proteins using gene targeting in mouse embryonic stem cells (ES cells) and transgenic mice. At the same time I have determined the chromosomal localisation of five centromere protein genes and supervised the mapping of another, with a view to identifying whether any candidate mouse mutants bearing a mutation in one of the these genes already exist in databases.

b) Aims of studies

The aim of these studies was to generate and analyse mouse mutants bearing germline loss-of-function mutations in Cenpa, Cenpb, Cenpc, Incenp, Bub3 and Api4 centromere-associated proteins and to map the chromosomal positions of *Cenpa*, *Cenph*, *Cenpe*, *Cenpf*, *Incenp* and *Bub3* genes.

c) Animal ethics approval

All studies were conducted under approval of the Royal Children's Hospital Animal Ethics Committee (RCH AEC).
Please note the RCH AEC reference numbers:
- A191, A282, A306, A375 and A388 covers the generation and characterisation of mice with targeted mutations in centromere protein genes.
- A263, covers the genetic mapping of centromere protein genes to mouse chromosomes.
- A269, A314, A338 and A345 covers the production of monoclonal antibody in mice and polyclonal antibodies in rabbits that were used to characterise the mice carrying specific mutations in centromere protein genes.

d) Contribution to Joint Publications by the Candidate

As part of the University of Tasmania requirements for enrolment the candidate was required to provide signed declarations from co-authors as to their contribution to each of the submitted publications. In addition the candidate was required to describe the development of research relevant to the publications describing:
i) functional analysis of cell lines and mouse bearing targeted loss-of-function mutations in centromere protein genes: *Cenpa*, *Cenpb*, *Cenpc*, *Incenp*, *Api4* and *Bub3*

Generation of mice with disrupted Cenpa, Cenpb, Cenpc, Incenp and Bub3 genes
The successful production of mice bearing precise targeted mutations depends on many steps being optimal (Mansour et al, 1988). To generate mice with disrupted *Cenpa*, *Cenpb*, *Cenpc*, *Incenp* and *Bub3* genes I worked closely with Prof Choo's team to improve the homologous recombination frequency in parental ES cells (derived from 129 mouse substrains) by ensuring isogenic genomic DNA libraries were used for gene isolation and subsequent generation of the replacement targeting constructs. The incorporation of sufficient homology was optimised in the constructs (Hasty and Bradley, 1993). Despite these efforts no recombinants were obtained with the first 750 colonies analysed for *Cenpc* and the initial 1250 colonies screened for *Cenpb*.

This led to my inviting Dr Peter Mountford to the Murdoch Childrens Research Institute. Dr Mountford had recently returned from Edinburgh where he had refined a genetrap method that makes use of a picornavirus internal ribosomal entry site (IRES) and had achieved recombinants in up to 70-86% of screened colonies (Mountford et al, 1994). This method was subsequently adopted in our own laboratory and used successfully to generate ES cell lines with disrupted *Cenpa* (Newson, 1997; Redward, 1998; Howman, 2000), *Cenpb* (Hudson, 1998), *Cenpc* (Kalitsis, 1998), *Incenp* (Kile, 1997) and *Bub3* (Dr Paul Kalitsis, personal communication) genes with much improved targeting frequencies.

I then microinjected these cell lines into C57BL/6 mouse blastocysts and transferred them to pseudopregnant recipient mice to generate mouse chimaeras. Unfortunately the first batch of *Cenpc* high grade chimaeras were infertile despite the parental E14 ES cells (which I had received from Dr Martin Hooper, University of Edinburgh) having been proven germline while under my care at The Ludwig Institute (Mann et al 1993, Leischke et al, 1994). This led me to review and improve the tissue culture facilities at The Murdoch Childrens Research Institute. Major steps included the implementation of rigorous quality control of the ES cells and media, karyotyping of targeted lines, and improved freezing and storage conditions for potential targeted cell colonies that were undergoing screening. I also obtained a number of new parental ES cell lines from external sources for this work. Of these the R1 (from Dr Steve Delaney, University of Queensland), W9.5, W9.8 (from Dr Jeff Mann, Beckman Institute) and 129/1 cell lines (from Dr Graham Kay, QIMR), grown on STOneoR mouse feeder cells (from Dr Liz Robertson, Columbia University), were successful in giving high grade germline transmitting mouse chimaeras in my hands. Additionally I established drug tolerance titration curves for G418 (neomycin) and hygromycin (the selection markers used in conjunction with the IRES cassette) and determined the minimal dosage of these chemicals required to select against non-targeted parental ES cells following electroporation of gene targeting constructs.

Once targeted ES cell lines were identified by Southern analysis using an external probe I facilitated members of Prof Choo's team to develop efficient PCR screening strategies for the rapid detection of wildtype, heterozygous and nullizygous (knockout) offspring postnatally and prenatally. The ability to perform PCR

genotyping on the latter was particularly critical if the gene disruption resulted in embryonic lethality. I was also very active along with Prof Choo in helping group members to develop essential analytical tools such as morphological and immunofluorescence techniques especially for the embryos that may be required for phenotypic analysis of the mouse mutants.

The successful generation of the many transgenic mouse strains at The Murdoch Childrens Research Institute stretched existing resources at the RCH and it was necessary for me to arrange offsite housing of these mice under the care of my staff (Sophie Gazeas, Anick Sylvain and Jodi Ladhams). This required organising health care and testing, rederiving mouse strains by Caesarean section, giving clear instruction as to how the mouse colonies were to be bred and maintained, planning and designing breeding experiments and ensuring that the relevant RCH AEC approvals had been obtained prior to experimentation.

In addition to generating and breeding the mice I have been heavily involved with the phenotypic characterisation of the *Cenpb*-null and *Cenpb* targeted revertant control mice and the embryonic lethality observed in the *Cenpa*-, *Cenpc*-, *Incenp*-, *Api4*- and *Bub3*-nullizygous mice. The *Api4* knockout mice were generated by Dr David Vaux's laboratory, WEHI. Initially *Api4* (survivin) was described as an inhibitor of apoptosis (reviewed by Deveraux and Reed, 1999) however Dr Vaux's team has recently identified survivin as a centromere-associated protein. Subsequently Dr Vaux contacted Prof Choo to collaborate with the analysis of the *Api4*-disrupted mice.

Phenotypic characterisation of the embryonically lethal Cenpa, Cenpc, Incenp, Api4 and Bub3 knockout mice

My contribution to the phenotypic analysis of the *Cenpa*-, *Cenpc*-, *Incenp*-, *Api4*- and *Bub3*-deficient mouse strains comprised of:
- identification of embryonic lethality at specific timepoints in embryogenesis for each gene by dissecting out pre- and postimplantation mouse embryos from heterozygous breeding pairs for morphological studies and PCR analysis with Prof Choo's group and Dr Vaux's team.

- design and execution of *in vitro* experiments to further refine the *in vivo* observations by dissecting out preimplantation mouse embryos from heterozygous breeding pairs and testing their ability to form an inner cell mass and trophectoderm in cell culture systems.
- breeding and genetic backcross experiments of *Cenpa* and *Cenpc* heterozygous mice onto different inbred backgrounds, accompanied by PCR analysis with a view to modifying the phenotype ie rescuing the lethality or hastening the lethality.
- an extensive literature review of known mouse strains that display embryonic lethality. The key contribution of this survey was locating a publication that describes a mitosis defective embryonic lethal mouse strain that displays oliogosyndactaly known as *Os* (Magnuson and Epstein, 1984). This publication has been invaluable for suggestions on analysis of preimplantation embryos that were likely to display chromosomal abnormalities and has assisted Prof Choo's group to examine the centromeres and chromosomes of the *Cenpa-*, *Cenpc-*, *Incenp-*, *Api4-* and *Bub3-* disrupted embryos by mitotic index and staining with anti-centromere protein antibodies.

Phenotypic assessment of the non-lethal Cenpb knockout mice

My contribution to the phenotypic study of the *Cenpb*-deficient mice, cell lines and *Cenpb* revertant mice has been extensive in experimental design and execution. In order to follow up my observations Prof Choo and I set up of a number of external collaborations to understand the pathology and physiology of these mice.
These collaborations included:
- histopathological analysis of 20 organs from individual mice with Dr CW Chow, Department of Pathology, RCH.
- specific examination of the pathology of the testis with Prof David de Kretser, Institute of Reproduction and Development and Dr Nigel Wreford, Department of Anatomy, Monash University.
- pathological examination of the uterus with Dr Lois Salamonsen, Prince Henry's Institute.
- examination of uteri for the presence of opportunistic or pathogenic bacteria with the Department of Microbiology, RCH.
- *in situ* hybridisation of mouse tissues with Stephanie Edmondson, Centre for Hormone Research, RCH.

- FACS analysis to check for possible aneuploidy in specific mouse tissues with Andrew Fryga and Dianne Tucker, Department of Haematology, RCH.
- measurement of testosterone, 17β-estradiol and progesterone levels in the mice with Department of Biochemistry, RCH.
- whole body composition analysis of mice with Dr Brian Leury, Institute of Land and Food Resources, University of Melbourne.
- measurement of leptin levels to exclude hypophagia (suppressed food intake) with Dr Anne Thorburn, Department of Medicine, University of Melbourne.
- analysis of mouse longevity using Kaplan Meier survival plots with Dr Rory Wolfe, Department of Statistics, RCH.
- I also sought instruction in techniques such as: TUNEL staining to test for apoptosis from Pam Farmer, Department of Surgical Research, RCH as well as BUdR labeling of mouse tissues *in vivo* with Dr Cris Print, WEHI.

ii) the genetic mapping of centromere protein genes: *Cenpa, Cenph, Cenpe, Cenpf, Incenp* and *Bub3*

I initiated these studies using Recombinant Inbred mouse strains (RI strains) to map *Cenpa* and *Incenp* genes similar to my previous mapping studies that were used to determine the chromosomal localisation of relaxin and TGFα genes (Fowler et al, 1991; Fowler et al, 1993). My initial mapping of *Cenpa* using RI strains lead to an unexpected result. Subsequently I sought a collaboration with with Dr Christine Kozak (Chair of International Mammalian Genome Society Mouse Chromosome 5 Subcommittee) to independently confirm my mapping of *Cenpa* using her Backcross mouse DNA panel. I also worked with Prof Choo's group to verify the assignment of human *CENPA* using somatic cell hybrids (Newson, 1997).

After presenting my work at the Mouse Genome conference in Florida, 1997, I learnt of the recent availability of commercial Backcross panels (purchased from Dr Mary Barter and Dr Lucy Rowe, The Jackson Laboratory). These panels enabled the refined mapping of the *Cenph*, *Cenpe*, *Cenpf*, *Incenp* and *Bub3* centromere protein genes using probes provided by Prof Choo's group (MacDonald, 1996; Kile, 1997; Dr Paul Kalitsis and Dr Richard Saffery). Dr Anthony Lo was supervised by me to determine the genetic mapping of *Cenph*.

d) Structure of thesis

Chapter 1 is an introductory chapter that encompasses a review of the centromere literature with emphasis on the centromere-associated proteins. Chapters 2 and 3 describe the findings and summaries of the enclosed publications. These two chapters do not attempt to present the work in complete detail as it is included in the enclosed publications, rather they deliver it in the context of a thematic overview describing the function and chromosomal localisation of the centromere protein genes. The final Chapter 4 features the impact, future directions and implications of these studies.

Please note that a copy of each publication and general references are included in this thesis in accordance with the University of Tasmania PhD by previous publication guidelines. In addition all referenced publications resulting from the work relating to the present thesis are in bold and numbered by a superscript (eg **Fowler et al, 1997**[1]).

Chapter 1 – Introduction

1.1 Background

The centromere is the primary constriction in the dividing chromosome and the origin from which genetic recombination distances are measured (reviewed by Craig et al, 1999). It holds newly replicated sister chromatids together and allows the attachment of 15 to 30 microtubules that originate from centrosomes (Maney et al, 1999). These in turn facilitate sister chromatid separation to daughter cells during mitosis and meiosis by manoeuvring the chromosomes to opposite poles of the bipolar spindle prior to nuclear envelope reformation and completion of mitosis (for review see Alberts et al, 1994a). Problems in sister chromatid separation during cell division can lead to aneuploidy (ie abnormal chromosome number eg patients with Downs syndrome cells carry an extra chromosome 21), aging, cancer and cell death. Human aneuploidies, collectively, represent the most common cause of genetic abnormalities and are thought to be a major factor for patients with spontaneous abortion and recurrent miscarriage (Pellicer et al, 1998; Lomax et al, 2000). The possibility that some non-disjunction of chromosomes may be genetically determined is tantalising because if proven, it would allow the genetic diagnosis of patients and a better understanding of the aetiology of certain conditions which result from aneuploidy.

1.2 Centromere structure

The mammalian centromere is usually made up of highly repetitive, transcriptionally inactive DNA enveloped by a specialised proteinaceous structure known as the kinetochore (reviewed by the following: Rattner, 1991; Brinkley et al, 1992; Earnshaw and Tomkiel, 1992; Pluta et al, 1995; Choo, 1997a; Craig et al, 1999; Maney et al, 1999). A number of these reviews have identified the centromere of fully condensed metaphase chromosomes as having three major components: the pairing domain at the inner surface of the centromere where the sister chromatids are in intimate contact; the central domain representing the majority of the centromeric DNA, and the two kinetochore domains along each outer surface of the centromere (Figure1; Rattner, 1991; Choo, 1997a; Craig et al, 1999). Electron microscopy has identified the kinetochore domain of each sister chromatid as having three layers

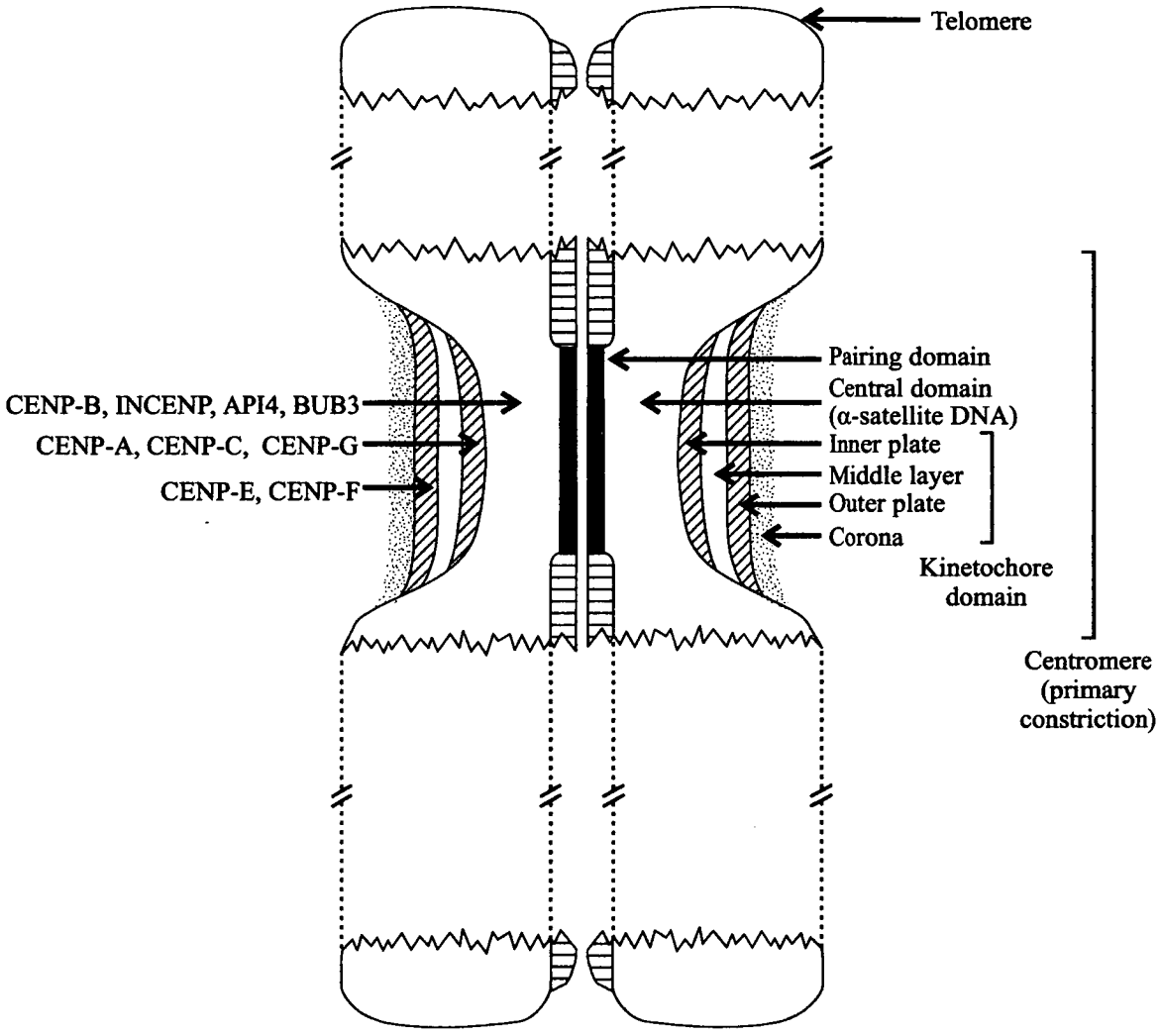

Figure 1 Schematic representation of structural domains (shown on right) and centromere-associated proteins (shown on left) of the centromere-kinetochore complex on human metaphase chromosome (figure based on Choo 1997a).

Note: CENP-B and INCENP broadly localise to the central domain which contains α-satellite DNA; API4 colocalises with INCENP; BUB3 with α-satellite DNA; CENP-A, CENP-C and CENP-G localise to the inner plate of the kinetochore domain; CENP-E and CENP-F to the outer plate of the kinetochore domain. CENP-E has also been localised to the fibrous corona which extends from the outer plate. The precise localisation of CENP-H at the kinetochore domain is unknown at present. The positioning of several constitutive and facultative proteins throughout the cell cycle and at the centromere-kinetochore complex has been further defined by confocal immunofluorescence microscopy (Martineau-Thuillier et al, 1998; **Uren et al, 2000**[12]) and immunoelectron microscopy using antibodies (reviewed by Craig et al, 1999).

known as the inner plate, middle layer or interzone and outer plate with a distinct corona (fibrous coat) on the outer plate (Figure 1). The inner plate contains the outermost centromeric DNA and several centromere-associated proteins known as CENPs [a]. Whereas the outer plate is the site of microtubule attachment and cell cycle checkpoint control ie a cellular control mechanism that ensures cell cycle progression proceeds only after the microtubules are properly attached to the centromeres of all chromosomes (Pluta et al, 1995; Choo, 1997a; Craig et al, 1999).

1.3 Centromeric DNA

The role of the block of tandemly-repeated, late-replicating DNA that underlies the kinetochore protein structure of centromeres and how it separates during mitosis is unclear (reviewed by the following: Holm, 1994; Choo, 1998a; Craig et al, 1999). Besides human and mouse, centromeric DNA has been cloned from many organisms including *Schizosaccharomyces pombe* (a fission yeast with 40 to 100 kb size centromeres), *Saccharomyces cerevisiae* (budding yeast with <0.2 kb size 'point' centromeres), *Drosophila melanogaster* (fly), fish, *Muntiacus muntjac* (Indian muntjac deer), cow and pig (reviewed by Choo, 1998a) as well as *Neurospora crassa* (filamentous fungus; Cambareri et al, 1998), water buffalo (Tanaka et al, 1999), *Arabidopsis thaliana* (small herb plant; Copenhaver et al, 1999) and *Plasmodium falciparum* (mosquito; Bowman et al, 1999). With the exception of *S. cerevisiae*, all eukaryotic centromeres have a large amount of repetitive DNA sequences (Choo, 1998a). These repeat DNA sequences constitute up to 5% of the human genome and 10% of the mouse genome (Brinkley et al, 1992). However unlike the telomere (Figure 1) which consists of tandem repeats of the sequence TTAGGG (Blackburn

[a] The nomenclature for the centromere proteins and genes in species other than mouse are written in capital letters with a hyphen (eg CENP-A) for protein and *CENPA* for gene symbol in keeping with the current literature and Genome Database (GDB). The symbol for the mouse centromere proteins is written in small letters with no hyphen (eg Cenpa) for protein and *Cenpa* for gene symbol as approved by International Committee on Standardised Genetic Nomenclature for Mice which restricts the use of capital letters and hyphens in mouse genes or loci.

and Greider, 1995), little or no DNA sequence homology has been observed in the cloned centromeres from the above species, which range in size from 40 to 5000 kb. This suggested that the DNA sequences which form the structural backbone of the centromere are not crucial for conserved centromere function (Choo, 1998a; Baum and Clarke, 2000).

Furthermore, there is a scarcity of expressed genes in the centromeric regions of most species and genetic recombination is dramatically reduced in the region (for commentary see Choo, 1998b). Indeed many human and *Drosophila* genes become inactive when inserted near the centromere. However there are several organisms such as *S. cerevisiae*, *S. pombe*, *Drosophila* and *Arabidopsis* that have expressed genes residing very close to, or within defined centromeric regions (Copenhaver et al, 1999) adding to the complexity of understanding the primary role of DNA in centromere formation.

1.3.1 Human centromeric DNA

In humans, the central domain of centromeres is made up of large arrays (2-4 Mb on each chromosome) of highly repetitive 171-bp A+T rich DNA alphoid satellite DNA monomers (also known as α-satellite DNA) which contain 17-bp box motifs that have the ability to bind one of the centromere proteins, CENP-B (Rattner, 1991; Choo, 1997b). Although α-satellite DNA has been shown experimentally to display functional centromeric activity, evidence exists that this sequence may be redundant because of the ability of the human genome to form functional, analphoid (α-satellite DNA-deficient) new centromeres (neocentromeres) in noncentromeric regions of the genome (reviewed by Choo, 1997b).

Approximately 40 neocentromeres have been described in humans as well as one in *Drosophila* (reviewed by Choo, 1998a; Williams et al, 1998; Slater et al, 1999; Voullaire et al, 1999a; Tyler-Smith and Floridia, 2000). The best characterised of these is the human chromosome 10-derived neocentromere known as mardel (10). This mitotically stable neocentromere has been cloned and sequenced from a 80-kb region on 10q25 with only minor similarity to known centromeric DNA sequences being detected (Voullaire et al, 1993; du Sart et al, 1997; Barry et al, 1999). Despite

this, the mardel (10) neocentromere has been shown to display identical binding of more than 20 different centromere-associated proteins except for the lack of CENP-B binding, when compared to normal α-satellite-based centromeres (Saffery et al, 2000). The paucity of detectable CENP-B binding complements the DNA sequence study, which identified only one copy of a CENP-B box-like motif in mardel (10) DNA (Barry et al, 1999).

These recent studies highlight that although α-satellite-rich DNA may be the preferred site of human centromere formation in its absence other latent genomic regions may become activated presumably by an epigenetic event (ie a sequence-independent mechanism) or a particular DNA conformation that results in a cascade of centromere-associated protein binding and the creation of functional new centromeres (du Sart et al, 1997; Barry et al, 1999; Saffery et al, 2000). Moreover it adds support to the notion that specific centromeric DNA sequences are not required for centromere activity, although the sequencing of other neocentromeres may yet identify a common predetermining feature in centromeric DNA such as islands of A+T-rich sequence (Choo, 1998a; Barry et al, 1999).

1.3.2 Mouse centromeric DNA

In the mouse, *Mus musculus* there are two main subclasses of satellite DNA known as major (an A+T-rich 234-bp monomer) and minor (a 125-bp monomer) with colocalisation of the centromere-associated proteins and the 17-bp Cenpb box being present only in the minor satellite DNA (Brinkley et al, 1992). Mouse centromeres are acrocentric with the minor satellite present at the X chromosome and autosomes being flanked by telomeric DNA on one side and major satellite on the other (Tyler-Smith and Willard, 1993). The mouse Y chromosome contains no detectable minor or major satellite DNA and like the human Y chromosome Cenpb binding sites are absent (Rattner, 1991). In the male, the necessary pairing off of the sex chromosomes in meiosis is unlike the homologous chromosomes that undergo sister centromere pairing. Instead it is achieved via the pseudoautosomal regions on the X and Y chromosome uniting and partitioning into two daughter nuclei (Alberts et al, 1994b).

Besides *Mus musculus* (*M. musculus*), the distribution of centromeric DNA has been examined in two other *Mus* genus members, *Mus spretus* (*M. spretus*) and *Mus caroli* (*M. caroli*). Both these species have been shown to contain major satellite DNA at the centromere as well as along the chromosomal arm regions. The minor satellite DNA, which was only found at the kinetochore region of *M. musculus*, has been found distributed throughout the centromere in *M. spretus*. In the case of *M. caroli* the minor satellite centromeric DNA is made up of 79-bp repeat monomers with minimal (9 of 17-bp conserved) Cenpb binding sequences (Brinkley et al, 1992; Kipling et al, 1995; Pluta et al, 1995; Sunkel and Coelho, 1995). Apart from Cenpb little is known about the profile of the centromere-associated proteins in *M. spretus* and *M. caroli*.

1.4 Centromere-associated proteins

There are five constitutive centromere proteins known as: CENP-A, CENP-B, CENP-C (reviewed by Maney et al, 1999), CENP-G (Figure 1; He et al, 1998) and CENP-H (Sugata et al, 1999) that are constantly present at the mammalian centromere throughout the cell cycle including during interphase. Several of these constitutive proteins (eg CENP-A, CENP-B, CENP-C) were identified initially through the use of autoimmune sera from patients with calcinosis, Raynaud phenomenon, esophageal dismotility, sclerodactyly, telangiectasia (CREST) syndrome (Moroi et al, 1980; Earnshaw and Rothfield, 1985) or 'Watermelon syndrome' (CENP-G; He et al, 1998) [b].

[b] Another centromere protein known as CENP-D was identified as a 47-kDa protein that localised to the kinetochore domain of both human and Indian muntjac deer cells (reviewed by Maney et al, 1999). CENP-D has been omitted from this present study as subsequent work has shown CENP-D to be homologous with another 45-kDa mammalian protein known as RCC1 (Regulator of Chromosome Condensation 1). RCC1 is a cellular guanine exchange factor and an unlikely centromere protein (Choo, 1997a).

As well, there are approximately 20 known facultative or chromosome passenger proteins, that briefly associate with the centromere for a certain portion of the cell cycle. These include proteins such as CENP-E, CENP-F or mitosin, INCENP, API4 or survivin, cytoplasmic dynein intermediate chains and many other proteins (reviewed by the following: Craig et al, 1999; Maney et al, 1999; Saffery et al, 2000). These proteins appear to use the centromere during metaphase as a marshalling area before transferring from the chromosome to the mitotic spindle in early anaphase and performing cytoskeletal functions toward the end of mitosis (Craig et al, 1999).

A subgroup of these transiently associated centromeric proteins are involved in cell cycle regulation via a feedback control mechanism known as a mitotic spindle checkpoint. This group of proteins include members of the BUB (Budding Uninhibited by Benzimidazole)-family such as BUB1, BUB3 and BUBR1 (BUB1-related protein kinase) as well as other proteins including the MAD (Mitotic Arrest Deficient)-family members known as MAD1-3 (for reviews see: Craig et al, 1999; Maney et al, 1999; Saffery et al, 2000). These proteins control metaphase to anaphase transition by inhibiting the onset of anaphase until all the chromosomes achieve bipolar microtubule attachments and are correctly aligned on the mitotic spindle. Unattached kinetochores generate an inhibitory transduction signal or 'checkpoint', whereas secured kinetochores experience tension due to opposing spindle forces. Subsequently tension-sensitive proteins located at the kinetochore have been postulated to lose activity thus allowing anaphase to proceed (Taylor et al, 1998). However evidence also exists to suggest that the onset of anaphase is initiated by cleavage of specific sister chromatid cohesion proteins rather than the sole activity of tension-generating spindle fibres (reviewed by Nasmyth et al, 2000). Degradation of these cohesion proteins is believed to be linked to the BUB and MAD checkpoint pathways via MAD2 kinetochore complexes diffusing throughout the cell and inactivating a structure known as the anaphase promoting complex (APC)/cyclosome ubiquitin ligase which marks proteins for degradation by tagging with ubiquitin. When inactivate, the APC is unable to ubiquinate the cohesion proteins and initiate anaphase (Maney et al, 1999; Dobles et al, 2000).

Understanding the role of Cenpa, Cenpb, Cenpc, Incenp, Api4 and Bub3 proteins in centromere formation and function together with determining the chromosomal

positions of *Cenpa*, *Cenph*, *Cenpe*, *Cenpf*, *Incenp* and *Bub3* genes is the major focus of the presented publications (**Fowler et al, 1997[1]; Kalitsis et al, 1998a[2]; Hudson et al, 1998[3]; Fowler et al, 1998a[4]; Fowler et al, 1998b[5]; Cutts et al, 1999[6]; Fowler et al, 1999[7]; Fowler et al, 2000[8]; Howman et al, 2000[9]; Lo et al, 2000[10]; Kalitsis et al, 2000[11]; Uren et al, 2000[12]**). It was not necessary to localise *Cenpb*, *Cenpc* and *Api4* loci as these have already been described (Carlson et al, 1993; McKay et al, 1994; Li and Altieri, 1999). Also, *Cenph*, *Cenpe* and *Cenpf* were cloned in Prof Choo's laboratory and mapped in this study with the view to generate knockout mice in the future. Subsequently the remainder of this Chapter has concentrated on introducing: CENP-A, CENP-B, CENP-C and CENP-H constitutive centromere proteins as well as CENP-E, CENP-F, INCENP, API4 and BUB3 facultative centromere proteins.

1.4.1 Constitutive centromere proteins

1.4.1.1 CENP-A

CENP-A is a 17-kDa protein that was first identified using CREST antisera on human centromeres during mitosis and interphase (reviewed by the following: Choo, 1997a; Maney et al, 1999). This protein, like CENP-C has been localised to the inner kinetochore plate (Figure 1; Warburton et al, 1997). Also, it has been detected at mammalian and chicken centromeres (reviewed by Choo, 1997a; Saffery et al, 1999b) as well as *S. cerevisiae* (Stoler et al, 1995), *Caenorhabditis elegans* (nematode worm; Buchwitz et al, 1999); *S. pombe* and *Drosophila* (Pidoux and Allshire, 2000) where CENP-A protein homologs are known as CSE4p (chromosome segregation protein) and HCP-3 (holocentric protein-3), Cnp1 and Cid1 respectively. Furthermore CENP-A has been has been detected at neocentromeres (Saffery et al, 2000) and is not present at inactive centromeres on dicentric chromosomes (Warburton et al, 1997).

CENP-A protein was originally purified from bull sperm and a partial cDNA sequence, as well as cDNA sequences for mouse and human CENP-A have been reported (Sullivan et al, 1994; Kalitsis et al, 1998b). Sequence analysis has revealed the carboxyl-terminus (C-terminus) of CENP-A to have significant regions of

homology with histone H3 (Sullivan et al, 1994; Kalitsis et al, 1998b). Besides H3 there are three other specialised histone proteins (H2A, H2B and H4) that are responsible for packing or condensing very long eukaryotic DNA into the nucleus. DNA that is associated with histones is known as chromatin and the fundamental DNA-histone packing unit is known as the nucleosome (reviewed by Alberts et al, 1994c). The acetylated state of histones H3 and H4 has been implicated in centromere structure and function as have other post-translational changes such as phosphorylation and ribosylation (Pidoux and Allshire, 2000).

Further CENP-A analyses suggest that the inner kinetochore plate consist partly of CENP-A/DNA nucleosomes that have been formed by the C-terminal end of CENP-A binding to a certain DNA conformation rather than a particular DNA sequence (reviewed by Maney et al, 1999). Collectively a number of studies indicate that CENP-A may have an important role in the packaging of centromere chromatin. Additionally mammalian CENP-A is expressed in late S-phase coinciding with the late timing of kinetochore DNA replication, possibly providing an early epigenetic marker for centromere formation on chromosomes (reviewed by the following: Karpen and Allshire, 1997; Csink and Henikoff, 1998; Van Hooser et al, 1999, Pidoux and Allshire, 2000).

Evidence for the functional role of CENP-A comes from anti-CENP-A antibody microinjection experiments in human HeLa cells (Figueroa et al, 1998) and gene disruption experiments in the *S. cerevisiae CSE4* gene (Stoler et al, 1995). HeLa cells injected into the nucleus during early replication stages of the cell cycle with antibody raised against the amino-terminus (N-terminus) of CENP-A, arrested in interphase and lost viability. Whereas cells injected during different stages of mitosis progressed through the cell cycle at a slower rate suggesting that once CENP-A has organised the centromeric chromatin during interphase the cell is protected from any adverse effects of the anti-CENP-A antibody (Figueroa et al, 1998).

Earlier studies on the *cse4-1* temperature-sensitive yeast mutant revealed arrest and inviability at higher temperatures however the arrest occurred after DNA replication and spindle assembly but before the onset of sister chromatid separation during anaphase suggesting that CSE4 protein functions in chromosome segregation as opposed to DNA replication (Stoler et al, 1995). Exploring the purpose of Cenpa in

centromere biology and determining the genetic mapping of the mouse *Cenpa* locus forms the basis of experiments that are presented in Chapters 2 and 3, respectively.

1.4.1.2 CENP-B

Human CENP-B has been identified as an 80-kDa protein, which is distributed throughout the centromeric heterochromatin beneath the inner plate of the kinetochore (Figure 1; Cooke et al, 1990). This protein is encoded by a single intron-less gene and has 96% cDNA sequence homology with the cloned mouse *Cenpb* gene (Earnshaw et al, 1987; Sullivan and Glass, 1991). The human and mouse genes have been localised to a homologous region on human chromosome 20p13 (Seiki et al, 1994) and mouse chromosome 2 (Carlson et al, 1993; 74.2 cM region, MGD). Besides human and mouse, the CENP-B amino acid sequence is highly conserved in hamster, African green monkey, great ape, tupaia (tree shrew), calf, Indian muntjac deer and sheep (reviewed by the following: Kipling and Warburton, 1997; Maney et al, 1999) as well as in the higher plant known as *Phaseolus vulgaris* (Barbosa-Cisneros et al, 1997). Furthermore immunofluorescent staining with antisera to human CENP-B has revealed the conservation of this protein in chicken, mouse and human centromeres (Saffery et al, 1999b).

Sequence analysis has shown that the N-terminus of CENP-B encodes a DNA-binding domain whereas the C-terminus houses the CENP-B dimerisation domain (reviewed by Maney et al, 1999). CENP-B binds to α-satellite DNA in human or minor satellite DNA in mouse via a 17-bp sequence known as the CENP-B box motif. This motif has been found in the centromeric DNA of a wide variety of vertebrates (Maney et al, 1999) and plants (Aragon-Alcaide et al, 1996; Nagaki et al, 1998; Weide et al, 1998). The dual DNA-binding and dimerisation properties of CENP-B suggest that this protein organises the assembly of repetitive DNA at the primary constriction facilitating centromere/kinetochore formation (Yoda et al, 1992).

A second CENP-B related protein known as *jerky* has been identified in an insertional mouse mutant as have three human *jerky* gene products (Toth et al, 1995; Baum and Clarke, 2000). The *jerky* mouse suffers epileptic seizures and its locus has

been mapped to the 42.8 region on chromosome 15 (MGD). The role of the 58-kDa *jerky* protein on chromosomes and centromeres is at present unknown (Toth et al, 1996; reviewed by Craig et al, 1999). Also, mammalian CENP-B has sequence similarity with two centromere-binding proteins in *S. pombe* known as Abp1p and Cbh1p which are believed to bind DNA via N-terminal domains, as well as with the *Tigger1*, *2* and *pogo* transposases which have the ability to cause single-stranded DNA breaks that may facilitate evolution (Kipling and Warburton, 1997; Baum and Clarke, 2000).

The role of CENP-B in centromere biology has been controversial for many years with its extraordinarily conserved sequence and anti-CENP-B antibody microinjection experiments suggesting that it is an indispensable protein (Bernat et al, 1990, 1991). This is further supported by a yeast strain carrying deletions in both CENP-B homologs Abp1p and Cbh1p, having a profound effect on chromosome segregation and growth (Baum and Clarke, 2000).

On the other hand there are many lines of evidence to suggest that CENP-B is non-essential. These include the presence of CENP-B binding on both active and inactive centromeres of dicentric human chromosomes (Earnshaw et al, 1989). Additionally the amount of CENP-B varies considerably on chromosomes and there is a lack of CENP-B boxes or bound protein on human or mouse Y chromosomes (Sunkel and Coelho, 1995). Likewise CENP-B is absent from human analphoid neocentromeres (Choo, 1998a) and is virtually undetectable on African green monkey centromeres which are composed of α-satellite DNA (Goldberg et al, 1996). This plethora of observations marked Cenpb as an ideal protein for further functional studies discussed in Chapter 2.

1.4.1.3 CENP-C

CENP-C was identified by CREST antisera as a 140-kDa protein and has been localised to the inner kinetochore plate near the centromeric chromatin (Figure 1; reviewed by the following: Craig et al, 1999; Maney et al, 1999). Antisera to mouse or human CENP-C has revealed the conservation of this protein in chicken, mouse, human and *Xenopus* (Lanini and McKeon, 1995; Saffery et al, 1999b). Human, sheep

and mouse cDNAs have been cloned with sequence similarity being observed with the chromosome segregation protein Mif2p in *S. cerevisiae*, Cnp3 in *S. pombe*, TO3F1.9 in *C. elegans*, AtCENP-C in *A. thaliana* and three maize homologs known as CenpcA, CenpcB and CenpcC (reviewed by Kalitsis et al, 1998b; Pidoux and Allshire, 2000; Tyler-Smith and Flordia, 2000). Furthermore the genomic structure of the mouse gene has been determined (Kalitsis et al, 1998b) and mapped to chromosome 5E2-E5 in a region of homology with human chromosome 4q12-q13.3 (McKay et al, 1994). A non-functional mouse and human CENP-C pseudogene has also been localised on chromosomes 2B and 12q21.2-q21.33 respectively (McKay et al, 1994).

CENP-C has been shown to interact with: DNA (Yang et al, 1996); the nucleolar transcription factor UBF/NOR90 (Pluta and Earnshaw, 1996); and Hdaxx, a protein involved in apoptosis (programmed cell death; Pluta et al, 1998). It has been shown to be present on active centromeres of dicentric chromosomes (Earnshaw et al, 1989; Page et al, 1995) and on neocentromeres (reviewed by Choo, 1997b) suggesting that CENP-C has an essential role in centromere function.

The biological role of CENP-C has been explored *in vitro* by microinjection of CENP-C antisera into porcine and human cells (Tomkiel et al, 1994). Anti-CENP-C microinjection experiments resulted in cells arresting in metaphase and the formation of kinetochores with a significantly smaller diameter (Tomkiel et al, 1994). However, antibody injection experiments can be fraught with limitations such as lack of efficiency and specificity that may restrict their interpretation (Alberts et al, 1994d; Maney et al, 1999). The functional role of Cenpc *in vitro* and *in vivo* is investigated further in Chapter 2.

1.4.1.4 CENP-H

CENP-H, or perhaps more correctly Cenph was identified as a 33-kDa novel mouse kinetochore protein during the course of isolating erythropoietin-inducible transcripts by differential display in mouse SKT6 cells (Sugata et al, 1999). Antibody raised to mouse Cenph recognised mouse and human CENP-H in immunofluorescence stainings. The observed paired CENP-H stainings were also shown to colocalise with human anti-centromere specific antibody. However, no indication was given as to

whether the staining was uniform on the centromere/kinetochore complex of all chromosomes or whether some variation was observed similar to the pattern observed with CENP-B in human, mouse and chicken cells (Saffery et al, 1999b).

Surprisingly, unlike other centromere proteins such as Cenpa, Cenpb, Cenpc or Incenp that have detectable mRNA levels in non-haemopoietic mouse tissues by Northern blot analyses (Redward, Fowler and Kalitsis, unpublished observations; Saffery et al, 1999a) *Cenph* RNA expression levels were too low to detect using this method (Sugata et al, 1999). Being a relatively new centromere protein the precise localisation of CENP-H at the kinetochore domain remains to be elucidated. In addition, insight into the function of this protein in mitosis and meiosis could be gained by targeting the *Cenph* gene to produce a deficient mouse. As an initial step, however *Cenph* genetic mapping studies described in Chapter 3 were performed to find out whether *Cenph* shows concordance with any pre-existing mouse mutant.

1.4.2 Facultative centromere proteins

1.4.2.1 CENP-E

CENP-E belongs to a second much larger group of facultative centromere proteins that are only transiently associated with the centromere during the cell cycle. CENP-E was originally identified using a monoclonal antibody raised against a chromosomal scaffold fraction prepared from mitotic chromosomes (Yen et al, 1991). This 312-kDa kinesin-related motor protein localises on the outer kinetochore plate including the fibrous corona, of the mammalian centromeres throughout prometaphase, during metaphase (Figure 1; Cooke et al, 1997) and anaphase when cells were undergoing chromatid movement. CENP-E starts to diminish from the centromeres at anaphase but remains at detectable levels at kinetochores of decondensing chromosomes in telophase (Yen et al, 1991, 1992; Lombillo et al, 1995; Cooke et al, 1997). In late anaphase and during telophase the bulk of CENP-E concentrates in the midbody on the stem body material that coats the overlapping

antiparallel microtubules of the central spindle [c]. Following the completion of mitosis CENP-E is largely destroyed by proteolysis (Cooke et al, 1997).

CENP-E appears to be conserved in multicellular organisms with human, *Xenopus* and 2 *Drosophila* homologs known as CENP-meta and CENP-ana being cloned (reviewed by Maney et al, 1999; Yucel et al, 2000). Also, CENP-E antisera (antihuman) has been used to detect CENP-E at the centromeres of human, Indian muntjac deer, rat kangaroo, mouse and chicken chromosomes (Cooke et al, 1997; Saffery et al, 1999b).

Recently it has been shown that the kinetochore localisation domain of CENP-E interacts with CENP-F and the spindle checkpoint protein BUBR1 (Chan et al, 1998). Additional analysis has revealed that CENP-F localises to the kinetochore, prior to BUBR1 which is followed by CENP-E suggesting that the association between CENP-F and BUBR1 with the kinetochore produces a CENP-E/kinetochore binding site (reviewed by Maney et al, 1999). *In vitro* studies using antibodies or antisense oligonucleotides to CENP-E have shown that this protein was essential for monopolar chromosomes to establish bipolar connections and for chromosomes with connections to both spindle poles to congress (move) and align at the spindle equator (Thrower et al, 1995; Schaar et al, 1997; Wood et al, 1997; Yao et al, 2000). To further understand CENP-E and to test the hypothesis that the *Os* mouse mutant could be a candidate carrying a mutated *Cenpe* gene, genetic mapping experiments were carried out as described in Chapter 3.

[c] The midbody forms during cytokinesis when cleavage furrowing of cellular cytoplasm is near completion. The midbody is constructed from the remaining overlapping microtubules from the two opposing spindle poles and is tightly packed together with dense matrix material. Cytokinesis begins after a cell has duplicated its genetic material and is completed by the destruction of the midbody and restoration of an intact cell membrane around each of the daughter cells (Alberts et al, 1994a; Bischoff and Plowman, 1999).

1.4.2.2 CENP-F

CENP-F is also known as mitosin. Human CENP-F was identified through screening cells with sera from patients with nonsclerodermal rheumatic disease whereas mitosin was isolated by others screening human cells for proteins that interact with the retinoblastoma protein (for review, see Maney at al, 1999). CENP-F is a 367-kDa nuclear matrix-associated chromosome passenger protein predicted to contain putative kinase phosphorylation sites (Rattner et al, 1993; Liao et al, 1995). CENP-F has been shown to be present at the centromeres of human, mouse and chicken chromosomes (Saffery et al, 1999b) and two CENP-F homologs known as HCP-1 and HCP-2 have been identified in *C. elegans* (Pidoux and Allshire, 2000).

Moreover this protein has been shown to be uniformly distributed in the cell nucleus during S-phase, localising onto the outer kinetochore plate from late G_2/M-phase to metaphase (Figure 1; Rattner et al, 1993) where it has been shown to physically interact or precipitate with CENP-E (see above) (Chan et al, 1998; Yao et al, 2000). In anaphase CENP-F relocates to the spindle midzone region where the metaphase plate once was. By telophase CENP-F concentrates either side of the midbody before being degraded following completion of mitosis (Rattner et al, 1993; Liao et al, 1995; Mancini et al, 1996).

The functional role of CENP-F is not well understood however the localisation of CENP-F/mitosin during kinetochore formation has been accompanied by an increase in chromatin condensation. This and some of CENP-F sequence properties suggest that it may have an active role in chromatin condensation prior to mitosis (reviewed by Maney et al, 1999). In addition, CENP-F has been shown to be a valuable proliferation marker for various brain tumours (Landberg et al, 1996). To gain further insight into CENP-F, the chromosomal position of mouse *Cenpf* was determined as described in Chapter 3.

1.4.2.3 INCENP

Two proteins known as INCENP I and II (INner CENtromere Proteins) were the first of the chromosome passenger group of centromere proteins to be described. These were originally identified in chicken with a monoclonal antibody raised against the bulk proteins of a mitotic chromosome scaffold fraction (Cooke et al, 1987). Subsequently INCENPs I and II were shown to be 96-kDa and 101-kDa respectively, and to be encoded by the same single gene (Mackay et al, 1993). Both *Xenopus* (130-kDa) and mouse (101-kDa) homologs of chicken INCENP have been identified and protein analysis has revealed the presence of many putative kinase phosphorylation sites (Stukenburg et al, 1997; Saffery et al, 1999a). Furthermore this protein has been shown to be conserved in chicken, mouse and human cells (Ainsztein et al, 1998; Saffery et al, 1999b) and the single-copy mouse *Incenp* gene has been cloned (Saffery et al, 1999a).

During prophase INCENP protein has been found along the chromosomal arms, progressively accumulating in the central domain of the centromere during prometaphase and early metaphase (Ainsztein et al, 1998). At metaphase INCENP is broadly distributed throughout the heterochromatin beneath the kinetochore similar to CENP-B (Figure 1; Eckley et al, 1997). At late metaphase, INCENP starts to leave the centromeres and during metaphase-anaphase transition becomes associated with the stem body material which coats the overlapping microtubules of the central spindle. By mid anaphase some INCENP staining appears at the cell cortex in the region of the actin-mediated contractile ring where the cleavage furrow will later form. During telophase INCENP staining concentrates in the midbody in the intercellular bridge where it disappears following cytokinesis (Earnshaw and Cooke, 1991).

Recent *in vitro* studies have used different mutant forms of INCENP to study its functional role. The first assayed the effects of a CENP-B:$INCENP_{43-839}$ overexpression construct in HeLa cells within 24-48 hour after transfection. This chimaeric transgene tethered the $INCENP_{43-839}$ protein to the heterochromatic domain of the centromere throughout the mitosis producing a dominant-negative effect on endogenous INCENP that disrupted cytokinesis. Without the CENP-B to

secure it to the centromere the $INCENP_{43-839}$ truncation mutant lacked the ability to concentrate at centromeres during metaphase and to transfer to the spindle at the metaphase-anaphase transition (Eckley et al, 1997).

The second study used transient transfection of HeLa cells with a series of truncated molecules to map INCENP regions that are essential for centromere targeting and transfer to the spindle during anaphase. One of these mutants, $INCENP_{1-405}$ targets centromeres but lacks the microtubule association region. This dominant-negative mutant interferes with chromosomal congression during prometaphase and completion of cytokinesis by displacing wildtype INCENP (Mackay et al, 1998). However one possible disadvantage with these dominant-negative approaches is the presence of endogenous INCENP protein that may interfere with the observed phenotypes. To overcome this, the functional role of Incenp is examined further using knockout mouse technology in Chapter 2. The genetic mapping of the *Incenp* locus is described in Chapter 3.

1.4.2.4 API4

Apoptosis inhibitor 4 protein (API4) or survivin encodes a 16.5-kDa protein (Li et al, 1998) and belongs to the Inhibitor of Apoptosis (IAP) family of proteins that contain a baculoviral IAP repeat (BIR) of approximately 70 amino acids. IAPs were originally discovered in baculoviruses and have been shown to block apoptosis in response to viral infection of host insect cells. Qualification for IAP membership is generally restricted to proteins encompassing BIR domains that suppress apoptosis. However survivin and several other BIR-bearing proteins have been implicated in cell division rather than purely anti-apoptotic activities. To date, survivin-related proteins have been identified in *S. pombe* (Bir1), *S. cerevisiae* (Bir1p), *C. elegans* (BIR-1), human (API4) and mouse known as Api4 (for review, see Deveraux and Reed, 1999). The human *API4* gene has been localised to 17q25 whereas the mouse locus, *Api4* has been assigned to the distal region of chromosome 11E2 (Li and Altieri, 1999; Mouse Genome Database, 2000).

Recent studies using independently derived, affinity-purified polyclonal antibodies to a unique N-terminal peptide of human survivin have localised survivin in HeLa cells.

The first study has identified survivin as a non-centromeric G_2/M mitotic checkpoint protein that closely associates with microtubules, midbodies, centrosomes (organelles from which the mitotic spindle develops) and the apoptosis effector caspase-3 during the cell cycle (Li et al, 1998; Li et al, 1999). Whereas a subsequent study has found survivin to be a transient centromere-associated protein with an immunostaining profile resembling that of the chromosome passenger protein INCENP (Figure 1; **Uren et al, 2000**[12]). Furthermore, INCENP has been shown to colocalise with another passenger protein known as Telophase Disc 60 (TD-60; Martineau-Thuillier et al, 1998). This protein has been shown to localise with the serine/threonine kinase Aurora1 which is required for the successful completion of cytokinesis (Martineau-Thuillier et al, 1998; Bischoff and Plowman, 1999).

The expression of survivin during the cell cycle and in development as well as in human cancers has lead to the proposal of survivin having a direct role in oncogenesis (LaCasse et al, 1998). Survivin mRNA has been found to be upregulated approximately 40 fold at the G_2/M-phase of the mammalian cell cycle (Li et al, 1998). Northern analysis has detected survivin in many tissues derived from day 11.5pc (post conceptus) mouse embryos but expression became restricted to a few locations by late gestation and was rare in normal adult mouse or human tissues (Adida et al, 1998). In contrast survivin was overexpressed in many transformed cell lines and human cancers. Interestingly survivin levels in colorectal cancer inversely correlated with five year survival rates suggesting that this protein may be of prognostic value for patients with certain tumours (LaCasse et al, 1998; Deveraux and Reed, 1999). Further support for survivin having a role in tumour progression has been attributed to the continuous expression of survivin abnormally prolonging cell survival by preventing apoptosis via binding to and inhibiting caspase-3 and caspase-7 thus protecting the mitotic spindle from caspase damage and allowing transformed cells to multiply unchecked (LaCasse et al, 1998; Miller, 1999).

The functional role for survivin in cell division and death is debatable. Studies in some organisms such as *C. elegans* and yeast that lack caspase-inhibiting IAPs suggest that survivin are involved in cell division. *C. elegans* embryos that were rendered

BIR-1-deficient using RNA interference strategy were unable to undergo cytokinesis and became polyploid, whereas *S. pombe Bir1*- and *S. cerevisiae Bir1p*- null mutants failed to accurately transmit chromosomes (Fraser et al, 1999; Uren et al, 1999). However investigations in cultured mammalian cells suggest that survivin has a dual role in cell cycle regulation and control of cell death (reviewed by Reed and Reed, 1999). Disruption of survivin-microtubule interactions in HeLa cells using various microtubule-depolymerising chemicals (eg nocadozole or colchcine) and the microtubule-stabilising agent taxol; antisense oligonucleotides and a dominant-negative survivin mutant resulted in a loss of survivin-microtubule interaction and apoptosis inhibition (Li et al, 1998; Li et al, 1999). Cells with depleted survivin were characterised by supernumerary centrosomes, multipolar mitotic spindles, multinucleation and polyploidy suggestive of failed centrosome function and/or cytokinesis (Li et al, 1999).

To help resolve the important question as to whether mammalian survivin is a unique checkpoint protein that has a double act in cell division and caspase-mediated cell death versus being a chromosomal passenger protein that has little to do with being a caspase inhibitor, analysis of survivin-depleted mice was undertaken as described in Chapter 2.

1.4.2.5 BUB3

BUB3 is a member of the BUB-family of mitotic spindle checkpoint proteins first identified in a genetic screen of *S. cerevisiae*. The BUB mutants, unlike normal cells, failed to arrest in anaphase following exposure to benzimidazole-related, spindle-damaging agents (Hyot et al, 1991). Subsequently homologs of budding yeast BUB3 (ScBUB3) have been reported in *Xenopus*, *Drosophila*, human (BUB3) and mouse known as Bub3 (Basu et al, 1998; Efimov and Morris, 1998; Taylor et al, 1998; Goto

and Kinoshita, 1999; Martinez-Exposito et al, 1999) [d]. The human *BUB3* gene encodes a 37-kDa protein that is 69% similar to *S. cerevisiae BUB3* (Taylor et al, 1998). Like the yeast and human genes, mouse *Bub3* contains a *Bub1* binding domain and four WD40-repeats that are postulated as having a role in protein-protein interactions (Martinez-Exposito et al, 1999). Note: WD40-motifs are comprised of 40 amino acids that end with the sequence Trp-Asp (WD; Neer et al, 1994).

The *BUB3* locus has been assigned to human chromosome in the region of 10q24-26 (Cahill et al, 1999; Seeley et al, 1999; Kwon et al, 2000). Chromosome deletions in this location appear in cancers from a number of tissues suggesting that *BUB3* may function as a tumour suppressor gene (Seeley et al, 1999). Moreover mutations of the *BUB1* kinase gene have been identified in colon cancer cell lines that display an altered mitotic checkpoint status as well as chromosome instability phenotype (Cahill et al, 1998).

Similar to human BUB1 and BUB3, mouse Bub3 cytosolic protein localises to the kinetochore during early mitosis (Taylor et al, 1998; Martinez-Exposito et al, 1999). Anti-kinetochore staining of human HeLa and mouse 3T3 cells with CREST antisera and α-satellite probes revealed colocalisation with Bub3 antisera during prophase, prometaphase and metaphase (Figure1; Martinez-Exposito et al, 1999). However at metaphase the amount of Bub3 at the kinetochores of spindle-aligned chromosomes decreased dramatically. Indeed it has been estimated to reduce 3- to 5-fold on the centromeres of HeLa chromosomes and stay that way until the end of anaphase (Martinez-Exposito et al, 1999).

To further explore this phenomenon, HeLa cells were treated with nocodazole and taxol at concentrations that did not affect the gross structure of the mitotic spindle

[d] The nomenclature for the family of BUB proteins appears in the literature as eg hBUB3, hBub3, HBUB3 or BUB3 for the human homolog; mBUB3, mBub3, MBUB3 or Bub3, for the mouse homolog. I have elected to use BUB3 for human and Bub3 for mouse proteins respectively as well as *BUB3* and *Bub3* for the human and mouse gene symbols, respectively in keeping with International Committee on Standardised Genetic Nomenclature for Mice.

but increased the number of non-aligned chromosomes. Significantly these lagging metaphase-like chromosomes selectively retained high levels of BUB3 and low levels of tubulin suggesting that BUB3 levels on kinetochores varies with the number of attached microtubules and that the binding of microtubules to kinetochores may displace BUB3-related checkpoint complexes (Martinez-Exposito et al, 1999). Earlier studies have shown that BUB3 interacts with BUB1 to form a protein kinase complex that is capable of sequestering other proteins such as BUBR1 kinase to form additional complexes (Roberts et al, 1994; Taylor et al, 1998; Martinez-Exposito et al, 1999). As discussed previously, BUBR1 has been shown to associate with CENP-E thus linking the checkpoint role of BUB family members on centromeres to microtubule activity via the CENP-E motor protein (Chan et al, 1998; Yao et al, 2000).

Studies in *S. cerevisiae* bearing mutations at the *ScBUB1* and *ScBUB3* loci suggested that in the absence of ScBUB3, ScBUB1 is unable to localise at the centromere and hence the checkpoint remains non-responsive to unattached kinetochores. This cumulates in an early onset of anaphase, mitotic errors and subsequent laggard growth (Roberts et al, 1994; Taylor et al, 1998). In addition, a similar slow-growth phenotype was observed in *Aspergillus nidulans* (filamentous fungus) transformants bearing mutations in BUB1 and BUB3 genes known as *sldA* and *sldB*, respectively (Efimov and Morris, 1998). To further explore the functional requirement of BUB3 in mammalian cells and to consider the possibility that defective *BUB3* may contribute to aneuploidy, *Bub3*-null mice were generated and the genetic mapping of the *Bub3* gene was determined as described in Chapters 2 and 3, respectively.

Chapter 2 - Functional Analysis of Mouse Centromere Proteins

2.1 Background

One of the strategies for studying the functional role of a particular protein of interest has been to inactivate it by microinjecting somatic cells with a specific antibody (Alberts et al, 1994d). This method has been employed to study the role of a range of proteins including some of the centromere-associated proteins eg CENP-A, CENP-B, CENP-C and CENP-E (Bernat et al, 1990,1991; Tomkiel et al, 1994; Schaar et al, 1997; Figueroa et al, 1998). However this approach has some limitations. For instance, some antigenic sites may be inaccessible to the antibody and antibody-binding may not necessarily inactivate protein function (Alberts et al, 1994d).

Genetic approaches may circumvent these problems. Proteins are synthesised gene products and can be altered by replacing the normal gene with a cloned mutant gene. Mutants that lack or over-express a specific protein, or generate an aberrant form of protein may quickly reveal the function of the normal molecule (Alberts et al, 1994d). Consequently, many experimental approaches such as mutagenesis and transgenesis including antisense RNA, ribozyme and dominant-negative strategies have been widely used to study gene (and protein) function in a variety of cell lines and model organisms such as yeast, *Drosophila*, *C. elegans*, *Rattus norvegicus* (rat) and mouse. Of these, transgenic mouse technology offers one of the most powerful tools for studying mammalian gene regulation and function (Hammes and Schedl, 2000).

2.1.1 Transgenic mice

Transgenic animals are those that have foreign DNA sequences integrated into their genome as a consequence of the introduction of DNA. Foreign genes may be introduced into the genome by microinjection into the pronucleus of a fertilised embryo, or by viral infection of an embryo, or by manipulation of mouse embryo stem cells (ES cells). The development of ES cells, homologous recombination with embryo manipulation and chimaera formation in the 1980's has provided a remarkable means for examining gene function. At its simplest, gene targeting ES cells allows disrupting or knocking out the endogenous allele of interest *in vitro*, returning the mutant cells to mouse blastocysts and generating transgenic mice

bearing a precise null mutation for *in vivo* experimental study (reviewed by Joyner, 1993; Silver, 1995).

Since the first knockout mice were described in 1988 (Mansour et al, 1988), targeting vectors have been refined to greatly improve the frequency of homologous recombination. This has been achieved by the use of isogenic vector DNA, increasing the length of homologous DNA in the targeting construct (Hasty and Bradley, 1993) and making use of efficient selectable marker cassettes such as one that employs an internal ribosomal entry site (IRES) to generate bicistronic mRNA (Mountford et al, 1994).

In addition new types of gene targeting strategies have been described. These include Cre/loxP and Flp/frt site-specific recombination-based methods. These approaches enable subtle or point mutations to be introduced in any gene as well as providing a means for deleting up to several centiMorgans (cM) of genomic DNA. These recombinase systems can be also utilised to study conditional mutations in mice at a certain time during development or in a particular cell lineage where the constitutive null mutation is lethal (for reviews see Muller, 1999; Plagge et al, 2000).

2.2 Rationale

In order to gain insight into the role of Cenpa, Cenpb, Cenpc, Incenp, Api4 and Bub3 centromere-associated proteins we chose to generate and analyse mouse mutants bearing targeted loss-of-function germline mutations in the specific loci that encode these proteins (**Kalitsis et al, 1998a**[2]; **Hudson et al, 1998**[3]; **Cutts et al, 1999**[6]; **Fowler et al, 2000**[8]; **Howman et al, 2000**[9]; **Kalitsis et al, 2000**[11]; **Uren et al, 2000**[12]). This strategy has several advantages. First, it permits not only the mitotic function of the centromere proteins to be studied *in vitro* and *in vivo*, but also the role of these proteins in meiosis and embryogenesis. Second, it allows for the possible identification of candidate disease-causing loci in humans and other mammals as studies in other fields have shown (Epping and Nadeau, 1995; Paigen, 1995). Third, it offers an alternative and more elegant system than the conventional strategy of microinjecting polyclonal antibodies against centromere-associated proteins into cells and studying their effects on centromere function and cell division since the side-

effects of injected antibodies are difficult to ascertain (**Kalitsis et al, 1998a**[2]; Maney et al, 1999). Fourth, it makes for a more precise system than dominant-negative genetic approaches that may be complicated by residual endogenous CENP protein (**Cutts et al, 1999**[6]). Fifth, the mouse centromere shares many common features with the human centromere. For example both centromeres contain repetitive DNA (α-satellite DNA in the human and minor satellite DNA in mouse) that carry the CENP-B box motif to which CENP-B protein binds (for reviews see: Choo, 1997a; Pluta et al, 1995). Additionally it has been shown that both mouse and human centromeres bind antibodies to CENP-A, CENP-B, CENP-C, CENP-E, CENP-F, CENP-G, CENP-H, INCENP and BUB3 proteins (Choo, 1997a; He et al, 1998; Maney et al, 1999; Sugata et al, 1999; Saffery et al, 1999b, Martinez-Exposito et al, 1999). Sixth, the gene structure or molecular sequence of mouse *Cenpa*, *Cenpb*, *Cenpc*, *Cenpe*, *Cenpf*, *Cenph*, *Incenp*, *Api4* and *Bub3* genes have been determined (Kalitsis et al, 1998b; **Hudson et al, 1998**[3]; **Fowler et al, 1998a**[4]; **Fowler et al, 1998b**[5]; Martinez-Exposito et al, 1999; Saffery et al, 1999a; Sugata et al, 1999; **Uren et al, 2000**[12]).

2.3 Generation of mice carrying *Cenpa*, *Cenpb*, *Cenpc*, *Incenp*, *Api4* and *Bub3* targeted mutations

Mice bearing disrupted *Cenpa*, *Cenpb*, *Cenpc*, *Incenp* and *Bub3* genes were generated by gene targeting mouse ES cells (R1, W9.5 and 129/1) derived from 129 mouse substrains with promoterless targeting vectors that incorporated an IRES-neomycin or IRES-hygromycin marker (Mountford et al, 1994). The *Api4*-null mouse model was created at WEHI, by gene targeting C57BL/6 ES cells (BRUCE4) with a replacement targeting construct containing a neomycin selectable marker (**Uren et al, 2000**[12]).

Heterozygous cell lines for each gene were identified by Southern blot using specific external probes. The IRES-neomycin vectors were instrumental in achieving efficient homologous recombination frequencies of: 54% (129/1) for *Cenpa* (**Howman et al, 2000**[9]); 2% (R1), 3.5% (W9.5) and 1.3% (W9.8) for *Cenpb* (**Hudson et al, 1998**[3]); 74% (R1) for *Cenpc* (**Kalitsis et al, 1998a**[2]); 3.7% (129/1) and 4.6% (W9.5) for

Incenp (**Cutts et al, 1999**[6]); 10% (129/1) and 30% (W9.5) for *Bub3* (Dr Paul Kalitsis, personal communication). This was accomplished by selecting for homologous recombination events downstream of the endogenous promoters and translation of the neomycin or hygromycin gene products via the IRES (**Cutts et al, 1999**[6]).

Targeted cell lines were then injected into C57BL/6 blastocysts and transferred to pseudopregnant recipient female mice to produce germline chimaeras. The chimaeras were mated to C57BL/6 mice to generate heterozygous progeny. The heterozygous offspring were intermated to obtain wildtype, heterozygous and homozygous progeny. Individual mice were initially genotyped by Southern analysis, followed by PCR screening. Nested PCR strategies were used for genotyping mouse embryos (**Kalitsis et al, 1998a**[2]; **Hudson et al, 1998**[3]; **Cutts et al, 1999**[6]; **Fowler et al, 2000**[8]; **Howman et al, 2000**[9]; **Kalitsis et al, 2000**[11]; **Uren et al, 2000**[12]).

2.4 Analysis of mice bearing loss-of-function mutations in centromere protein genes

2.4.1 *Cenpa*

Clues to the essential requirement for *Cenpa* during mouse development were evident from the reduced average litter size of 6.0 ± 2.4 (n=23 litters) for *Cenpa* heterozygous mouse crosses as compared to 9.1 ± 2.6 (n=31 litters) for wildtype crosses. Furthermore no null offspring were observed in 186 live born progeny from heterozygous matings. To further investigate the timepoint of *Cenpa*-null lethality, embryos from heterozygous crosses were genotyped at day-2.5 and -8.5 post conceptus. Analysis revealed that *Cenpa*-null embryos were morphologically healthy at day-2.5 but presented as resorptive implantation sites at day-8.5 and were unable to be dissected. This indicated that the point of lethality was likely to be somewhere in the postimplantation period between day 3.5 and 8.5-day gestation (**Howman et al, 2000**[9]).

To explore the postimplantation development, day-3.5 embryos from heterozygous crosses were collected and cultured individually. These embryos were photographed

daily or stained with Giemsa stain. At 5.5-day pc (ie 3.5 days *in utero* plus 2 days in culture), a number of embryos displayed degeneration of the inner cell mass (ICM) and the trophectoderm[e]. By day-6.5, a defined ICM was no longer visible, while the number of trophectoderm cells was also in decline. These sick embryos were collected for PCR analysis while the remaining healthy embryos were cultured to day-8.5 before collection. The results indicated that all the healthy day-8.5 embryos were either wildtype or heterozygous whereas the 6.5-day degenerating embryos were *Cenpa*-null (**Howman et al, 2000**[9]).

Giemsa staining and chromosomal analysis of cultured null embryos at day-5.5 and 6.5 revealed severe mitotic problems including mitotic delay, highly condensed metaphase chromosomes, micro- and macronuclei formation, nuclear bridging ie joined nuclei, and chromatin blebbing. Not surprisingly the 6.5-day null embryos displayed an increase in the degree of severity with most cells being macronucleated, suggesting that cell division had come to a halt. Indeed no discernible mitotic chromosomes were observed in these embryos whereas mitotic indices of 5.5-day cultured embryos were 1.1% for *Cenpa*-null embryos and 4.7% for normal embryos (**Howman et al, 2000**[9]). The mitotic index is calculated by counting the number of mitotic spreads over the total number of cells for each embryo (**Kalitsis et al, 1998a**[2]).

To investigate the cause of the observed mitotic disarray and verify the completeness of the *Cenpa* gene targeting strategy, immunofluorescence studies were performed. Analyses demonstrated an absence of Cenpa protein, and an abnormal dispersion of Cenpb and Cenpc proteins throughout the nuclei of interphase cells, instead of the usual discrete and compact signals. This indicated that Cenpb and Cenpc are

[e] In normal healthy embryos the ICM gives rise to the embryo proper and the trophectoderm forms the extra-embryonic tissues (Robertson, 1987). Mouse trophectoderm is comprised of trophoblasts that arise from day-4.5 embryonic cells that stop dividing and undergo many cycles of S-phase generating giant cells with polypoid nuclei (Dobles et al, 2000).

incapable of kinetochore formation in the absence of Cenpa and that this failure is likely to explain the progressive deterioration of mitosis and eventual cell death observed in the *Cenpa*-null embryos (**Howman et al, 2000**[9]).

Overall the results suggest that Cenpa plays an early role in organising centromeric chromatin in interphase in preparation for subsequent kinetochore/centromere assembly. These findings are consistent with the proposal that CENP-A is a good candidate epigenetic marker that stamps a chromosomal region for centromere formation (**Howman et al, 2000**[9]).

2.4.2 *Cenpb*

To better understand the role of Cenpb, gene targeting of R1, W9.5 and W9.8 ES cell lines was used to generate cell lines and mice (R1 and W9.5 only) with a null mutation at the *Cenpb* locus. The null status of the double targeted ES cell lines was verified by an absence of Cenpb binding on centromeres by direct immunofluorescence using anti-Cenpb monoclonal antibody (**Hudson et al, 1998**[3]). Breeding pairs of heterozygous mice gave birth to normal-sized litters with the expected Mendelian ratio of offspring indicating that the *Cenpb*-null progeny were viable.

The R1 *Cenpb* knockout mice appeared mitotically and meiotically normal but developed lower body-weight with the difference reaching significance ($p < 0.05$) after 22 weeks in males and 12 weeks in females (**Hudson et al, 1998**[3]). This difference in weight was explored by analysing the body composition of 20-week-old mice in terms of their dry weight, ash weight, moisture, protein and fat. When the results were expressed as a percentage of fresh body weight, no significant difference was observed suggesting that *Cenpb*-null mice were proportionally smaller than control mice (**Fowler et al, 2000**[8]). In addition, plasma leptin levels were measured and found to be similar between *Cenpb*-null and wildtype mice suggesting that hypophagia (suppressed food intake) was unlikely to be responsible for the reduced body weight in the knockout mice (**Fowler et al, 2000**[8]).

To further examine the reduced size of R1 *Cenpb*-null mice a large number of organs were dissected and weighed from age- and sex-matched mice. Surprisingly the testis, uterus and epididymis weights of 10-week-old R1 null mice were significantly smaller (29%, $p<0.001$ for testis, **Hudson et al, 1998**[3]; 31%, $p = 0.032$ for uterus, **Fowler et al, 2000**[8]; 18%, $p = 0.039$ for epididymis, Fowler, unpublished observations) when compared to wildtype mice. Cytogenetics and FACS analysis of testis, bone marrow and spleen revealed no abnormality. A closer look at male meiosis using histology, advanced sperm counting and stereology detected no substantial difference in the efficiency of mitotic or meiotic division (**Hudson et al, 1998**[3]). Furthermore, a long term breeding study over two years with R1 *Cenpb*-null male mice failed to demonstrate any effect on fertility and longevity as compared to wildtype males (**Fowler et al, 2000**[8]).

To further explore these early observations, R1 heterozygous mice were backcrossed to generate C57 *Cenpb*-null congenic and C57 control mice. Also the W9.5 heterozygotes were intercrossed to produce W9.5 *Cenpb*-null and control offspring. Follow-up studies demonstrated that the significant testis- and uterus-weight reduction was seen in *Cenpb*-null mice on all three different genetic backgrounds (denoted R1, C57 and W9.5) whereas body weight was dependent on genetic background as well as the sex of the mice.

In a concurrent study to determine whether cell lines deficient in Cenpb had an altered growth rate, the population doubling times of three null ES cell lines were compared to wildtype and heterozygous cell lines. No significant difference was observed between the cell lines over 400 cell divisions. Karyotyping of the late passage cell lines revealed no increase in aneuploidy compared to the control lines. This suggested that the *Cenpb*-null cell lines grew normally, unlike telomerase-deficient ES cells that deteriorated in doubling times over a similar test period (Niida et al, 1998).

To examine whether the Cenpb construct had unintendedly interfered with expression of a neighbouring gene, 'revertant' mice were generated. These mice lacked the targeted *Cenpb* frameshift mutation but not the other components of the targeting construct. This mutation was shown to have no noticeable effect on Cenpb

protein expression of fibroblast cell lines derived from revertant mice (Front cover, **Fowler et al, 2000[8]**). Moreover it corrected the phenotype seen in the *Cenpb*-null mice indicating that the observed features were not caused by the targeting cassette inadvertently affecting a closely located gene (**Fowler et al, 2000[8]**) as described in other studies (Olson et al, 1996; Muller, 1999).

Besides displaying a small uterus, *Cenpb* knockout female mice demonstrated an age-dependent reproductive dysfunction that was more severe in the C57 background. Breeding studies with 8- to 15-week-old C57-null female mice demonstrated slow or difficult delivery of pups whereas the R1 and W9.5 *Cenpb*-null females bred normally for the first three to four litters. However these females displayed pregnancy problems by age 9-month. In many cases pregnant females sickened because of being overdue by up to 10 days. Autopsy of these mice revealed dead intact or resorbing foeti and pyometra (uterine infection; **Fowler et al, 2000[8]**).

To further investigate the causes for the female reproductive phenotype, progesterone and ß-estradiol levels were measured in non-mated females in all three backgrounds. In addition, fertilised eggs and ovaries from day-0.5 pc females were collected. No difference in hormone levels or embryo number was detected when compared to age-matched wildtype female mice. Also histology and weigh analyses of ovarian tissues failed to reveal any abnormality. However, histological analysis of uterine tissue from 10-week-old C57 and 6- to 9-month-old R1 females revealed abnormal luminal and glandular epithelium, fewer endometrial glands, increased leucocyte infiltration, haemorrhage and infection in the *Cenpb*-null mice. Close examination of the abnormal uterine epithelial layer revealed the presence of 'clear' apoptotic cells that were positive on TUNEL assay (**Fowler et al, 2000[8]**).

In situ hybridisation was used to determine the *Cenpb* mRNA expression pattern in normal uterus. A specific *Cenpb*-antisense probe detected high levels of *Cenpb* expression in the epithelial lining of the uterine lumen and endometrial glands of normal mice. Collectively these results suggested that Cenpb protein may have an important functional role in maintaining the epithelial layer of the uterus and subsequent reproductive performance (**Fowler et al, 2000[8]**).

2.4.3 *Cenpc*

To study the biological role of Cenpc protein, mice bearing a disrupted *Cenpc* allele were generated and intermated. PCR analysis of 276 progeny identified 85 wildtype, 191 heterozygotes and no liveborn nullizygous pups. Male and female heterozygotes were normal-sized, healthy and fertile. To determine the stage of embryonic lethality 30 embryos were dissected for genotyping from heterozygous crosses at 13.5-, 10.5- and 8.5-day post conceptus. No *Cenpc*-null postimplantation embryos were identified prompting the investigation of day-3.5 embryos. Morphological and PCR analysis of 50 embryos revealed 17 wildtype, 18 heterozygous and 10 null embryos. 80% of these *Cenpc*-disrupted embryos were significantly delayed in development when compared to the heterozygous and wildtype embryos. Instead of being at the blastocyst stage the majority of the null embryos were classified as morula, degenerating morula and less than 16-cell stage of development (**Kalitsis et al, 1998a**[2]).

To further examine the morphology and mitotic index of the aberrant embryos, 155 day-3.5 embryos from heterozygous crosses as well as 64 day-3.5 control embryos from wildtype intermatings or wildtype x heterozygous matings were analysed using phase contrast microscopy followed by Giemsa staining. Overall 75% of the unstained embryos in the 3.5-day control group reached the blastocyst stage as compared to 56.8% of the heterozygous-cross cohort. Examination of the Giemsa-stained embryos revealed 25.2% to have irregular-sized interphase nuclei, scattered and highly condensed chromosomes as well as an abundance of micronuclei whereas none of the control embryos showed any micronuclei formation. The mitotic indices measured an average of 6.9% for the morphologically abnormal embryos 3.6% for the normal embryos indicating that mitotic arrest had taken place (**Kalitsis et al, 1998a**[2]).

To explore whether day-2.5 preimplantation embryos displayed a similar or milder phenotype at an earlier age, 52 embryos from heterozygous matings and 32 wildtype embryos were morphologically assessed, incubated in colcemid and Giemsa-stained to examine chromosomes for aneuploidy. The results indicated that there was no difference in embryonic development or chromosome number. Furthermore no

micronuclei were observed suggesting that day-2.5 *Cenpc*-deficient embryos underwent normal mitosis for the first 3 division cycles before the maternal pool of Cenpc was depleted (**Kalitsis et al, 1998a**[2]).

As shown with the *Cenpb*-disrupted mice and in other unrelated mutant mouse strains, the phenotypic characteristics of mice can be modified by backcrossing mice onto different genetic backgrounds (Moser et al, 1992; Banbury, 1997; **Fowler et al, 2000**[8]). Indeed an earlier study has shown that the embryonic lethality observed in *Egfr* nullizygous mutants could be rescued by crossing onto CD-1 or MF1 Swiss backgrounds (Sibilia and Wagner, 1995; Threadgill et al, 1995). However the subsequent breeding of the *Cenpc*-null allele on C57BL/6 and FVB Swiss congenic mouse backgrounds failed to rescue the phenotype as the early lethality of *Cenpc*-deficient embryos persisted (Fowler and Kalitsis, unpublished observations).

As a group these observations suggested that progression of *Cenpc*-null embryos through mitosis was severely impeded at day-3.5 *in utero* with most chromosomes failing to align onto the metaphase plate. Despite this, some chromosomes were still able to undergo post-metaphase steps and form micronuclei structures (**Kalitsis et al, 1998a**[2]). Overall the *Cenpc* knockout mouse model provides *in vivo* evidence that Cenpc is a functionally essential protein for correct segregation during mitotic cell division.

2.4.4 *Incenp*

The function of Incenp was studied *in vivo* and *in vitro* via the generation of a knockout *Incenp* mouse model. Mice heterozygous for the targeted *Incenp* mutation were phenotypically indistinguishable from their wildtype littermates. The intercrossing of heterozygotes resulted in 102 progeny of which 73 were heterozygotes and 29 were wildtype. This suggested that the null offspring were embryonic lethal which was further supported by the smaller litter size (7.5 ± 1.0) for heterozygous intercrosses compared to 9.6 ± 2.4 for wildtype crosses (**Cutts et al, 1999**[6]).

To define the point of lethality, 23 day-8.5 postimplantation embryos were harvested from heterozygous matings, 16 were heterozygotes and 7 were wildtype. A further 35 preimplantation day-3.5 pc embryos were flushed from uteri and individually cultured for 6 days. Of these, 31 embryos hatched from their zona pellucida, attached and formed characteristic trophectoderm and ICM layers. Genotyping of these revealed 23 heterozygotes and 8 wildtype embryos. Three of the remaining 4 embryos were unable to hatch from their zona and showed signs of degeneration whereas the last embryo eventually attached but did not progress in its development. These 4 putative null embryos represented 11% of the total embryos and lead to the experiment being repeated by harvesting and culturing 21 embryos flushed from the oviducts and uteri of 3.5-day pc mice. Of these, 24% (5 of 21) were nullizygous, suggesting that affected embryos may have an increased stay in the oviduct. At the same time 44 control embryos developed healthy ICM and trophectoderm layers *in vitro* (**Cutts et al, 1999**[6]).

The phenotype of 39 day-3.5 embryos from heterozygous crosses was correlated with genotype by photographing the embryos examined with phase contrast microscopy prior to PCR analysis. Of these, 8 (21%) were null and contained large abnormal cells without any distinct blastocoel cavity, ICM or trophectoderm layers when compared to the 22 (56%) heterozygous and 9 (23%) wildtype embryos. Further analysis of Giemsa-stained day-3.5 embryos revealed the *Incenp*-disrupted embryos to have approximately 7 large nuclei as compared to normal blastocysts, which contained an average of 40-50 uniform nuclei. These embryos displayed a significantly increased mitotic index of 20% compared to 3.9% for the unaffected embryos indicating a severe delay or arrest in mitosis (**Cutts et al, 1999**[6]).

The nuclear morphology of day-3.5 affected embryos displayed a plethora of defects including micronuclei and giant nuclei with an increased number of nucleoli and chromosomes. The mitotic chromosomes of the null embryos were condensed, scattered and did not represent any specific stage of mitosis. To investigate earlier events related to this phenotype day-2.5 embryos were harvested from heterozygous crosses and analysed. Similarly the day-2.5 null embryos displayed nuclei of varying sizes ranging from micro- to macronuclei (up to 10x normal size) with an increased number of nucleoli and chromosomes. One unusual feature of these nuclei was the

presence of internuclear bridges and binucleation indicating a problem with nuclear reformation.

The integrity of the mitotic spindle of day-2.5 and -3.5 *Incenp*-disrupted embryos was examined by anti-tubulin antibody staining. This antibody was selected to evaluate the mitotic spindle because microtubules are formed from molecules of α- and β-tubulin heterodimers (Alberts et al, 1994e). Anti-tubulin staining revealed a complete absence of midbodies that normally form during telophase/cytokinesis. Moreover severely affected embryos exhibited aberrant bundling of microtubule spindle fibres into gigantic spindle 'cords' as demonstrated by anti-tubulin antibody staining (front cover, **Cutts et al, 1999**[6]). The findings of this study suggest that Incenp has a vital role in mitosis, at the level of microtubule function and/or cytokinesis.

2.4.5 *Api4*

To study the requirement for survivin during the mammalian cell cycle and development, *Api4*-targeted mice were generated. Heterozygous breeding pairs were healthy and fertile but failed to generate live born survivin-null offspring (**Uren et al, 2000**[12]). Dissection of day-6.5 and day-8.5 implantation sites from heterozygous crosses revealed an absence of nullizygous embryos suggesting that the deletion of mouse survivin gene caused embryonic lethality.

Further analyses using phase contrast microscopy and PCR of 96 explanted day-2.5 and -3.5 embryos revealed 23 phenotypically abnormal null embryos and 73 normal wildtype or heterozygous embryos after 3-4 days culture. By day-5.5 and -6.5 all of the *survivin*-disrupted embryos had failed to hatch their zona pellucida and implant *in vitro* in contrast with the remaining embryos which had hatched and formed healthy ICM and trophectoderm layers. Some degeneration was apparent in the depleted embryos at day-2.5 however a small number of embryos were no different from wildtype or heterozygous progeny up until day-4.5. By day-5.5 to -6.5 all null embryos were grossly abnormal with an absence of distinct ICM, blastocoel cavity or trophoblasts. Notably these embryos contained giant cells reminiscent of the

phenotype observed in the *Incenp*-disrupted embryos (**Cutts et al, 1999[6]; Uren et al, 2000[12]**).

To further examine the phenotypic features of these embryos a series of day-2.5 embryos were cultured for 1-3 days and stained daily with DAPI or Giemsa as well as with anti-tubulin immunofluorescence for nuclear and microtubule morphologies, respectively. Signs of early mitotic deterioration included micronuclei formation, nuclear sizes and appearance, and multinucleation. As the embryos progressed, cells failed to complete mitosis and the decreasing pool of normal cells were replaced with an average of 13 giant cells with bizarre nuclei, bridging and blebbing compared to >200 nuclei in the control embryos at day-5.5. Like *Incenp*-null embryos, tubulin staining demonstrated a lack of normal mitotic spindle structures, intercellular midbodies and bundling of microtubules indicating a defect affecting microtubule dynamics and/or cytokinesis (**Uren et al, 2000[12]**).

These results, when taken with other findings described in this study such as the failure of centromere proteins to colocalise with caspase-3 during the cell cycle (Dr Lee Wong, unpublished observations) and the centromeric association of survivin with INCENP along a novel para-polar axis during mitosis, suggest that survivin's expression pattern in cancer maybe due to the cell cycle role of survivin, rather than survivin contributing to tumorigenesis through inhibition of apoptosis (**Uren et al, 2000[12]**).

2.4.6 *Bub3*

Early studies in *S. cerevisiae* and *A. nidulans* that suggested BUB3 might be dispensable in mammalian cells were quickly refuted when healthy heterozygous mice bearing a targeted *Bub3* allele were intermated. No live nullizygous progeny were observed among the first 91 weanlings, instead a wildtype to heterozygous offspring ratio of 1:2 was noted. Backtracking through pregnancies revealed that the *Bub3*-null embryos were unable to survive the early postimplantation period. The timepoint of embryonic lethality was refined by placing 32 day-3.5 embryos from heterozygous crosses into culture, photographing them daily for 4 days followed by molecular analysis. PCR genotyping and photomicroscopy revealed that there were

25 phenotypically normal embryos (10 wildtype and 15 heterozygous) and 7 *Bub3*-disrupted embryos that had noticeably smaller ICMs on day-6.5. The following day, the ICM of day-7.5 *Bub3*-null embryos displayed significant degeneration while the trophectoderm which undergoes endoreduplication was normal-sized (**Kalitsis et al, 2000**[11]).

To further explore these observations day-3.5 to day-6.5 cultured embryos from heterozygous crosses were stained each day with DAPI. No apparent nuclear defects were observed in day-3.5 embryos however close examination of day-4.5 embryos revealed a significant increase in the number of micronuclei per affected embryo from 7.4 ± 4.2, as compared to 1.1 ± 1.3 micronuclei per normal embryo. At day-5.5, 12 out of 42 embryos displayed a 35% decrease in cell number from 200 ± 82 per non-affected embryo to 130 ± 32 cells in the embryos that contained micronuclei. These putative null embryos also had a significantly lower mitotic index of 3.2 ± 2.6% as compared to 7.0 ± 2.1% ($p < 0.001$) for the normal embryos, indicating a slowing down in mitosis. The next day, 10 out of 37 day-6.5 embryos were even more affected showing ICMs that were down to 50-100 cells compared to 300-500 cells in the non-affected embryos. These embryos contained a number of nuclear and chromosomal abnormalities that included macro- and micronuclei formation, nuclear bridging and lagging chromosomes that had failed to attach to microtubules (**Kalitsis et al, 2000**[11]).

The role of Bub3-mediated checkpoint activity was further assessed in *Bub3*-disrupted embryos by culturing embryos from wildtype and heterozygous crosses in the presence of the antimicrotubule chemical nocodazole at a level that deterred attachment of kinetochores with the mitotic spindle. Exposure to nocodazole induced a more pronounced phenotype in day-4.5 presumed null embryos. Six affected embryos out of 27 embryos from heterozygous parentage displayed an increase in the number of micronuclei from approximately 7.4 ± 4.2 per embryo in the untreated cohort to 17 ± 10 ($p = 0.039$) in the treated embryos. In comparison the number of micronuclei in normal progeny from heterozygous or wildtype crosses averaged approximately one micronucleus per embryo irrespective of treatment with nocodazole. Additionally the affected embryos showed no real difference in their mitotic index from 1.6 ± 1.3% for the untreated group to 3 ± 1.2% ($p = 0.071$) for the

nocodazole-treated embryos. On the other hand, the mitotic index for untreated normal embryos from heterozygous crosses dramatically increased approximately 9-fold from 2.1 ± 2.2% to 19 ± 6.6% indicating that normal embryos arrest when their kinetochore-spindle connection is disrupted. Whereas *Bub3*-deficient embryos were able to escape the checkpoint and proceed through the final stages of mitosis in a manner that resulted in aneuploidy and eventual cell death (**Kalitsis et al, 2000**[11]).

In conclusion, this study has found that Bub3 is an essential requirement for normal activation of the mitotic spindle checkpoint pathway in mammalian development. In the absence of Bub3, unchecked cell division results in rapid accumulation of mitotic errors and embryonic death.

2.5 Summary

This chapter describes a series of publications where gene targeting has been used to analyse the role of Cenpa, Cenpb, Cenpc, Incenp, Api4 and Bub3 centromere proteins. With the exception of Cenpb, the mouse knockouts resulted in early embryonic lethality. These studies demonstrated that Cenpa, Cenpc, Incenp, Api4 and Bub3 proteins are vital for mitosis during mouse development. Embryos bearing a disruption of both alleles displayed severe nuclear morphological degeneration, mitotic arrest and death. However, heterozygous mice were healthy, fertile, normal-sized and showed no sign of tumorigenesis or shortened lifespan when compared to wildtype littermates suggesting that inactivation of one allele does not produce a dominant-negative effect or haploinsufficiency. The timing of embryonic lethality varied over several days with the *Cenpc*-, *Incenp*-, and *Api4*-disrupted embryos failing to hatch and implant, whereas the *Cenpa*- and *Bub3*-deficient strains progressed further forming trophectoderm and ICM outgrowths before cessation of cell division. The observed window of viability for each mutant may have been a reflection of the essential nature of each protein however the *Cenpa*- and *Bub3*-null embryos may have survived longer due to a greater stability of residual maternal Cenpa or Bub3 mRNA and/or protein.

In contrast, *Cenpb*-null mice appear mitotically and meiotically normal despite displaying a mild reduction affecting body weight that is dependent on genetic

background. In addition *Cenpb*-deficient mice have smaller testis, epididymis and uteri with uterine function being severely compromised in 10-week-old females on a C57 background due to defective luminal epithelium. The finding that genetic background affects the phenotype of *Cenpb*-disrupted mice is important as two other groups have reported targeted-*Cenpb* mice with no obvious phenotype using different ES cell lines (Kapoor et al, 1998; Perez-Castro et al, 1998) and a third mouse strain for chimaera matings (Perez-Castro et al, 1998).

In summary the key findings of each of the individual targeted mouse mutant studies are:

- in the absence of Cenpa, centromere chromatin organisation is severely compromised;
- Cenpb is not necessary for mitosis or meiosis but nonetheless it has a key role in uterine morphogenesis that is subject to gene modifiers;
- Cenpc has a non-replaceable function at the metaphase stage during mitosis presumably due to its direct involvement in the maintenance of proper kinetochore structure and function;
- Incenp and Api4 have crucial roles in the regulation of microtubule dynamics and/or the final stages of mitosis such as cytokinesis;
- Bub3 is an essential component of the mitotic spindle checkpoint pathway that functions during mammalian cell division.

Furthermore, these mouse mutants provide a valuable resource for future centromere studies that are discussed in Chapter 4.

Chapter 3 - Genetic Mapping of Mouse Centromere Protein Genes

3.1 Background

The mapping of mouse genes on chromosomes provides a powerful means of progressing from genetic disease to the causative DNA sequence. In the reverse sense, mapping can generate new valuable clues for gene function by showing correlation of novel DNA sequences (clones) with phenotypic variation (Silver, 1995). Knowing where one gene or disease-causing locus maps in one species can be a great resource for identifying its location in another. The mapping of mouse genes has been a particularly useful strategy for identifying new human and animal disease loci (Epping and Nadeau, 1995; Bedell et al, 1997). It also allows the dissection of genetic versus environmental components of complex traits such as body-weight (Silver, 1995; Taylor, 2000) and the examination of genes which may be subject to parental imprinting, as was found in heterozygous mice bearing a disrupted *Igf2* gene (Dechiara et al, 1991).

3.1.1 Genetic Map

At present approximately 7,000 genes of the estimated 50 to 150,000 genes that make up the mammalian genome have been mapped in the mouse (Silver, 1995; Mouse Facts, 2000). The genetic map of the mouse is a composite map that includes linkage, chromosomal and physical mapping data with the linkage or recombination map generating much of the genetic mapping information. A locus is placed on the map whenever it is found to have linkage with a previously assigned gene or microsatellite marker. The genetic distance between loci is measured in centiMorgan(s) (cM) with one cM being equivalent to a recombination or crossover rate of 1%. Given that the mouse haploid genome has been estimated to contain approximately 3x 10^9 basepairs (bp) and to be 1575 cM in size, one cM equates to an average physical distance of two megabases (Mb; Taylor, 2000). Individual mouse chromosomes vary in size with the longest being chromosome 1 at 111.1 cM down to the shortest, the Y chromosome at 3.0 cM (Mouse Facts, 2000).

The chromosomal map is based on the karyotype of the mouse genome. The mouse has 20 pairs of acrocentric chromosomes including 19 pairs of autosomes as well as X and Y sex chromosomes. Crude chromosomal assignments can be made by the use of somatic cell hybrids that contain a specific mouse chromosome in a genetic

background from another species. More precise chromosomal mapping can be achieved by *in situ* hybridisation methods that demonstrate localisation of the gene of interest with a specific chromosomal band (Silver, 1995). However, this technique is not as accurate as linkage or physical mapping strategies.

The physical mapping of the mouse genome has begun in earnest with the private company Celera Genomics having sequenced about one-third of the 129/SvJ mouse strain (Abbott, 2000). At the same time the National Institutes of Health (NIH) has began to sequence the C57BL/6 mouse strain. Celera Genomics plan to have the full genome sequenced by the end of this year whereas NIH has a projected completion date of 2003 (Abbott, 2000; Golden and Lemonick, 2000). At present, the C57BL/6 map consists of overlapping DNA clones that cover specific chromosomal regions of 0.65% of the mouse genome (Mouse Genome Sequencing, 2000). As the physical map increases in density it has been claimed that the Mb will replace the cM as the reference unit for gene assignments and mapping distances on chromosomes (Silver, 1995).

3.1.2 Mapping genes by linkage analysis

Commercially available Recombinant Inbred strains (RI strains) and interspecific backcross panels (The Jackson Laboratory, Maine USA) with a good representation of previously assigned markers and gene loci provide a means of mapping genes by linkage analysis (reviewed by Silver, 1995; Taylor, 2000). Crossing two parental inbred strains then selecting pairs at random and brother-sister mating for 20 generations derives RI strains. Whereas interspecific backcross panels are generated by crossing an inbred *M. musculus* strain with one of the inbred *M. spretus* strains followed by backcrossing the first generation female progeny with one of the parental strains.

In both scenarios the genomes of the founder strains are randomly mixed and each genetic marker that is polymorphic between these strains has a characteristic blueprint known as the strain distribution pattern (SDP) for the RI strains or haplotype for the backcross panels. The founder genes that are closely linked tend to be inherited together and the closer this is, the more likely it is that their SDP or haplotype will be similar. The backcross panels have a clear advantage over the RI

strains because the evolutionary genetic distance between the founder strains is likely to facilitate finding a polymorphism. Furthermore the backcross panels have a considerably larger number of set members for calculating recombination frequencies and confidence limits (Green, 1981; Silver, 1985; Manly, 1993). Subsequently these panels eg BSS and BSB Panels (The Jackson Laboratory) have provided a detailed map of proven locus order to a maximum resolution of 0.5 to 1.0 cM (The Jackson Backcross map; Rowe et al, 1999).

Recently the recombination-based Jackson Backcross map has been cross-referenced to mapping data generated by the analysis of whole genome radiation hybrids (Rowe et al, 1999). The T31 radiation hybrid panel (RH panel; Research Genetics, Inc) consists of a random smattering of very small fragments of the 129/aa mouse genome in a A23 hamster background and has a map resolution of 0.2 to 0.5 cM (McCarthy et al, 1997). However the gathering and interpreting of RH data may be fraught with difficulty and therefore it may be necessary to verify gene assignments by repeating the RH panel analysis as well as mapping by other means (Rowe et al, 1999).

3.2 Chromosomal assignment of mouse centromere protein genes

Mindful that it is sometimes a redundant exercise to generate a mouse model using transgenesis because in some instances nature or earlier mutagenesis experiments have already provided these for us (Fowler et al, 1993; Mann et al, 1993; Fowler et al, 1995; Bedell et al, 1997), the genetic mapping of *Cenpa*, *Cenph*, *Cenpe*, *Cenpf*, *Incenp* and *Bub3* genes to specific subregions of mouse chromosomes was determined (**Fowler et al, 1997**[1]; **Fowler et al, 1998a**[4]; **Fowler et al, 1998b**[5]; **Fowler et al, 1999**[7]; **Lo et al, 2000**[10]). This exercise has explored the possibility that formerly described aberrant mouse strains may carry mutations in these genes. The other centromere protein genes of interest: *Cenpb*, *Cenpc* and *Api4* genes have been previously mapped in the mouse (Carlson et al, 1993; McKay et al, 1994; Li and Altieri, 1999) and there appeared to be no pre-existing mouse mutants for these genes.

3.2.1 *Cenpa*

The chromosomal assignment of the mouse *Cenpa* gene has been determined by two independent means (**Fowler et al, 1997**[1]). In the first instance an informative restriction fragment length polymorphism (RFLP) was identified around the *Cenpa* gene of the AKR/J (AK) and C57L/J (L) progenitor RI mouse strains using a specific *Cenpa* cDNA probe. This polymorphism was used to genotype DNA from the AKXL set of RI strains. The resulting SDP demonstrated that *Cenpa* localises to the proximal region of mouse chromosome 5 near *Adra2c, D5H4S43E* and *Qdpr* markers. This result was unexpected as the Genome Database (GDB) had previously reported human *CENPA* to localise to chromosome 2p24-p21 and there was no prior known area of homology with proximal mouse chromosome 5 and human chromosome 2.

Further experiments were performed to independently confirm the mapping of *Cenpa* to mouse chromosome 5 using a *M.spretus*-based backcross panel as well as *CENPA* to human chromosome 2 using somatic cell hybrids. The *M. spretus*-based linkage analysis refined the position of *Cenpa* to the proximal region of chromosome 5, between *Il6* and *Yes1* loci near [*Adra2c-D5H4S43E-Hdh*] markers. Interestingly the *Il6* mouse locus (17 cM region; MGD) marks the end of a region of homology with human chromosome 7, whereas the [*Adra2c-D5H4S43E-Hdh*] loci (20 cM region; MGD) signal the beginning of a larger stretch of homology with chromosome 4p. In between these two regions there are two small subregions of homology between proximal mouse chromosome 5 and human chromosomes 18 encompassing *Yes1* and *Tyms* loci, and 2p24-p21 where *Fosl2* and *Cenpa* loci reside (**Fowler et al, 1997**[1]).

3.2.2 *Cenph*

The mouse *Cenph* locus has been localised to chromosome 13D1 by fluorescence *in situ* hybridisation (FISH) using a BAC-derived genomic probe specific to the 5′ end of the *Cenph* gene on normal mouse metaphase chromosomes. The identity of chromosome 13 was verified by colocalisation with a commercially available chromosome 13 probe (**Lo et al, 2000**[10]).

Additionally, the chromosomal positioning of *Cenph* was confirmed and refined by linkage analysis of The Jackson BSS and BSB Panels using a polymorphic microsatellite marker $(CA)_n$ in the intronic region of the 3′ end of the *Cenph* gene of the progenitor strains. No recombinants in a total of 188 informants were observed with the microtubule-associated protein 5 gene (*Mtap-5*; 0.0-1.6 cM, 95% limits; Dr Mary Barter, personal communication) and many microsatellite markers on distal region of chromosome 13 in both panels (**Lo et al, 2000**[10]). The assignment of *Cenph* on mouse chromosome 13 (51.0 region, MGD) is consistent with the presence of a BAC containing the human homolog (*CENPH*) on chromosome 5q (Dr Paul Kalitsis, personal communication). This well-established region of mouse-human homology encompasses approximately 50 genes spanning the mid- to distal region on mouse chromosome 13 and human chromosome 5q (MGD).

3.2.3 *Cenpe*

The genetic mapping of the mouse *Cenpe* gene was carried out with a specific hypothesis in mind. Previously, the human *CENPE* gene has been assigned to chromosome region 4q24-q25 (Testa et al, 1994) in a region of homology with mouse chromosome 8 (42 cM region; MGD). This area encodes the mouse *Os* mutant that displays embryonic lethality due to a mitotic arrest defect phenotype (Magnuson and Epstein, 1984). Besides *CENPE*, 15 other genes on human chromosome 4q23-q35 have been shown to share homology with mouse chromosome 8 (MGD). This initially suggested the possibility that the *Os* mouse mutant could be a candidate for carrying a mutated *Cenpe* gene (**Fowler et al, 1998a**[4]). However the localisation of *Cenpe* near the centromere region on chromosome 6 by linkage analysis of the AXB set of RI strains and The Jackson BSS Panel has excluded the possibility that the *Os* locus may encode a *Cenpe* mutation.

The mapping position of *Cenpe* was somewhat unexpected, given that there has been only one other prior report of homology between mouse chromosome 6 and human chromosome 4. The human homolog of the *Drosophila* atonal homolog 1 gene (*ATOH1*) has been assigned to 4q22 (Ben-Arie et al, 1996) whereas mouse *Atoh1* gene was mapped to the 30.5 cM region on chromosome 6. The *Atoh1* gene is separated from *Cenpe* (0.1 cM region, MGD) by a large segment of approximately

30 cM on chromosome 6 that has extensive homology to human chromosome 7, encompassing more than 40 genes (MGD). This segment includes six genes (*Cappa2*, *Dlx6*, *Ggc*, *Met*, *Ptn*, *Tcrb*) that have linkage to *Cenpe* as well as a smaller region that has homology with human chromosome 2. The results of the present analysis have therefore established a new region of homology on mouse proximal chromosome 6 and the human 4q24-q25 region (**Fowler et al, 1998a**[4]).

3.2.4 *Cenpf*

The mouse *Cenpf* gene was mapped by identifying a polymorphism around the *Cenpf* locus and using it to genotype DNA from The Jackson BSS Panel (**Fowler et al, 1998b**[5]). The resulting haplotype indicated linkage to a large bin of genes and markers on the distal region of mouse chromosome 1. This assignment conformed with the expected mouse-human mapping region, since human *CENPF* has been localised to human chromosome 1q32-1q41 (Testa et al, 1994). Beside *CENPF* there are in excess of 50 genes that have homology with human 1q and the distal region of mouse chromosome 1 including *Apoa2* gene (92.6 region, MGD) that was shown to have linkage with *Cenpf* (**Fowler et al, 1998b**[5]).

3.2.5 *Incenp*

The mouse *Incenp* gene was assigned to the proximal region of mouse chromosome 19 by two different methods of linkage analysis (**Fowler et al, 1998a**[4]). In the first instance *Incenp* was mapped using the AKXL set of RI strains. No recombinants were observed between *Incenp*, *Fosl1*, *D19Mit59*, *Ltbpp2*, *Cd98*, *or Xmmv42* (0.0-6.9 cM, 95% limits). To further refine the chromosomal location of *Incenp*, the locus was also mapped by analysis of The Jackson BSS Panel. The observed haplotype indicated linkage to *Chk*, *D19Mit32*, *D10Mit93*, and *Nofl* markers (0.0-3.8 cM, 95% limits). This linkage was consistent with the RI strain data and extended the data by placing *Incenp* closer markers assigned to the centromere region of chromosome 19 (3 cM region, MGD) in a popular region of homology with human chromosome 11q11-q13. This suggested that human *INCENP*, whose present chromosomal location remains unknown, may be in that particular region on chromosome 11 (**Fowler et al, 1998a**[4]).

3.2.6 *Bub3*

The chromosomal position of the mouse mitotic spindle checkpoint gene *Bub3* was mapped by analysis of The Jackson BSS Panel (**Fowler et al, 1999**[7]). The observed haplotype indicated linkage to several genes and markers on the distal region of mouse chromosome 7, including the *Cyp2e1* gene (68.4 cM region, MGD). The mapping of *Bub3* to this region conformed with the expected mouse-human region of homology, since *BUB3* has been mapped to human chromosome 10q24 (Seeley et al, 1999), 10q24-q26 by radiation hybrid mapping (Cahill et al, 1999) and to 10q26 by *in situ* hybridisation (Kwon et al, 2000). Beside *Bub3*, there are ten genes that have homology with human chromosome 10q24-q26 and the distal region of mouse chromosome 7 including *Cyp2e1* (**Fowler et al, 1999**[7]).

3.3 Summary

The genetic mapping of *Cenpa*, *Cenph*, *Cenpe*, *Cenpf*, *Incenp* and *Bub3* loci to mouse chromosomes 5, 13, 6, 1, 19 and 7 respectively, did not highlight any existing morphological mouse mutants. However the mapping of *Cenpa* and *Cenpe* to mouse chromosomes 5 and 6 respectively, has extended or identified novel regions of mouse-human homology. These findings were quite unexpected given the extensive amount of mapping data that exists for the mouse and human genomes (MGD; GDB). Since completing the mapping of *Cenpa*, the relevant mouse-human region of homology has been extended to encompass many more loci (MGD) whereas the mapping of *Cenpe* has stimulated a collaborative study. This collaboration and the impact of these genetic mapping studies are discussed further in Chapter 4.1 - Impact of Centromere Studies.

Chapter 4 – Impact and Implications of Centromere Studies

4.1 Impact of centromere protein studies

When assessing the impact of the publications presented in this thesis in advancing the field of study, it is important to take into consideration the quality of the journal, the time elapsed since publication and the outcome of concurrent and subsequent studies by our laboratory and other groups.

4.1.1 Impact factor of journals

The quality of the international, peer-reviewed journal in which the papers were published can be assessed by the impact factor rating of the journal (Online Journals and Impact Factors, 2000). The papers describing the *Cenpa*, *Cenpb*, *Cenpc*, *Incenp*, *Bub3* and *Api4* gene knockout studies (**Kalitsis et al, 1998a**[2]; **Hudson et al, 1998**[3]; **Cutts et al, 1999**[6]; **Fowler et al, 2000**[8]; **Howman et al, 2000**[9]; **Kalitsis et al, 2000**[11]; **Uren et al, 2000**[12]) were published in the following: Proceedings of the National Academy of Sciences USA, Journal of Cell Biology, Human Molecular Genetics, Genome Research, Genes and Development and Current Biology which have impact factors of: 9.82, 12.79, 9.31, 7.71, 19.07 and 7.86 respectively (Online Journals and Impact Factors, 2000). Two of these publications were featured as first articles in Journal of Cell Biology (**Hudson et al, 1998**[3]) and Human Molecular Genetics (**Cutts et al, 1999**[6]). The latter was also featured on the front cover of Human Molecular Genetics as was the recent follow-up *Cenpb* knockout mouse study (**Fowler et al, 2000**[8]) in Genome Research. The above cited journals all fall within the top 90 of the 1123 bioscience-related journals listed in PubMed (Online Journals and Impact Factors, 2000; PubMed, 2000) reflecting a clear acknowledgment of the significance of these studies by our peer group.

The brief reports describing the chromosomal assignment of human *CENPA* and mouse *Cenpa*, *Cenph*, *Cenpe*, *Cenpf*, *Incenp* and *Bub3* genes (**Fowler et al, 1997**[1]; **Fowler et al, 1998a**[4]; **Fowler et al, 1998b**[5]; **Fowler et al, 1999**[7]; **Lo et al, 2000**[10]) were published in the Animal Cytogenetics and Comparative Mapping section in Cytogenetics and Cell Genetics. Despite being a specialist journal for publishing the

chromosomal localisation of genes this periodical is ranked in the top 200 bioscience journals and has an impact factor of 1.88 (Online Journals and Impact Factors, 2000).

4.1.2 Time elapsed since publication

Another factor for consideration is whether scientific community has been able to build further on the published studies. With this particular point one needs to keep in mind whether enough time has elapsed since publication for the work to mature. This is quite important when assessing the impact of these publications as these studies are contemporary with the first paper being published in December 1997 (**Fowler et al, 1997**[1]) and the most recent being accepted in September 2000 (**Uren et al, 2000**[12]). Nonetheless these publications are already well cited in the literature by other workers.

4.1.3 Concurrent and subsequent publications

The significance of these studies was mirrored in the number of competitive studies being done by independent major international groups. In every instance the submitted publications were the first to describe a knockout mouse model for the protein studied. Besides being competitive, these publications were also complementary in the centromere protein gene field. For example: prior to commencing the targeted mutation of the mouse *Cenpa* gene there were limited functional studies available for CENP-A. Previously, gene disruption experiments had been described for the *CSE4* gene, a *S. cerevisiae* homolog of *CENPA* (Stoler et al, 1995). However during the course of our analysis an important study was published describing anti-CENP-A antibody microinjection experiments in human HeLa cells (Figueroa et al, 1998). Furthermore less than a week after the manuscript describing the *Cenpa*-null mice (**Howman et al, 2000**[9]) was submitted, a publication appeared in Nature describing comparable phenotypic effects by disrupting a *CENPA* homolog in *C. elegans* using RNA-mediated interference experiments (Buchwitz et al, 1999). Similarly, a few days after the *Bub3* knockout mouse paper (**Kalitsis et al, 2000**[11]) was sent claiming to be the first mammalian spindle checkpoint gene to be disrupted, a publication appeared in Cell describing an analogous phenotype in *Mad2*-deficient mice for a different spindle checkpoint protein (Dobles et al, 2000).

Likewise, while the manuscript describing the *Cenpc* knockout mice (**Kalitsis et al, 1998a**[2]) was under review another *CENPC* knockout mutation was reported in cultured DT-40 chicken cells as having matching phenotypic effects *in vitro* (Fukagawa and Brown, 1997).

With regard to the first publication describing the *Cenpb* knockout mouse (**Hudson et al, 1998**[3]) two other groups have subsequently described in lesser detail the phenotypic effects in independently derived *Cenpb* knockout mice (Kapoor et al, 1998; Perez-Castro et al, 1998). Neither group has reported any abnormality in their mice whereas I have built further on my initial observations (**Hudson et al, 1998**[3]) which has resulted in another publication (**Fowler et al, 2000**[8]).

The recent publication describing the generation and phenotypic characterisation of the *Incenp* knockout mice (**Cutts et al, 1999**[6]) drew the attention of Dr David Vaux, WEHI. Subsequently a collaboration was embarked upon characterising the mice bearing a null mutation in the survivin or *Api4* centromere protein gene (**Uren et al, 2000**[12]). At present the structure and function of survivin continue to be extensively studied by many international groups. Just prior to the survivin studies being accepted for publication the crystal structure for survivin was determined by several laboratories (Chantalat et al, 2000; Muchmore et al, 2000; Shi, 2000; Verdecia et al, 2000). Moreover gene interference studies with survivin and Aurora-like kinase homologs in *C. elegans* were published last month that revealed similar defects in cytokinesis (Speliotes et al, 2000). At the same time, others have shown in *Xenopus* that INCENP and Aurora-related kinase bind one another *in vitro* and that INCENP was required to correctly target this kinase to the centromere and central spindle in HeLa cells (Adams et al, 2000). These studies support the signal pathway model linking survivin, INCENP and Aurora 1 kinase described in section 4.2.4 (**Uren et al, 2000**[12]).

Like a number of the gene knockout publications, the publication describing an uncommon region of mouse-human homology around the *Cenpa* locus (**Fowler et al, 1997**[1]) coincided with another relevant publication. While the *Cenpa* manuscript was in preparation, the *Fosl2* gene was reported as mapping to a similar homologous

region (Poirier et al, 1997). Dr Poirier kindly forwarded details of his data which I subsequently incorporated in our paper (**Fowler et al, 1997**[1]). Furthermore while under review, two more loci, *Gckr* and *Khk* were shown to have analogous homology. At present the MGD reports 6 genes (including *Cenpa*) in this region of homology (MGD; July, 2000).

The mapping of *Cenpe* to the proximal region of chromosome 6 and the identification of a novel mouse-human region of homology (**Fowler et al, 1998a**[4]) has stimulated a collaboration with Dr Rosemary Elliott, Chair of International Mammalian Genome Society Mouse Chromosome 6 Subcommittee. Dr Elliott has used PCR analysis of the T31 RH panel with *Cenpe* primers to verify the chromosomal localisation of *Cenpe* close to the centromere on mouse chromosome 6 (0.1 cM region, MGD). Subsequently another group has identified 2 CENP-E homologs in *Drosophila* as well as 2 *Cenpe*-related loci on mouse chromosomes 3 and 6 suggesting that there may be 2 CENPE-like proteins in mammals (Yucel et al, 2000). Genetic sequencing of the mouse genome promises to confirm whether another homolog of *Cenpe* exists on chromosome 3 as well as revealing whether or not other expressed gene loci reside between *Cenpe* and the centromere on chromosome 6.

The assignment of the mouse *Cenpf* and *Bub3* loci in well-established regions of mouse-human homology (**Fowler et al, 1998b**[5]; **Fowler et al, 1999**[7]) has helped expand these regions. With respect to *Cenpf* and *CENPF* loci there were in excess of 50 genes that shared similar homology (MGD; April, 1998) whereas at present the MGD reports this region of homology as encompassing more than 90 genes (MGD; September, 2000). In the case of *Bub3* and *BUB3* the homologous region on mouse chromosome 7 and human chromosome 10 respectively, has been expanded from 10 to 12 genes (MGD; September, 2000).

4.2 Future studies with mouse mutants

The mouse mutants described in this study provide a valuable resource for future investigations such as immuno-electron and -confocal microscopy analyses to determine the effect of the absence of a particular centromere protein on kinetochore formation and structure (Martineau-Thuillier et al, 1998; Craig et al, 1999). Time lapse photography of dividing nuclei from *Cenpa-*, *Cenpc-*, *Incenp-*, *Api4-* and *Bub3-* defective embryos and *Cenpb*-null uterine epithelial cells also offers an elegant means for examining possible aberrant chromosomal movements during mitosis (Reider and Cole, 1998).

4.2.1 *Cenpa-*, *Cenpc-*, *Incenp-*, *Api4-* and *Bub3*-null mice

Apparent healthy heterozygous mice bearing one targeted allele continue to be studied for tumorigenesis and longevity. The most recently generated mice are the *Bub3* mutants (**Kalitsis et al, 2000**[11]). These mice are of particular interest given that some human intestine and lung tumours have been shown to encode mutations in *BUB1* and *MAD1* mitotic spindle checkpoint genes, respectively (Cahill et al, 1998; Nomoto et al, 1999). Moreover heterozygous *Mad2* mice were observed to have subtle differences in morbidity and a possible increase in tumour incidence when compared to age-matched wildtype offspring (Dobles et al, 2000). Tumour susceptibility in the *Cenp*-depleted mice could be explored further by exposing heterozygous mice to tumour-inducing agents (Sivak, 1982) or by backcrossing the mice onto genetically conducive backgrounds (Kozak, 1996).

The observed embryonic lethality in the *Cenpa-*, *Cenpc-*, *Incenp-*, *Api4-* and *Bub3-* null mice paves the way for examining the role of these proteins via conditional mutants that allow a gene product to be expressed in a tissue-specific or temporal manner. Systems such as Cre/LoxP permit a targeting construct flanked by LoxP sites to be inserted into mice via homologous recombination in ES cells. The transgene is then deleted in cells or tissues following the mating of LoxP mice with mice expressing Cre recombinase under the control of a specific promoter (Plagge, 2000). The challenge in this approach is to choose a tissue- or cell-specific promoter eg spleen- or testis-specific that would allow the centromere protein of interest to be

studied in a particular cell or tissue without necessarily causing death to the animal. An additional advantage with this design is that it allows removal of antibiotic selection cassettes that may cause sporadic effects on neighbouring genes as observed in other studies (Olson et al, 1996; Muller, 1999).

Another strategy for studying patterns of gene expression has been the use of targeting constructs that contain reporter genes such as *lacZ* β-galactosidase (*lacZ*) of *Escherichia coli* (bacteria; Gossler and Zachgo, 1993) or the green fluorescent protein (GFP) of *Aequorea victoria* (jellyfish; Kanda et al, 1998). The IRES cassettes used in the *Cenpa*, Cenpc and *Bub3* targeting constructs have a *lacZ*-neomycin or -hygromycin fusion gene (**Kalitsis et al, 1998a**[2]; **Howman et al, 2000**[9]; **Kalitsis et al, 2000**[11]) however initial analysis of the *Cenpc*-targeted cells detected the *lacZ* transcript as an uninformative cytoplasmic product rather than a precise nuclear signal (Dr Paul Kalitsis, unpublished observations). Previously, GFP has been successfully used to fluorescently tag specific chromosomal regions including histone protein H2B (Kanda et al, 1998). Subsequently ES cell lines with incorporated *Cenpa*-GFP have been generated in our laboratory (Redward, 1998). At present these cell lines are being used to generate mice that promise to allow visual analysis of *Cenpa*-GFP during mitosis, meiosis and trophectoderm formation via endoreduplication.

Interestingly, *Cenpa*-null trophectoderm cells deteriorated *in vitro* whereas *Bub3*-, like *Mad2*-deficient trophectoderm layers remained healthy despite the mitotically active ICMs dramatically diminishing in cell number by day-5.5 to-6.5 post conceptus (Dobles et al, 2000; **Howman et al, 2000**[9]; **Kalitsis et al, 2000**[11]). These observations support a role for *Cenpa* in S-phase and invite extra study by labeling *Cenpa*-null blastocyst outgrowths *in vitro* or implantation sites *in vivo* with the thymidine analogue, 5-bromo-2′-deoxyuridine (BUdR) which labels replicating DNA of newly formed sister chromatids during S-phase. Likewise the observed cell death in *Cenpa*-null and other knockout embryos warrants additional examination given that Giemsa staining of *Cenpa*-null embryos revealed nuclear blebbing indicative of apoptosis (**Howman et al, 2000**[9]). In addition, other studies have demonstrated an interaction of Cenpc with the apoptotic protein known as Hdaxx (Pluta et al, 1998) and programmed cell death has been observed in *Mad2*-deficient embryos (Dobles

et al, 2000) suggesting that *Cenpc*- and *Bub3*-null embryos also deserve further analysis using an assay for apoptosis such as TUNEL (Gavrieli et al, 1992).

4.2.2 *Cenpb*-null mice

Studies continue with the *Cenpb*-disrupted mice to determine whether *Cenpb* deficiency subtly affects some aspect of centromere function in a tissue-specific manner that results in a slower rate of progression through the cell cycle or whether Cenpb has another biological role that may be unrelated to centromere function *per se* (Kipling and Warburton, 1997). Clues to this maybe elucidated by studying the mechanism that leads to the degeneration of the uterine epithelium in *Cenpb*-null mice (**Fowler et al, 2000**[8]). *In vitro* separation of this layer from *Cenpb*-deficient and control mice using various enzymes (eg dispase, trypsin, pancreatin and collagenase) and cell culture conditions (Glasser and M^{c}Cormack, 1981; Glasser and Julian, 1986; Jacobs et al, 1990) has failed to yield enough metaphases for assessment. Likewise, examination of fresh single cell suspensions from dissected uterine epithelial tissue has generated inconsistent cell cycle profiles by FACS analysis or too few mitotic figures for karyotyping.

Instead of pursuing an *in vitro* analytical approach, studies have begun to examine the role of Cenpb by labeling uteri from ovariectomised, estrogen-stimulated, age-matched *Cenpb*-null and wildtype control mice with BUdR *in vivo* as described in other studies (Orimo et al, 1999). This procedure is designed to maximise the number of uterine epithelial cells undergoing mitosis (personal communication; Dr Robert Bigsby, Indiana University School of Medicine, USA). Besides providing a source of material for examining S-phase and mitotic indices, transverse sections of uteri can also be used to assess the fraction of cells in mitosis by immunostaining for phosphorylated-histone H3 or for other cell cycle stages using specific antibodies (Sher, 1996; Dobles et al, 2000; Liu et al, 2000; Takai et al, 2000).

The observed small testis and uteri of *Cenpb*-null mice is reminiscent of telomerse-deficient mice following intermating of telomerase-depleted mice for up to 6 generations (Lee et al, 1998). Generation 4 telomerase knockout mice were found to have significantly smaller litters whereas generation 6 intercrosses exhibited

infertility due to defective spermatogenesis and apoptosis as well as a decrease in oocytes following ovulation and a possible compromise in uterine structure and function. The worsening phenotype of the telomerase-null mice was linked to a reduction in telomere-length and chromosomal abnormalities (Lee et al, 1998). These observations together with a possible role for CENP-B in genome evolution (Kipling and Warburton, 1997) has stimulated a similar ongoing breeding program in my own study for *Cenpb*-null mice examining testis-, uterus-, ovary- and litter-size over a number of generations.

The variation in bodyweight and female reproductive performance of *Cenpb*-null mice on different genetic backgrounds can be explored further by linkage analysis of backcross breeding programs that are designed to identify candidate genetic modifiers or quantitative trait loci (QTL; Taylor, 2000). Such breeding programs in mice have provided the basis for identifying many modifier loci including a specific cystic fibrosis (CF) modifier locus for meconium ileus (severe intestinal obstruction in a subset of CF patients at birth) on mouse chromosome 7 (Rozmahel et al, 1996). Subsequently its human homolog has been discovered on human chromosome 19q13 (Zielenski
et al, 1999).

4.2.3 *Os* and *jerky* mice

The sequencing and genetic mapping of the centromere-associated genes to locations other than mouse chromosomes 8 and 15 has excluded *Cenpa*, *Cenph*, *Cenpe*, *Cenpf*, *Incenp* and *Bub3* as being responsible for the phenotypes observed in the *Os* and *jerky* mouse mutants (**Fowler et al, 1997**[1]; **Fowler et al, 1998a**[4]; **Fowler et al, 1998b**[5]; **Fowler et al, 1999**[7]; **Lo et al, 2000**[10]). However this does not discount the possibility of causative mutations existing in the dozen or more unsequenced and/or unmapped known centromere proteins including CENP-G or ZW10 (for review, see Saffery et al, 2000; MGD), or yet to be identified centromere proteins. At present one of the cytoplasmic dynein intermediate chain genes, known as *Dnclic2* has been assigned to the 50 cM region of chromosome 8 (MGD) making it a possible contender for the mitotic phenotype observed in the *Os* mouse mutant (Magnuson and Epstein, 1984). Previously, cytoplasmic dynein intermediate chains have been

shown to transiently bind kinetochores and have a role in mitotic spindle organisation (Pfarr et al, 1990; Steuer et al, 1990; Purohit et al, 1999).

4.2.4 Redundancy and signal pathway models

Two of the centromere protein knockout projects have led to proposed redundancy and signal pathway models for CENP-B and API4 proteins, respectively. With regard to CENP-B, Prof Andy Choo has hypothesised that a lower affinity protein designated CENP-Z can organise the large amount of repetitive centromeric DNA in the absence of CENP-B protein or CENP-B binding sites (**Hudson et al, 1998**[3]). This is supported by functional studies in *S. pombe* that demonstrate more than one CENP-B-related protein family member is required for proper chromosome segregation and growth (Baum and Clarke, 2000). At present, 2 proteins (pJα and CENP-G) that bind the centromeres of CENP-B-deficient Y chromosomes have been suggested as likely candidates for functional redundancy with CENP-B (**Hudson et al, 1998**[3]; Baum and Clarke, 2000) however the gene sequence and knockout status of these proteins are yet to be determined. Nevertheless, the *Cenpb*-null mice and cell lines generated in this study provide a resource for identifying and confirming the existence of these proposed or other unknown Cenpb-related proteins.

The observed phenotypic similarities between *Api4*- and *Incenp*-deficient mouse homologs has prompted Dr David Vaux to explore the likelihood of a possible common signaling pathway between these 2 proteins (**Uren et al, 2000**[12]). Besides the phenotypic knockout data, INCENP, API4 and the kinase known as Aurora1 share comparable cell cycle and centromere localisation patterns. Furthermore, studies in *S. cerevisiae* have linked Bir1p (API4 homolog), Ipl1p (Aurora1 homolog) with an 'INCENP-box' bearing protein known as Sli15, suggesting that a similar liaison may exist in other organisms (**Uren et al, 2000**[12]). The *Incenp*- and *Api4*-knockout models characterised in this study supply a helpful tool for addressing this hypothesis in mammals.

4.3 Implications of centromere studies

Understanding the molecular mechanism of how centromere proteins participate in the formation of centromeres as well as how they take part in the regulation of mitotic steps is critical for areas of research that aim to: 1) generate mammalian artificial chromosomes for gene therapy purposes; 2) comprehend the wide spectrum of aneuploid-related clinical conditions in human and veterinary medicine.

4.3.1 Mammalian artificial chromosomes

Mammalian artificial chromosomes or MACs, which approximate 2-5 Mb in size, are miniaturised versions of normal chromosomes. Originally, artificial chromosomes were constructed in yeasts and consisted of specific cloned DNA sequences that include telomeres, origin(s) of replication and a centromere (reviewed by Brown et al, 2000). In mammals there have been 2 major approaches employed to generate MACs with limited success. One way has been to assemble mini-chromosomes from the basic chromosome components *in vitro* whereas another has been to reduce the size of an existing chromosome by site-specific recombinases such as Cre/loxP and seeding with telomeric DNA. The Cre/loxP recombinase system has been also utilised to introduce large arrays of DNA into MACs for future delivery into host cells (reviewed by Willard, 1998; and Brown et al, 2000). Besides being an invaluable vector for transfer of therapeutic genes, MACs can be used for studying chromosome function and large-scale transgenesis (Choo, 1997b; Brown et al, 2000). Indeed, recent studies in mice have demonstrated the feasibility of introducing mini-chromosomes into the mouse germline via ES cells or microinjection into the pronuclei of fertilised eggs (Shen et al, 1999; Co et al, 2000).

One stumbling block to the efficient construction of mammalian artificial chromosomes has been defining, manipulating and activating the minimal centromeric DNA sequences that are required for centromere function. The recent cloning of novel DNA sequences from the human neocentromere known as mardel (10) offers an alternative centromeric DNA base for chromosome construction however further structure-function studies are required to elucidate the mechanism which activates centromere function (Choo, 1997b).

4.3.2 Clinical conditions

Like *Cenpa-*, *Cenpc-*, *Incenp-* and *Api4-* it is probable that *Bub3*-null mutations in humans would lead to early lethality and pregnancy wastage. As such, similar mutations in humans could be partly responsible for the high rate of implantation failure and spontaneous loss in early pregnancies due to aneuploidy (Wilcox, 1988; Qumsiyeh et al, 2000). FISH analysis or comparative genome hybridisation (CGH) in combination with flow cytometry on blastomere biopsies taken from preimplantation embryos obtained from women undergoing *in vitro* fertilisation (IVF) have detected numeric chromosomal abnormalities (Pellicer et al, 1998; Lomax et al; 2000). Furthermore, whole genome amplification in concert with CGH has demonstrated not only diagnosis of chromosomal aneuploidy in single cells and blastomeres (Voullaire et al, 1999b, 2000) but allows analysis of numerous specific gene loci (Wells et al, 1999). Together, these techniques offer a means for testing IVF embryos at risk for mutation in centromere protein genes or other genes that may be essential for embryonic survival.

Similarly, the *Cenpb* mouse studies may help shed light on the high rate of unsuccessful pregnancies in women (Wilcox et al, 1988; Qumsiyeh et al, 2000) as well as conditions like pyometra which is a considerable problem in veterinary medicine (Santschi et al, 1995; Lawler, 1998; Dhaliwal et al, 1998). At present, Prof Andy Choo's group (Andrew MacDonald and KJF) in collaboration with Helen Norse (Royal Women's Hospital) and Dr Kate Stern (Mercy Maternity Hospital) are currently undertaking a study to determine whether abnormal reproductive performance in certain women is associated with mutations in *CENPB*. Several methods for mutation screening including DNA sequencing (Barry et al, 1999), mutation-specific cleavage detection (Babon et al, 1999), immunophenotyping (**Hudson et al, 1998**[3]; **Fowler et al, 2000**[8]) and microarray (DNA-chip)-based hybridisation (reviewed by Hacia, 2000) are being explored. Given the power and efficiency of the chip technology (for reviews see: The Chipping Forecast, 1999) the microarray DNA templates have been expanded to include other candidate genes such as leukaemia inhibitory factor, interleukin 11 and estrogen receptor α. These genes have been chosen because knockout studies in mice have resulted in reduced uterus size and function (Stewart et al, 1992; Robb et al, 1998; Orimo et al, 1999).

The recent discovery that genes involved in mitosis (eg *CENPA*, *CENPE* and *CENPF*) and extracellular remodeling, are down-regulated in early passage fibroblasts from 90-year-old individuals when compared to young- and middle-age individuals using high-density oligonucleotide microarrays has emphasised the power of this technique (Cristofalo, 2000; Ly et al, 2000). Besides being used to study centromere protein gene expression profiles in aging and *CENPB*-mutation detection, microarrays can be diagnostic tools for examining centromere protein genes in relation to a broad variety of aneuploid-related conditions including cancer and embryonic lethality. Overall the studies presented in this thesis have identified vital roles for centromere protein genes in whole animals thus providing insight into the genetic basis of chromosomal pathologies that lead to reproductive failure in humans and animals.

PUBLICATION 1

K.J. FOWLER, A.J. NEWSON, A.C. MACDONALD,
P. KALITSIS, M.S. LYU, C.A. KOZAK AND K.H.A. CHOO
(1997)

CHROMOSOMAL LOCALIZATION OF MOUSE *CENPA* GENE.

CYTOGENETICS AND CELL GENETICS, 79: 298-301.

Cytogenet Cell Genet 79:298–301 (1997)

Cytogenetics and Cell Genetics

Chromosomal localization of mouse *Cenpa* gene

K.J. Fowler,[a] A.J. Newson,[a] A.C. MacDonald,[a] P. Kalitsis,[a] M.S. Lyu,[b] C.A. Kozak,[b] and K.H.A. Choo[a]

[a] The Murdoch Institute for Research into Birth Defects, Royal Children's Hospital, Parkville, Victoria (Australia), and [b] Laboratory of Molecular Microbiology, National Institute of Allergy and Infectious Diseases, National Institutes of Health, Bethesda, MD (USA)

Abstract. Using a previously isolated mouse centromere protein A *(Cenpa)* probe, we have localized the gene to the proximal region of mouse Chromosome 5, between the known *Il6* and *Yes1* loci near [*Adra2C-D5H4S43-Hdh*]. Comparison of this localization with that of human CENPA, which maps to chromosome 2, is consistent with the presence of a new region of conserved synteny between the two species.

The centromere is a highly differentiated structure of the mammalian chromosome that plays a key role in the proper segregation of replicated chromosomes during mitosis and meiosis. On metaphase chromosomes, an active centromere forms a primary constriction that is usually, but not always (e.g., Voullaire et al., 1993; du Sart et al., 1997), associated with heterochromatin and C-banding. The centromere binds three constitutive proteins (CENPA, CENPB, and CENPC) and a host of other proteins that are transiently present during specific stages of the mitotic cell division cycle (reviewed by Brinkley et al., 1992; Earnshaw and MacKay, 1994; Choo, 1997).

CENPA has been found to be associated with histone H4 and the other core histones in particles that co-purify with the nucleosome core (Palmer and Margolis, 1985; Palmer et al., 1987). Direct sequence analysis of cloned human and bovine CENPA cDNA demonstrated a high degree of homology with mammalian histone H3 and led to the suggestion that CENPA acts as a histone H3 homolog to replace one or both copies of histone H3 in centromeric nucleosomes (Sullivan et al., 1994). In addition, CENPA shares a significant homology with the yeast *(Saccharomyces cerevisiae)* protein Cse4p, another member of the histone H3-like class of proteins (Sullivan et al., 1994; Wilson et al., 1994; Stoler et al., 1995) that has been shown to be required for proper chromosome segregation (Stoler et al., 1995).

In a recent study, we have isolated and determined the full-length cDNA sequence and complete genomic structure of mouse *Cenpa* (Kalitsis et al., 1998). Here, we describe the use of a mouse *Cenpa* probe to localize this gene on the mouse linkage map. We compared this localization with the map position of human CENPA and confirm a new region of conserved synteny between the two species.

Materials and methods

Mouse genetic mapping

Genomic DNA from inbred mouse strains AKR/J and C57L/J and the AKXL recombinant inbred (RI) mouse sets were purchased from Mouse DNA Resource, The Jackson Laboratory, Bar Harbor, ME. Aliquots (10 or 20 μg) of genomic DNA were digested to completion with *Pvu*II (Boehringer Mannheim), resolved on 1% agarose gels, transferred in 0.4% NaOH onto Hybond N+ membrane filters (Amersham), and hybridized with a ^{32}P-labeled 5′ *Cenpa* cDNA fragment (nucleotide positions 1–274, GenBank accession No. AF012709). Posthybridization washes were carried out in 0.1% SDS, 1 × SSC at 65°C.

Data for mouse chromosome maps and all known strain distribution patterns (SDPs) of AKXL recombinant inbred mice were obtained from the Mouse Genome Database (MGD), Mouse Genome Informatics, The Jackson Laboratory (http://www.informatics.jax.org) and date from July 1997. Recombination frequencies *(r)* were calculated using the formula $r = R/(4 - 6R)$, where R is the proportion of discordant strains in the RI set (Green, 1981). The 95% confidence intervals (Table 1) for linkage analysis with RI mice are those tabulated by Silver (1985).

Cenpa was also mapped by analysis of the cross (NFS/N × *M. spretus*) × *M. spretus* or C58/J (Adamson et al., 1991). Progeny of this cross have been typed for about 800 markers, including the Chromosome 5 markers *En2* (engrailed-2), *Il6* (interleukin 6), *Yes1* (yes1 oncogene), *Hdh* (Huntington disease homolog), and *Msx1* (homeobox msh-like 1). *En2*, *Il6*, and *Msx1* were

Supported by the National Health and Medical Research Council of Australia. K.H.A.C. is a Principal Research Fellow of the Council.

Received 9 September 1997; revision accepted 20 December 1997.

Request reprints from K.J. Fowler, The Murdoch Institute for Research into Birth Defects, Royal Children's Hospital, Flemington Road, Parkville 3052 (Australia); telephone: 03-9345-5081; fax: 03-9348-1391; e-mail: fowlerk@cryptic.rch.unimelb.edu.au.

KARGER

E-mail karger@karger.ch
Fax + 41 61 306 12 34
http://www.karger.com

0301–0171/97/0794–0298$15.00/0

This article is also accessible online at:
http://BioMedNet.com/karger

typed as previously described (Wada et al., 1993; Yamanaka et al., 1994). *Yes1* was typed as an *Eco*RI polymorphism using as probe the 500-bp insert of pXEyes (Sukegawa et al., 1987), obtained from the American Type Culture Collection (Rockville, MD). *Hdh* was typed as an *Eco*RI polymorphism using as probe IT15, which was kindly provided by Dr. T. Vo (Wayne State University, Detroit, MI).

Human chromosome localization

Two primers, hcenpa-1 (5'-GCT GTT GTG AAG AAT GCC G-3') and hcenpa-2 (5'-GGC CAA TGA GAG TAT GCA CC-3'), were generated from the 5' sequence of the human CENPA gene (GenBank accession No. U82609 [Shelby et al., 1997]). PCR was performed with Ampli*Taq* DNA polymerase (Perkin Elmer) on a somatic cell hybrid panel containing the 22 human autosomes and two sex chromosomes in a Chinese hamster or mouse cell background (Coriell Cell Repositories, NIGMS Mapping Panel #2 DNA). Each 50-µl reaction contained 50 ng of hybrid genomic DNA, 250 ng of each primer, and 1.5 mM Mg^{++} buffer (Perkin Elmer). PCR began with a "hot start" at 95°C, followed by 35 cycles of denaturation at 95°C for 1 min, annealing at 60°C for 1 min, and extension at 72°C for 90 s. In the final cycle, the extension time was increased to 5 min at 72°C.

Data for the human chromosome maps were obtained from the Genome Database (GDB) and date from July 1997 (http://gdbwww.gdb.org).

Results

Mouse genetic mapping

Using a 5' fragment of the mouse *Cenpa* cDNA, an informative polymorphism was identified with *Pvu*II between the progenitor RI mouse strains. The enzyme revealed two bands at 5.2 kb and 1.3 kb in AKR/J, and two bands at 5.6 kb and 1.3 kb in C57L/J. This polymorphism was used to genotype DNA from the AKXL set of RI mouse strains. The resulting SDP is summarized in Table 1. Comparison of the SDP for *Cenpa* with those of other markers mapped using these strains indicated that *Cenpa* localizes to the proximal region of Chromosome 5. No recombinants (0.0–6.9 cM; 95% limits) were observed between *Cenpa* and *D5H4S43E*, *Adra2c*, or *Qdpr* (Table 1).

Southern blot analysis also identified *Bam*HI fragments of 5.9 kb in *M. spretus*, as well as 4.3 kb and 2.9 kb in C58/J and NFS/N. Inheritance of the variant fragment was typed in progeny DNA, and the observed pattern indicated linkage to markers on proximal Chromosome 5 (Fig. 1a). This linkage analysis

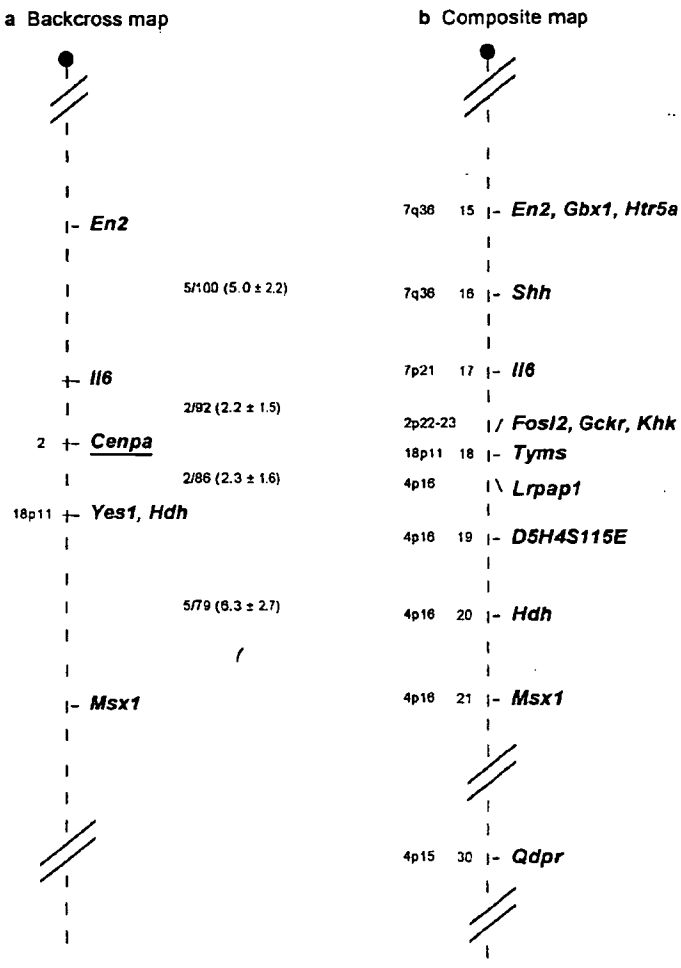

Fig. 1. (**a**) Genetic map location of *Cenpa* on mouse chromosome 5 by analysis of the cross (NFS × *M. spretus*) × *M. spretus* or C58/J. Recombination fractions for adjacent loci are shown to the right of the map, with the recombination distance (cM) (95% limits) given in brackets. No recombinants were found between *Yes1* and *Hdh* in 78 mice. The map locations of the human homologs for each of the mouse genes are indicated to the left of the map. (**b**) An abbreviated composite map of the proximal mouse Chromosome 5 loci (15–30 cM region; Kozak and Stephenson, 1997), highlighting the four regions of conserved synteny between proximal Chromosome 5 and human chromosomes 2, 4, 7, and 18. The localization of *Gckr* and *Khk* is based on Wightman et al. (1997).

Table 1. Strain distribution patterns for the AKXL set of RI mouse strains for *Cenpa*

	AKXL strain distribution patterns																		Percent recombination (cM) (95% limits) with *Cenpa*
	5	6	7	8	9	12	13	14	16	17	19	21	24	25	28	29	37	38	
Mpmv13 (modified polytrophic murine leukemia virus 13)	L	L	L	L	A	L	A	A	L	A	L	A	A	L	A	L	L	A	8.3 (1.8–41.7)
Adra2c (adrenergic receptor alpha 2c)	A	L	A	L	L	L		L	L	A	L	A	A	L	A	L	L	A	0.0 (0.0–6.9)
D5H4S43 (DNA segment)	A	L	A	L	L	L	A	L	L	A	L	A	A	L	A	L	L	A	0.0 (0.0–6.4)
Cenpa	A	L	A	L	L	L	A	L	L	A	L	A	A	L	A	L	L	A	
Qdpr (quinoid dihydropteridine reductase)	A	L	A	L	L	L	A	L	L	A	L	A	A	L	A	L	L	A	0.0 (0.0–6.4)
D5Btr3 (DNA segment)	A	L	A	L	L	L	A	A	L	A	L	A	A	A	L	L	L	A	5.6 (1–27.3)
Mpmv7 (modified polytrophic murine leukemia virus 7)	A	L	A	L	L	L	A	A	L	A	L	A	A	A	L	L	L	A	5.6 (1–27.3)

thus positioned *Cenpa* between *Il6* and *Yes1* and is therefore consistent with the RI strain data. The human homologs of *Il6* and *Yes1* have been mapped to 7p21→p15 (Ferguson-Smith et al., 1988) and 18p11.3 (Silverman et al., 1993), respectively, suggesting that the human CENPA gene could map to either of these chromosomes.

Human chromosome localization

A database search for the chromosomal localization of human CENPA has identified an entry on chromosome 2p24→p21 between the markers D2S174 and D2S390 (GDB; Whitehead Transcript Map WI-7987). Since our mapping data has placed mouse *Cenpa* in a region that was not previously known to be homologous with this human CENPA entry, we decided to confirm the human gene localization independently. This was achieved by PCR analysis of a somatic cell hybrid panel using a human CENPA-specific set of primers. The results indicated that only the hybrid cell line containing human chromosome 2 gave the expected PCR product (data not shown), thus confirming the localization of CENPA on human chromosome 2.

Discussion

Genetic mapping of mouse *Cenpa* to Chromosome 5, between the *Il6* and *Yes1* loci and near [*Adra2c-D5H4S43-Hdh*], and the assignment of human CENPA to chromosome 2 has confirmed the existence of a small region of mouse-human conserved synteny. The mouse *Il6* locus (17 cM; MGD) marks the end of a region of homology with human chromosome 7, whereas the [*Adra2c-D5H4S43-Hdh*] loci (20 cM; MGD) signal the beginning of a relatively large stretch of homology with human chromosome 4p (Kozak and Stephenson, 1997; Searle and Selley, 1997), which, as recently demonstrated by Poirier et al. (1997), is disrupted by the *Fosl2* (Fos-like antigen 2) locus at Chromosome 5 (18 cM; MGD). Furthermore, within the *Il6* and [*Adra2c-D5H4S43-Hdh*] segment of Chromosome 5, *Yes1* and *Tyms* (thymidylate synthase) constitute a small region of homology with human chromosome 18p11.3 (Silverman et al., 1993; Fig. 1b).

In addition to *Cenpa* and *Fosl2*, the earlier finding of another human chromosome 2 homolog, *Mpv17* (nephrotic syndrome associated with retroviral insertion), on Chromosome 5 (Karasawa et al., 1993) is of interest. However, because this assignment was based on an analysis of somatic cell hybrids, specific localization of this homology region on the mouse linkage map could not be established. Given that MPV17 has been localized to human chromosome 2p23→p21 (Karasawa et al., 1993), FOSL2 to 2p23→2p22 (MGD), and CENPA to 2p24→p21 (GDB), our data thus confirmed this region of homology on proximal mouse Chromosome 5 and also predicted a more refined location for *Mpv17* on Chromosome 5.

In a previous study, another human centromere protein, CENPC, was localized to 4q12→q13.3, while its mouse homolog *(Cenpc)* was mapped to Chromosome 5E2-E5 (McKay et al, 1994). Thus, whereas mouse *Cenpa* and *Cenpc* demonstrated co-localization on Chromosome 5, albeit some distance apart, this linkage was absent in humans. At present, the significance, if any, of the chromosomal linkage of two constitutively expressed but structurally unrelated centromere proteins on mouse Chromosome 5 is not known.

Acknowledgements

We thank Vivien Bonazzi, Richard Saffery, and David Shaw for assistance with informatics.

References

Adamson MC, Silver J, Kozak CA: The mouse homolog of the gibbon ape leukaemia virus receptor: genetic mapping and a possible receptor function in rodents. Virology 183:778–781 (1991).

Brinkley BR, Ouspenski I, Zinkowski RP: Structure and molecular organization of the centromere-kinetochore complex. Trends Cell Biol 2:14–21 (1992).

Choo KHA: The Centromere (Oxford University Press, Oxford 1997).

Earnshaw WC, MacKay AM: Role of nonhistone proteins in the chromosomal events of mitosis. FASEB J 8:947–956 (1994).

Ferguson-Smith AC, Chen YF, Newman MS, May LT, Sehgal PB, Ruddle FH: Regional localization of the interferon-beta 2/B-cell stimulatory factor 2/hepatocyte stimulating factor gene to human chromosome 7p15→p21. Genomics 2:203–208 (1988).

Green MC: Gene mapping, in Foster HL, Small JD, Fox JG (eds): The Mouse in Biomedical Research, History, Genetics, and Wild Mice, Vol 1, pp 105–117 (Academic Press, New York 1981).

Kalitsis P, MacDonald AC, Newson AJ, Hudson DF, Choo KHA: Gene structure and sequence analysis of mouse centromere proteins A and C. Genomics (1998, in press).

Karasawa M, Zwacka RM, Reuter A, Fink T, Hsieh CL, Lichter P, Francke U, Weiher H: The human homolog of the glomerulosclerosis gene *Mpv17*: structure and genomic organization. Hum molec Genet 2:1829–1834 (1993).

Kozak C, Stephenson D: Mouse Chromosome 5. Mammal Genome 8:S80–S99 (1997).

McKay S, Thomson E, Cooke H: Sequence homologies and linkage group conservation of the human and mouse *Cenpc* genes. Genomics 22:36–40 (1994).

Palmer DK, Margolis RL: Kinetochore components recognized by human autoantibodies are present on mononucleosomes: Mol Cell Biol 5:173–186 (1985).

Palmer DK, O'Day K, Wener MH, Andrews BS, Margolis RL: A 17-kD centromere protein (CENP-A) copurifies with nucleosome core particles and with histones. J Cell Biol 104:805–815 (1987).

Poirier C, Laloutte A, Folletta VC, Cohen DR, Guenet JL: The gene encoding the Fos-related antigen 2 *(Fosl2)* maps to mouse Chromosome 5. Mammal Genome 8:223 (1997).

Sart D du, Cancilla MR, Earle E, Mao J, Saffery R, Tainton KM, Kalitsis P, Martyn J, Barry AE, Choo KHA: A functional neo-centromere formed through activation of a latent human centromere and consisting of non-alpha-satellite DNA. Nature Genet 16:144–153 (1997).

Searle GA, Selley RL: Tables of genetic homology. Mouse Genome 95:106–160 (1997).

Shelby RD, Vafa O, Sullivan KF: Assembly of CENP-A into centromeric chromatin requires a cooperative array of nucleosomal DNA contact sites. J Cell Biol 136:501–513 (1997).

Silver J: Confidence limits for estimates of gene linkage based on analysis of recombinant inbred strains. J Hered 76:436–440 (1985).

Silverman GA, Kuo WL, Taillon-Miller P, Gray JW: Chromosomal reassignment: YACs containing both YES1 and thymidylate synthase map to the short arm of chromosome 18. Genomics 15:442–445 (1993).

Stoler S, Keith KC, Curnick KE, Fitzgerald-Hayes M: A mutation in *CSE4*, an essential gene encoding a novel chromatin-associated protein in yeast, causes chromosome nondisjunction and cell cycle arrest at mitosis. Genes Devel 9:573–586 (1995).

Sukegawa J, Semba K , Yamanashi Y, Nishizawa M, Miyajima N, Yamamato T, Tokoshima K: Characterization of cDNA clones for the human c-*yes* gene. Mol Cell Biol 7:41–47 (1987).

Sullivan KF, Hechenberger M, Masri K: Human CENP-A contains a histone H3 related histone fold domain that is required for targeting to the centromere. J Cell Biol 127:581–592 (1994).

Voullaire LE, Slater HR, Petrovic V, Choo KHA: A functional marker centromere with no detectable alpha-satellite, satellite III, or CENP-B protein: activation of a latent centromere? Am J hum Genet 52:1153–1163 (1993).

Wada K, Zimmerman KL, Adamson MC, Yokotani N, Wenthold RJ, Kozak CA: Genetic mapping of a mouse gene encoding dipeptidyl aminopeptidase-like proteins. Mammal Genome 4:234–237 (1993).

Wightman PJ, Haywood BE, Bonthron DT: The genes encoding glucokinase regulatory protein and hexokinase co-localize to mouse chromosome 5. Mammal Genome 8:700–701 (1997).

Wilson R, Ainscough R, Anderson K, Baynes C, Berks M, Bonfield J, Burton J, Connell M, Copsey T, Cooper J, Coulson A, Craxton M, Dear S, Du Z, Durbin R, Favello A, Fraser A, Fulton L, Gardner A, Green P, Hawkins T, Hillier L, Jier M, Johnston L, Jones M, Kershaw J, Kirsten J, Laisster N, Latreille P, Lightning J, Lloyd C, Mortimore B, O'Callaghan M, Parsons J, Percy C, Rifken L, Roopra A, Saunders D, Shownkeen R, Sims M, Smaldon N, Smith A, Smith M, Sonnhammer E, Staden R, Sulston J, Thierry-Mieg J, Thomas K, Vaudin M, Vaughan K, Waterston R, Watson A, Weinstock L, Wilkinson-Sproat J, Wohldman P: 2.2 Mb of contiguous nucleotide sequence from chromosome III of *C. elegans*. Nature 368:32–38 (1994).

Yamanaka S, Johnson ON, Lyu MS, Kozak CA, Proia RL: The mouse gene encoding the GM2 activator protein *(Gm2a)*: cDNA sequence, expression, and chromosome mapping. Genomics 24:601–604 (1994).

Note added in proof

While this manuscript was under review, two more Chromosome 5 loci, *Gckr* and *Khk*, have been shown to share homology with human chromosome 2 (Wightman et al., 1997) and were added to the composite map (MGD; November 1997).

PUBLICATION 2

P. KALITSIS, **K.J. FOWLER**, E. EARLE, J. HILL, AND K.H.A. CHOO
(1998)

TARGETED DISRUPTION OF MOUSE CENTROMERE PROTEIN C LEADS TO MITOTIC DISARRAY AND EARLY EMBRYO DEATH.

PROCEEDINGS OF THE NATIONAL ACADEMY OF SCIENCES USA,
95: 1136-1141.

Proc. Natl. Acad. Sci. USA
Vol. 95, pp. 1136–1141, February 1998
Genetics

Targeted disruption of mouse centromere protein C gene leads to mitotic disarray and early embryo death

PAUL KALITSIS, KERRY J. FOWLER, ELIZABETH EARLE, JOANNE HILL, AND K. H. ANDY CHOO*

The Murdoch Institute for Research into Birth Defects, Royal Children's Hospital, Flemington Road, Melbourne 3052, Australia

Communicated by Yuet Wai Kan, University of California, San Francisco, CA, November 26, 1997 (received for review September 29, 1997)

ABSTRACT **Centromere protein C (CENPC) is a key protein that has been localized to the inner kinetochore plate of active mammalian centromeres. Using gene targeting techniques, we have disrupted the mouse *Cenpc* gene and shown that the gene is essential for normal mouse embryonic development. Heterozygous mice carrying one functional copy of the gene are healthy and fertile, whereas homozygous embryos fail to thrive. In these embryos, mitotic arrest and gross morphological degeneration become apparent as early as the morula stage of development. The degenerating embryos demonstrate highly irregular cell and nuclear morphologies, including the presence of a large number of micronuclei. Mitotic chromosomes of these embryos display a scattered and often highly condensed configuration and do not segregate in an ordered fashion. These results describing the phenotype of the mutant mouse embryos indicate that CENPC has a direct role in the mitotic progression from metaphase to anaphase.**

The centromere is a functional chromosomal domain that is responsible for the accurate segregation of eukaryotic chromosomes during mitotic and meiotic cell divisions. It is involved in sister chromatid cohesion and is the attachment site for spindle microtubules. Through its interaction with molecular motors, the centromere assists in the alignment of the replicated chromosomes onto the metaphase plate and the poleward movement of chromosomes during anaphase. Problems in sister chromatid separation can lead to aneuploidy, cancer, and cell death.

The centromere of the budding yeast *Saccharomyces cerevisiae* has been extensively characterized at the structural, biochemical, and genetic levels (1). It is made up of a 125-bp cis-acting CEN DNA unit that is known to associate with a number of proteins in forming a functional structure. Mutations in the CEN DNA and the centromere proteins have been shown to result in chromosome missegregation and mitotic arrest (2, 3). In comparison with the centromere of *S. cerevisiae*, the centromeres of the fission yeast *Schizosaccharomyces pombe* are significantly larger. They range in size from 35 to 110 kb and are made up of both repeated and unique DNA (4–6).

Mammalian centromeres, like those of *Sch. pombe*, are typically made up of long tracts of tandemly, repeated satellite DNA. For example, human centromeric DNA primarily consists of a 171-bp α-satellite DNA that spans several megabases on each chromosome (reviewed in ref. 7), whereas the mouse centromere is composed of a 120-bp tandem repeat known as minor satellite (8). Interestingly, a number of functional human centromeres that are devoid of normal centromeric repeats have recently been described on mitotically stable marker chromosomes (9–11).

To date, several mammalian centromere proteins have been isolated and characterized. These proteins can be subdivided into two categories, those that are present throughout the cell cycle and those that appear at specific stages of the cell cycle. Three proteins that are known to be present throughout the cell cycle include CENPA, CENPB, and CENPC (12). CENPA is a histone H3-like protein that is thought to be associated with the formation of centromere-specific chromatin (13). CENPB is a DNA-binding protein that interacts with a 17-bp CENPB box motif found on α satellite and mouse minor satellite DNA (14, 15), and it has been proposed to have a role in the specific packaging of centromeric heterochromatin (16). CENPC is a highly basic protein with DNA-binding properties and is located at the inner kinetochore plate (17, 18). All three proteins are presumed to form the kinetochore precursor onto which the transient proteins associate to form a functionally active kinetochore. The transient group of proteins includes the motor proteins CENPE and MCAK, CENPF, and the inner centromere protein, INCENP (reviewed in refs. 19 and 20).

Studies of human dicentric chromosomes (21, 22) and marker chromosomes containing neocentromeres (10, 11) have shown that CENPC is present on active but not inactive centromeres, suggesting that CENPC has an essential role in centromere function. In agreement with this idea, cells microinjected with anti-CENPC antibodies exhibit mitotic delay and formation of shortened and disrupted kinetochores (23). Transient expression studies of truncated forms of CENPC have revealed two functional regions of the protein. The first is an instability domain located at the amino terminus and is thought to be involved in the regulation of the temporal destruction of the protein at specific stages of the cell cycle. The second functional region is a DNA-binding and centromere-targeting domain located in the central portion of the protein (18, 24). Furthermore, CENPC shares a region of homology with the *S. cerevisiae* protein Mif2p (25, 26). Mutations in the *MIF2* gene have been shown to result in defective chromosome segregation and delayed progression through mitosis (25). Recent evidence suggests that *MIF2* is located at the centromere (26).

To directly investigate the role and biological significance of CENPC in mouse, we have disrupted the gene by homologous recombination. We describe here the phenotype and the consequence of such a gene disruption.

METHODS

Construction of *Cenpc* Targeting Construct. Using a mouse *Cenpc* cDNA fragment as a probe, we isolated a clone from a mouse genomic 129/Sv phage library (Stratagene). The clone contained exons 5–11 of the mouse *Cenpc* gene (27). From the clone, a 6.3-kb *Xba*I fragment containing exons 8 and 9 was

The publication costs of this article were defrayed in part by page charge payment. This article must therefore be hereby marked "*advertisement*" in accordance with 18 U.S.C. §1734 solely to indicate this fact.

Abbreviations: CENP, centromere protein; ES, embryonic stem; pc, post coitus; IRES, internal ribosome-entry site.

*To whom reprint requests should be addressed. e-mail: choo@cryptic.rch.unimelb.edu.au.

used to construct the targeting vector. A 700-bp *Xho*I–*Sal*I fragment covering the junction between intron 7 and exon 8 was deleted and replaced by a 6.7-kb splice acceptor-IRES-βgeo selectable marker. This construct, when homologously recombined into the mouse *Cenpc* locus, causes premature protein truncation that leads to the loss of the centromere-targeting domain, resulting in the abolition of CENPC function.

Transfection and Screening for Targeted Cell Lines. Mouse embryonic stem (ES) cell lines E14, R1, and W9.8 were used in transfection experiments to generate homologous recombinants. Cells (5×10^7) were electroporated with 40 μg of linearized construct DNA at 0.8 kV, 3 μF, and ∞ Ω (Bio-Rad Gene Pulser) and grown on STO-neo^R feeder cells (28) plus 10^3 units/ml leukemia inhibitory factor (LIF) (Amrad-Pharmacia). After 24 hours, G418 (GIBCO/BRL) selection was applied at an active concentration of 200 μg/ml. Resistant colonies were picked 7 to 10 days later and cell lines were established. Cells were grown up in 3-cm-diameter culture dishes to confluency, and genomic DNA was extracted, digested with *Eco*RI (Boehringer Mannheim), electrophoresed, and blotted onto Hybond N+ (Amersham) by using standard procedures. The filters were probed with a 3′ *Xba*I 1.2-kb probe (see Fig. 1*A*).

Blastocyst Injection and Chimeric Mouse Production. Targeted ES cell lines were injected into C57BL/6 blastocysts by standard methods (29). The injected blastocysts were then transferred into recipient pseudopregnant HSD Ola (Gpi-1bb) mice. Chimeric mice were selected by coat color and were mated with C57BL/6 mice to generate heterozygotes. Progeny from chimeric and heterozygous crosses were genotyped as described below. The heterozygous mice were crossed to obtain homozygotes.

Genotyping of Mice and Southern and PCR Analyses. DNA for Southern or PCR analysis was extracted from mouse tail by using the QIAamp Tissue Kit (Qiagen). Southern blotting and hybridization were carried out by standard methods. Mouse tail PCR was performed using a semiduplex strategy with the following primers: S, 5′-TTACCTTGAAGCAGTGCAGTG-3′; W, 5′-AACTGAGTACATGCAAGTATGG-3′; and neo1, 5′-CTTCCTCGTGCTTTACGGTATC-3′ (see Fig. 1*A*). PCR was performed with *Taq* DNA polymerase (Perkin–Elmer) with 1.5 mM $MgCl_2$, 0.2 mM dNTPs, and 100 ng of primers in a final volume of 20 μl. The cycling conditions were 95°C for 2 min, 58°C for 1 min, and 72°C for 90 sec, over 35 cycles. The predicted PCR products for S-W (wild-type allele) and neo1-S (targeted allele) are 995 bp and 580 bp, respectively.

Genotyping of Preimplantation Embryos. For mouse embryos up to the blastocyst stage, the limited amount of DNA template had necessitated the use of two rounds of nested PCR. Embryos were rinsed in M2 medium (Sigma) several times to remove any contaminating maternal cells, before they were taken up in 2 μl of medium and added to 23 μl of deionized H_2O. Prior to PCR, the samples were denatured at 95°C for 15 min to lyse the cells and denature any proteins. First round PCR used the *Cenpc* primers AK, 5′-AAGATG-AAGCTTCCGTCTCTC-3′; AL, 5′-TTCGTAGTCCTTTC-CCATGC-3′; and the βgeo primers GF1, 5′-AGTATCGGC-GGAATTCCAG-3′; GR1, 5′-GATGTTTCGCTTGGTGG-TC-3′) under the following cycling conditions: first cycle 95°C for 2 min, 55°C for 3 min, and 72°C for 90 sec, and second to thirtieth cycles 95°C for 60 sec, 55°C for 60 sec, and 72°C for 90 sec. The reaction mixture included 250 ng of primers AK, AL, GF1, GR1, 1.5 mM $MgCl_2$, 1.2 units of *Taq* DNA polymerase, and 0.2 mM dNTPs, in a final volume of 50 μl.

Second-round PCR involved two separate reactions using 100 ng of nested *Cenpc* primers: AM, 5′-CCGTCTCTCTAA-AGTGTTGCAG-3′; and AN, 5′-CTTCCTCTATTGGGTG-AGCC-3′; and βgeo primers, GF2, 5′-CCATTACCAGTTG-GTCTGGTG-3′; and GR2, 5′-CCTCGTCCTGCAGTTCAT-TC-3′; 1.5 mM $MgCl_2$, 0.5 unit of *Taq* DNA polymerase, and 1 μl of the first-round PCR product, in a final volume of 20 μl.

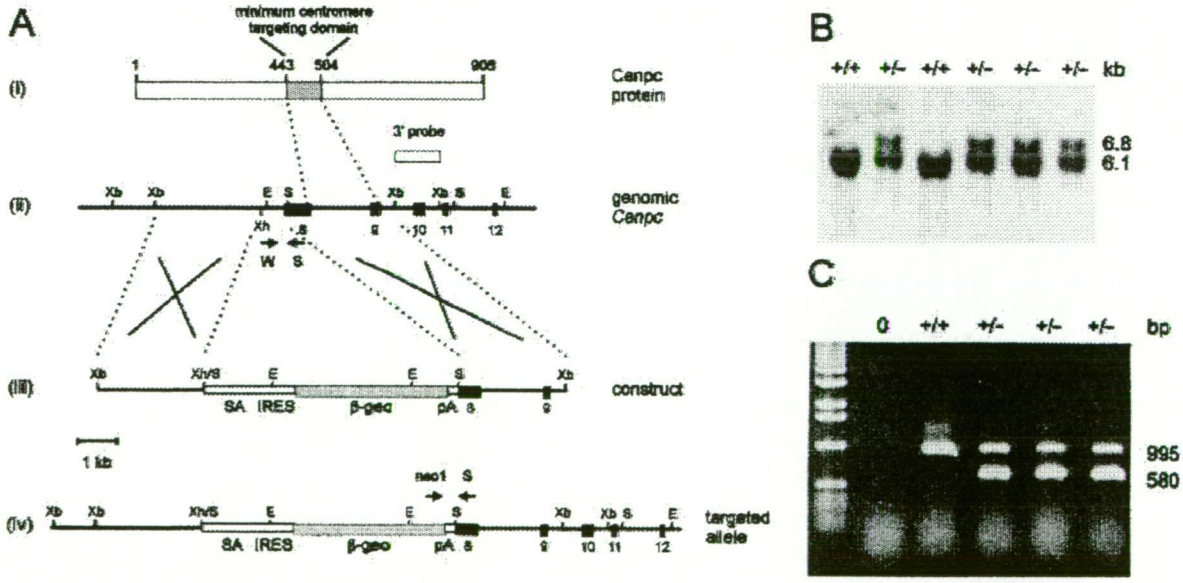

FIG. 1. Targeted disruption of the mouse *Cenpc* gene. (*A*) Gene replacement constructs and restriction maps. (*i*) Mouse CENPC protein, showing the amino acid positions of the minimum centromere-targeting domain (18) and the location of this domain downstream of the gene-disruption site. (*ii–iv*) Restriction maps for the *Cenpc* locus covering exons 8 to 12 (*ii*), the gene replacement construct (*iii*), and the *Cenpc* locus after targeted disruption (*iv*). Black boxes represent exons. The selectable marker cassette contained in the targeting construct consists of a splice acceptor site (SA), a picornaviral internal ribosome-entry site (IRES), a *lacZ*–neomycin-resistance fusion gene (βgeo), and a simian virus 40 polyadenylation sequence (pA) (27). A 1.2-kb *Xba*I fragment (designated 3′ probe) located downstream of the targeted region was used in the Southern screening strategy and detected a 6.1-kb wild-type *Eco*RI fragment in the untargeted locus or a 6.8-kb *Eco*RI fragment in the targeted locus. Arrows indicate positions of primers used in mouse tail and embryo PCR. Crosses denote expected sites of homologous recombination. Abbreviations for restriction enzymes are E, *Eco*RI; S, *Sal*I; Xb, *Xba*I; and Xh, *Xho*I. (*B*) Southern blot analysis of wild-type and correctly targeted ES cell lines. The sizes of wild-type 6.1-kb and homologous recombinant 6.8-kb bands are shown on the right. (*C*) PCR genotyping of mouse tail DNA or postimplantation embryos. The primer set S-W gives a 995-bp wild-type *Cenpc* product, whereas the neomycin-*Cenpc* primer set, neo1-S, gives a 580-bp targeted product.

The cycling conditions were as follows: first cycle 95°C for 2 min, 57°C for 60 sec, and 72°C for 90 sec, and second to thirtieth cycles 95°C for 60 sec, 57°C for 60 sec, and 72°C for 90 sec.

Embryo Staining and Determination of Mitotic Index. Day-3.5 post coitus (pc) preimplantation embryos were placed in a droplet of M16 medium (Sigma) under mineral oil (Sigma), photographed, and kept at 37°C until fixation. These embryos were not treated with any microtubule inhibitor at any stage. Each embryo was placed into a microwell containing 0.6% trisodium citrate for 4–8 min, then taken up in a minimal volume and placed onto a glass slide. A microdrop of methanol/acetic acid (3:1) was immediately placed over the embryo, allowing it to spread and dry. After two rinses in fixative, the slides were stained in Giemsa stain, pH 6.8 (Gurr), air dried, and mounted in DPX (BDH) for analysis.

A similar procedure was followed for the chromosome analysis of 2.5-day embryos except for the addition of 0.1 mg/ml Colcemid and incubation for up to 6 hr prior to harvesting. This allowed most cells to become arrested in mitosis so that chromosome numbers per cell could be counted.

The mitotic index of the day-3.5 embryos was determined by scoring the number of mitotic events over the total number of stained nuclei (which should correspond to the total number of cells, although individual cells were not recognizable as a result of membrane rupture during the hypotonic treatment). Because severely affected embryos expressing the −/− phenotype display a wide variation in nuclear morphology, including the formation of micronuclei, a nucleus was scored to represent a cell unit if it was at least half the size of a normal-looking nucleus.

RESULTS

Targeted Disruption of the Mouse *Cenpc* Gene. For the disruption of the mouse *Cenpc* gene in ES cells, we constructed a promoterless targeting construct that has included exons 8 and 9 of the mouse *Cenpc* gene (27) (Fig. 1*A*). In this construct, portions of intron 7 and exon 8 were deleted and replaced with a splice-acceptor–IRES–β-galactosidase–neomycin-resistance fusion marker (30). This disruption is expected to abolish any translation of the centromere-targeting region of *Cenpc* and render any truncated protein functionally inactive (18, 24). Following transfection of the construct into three different ES cell lines, Southern blot analysis (see Fig. 1*B* for typical results) revealed targeting frequencies of 11% (10 of 93 G418-resistant colonies), 74% (17 of 23), and 55% (11 of 20) for the cell lines E14, R1, and W9.8, respectively. A total of 18 cell lines carrying a targeted *Cenpc* allele were randomly picked from the three different cell lines and independently injected into C57BL/6 blastocysts for chimeric animal production. This resulted in the identification of three germ-line chimeras from an R1 cell line. These animals were used to generate the heterozygous (Fig. 1*C*) and homozygous (see below) progeny for further studies.

Disruption of *Cenpc* Causes Embryonic Lethality. Heterozygous male and female mice were phenotypically normal and showed no discernible impairment of growth and fertility. Intercrossing of the heterozygous mice produced 276 progeny, 85 of which were +/+ and 191, +/−. This result clearly indicated embryonic lethality of the homozygous mutant state. To determine the stage at which embryonic death occurred, we looked at postimplantation stages of development. Embryos at days 13.5, 10.5, and 8.5 pc were dissected out for genotyping. In the 30 embryos analyzed the homozygous mutant genotype was again absent, thus suggesting that lethality had occurred at an earlier stage.

We next looked for the presence of the −/− genotype in day-3.5 preimplantation embryos. Because of the limited amount of DNA in these early embryos, a two-round nested PCR strategy was developed for this study (Fig. 2). Fifty embryos were generated from multiple +/− × +/− crosses. As shown in Table 1, 10 −/− embryos were detected. When the stages of development of the different embryos were determined, it was apparent that the −/− embryos were, as a group, morphologically less healthy and/or delayed in their development, with 80% of embryos falling into this category (that is, morula, degenerating morula, and ≤16-cell stages; Table1) compared with 12% and 28% for the +/+ and +/− groups of embryos, respectively. These results suggested that developmental problems in the −/− embryos manifested as early as 3.5 days pc. This suggestion was further addressed by a closer examination of the individual cell morphology of the embryos.

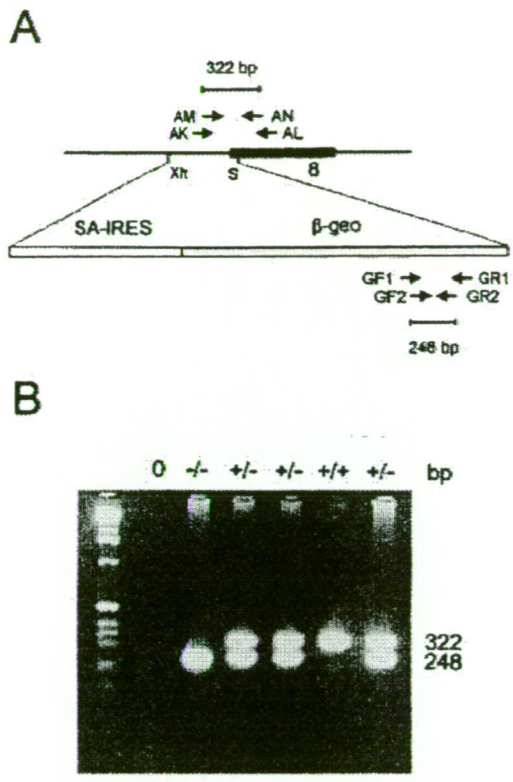

FIG. 2. PCR analysis of preimplantation embryos from +/− × +/− crosses. (*A*) Nested PCR strategy for genotyping embryos up to the blastocyst stage. *Cenpc* primer pairs include AK–AL for first-round synthesis and AM–AN for second-round synthesis, giving a final product of 322 bp for the untargeted allele. β-geo primer pairs include GF1–GR1 for first-round synthesis and GF2–GR2 for second-round synthesis, giving a final product of 248 bp for the targeted allele. Abbreviations for restriction enzyme sites are (Xh) *Xho*I and (S) *Sal*I. The black box indicates exon 8 of the mouse *Cenpc* gene (see Fig. 1*A*). (*B*) Nested PCR genotyping of day-3.5 embryos.

Aberrant Mitosis and Micronuclei Formation in Day-3.5 Embryos. One-hundred and fifty-five embryos at day 3.5 pc were collected from +/− × +/− matings and subdivided into

Table 1. Frequency of the different genotypes in day-3.5 preimplantation embryos of +/− × +/− matings

Developmental stage	No. of embryos (% of total) with genotype				
	Total	+/+	+/−	−/−	No result
Blastocyst	30 (60%)	15 (88%)	13 (72%)	2 (20%)	0
Morula	5 (10%)	1 (6%)	2 (11%)	2 (20%)	0
Degenerate morula	8 (16%)	1 (6%)	3 (17%)	3 (30%)	1
≤16 cells	7 (14%)	0	0	3 (30%)	4
Total	50	17	18	10	5

the different developmental stages by their morphology (Table 2). As controls, 64 embryos at day 3.5 pc were obtained from either +/+ × +/+ or +/+ × +/− matings. Comparison of the average litter sizes in the experimental and control groups indicated these to be 8.2 and 8.0, respectively, suggesting that fertilization was normal in both groups. Overall, the experimental group showed only 56.8% of embryos reaching the blastocyst stage compared with the control group value of 75%, indicating that the experimental group has a higher proportion of embryos that were developmentally delayed and/or unhealthy compared with the control group. Such a difference was consistent with the results shown in Table 1, in that it could be best explained by the developmental problems associated with the −/− embryos generated in the +/− × +/− matings.

To further investigate the embryos, they were fixed onto slides and stained with Giemsa stain. The results indicated that a substantial number of embryos in the experimental group showed irregular-sized nuclei and a high level of micronuclei (Fig. 3*C–F*). In total, 39 of the 155 embryos (or 25.2%) were shown to have this phenotype—a value that closely approximated the 25% expected frequency for the −/− genotype in +/− × +/− crosses. In contrast, none of the 64 control embryos showed any sign of micronuclei formation. When the relative number of embryos with irregular nuclei and micronucleated cells was ascertained in terms of developmental stage, a grossly disproportionate number (89.7%) was shown to be associated with embryos that demonstrated developmental delay or embryonic degeneration (Table 2). This result provided evidence that expression of the abnormal nuclear and micronuclear phenotype was directly responsible for the observed developmental problems in the −/− progeny.

The mitotic indices for the micronucleated and control group of embryos were determined. This involved counting the number of mitotic spreads over the total number of cells for each embryo. When the results for all the embryos within each group were pooled, an average mitotic index of 6.9% was obtained for the micronucleated embryos, whereas the value was 3.6% for their normal littermates, suggesting that some mitotic delay or arrest has occurred in the affected embryos. Furthermore, analysis of the mitotic stages of these embryos has indicated that metaphase chromosomes were not correctly aligning onto the metaphase plate and then not proceeding through an ordered anaphase, in contrast to the control group in which a significant proportion of cells showed normal progression through these stages. As shown in Fig. 3, the chromosomes of the affected embryos displayed a scattered configuration, with a substantial proportion of these chromosomes showing a highly condensed morphology.

To look for evidence of chromosome missegregation and aneuploidy at an earlier developmental stage, we have analyzed 2.5-day-old preimplantation embryos. Fifty-two embryos were obtained from +/− × +/− matings, and 32 embryos from +/+ × +/+ matings. The embryos were treated similarly to the 3.5-day embryos, except for a 3- to 6 hr-incubation in Colcemid to arrest mitosis to determine the chromosome number. The results indicated that 78.9% of embryos from the experimental group were at the expected eight- (or occasionally slightly more) cell stage compared with 78.1% in the control group, suggesting that embryonic development was not delayed at this stage. No micronuclei were observed in any of the embryos. When the number of chromosomes of the individual cells were counted, no aneuploidy was detected. These results therefore established that mitosis and embryonic development proceeded normally during the first three cell division cycles.

DISCUSSION

In a previous study, Tomkiel *et al.* (23) microinjected anti-human CENPC antibodies into cultured HeLa cells and demonstrated a transient arrest of cell division at metaphase. The arrested cells exhibited poor kinetochore structure and defective microtubule binding. The use of such a strategy, whilst offering useful preliminary insights into possible roles of centromere proteins, has a number of limitations. For example, the CENPC–antibody–antigen complex may interfere with other centromere or chromosomal proteins ,obscuring the real phenotype, or the anti-CENPC antibody may cross-react with other nuclear proteins to create a more complex effect. The question of whether the antibody used can completely inhibit the function of CENPC is also difficult to resolve completely. The production of specific null mutations of the *Cenpc* gene by homologous recombination in transgenic mice circumvents these uncertainties and provides a useful model system for the understanding of the functions of this protein. We report here the production of such a model for *Cenpc*, and describe the phenotype of this targeted transgenic mouse mutant.

Both human and mouse CENPC genes have previously been shown to be single-copy genes (17, 31). Our results demonstrate that disruption of this gene has no apparent effect on the growth and fertility of the heterozygous mice, suggesting that one functional copy of this gene is sufficient for full centromere activity. However, disruption of both the *Cenpc* alleles results in embryo lethality, as evident from our failure to detect the −/− genotype in any liveborns and in embryos at days 13.5, 10.5, and 8.5 pc. Clues to the observed lethality have come from direct examination of preimplantation embryos. When 3.5-day old embryos from +/− × +/− crosses were analyzed, approximately 25% of embryos displayed poor nuclear morphology and an abundance of micronuclei, which corresponds well with the expected frequency for the homozygous genotype. As a group, these embryos show slight to severe developmental delay or morphological degeneration. Although we

Table 2. Phenotypes of day 3.5 preimplantation embryos

	+/− × +/−		+/+ × +/+ or +/− × +/+	
Developmental stage	No. of embryos (% of total)	No. of embryos with micronuclei (% of total)	No. of embryos (% of total)	No. of embryos with micronuclei
Blastocyst	88 (56.8%)	4 (10.3%)	48 (75%)	0
Morula	38 (24.5%)	13 (33.3%)	8 (12.5%)	0
Degenerate morula	26 (16.8%)	22 (56.4%)	0	0
≤16 cells	2 (1.3%)	0	3 (4.5%)	0
Dead	1 (0.6%)	0	5 (8%)	0
Total no. of embryos	155	39	64	
No. of litters	19		8	
Avg. no. of embryos/litter	8.2		8.0	

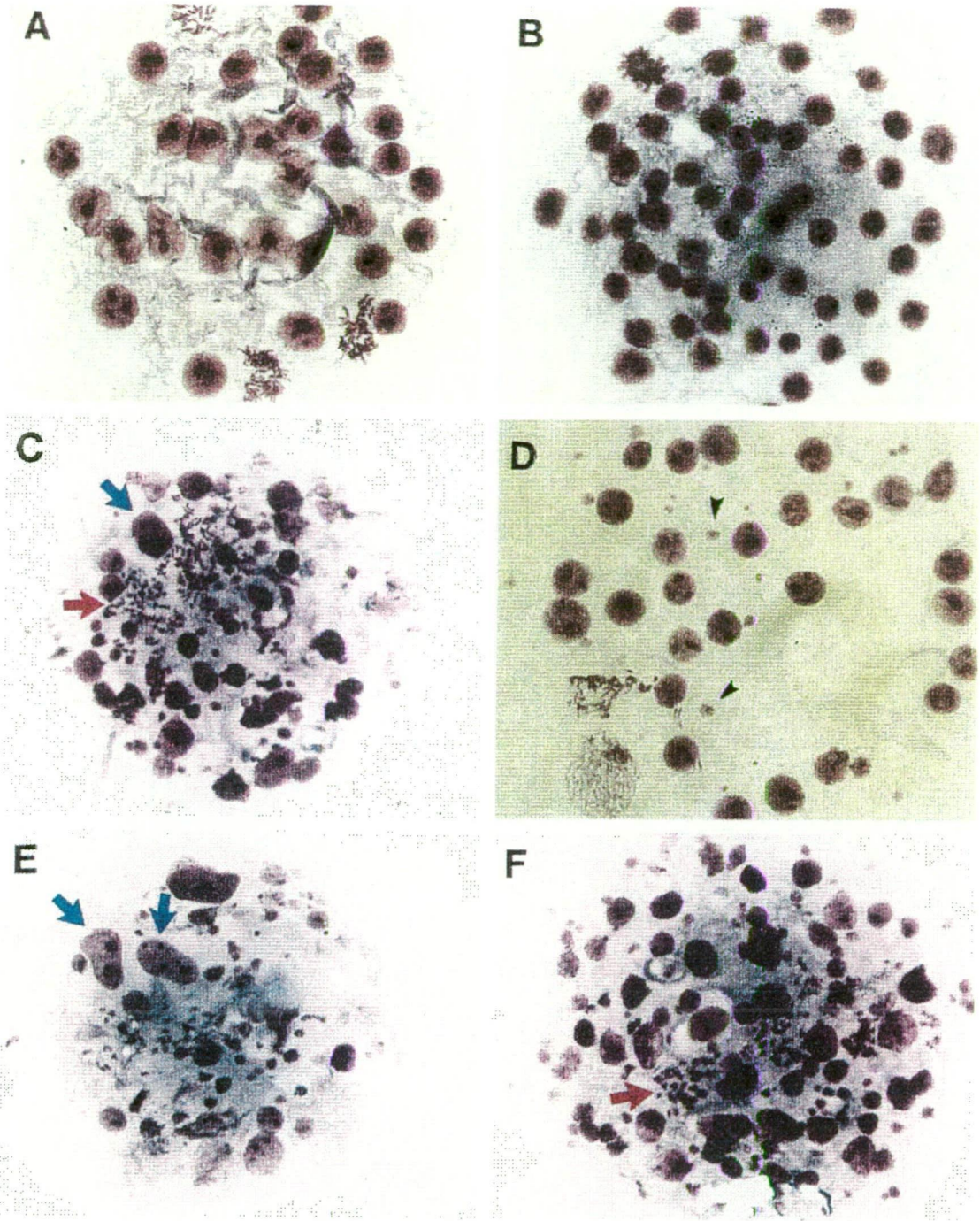

FIG. 3. Morphological analysis of Giemsa-stained day-3.5 embryos from +/− × +/− crosses. (*A* and *B*) Normal embryos, showing regular, round interphase nuclei and a number of cells undergoing mitosis. (*C–F*) Putative *Cenpc* homozygous mutant embryos, showing oversized interphase nuclei (blue arrows), scattered and highly condensed metaphase chromosomes (red arrows), and an abundance of micronuclei (black arrows). (×200.)

have not defined the exact stage of embryonic death, the severity of the phenotype (Fig. 3) suggests that the embryos are not likely to implant.

Based on the observed morphological and nuclear phenotype, the following model of mitotic and developmental events for the putative −/− embryos may be formulated. Because mitosis and the development of the 2.5-day embryos are normal, it can be assumed that the egg cytoplasm provides sufficient CENPC mRNA and/or protein for centromere function for up to three mitotic cell division cycles. After this period, the −/− embryos begin to misdivide, at first giving rise to predominantly normal-looking nuclei, with some micronuclei beginning to develop (Fig. 3*D*), However, without further replenishment of the maternal pool of CENPC, centromere function becomes progressively deficient, leading to increasing mitotic disarray and ultimately cell death.

Two observations suggest that mitotic disarray has its origin at the metaphase stage. First, the higher mitotic index for the affected group of embryos indicates that mitosis is delayed or arrested. Such a delay may be the result of a metaphase checkpoint that monitors a signal-generating mechanism at the kinetochore to delay anaphase onset until metaphase is completed, with all the chromosomes attaining bipolar attachment to microtubules and aligning properly at the spindle midzone (32). Our failure to detect any evidence for chromosomal congression at the metaphase plate in the 3.5-day affected embryos lends direct support to this possibility. Second, the mitotic chromosomes of the more severely affected embryos

display a scattered configuration and are often more condensed than chromosomes in the control embryos. These features, together with the observed failure of the chromosomes to congress at the spindle midzone, are similar to those of mitotic spreads from control embryos that have been treated with a microtubule inhibitor such as Colcemid.

Despite our failure to detect any proper congression of metaphase chromosomes and progression of the cells through anaphase, the metaphase arrest phenotype appears to be eventually lifted to allow the cells to proceed further along mitosis. These post-metaphase steps presumably involve highly disordered chromosomal segregation, as evident from the extensive number of micronuclei that are detected in the affected embryos; these micronuclei structures, which encapsulate missegregating or lagging chromosomes, are formed during nuclear membrane reformation at telophase, prior to cell cleavage. The finding of some nuclei that are significantly larger (occasionally doubling) in size compared with normal nuclei (e.g., Fig. 3 *C* and *E*) further suggests that in some cells, most or all replicated chromosomes may have failed to segregate, leading to a nuclear membrane being reformed around a presumed near-tetraploid genome.

The above observations provide *in vivo* evidence that CENPC is essential for proper mitotic cell division. Absence of this protein may prevent the ability of the other components of the centromere to form a mature kinetochore. This in turn could affect spindle morphology, or the function of kinetochores in segregating chromosomes. The severe phenotype of the $-/-$ embryos indicates that *Cenpc* is functionally nonredundant; recently, a number of other proteins that are involved in mitosis, including the *S. cerevisiae* centromere motor protein Kar3p, have been reported to show functional redundancy (33–35). On the basis of the severity of the observed phenotype in our mouse mutant, it may be extrapolated that null mutations of CENPC in humans will similarly lead to very early embryonic degeneration and spontaneous loss.

Earlier studies have shown that the phenotypes of some mouse mutants can be altered by genetic modifiers when crossed onto different mouse strains, as seen in the *Egfr* $-/-$ and the *Min*/+ mice (36–38). At present, it is not known whether any genetic modifiers exist for the *Cenpc* locus that may elicit a mitotic or meiotic phenotype in our heterozygous mice or partially correct the severe phenotype in the homozygous null mutants. We are currently determining this by breeding the targeted *Cenpc* allele onto mouse strains of different genetic background. In further studies, it would also be important to use targeted gene disruption in mice to determine the phenotype of null mutations for other known centromere proteins. Two of these proteins, CENPB and CENPE, are particularly interesting for this approach, because indirect evidence suggests that the former may be dispensable for function (9–11, 14, 39) whereas the latter, which is a motor protein (40), may be functionally redundant, as is the case for Kar3p (33–35). Judging from the amount of useful information that has come from the study of chromosome segregation mutants identified in *S. cerevisiae* and *Sch. pombe*, it would be feasible that the creation of a collection of mouse mutants would assist in the understanding of mitosis and meiosis in higher eukaryotes.

We thank Dr. Peter Mountford for the splice-acceptor-IRES-βgeo selection marker, Dr. Steve Delaney for the gift of R1 cells, and Dr. Leanda Wilton for technical advice on mouse embryos. We acknowledge Sophie Gazeas, Robin Breslin, and Rachel O'Dowd for excellent technical assistance. This work was supported by the National Health and Medical Research Council of Australia. K.H.A.C. is a Principal Research Fellow of the Council.

1. Clarke, L. & Carbon, J. (1985) *Annu. Rev. Genet.* **19,** 29–55.
2. Doheny, K. F., Sorger, P. K., Hyman, A. A., Tugendreich, S., Spencer, F. & Hieter, P. (1993) *Cell* **73,** 761–774.
3. Lechner, J. & Carbon, J. (1991) *Cell* **64,** 717–725.
4. Clarke, L., Amstutz, H., Fishel, B. & Carbon, J. (1986) *Proc. Natl. Acad. Sci. USA* **83,** 8253–8257.
5. Nakaseko, Y., Adachi, Y., Funahashi, S., Niwa, O. & Yanagida, M. (1986) *EMBO J.* **5,** 1011–1021.
6. Hahnenberger, K. M., Carbon, J. & Clarke, L. (1991) *Mol. Cell Biol.* **11,** 2206–2215.
7. Kalitsis, P. & Choo, K. H. A. (1997) in *The Centromere*, ed. Choo, K. H. A. (Oxford Univ. Press, Oxford), pp. 97–142.
8. Wong, A. K. & Rattner, J. B. (1988) *Nucleic Acids Res.* **16,** 11645–11661.
9. Voullaire, L. E., Slater, H. R., Petrovic, V. & Choo, K. H. A. (1993) *Am. J. Hum. Genet.* **52,** 1153–1163.
10. du Sart, D., Cancilla, M. R., Earle, E., Mao, J. I., Saffery, R., Tainton, K. M., Kalitsis, P., Martyn, J., Barry, A. E. & Choo, K. H. A. (1997) *Nat. Genet.* **16,** 144–153.
11. Depinet, T. W., Zackowski, J. L., Earnshaw, W. C., Kaffe, S., Sekhon, G. S., Stallard, R., Sullivan, B. A., Vance, G. H., Van Dyke, D. L., Willard, H. F., Zinn, A. B. & Schwartz, S. (1997) *Hum. Mol. Genet.* **6,** 1195–1204.
12. Earnshaw, W. C. & Rothfield, N. (1985) *Chromosoma* **91,** 313–321.
13. Palmer, D. K., O'Day, K., Trong, H. L., Charbonneau, H. & Margolis, R. L. (1991) *Proc. Natl. Acad. Sci. USA* **88,** 3734–3738.
14. Masumoto, H., Masukata, H., Muro, Y., Nozaki, N. & Okazaki, T. (1989) *J. Cell Biol.* **109,** 1963–1973.
15. Broccoli, D., Miller, O. J. & Miller, D. A. (1990) *Cytogenet. Cell Genet.* **54,** 182–186.
16. Muro, Y., Masumoto, H., Yoda, K., Nozaki, N., Ohashi, M. & Okazaki, T. (1992) *J. Cell Biol.* **116,** 585–596.
17. Saitoh, H., Tomkiel, J., Cooke, C. A., Ratrie, H., Maurer, M., Rothfield, N. F. & Earnshaw, W. C. (1992) *Cell* **70,** 115–125.
18. Yang, C. H., Tomkiel, J., Saitoh, H., Johnson, D. H. & Earnshaw, W. C. (1996) *Mol. Cell Biol.* **16,** 3576–3586.
19. Choo, K. H. A., ed. (1997) *The Centromere* (Oxford Univ. Press, Oxford).
20. Pluta, A. F., Mackay, A. M., Ainsztein, A. M., Goldberg, I. G. & Earnshaw, W. C. (1995) *Science* **270,** 1591–1594.
21. Earnshaw, W. C., Ratrie, H. & Stetten, G. (1989) *Chromosoma* **98,** 1–12.
22. Page, S. L., Earnshaw, W. C., Choo, K. H. A. & Shaffer, L. G. (1995) *Hum. Mol. Genet.* **4,** 289–294.
23. Tomkiel, J., Cooke, C. A., Saitoh, H., Bernat, R. L. & Earnshaw, W. C. (1994) *J. Cell Biol.* **125,** 531–545.
24. Lanini, L. & McKeon, F. (1995) *Mol. Biol. Cell* **6,** 1049–1059.
25. Brown, M. T., Goetsch, L. & Hartwell, L. H. (1993) *J. Cell Biol.* **123,** 387–403.
26. Meluh, P. B. & Koshland, D. (1995) *Mol. Biol. Cell* **6,** 793–807.
27. Kalitsis, P., MacDonald, A. C., Newson, A. J., Hudson, D. F. & Choo, K. H. A. (1998) *Genomics*, in press.
28. Robertson, E. J. (1987) in *Teratocarcinomas and Embryonic Stem Cells: A Practical Approach*, ed. Robertson, E. J. (IRL Press, Oxford), pp. 71–112.
29. Bradley, A. (1987) in *Teratocarcinomas and Embryonic Stem Cells: A Practical Approach*, ed. Robertson, E. J. (IRL Press, Oxford), pp. 113–152.
30. Mountford, P., Zevnik, B., Duwel, A., Nichols, J., Li, M., Dani, C., Robertson, M., Chambers, I. & Smith, A. (1994) *Proc. Natl. Acad. Sci. USA* **91,** 4303–4307.
31. McKay, S., Thomson, E. & Cooke, H. (1994) *Genomics* **22,** 36–40.
32. Li, X. & Nicklas, R. B. (1995) *Nature (London)* **373,** 630–632.
33. Meluh, P. & Rose, M. (1990) *Cell* **60,** 1029–1041.
34. Saunders, W. & Hoyt, M. (1992) *Cell* **70,** 451–458.
35. Goldstein, L. S. (1993) *J. Cell Biol.* **120,** 1–3.
36. Threadgill, D. W., Dlugosz, A. A., Hansen, L. A., Tennenbaum, T., Lichti, U., Yee, D., LaMantia, C., Mourton, T., Herrup, K., Harris, R. C., Barnard, J. A., Yuspa, S. H., Coffey, R J. & Magnuson, T. (1995) *Science* **269,** 230–234.
37. Sibilia, M. & Wagner, E. F. (1995) *Science* **269,** 234–238.
38. Moser, A. R., Dove, W. F., Roth, K. A. & Gordon, J. I. (1992) *J. Cell Biol.* **116,** 1517–1526.
39. Earnshaw, W. C., Bernat, R. L., Cooke, C. A. & Rothfield, N. F. (1991) *Cold Spring Harbor Symp. Quant. Biol.* **56,** 675–685.
40. Yen, T. J., Li, G., Schaar, B. T., Szilak, I. & Cleveland, D. W. (1992) *Nature (London)* **359,** 536–539.

PUBLICATION 3

D.F. HUDSON, **K.J. FOWLER**, E. EARLE, R. SAFFERY, P. KALITSIS, H. TROWELL, J. HILL, N.G. WREFORD, D.M. DEKRETSER, M.R. CANCILLA, E. HOWMAN, L. HII, S.M. CUTTS, D.V. IRVINE, AND K.H.A. CHOO (1998)

CENTROMERE PROTEIN B NULL MICE ARE MITOTICALLY AND MEIOTICALLY NORMAL BUT HAVE LOWER BODY AND TESTIS WEIGHTS.

THE JOURNAL OF CELL BIOLOGY, 141: 309-319.

Centromere Protein B Null Mice are Mitotically and Meiotically Normal but Have Lower Body and Testis Weights

Damien F. Hudson,* Kerry J. Fowler,* Elizabeth Earle,* Richard Saffery,* Paul Kalitsis,* Helen Trowell,* Joanne Hill,* Nigel G. Wreford,‡ David M. de Kretser,‡ Michael R. Cancilla,* Emily Howman,* Linda Hii,* Suzanne M. Cutts,* Danielle V. Irvine,* and K.H.A. Choo*

*The Murdoch Institute for Research into Birth Defects, Royal Children's Hospital, Parkville 3052, Australia; and‡Institute of Reproduction and Development, Monash University, Clayton 3168, Australia

Abstract. CENP-B is a constitutive centromere DNA-binding protein that is conserved in a number of mammalian species and in yeast. Despite this conservation, earlier cytological and indirect experimental studies have provided conflicting evidence concerning the role of this protein in mitosis. The requirement of this protein in meiosis has also not previously been described. To resolve these uncertainties, we used targeted disruption of the *Cenpb* gene in mouse to study the functional significance of this protein in mitosis and meiosis. Male and female *Cenpb* null mice have normal body weights at birth and at weaning, but these subsequently lag behind those of the heterozygous and wild-type animals. The weight and sperm content of the testes of *Cenpb* null mice are also significantly decreased. Otherwise, the animals appear developmentally and reproductively normal. Cytogenetic fluorescence-activated cell sorting and histological analyses of somatic and germline tissues revealed no abnormality. These results indicate that *Cenpb* is not essential for mitosis or meiosis, although the observed weight reduction raises the possibility that *Cenpb* deficiency may subtly affect some aspects of centromere assembly and function, and result in reduced rate of cell cycle progression, efficiency of microtubule capture, and/or chromosome movement. A model for a functional redundancy of this protein is presented.

THE protein components of the mammalian centromere can be broadly classified into two groups. Proteins from the first group are constitutively present on the centromere throughout the cell cycle, and include CENP-A, CENP-B, and CENP-C. The second group of proteins has been referred to as passenger proteins, since these proteins undergo complex relocations to other cellular organelles during the cell cycle, appearing on the centromere only during specific stages of the cycle (Brinkley et al., 1992; Earnshaw and Mackay, 1994). Examples of passenger proteins are INCENPs, MCAK, CENP-E, CENP-F, 3F3/2 antigens, and cytoplasmic dynein (reviewed by Earnshaw and Mackay, 1994; Pluta et al., 1995; Choo, 1997*a*). The proposed biological roles for these passenger proteins have included centromere formation and maturation, motor movement of chromosomes, sister chromatid cohesion and release, modulation of spindle dynamics, nuclear organization, intercellular bridge structure and function, and cytokinesis (reviewed by Choo, 1997a).

Amongst the constitutive centromere proteins, CENP-A has been localized to the outer kinetochore domain, and is a member of a growing class of proteins referred to as histone H3-like proteins whose members also include the *S. cerevisiae* homologue of CENP-A, CSE4p (Sullivan et al., 1994; Wilson et al., 1994; Stoler et al., 1995). Since CENP-A is found in association with histone H4 and the other core histones in particles that copurify with nucleosome core particles (Palmer and Margolis, 1985; Palmer et al., 1987), the protein is thought to act as a histone H3 homologue, replacing one or both copies of histone H3 in a certain set of centromeric nucleosomes, and is thought to serve to differentiate the centromere from the rest of the chromosome at the most fundamental level of chromatin structure: the nucleosome (Sullivan et al., 1994). CENP-C is located at the inner kinetochore plate, and has been shown to have an essential although yet undetermined centromere function as seen from its association with the active, but not the inactive centromeres of human dicentric chromosomes (Earnshaw et al., 1989; Page et al., 1995; Sullivan and Schwartz, 1995), arrest of mitotic progression after microinjection of anti-CENP-C antibodies into cul-

Address all correspondence to Dr. Andy Choo, The Murdoch Institute for Research into Birth Defects, Royal Children's Hospital, Flemington Road, Parkville 3052, Australia. Phone: 61-3-9345-5045; FAX: 61-3-9348-1391; E-mail: choo@cryptic.rch.unimelb.edu.au

The Journal of Cell Biology, Volume 141, Number 2, April 20, 1998 309–319
http://www.jcb.org

tured mammalian cells (Bernat et al., 1990; Tomkiel et al., 1994) or gene knockout (Fukagawa and Brown, 1997; Kalitsis et al., 1998), and the significant sequence homology it shares with Mif2, a protein involved in budding yeast chromosome segregation and believed to have a role in kinetochore function (Brown et al., 1993; Brown, 1995; Meluh and Koshland, 1995).

Human CENP-B is an 80-kD polypeptide that has been localized throughout the heterochromatin or central domain of the centromere (Earnshaw and Rothfield, 1985; Earnshaw et al., 1987; Cooke et al., 1990; Sullivan and Glass, 1991; Saitoh et al., 1992). The protein is encoded by an intronless gene present in a single copy within the genome (Sugimoto et al., 1993; Seki et al., 1994). The number of CENP-B protein molecules has been estimated to be ~20,000 per diploid genome in HeLa cells (Cooke et al., 1990; Muro et al., 1992). On different human chromosomes, variable but generally detectable levels of the protein have been observed (Earnshaw et al., 1987). A notable exception is the Y chromosome, which has been shown to consistently lack this protein (Earnshaw et al., 1987). Through the recognition of a 17-bp PyTTCGTTGGAA-PuCGGGA sequence known as the CENP-B box motif, CENP-B protein has been demonstrated to bind human centromeric α-satellite DNA directly (Masumoto et al., 1989; Muro et al., 1992; Pluta et al., 1992; Yoda et al., 1992).

Comparison of cloned human and mouse *CENP-B* gene sequences (Earnshaw et al., 1987; Sullivan and Glass, 1991) reveals a high degree of homology between the two species, with the coding regions showing an overall 96% sequence similarity and substantial stretches demonstrating 100% nucleotide identity between the two species (Sullivan and Glass, 1991). Of particular importance, both the NH_2-terminal DNA-binding and COOH-terminal dimerization domains are totally conserved. Surprisingly, even the 5′ and 3′ untranslated sequences demonstrate an unusually high level (95% and 83%, respectively) of homology that is suggestive of possible posttranscriptional regulatory mechanisms (Mullner and Kühn, 1988; Caput et al., 1986). Like its human counterpart, the mouse gene is single-copy and intronless. Although the mouse genome does not contain recognizable α-satellite DNA, CENP-B binding occurs through the 17-bp consensus *CENP-B* box motif that is found in the mouse centromeric minor satellite DNA (Pietras et al., 1983; Rattner, 1991). In addition to mouse and humans, the *CENP-B* gene is conserved in hamster, African green monkey, great ape, tupaias, calf, Indian muntjac, and sheep (Sullivan and Glass, 1991; Haaf and Ward, 1995; Yoda et al., 1996; Bejarano and Valdivia, 1996; EMBL accession no. U35655). Significant homology is also found between CENP-B and two *S. pombe* centromere DNA-binding proteins Cbh+ and Abp1p, where *cbh+* has been shown to be an essential gene (Lee et al., 1997), while *abp1*-deleted strains exhibit slower growth and a pronounced meiotic defect (Halverson et al., 1997). The CENP-B box motif has been found in the centromeric satellite DNA of species as diverse as primates, *Mus musculus*, *Mus caroli*, tree shrews, giant panda, gerbils, and ferrets (Pietras et al., 1983; Masumoto et al., 1989; Rattner, 1991; Muro et al., 1992; Pluta et al., 1992; Yoda et al., 1992; Haaf and Ward, 1995; Kipling et al., 1995; Kipling et al., 1994; Wu et al., 1990; Volobouev et al., 1995; Choo et al., 1991; Laursen et al., 1992; Haaf et al., 1995). Based on this observed conservation of CENP-B and its DNA-binding motif, it may be speculated that CENP-B is a functionally important component of the mammalian centromere.

Through its CENP-B box-binding and dimerization properties, the protein has the hallmark of a cross-linking protein that is involved in assembly of the large arrays of centromeric α-satellite or minor satellite DNA (Yoda et al., 1992; Muro et al., 1992). However, the absence of this protein on the Y chromosome in humans and mouse (Earnshaw et al., 1987), and on the centromeres of African green monkeys, which are known to be composed largely of α-satellite DNA containing little or no binding sites for CENP-B (Goldberg et al., 1996), suggests that this role may not be universal. In other studies, the protein has been shown to be present on both the active and inactive centromeres of mitotically stable pseudodicentric human chromosomes (Earnshaw et al., 1989; Page et al., 1995; Sullivan and Schwartz, 1995), suggesting that CENP-B binding does not immediately translate into centromere activity. Furthermore, an increasing number of stable human neocentromeric marker chromosomes (Voullaire et al., 1993; Ohashi et al., 1994; Choo, 1997*b*; Depinet et al., 1997; du Sart et al., 1997) have now been described that are capable of normal mitotic division in the absence of CENP-B binding, indicating that CENP-B is nonessential for mitotic chromosome segregation, at least for these marker chromosomes. Earlier attempts at defining the role of CENP-B in mammals have yielded conflicting results. Microinjection of polyclonal anti-CENP-B antibodies into human and mouse cells resulted in disruption of centromere assembly during interphase, and led to inhibition of kinetochore morphogenesis and function in mitosis (Bernat et al., 1990; Simerly et al., 1990; Bernat et al., 1991). However, a different study has indicated that expression of truncated versions of CENP-B in HeLa cells does not lead to a mitotic or cell cycle arrest phenotype (Pluta et al., 1992). To date, the role of CENP-B in meiosis has not been investigated.

To better understand the role of CENP-B in centromere function, we used gene targeting in mouse embryonic stem cells to derive animals with a null mutation in the *CENP-B* gene. A major advantage of such mouse mutants is that it enables us to study CENP-B functions not only in mitosis, but also in meiosis. We report that *CENP-B*–deficient mice appear to be mitotically and meiotically normal, but develop lower body and testis weights. We discuss the implications of these results and propose a model in favor of a redundancy of CENP-B in centromere function.

Materials and Methods

Construction of Targeting Vectors

A hybridization probe spanning the coding region of *Cenpb* was prepared from genomic DNA of mouse embryonic stem (ES)[1] cell line E14 by PCR using primers Bprot-1 (5′-GCGCAGATCTATGGGCCCCAAGCGGC-GGCAGC-3′) and Bprot-3 (5′-TCAGAATTCAGCTTTGATGTCCA-AGACCC-3′). Screening of mouse genomic phage libraries with this

1. *Abbreviations used in this paper*: ASC, advanced sperm count; ES, embryonic stem; RT, reverse transcription.

probe resulted in the identification of a positive clone (designated E1) from a 129/OLA library (gift of M. Kennedy) of E14 cells, and a second clone (designated D1) from a 129/SV library (Stratagene) of R1 mouse ES cells. An E1-derived fragment spanning nucleotides 920–2676 of mouse *Cenpb* gene (Sullivan and Glass, 1991, EMBL accession no. X55038) was ligated with a D1-derived fragment spanning 2676–5800 and cloned into a modified pSP72 vector (Promega Corp., Madison, WI). An oligonucleotide linker sequence designated D/TAA (5′-GTACCTAGGTATACTTTTAAACTGAC-3′) was inserted at position 1207, which is 72 amino acids downstream of the ATG start site of the 1.8 kb-coding sequence of *Cenpb* (Fig. 1*b*). This linker introduced a DraI site, a frameshift mutation, and three stop codons in all three reading frames, of which TAA was in frame with Cenpb translation, disrupting not only the critical NH_2-terminal 125–amino acid centromere DNA-binding domain (Yoda et al., 1992; Kitagawa at al., 1995), but also removing all remaining COOH-terminal regions including the dimerization domain (Yoda et al., 1992; Kitagawa et al., 1995). The IRES-neomycin (Mountford et al., 1994) and IRES-hygromycin (A. Smith, personal communication) markers were separately cloned into an AvrII site at position 3202 in the 3′ untranslated region before the polyadenylation signal to produce the targeting constructs IRES(neo) and IRES(hygro), respectively.

Southern Blot and PCR Analyses of Targeting Events

Correct gene targeting in ES cells and mouse tail genomic DNA was determined by Southern analysis using a 5′ genomic probe generated from the E1 phage clone with NheI (position 564) and SacII (position 920) situated outside the targeting construct sequence (see Fig. 1 *d*). For PCR genotyping, the following primers flanking the D/TAA linker were used: Fd-1 (5′-ACCATCCTGAAGAGAACAACGG-3′) and Rev-2 (TGGAACCAAGCATGAGAGAAG), which gave 128-bp and 154-bp products for wild-type and targeted alleles, respectively; or Fd-1 and Rev-3 (3′-TGGAACCAAGCATGAGAAG-5′), which gave a 173-bp and 199-bp product for wild-type and targeted alleles, respectively (see Fig. 1, *d* and *g*). PCR conditions were as follows: 95°C for 30 s, 55°C for 1 min, and 72°C for 1.5 min for a total of 35 cycles using a 50-μl vol containing 50–200 ng genomic tail DNA, 1 U Taq polymerase, 200 μM dNTPs, and 300 ng of each primer in 1 X Taq PCR buffer (Perkin-Elmer Corp., Norwalk, CT).

Generation of Targeted ES Cells and Mouse Chimeras

For transfection, 50 μg of the IRES(neo) construct was linearized at the 3′ end with AatII or SspI, or at the 5′ end with SacII, and electroporated into approximately 10^8 ES cells in 800 μl vol using a single pulse from a Bio-Rad Gene Pulser at 800 V, 3 μFD, ∄Ω. The ES cell lines used in this study were R1 (Nagy et al., 1993), W9.5, and W9.8 (Buzin et al., 1994). Transfected cells were plated onto mitomycin C-treated, neomycin-resistant, STO-neo^R (Robertson, 1987) plus 10^3U/ml LIF (Amrad-Pharamacia) and selected in G418 (Gibco-BRL) active at 300 μg/ml. One R1-derived G418-resistant colony, designated R1–26, demonstrated correct targeted disruption at the *Cenpb* allele, and was used for blastocyst injection to produce germline chimeric mice and for a second round of gene targeting to produce double-targeted, Cenpb-null cell lines in culture.

For chimeric mouse production, R1–26 cells were microinjected into host (C57 bla/6) blastocysts, followed by breeding of the resulting germline transmitting chimeras to generate heterozygous and homozygous Cenpb-null mice. For the second targeting event, the R1–26 cells were electroporated with 50 μg of the IRES(hygro) construct that has been linearized at the 3′ end with SspI. Transfected cells were grown in the absence of STO fibroblast feeder layer, and were selected in 300 μg/ml G418 and 110–140 μg/ml hygromycin. This resulted in a Cenpb-null cell line, designated R1–189N/H, in which both the *Cenpb* alleles were disrupted. This cell line was injected into C57 bla/6 blastocysts, and the resulting germline chimeras were used in a back-cross with C57 black mice to allow segregation of the two targeted alleles and the derivation of heterozygous and homozygous mouse strains carrying only the IRES(hygro)-targeted allele. In this way, mice with two independently targeted *Cenpb* alleles were generated.

Reverse Transcription (RT)-PCR Analysis and Sequencing

Total genomic RNA was extracted from wild-type R1 cells (+/+), the IRES(neo)-targeted cell line R1–26 (+/−), and the double-targeted cell line R1-189N/H (−/−). 0.5–1.0 μg total RNA was reverse-transcribed using a first-strand RT kit (Boehringer Mannheim Corp., Indianapolis, IN) and oligo-d(T) as primer. Annealing was carried out at room temperature for 10 min, followed by transcription at 42°C for 60 min and cooling at 4°C for 5 min. PCR was then performed on +/+, +/−, and −/− cell lines using conditions described for primers Fd-1 and Rev-2/Rev-3. For sequencing, the 199-bp Fd-1/Rev-3 PCR product from the −/− cell line was gel-isolated and cloned into the pGEM-T vector (Promega Corp., Madison, WI). Sequencing was performed on both strands in two separate clones using M13 Rev and T7 primers. Reactions were carried out using fluorescent dye terminator cycle sequencing (ABI PRISM™; Perkin-Elmer Corp., Norwalk, CT).

Immunohistochemistry

Autoimmune serum CREST no. 6 (gift of S. Wittingham and T. Kaye) was from a patient with calcinosis, Raynaud's phenomenon, esophageal dysmotility, sclerodactyly, and telangiectasia (Fritzler et al., 1980; Moroi et al., 1981; Brenner et al., 1981) and detects CENP-A and CENP-B (du Sart et al., 1997). Anti-CENP-B monoclonal antibody 2D-7 (Earnshaw et al., 1987) was purchased as hybridoma cells from American Type Culture Collection (Rockville, MD) and prepared as ascites fluid in pristane primed mice. Anti-Cenpc polyclonal antibody, Am-C1, was produced in a rabbit against a mouse Cenpc/GST-fusion product expressed in *Escherichia coli* (du Sart et al., 1997). Antihuman CENP-E antibody, HX1, was a gift from T. Yen (Yen et al., 1991; Yen et al., 1992). Cultured cells were arrested in mitosis with 10 μg/ml colcemid for 2 h. Immunofluorescence staining was performed as previously described (Jeppeson et al.,1992; du Sart et al., 1997). After the antibody binding, the cells were postfixed in 10% formalin, washed, and counterstained with DAPI and DABCO mountant. Images were analyzed using an Axioskop fluorescence microscope equipped with a 100× objective (Carl Zeiss, Inc., Thornwood, NY) and a cooled CCD camera (Photometrics Image Point) linked to a PowerMac computer.

Histology, Advanced Sperm Count (ASC), and Stereology

The organs analyzed for histology were dissected from 10-wk-old and 6 mo-old mice using standard techniques. Testicular determination of homogenization-resistant ASC was performed as previously described (Robb et al., 1978) on 10-wk-old animals. Stereological analysis was performed on testicular materials from 10-wk-old mice using the optical dissector (sic) technique (Wreford et al., 1995) to investigate the efficiency of meiosis by determining the ratio of pachytene spermatocytes to round spermatids associated with stages I–VIII of spermatogenesis. This ratio has an expected value of 4:1 if the efficiency of division through meiosis I and II is 100% and there is no loss of round spermatids after meiosis.

Cytogenetics and Flow Sorting

For karyotyping, −/− R1-189 N/H cell line as well as spleen and bone marrow cell cultures (with and without phytohaemagglutinin) were isolated from −/− mice and compared with the +/+ cell line and +/+ animal. Cells were treated with colcemid and GTL-stained using standard cytogenetic techniques. For flow sorting, 50,000 cells from spleen, bone marrow, or testis were isolated from 30-wk-old mice. These were analyzed by two-parameter analysis of DNA content vs. cell diameter using a FACScan™ (Becton Dickinson & Co., Sparks, MD) cell sorter equipped with an argon laser at 488 nm. Signals were collected by a FL2 detector with a 585-nm band pass filter. Testis cells were profiled into five main regions corresponding to the different steps in maturation from elongated and round haploid spermatids to diploid, S-phase, and tetraploid cells.

Results

Generation of Cenpb-null ES Cells and Mice

For disruption of the mouse *Cenpb* gene in ES cells, a promoterless targeting vector was constructed that incorporated a translation frame-shift linker, designated D/TAA, containing stop codons in all three reading frames, and the IRES-neomycin or IRES-hygromycin marker (Fig. 1 *b* and Methods). The D/TAA linker inserted 72 amino acids

downstream of the translation start site not only disrupted the critical NH_2-terminal 125–amino acid centromere DNA-binding domain (Kitagawa et al., 1995; Yoda et al., 1992), but also removed all remaining COOH-terminal regions including the dimerization domain (Kitagawa et al., 1995; Yoda et al., 1992). The IRES-neo and IRES-hygro selectable markers were placed in the 3′ untranslated region before the polyadenylation signal. For correct targeting and gene disruption, two homologous recombination events external to the linker and IRES(neo/hygro) regions were required (Fig. 1 *b*, solid-cross regions). When the IRES(neo) construct was linearized at the 3′ end with AatII or SspI and transfected into R1 and W9.5 cells, 2% (or 2 out of 103 neomycin resistant colonies) of R1 cells, 1.3% (1 out of 72 colonies) of W9.8, and 3.5% (12 out of 344 colonies) of W9.5 cells gave the desired targeted gene disruption (Fig. 1 *e*, lane *5*). Interestingly, a significantly higher frequency (90% for R1, 67% for W9.8, and 92% for W9.5) of an undesired targeting event was detected (Fig. 1 *e*, lanes *2*, *4*, *6*, and *7*) where incorporation of the IRES-neo element at the *Cenpb* locus had not been accompanied by the D/TAA linker. This result was due to recombinations occurring within the region between the IRES-neo cassette and the D/TAA linker (Fig. 1 *b*, broken-cross region) instead of in the region 5′ of the linker. The observation of a higher recombination frequency in this region was perhaps not surprising in view of the fact that 1995 bp of homologous DNA was present in this region compared with only 287 bp of homologous DNA between the D/TAA linker and the 5′ end of the construct. In subsequent experiments, it was further demonstrated that use of construct DNA linearized at the 5′ end using KspI to expose the *Cenpb* DNA end, as distinct from the plasmid vector DNA end using 3′ AatII or SspI, gave a 2.5-fold increase in the frequency of the desired targeting in R1 cells and a 3.8-fold increase in W9.5 cells (data not shown).

From the above screening, 21 heterozygous ES cell colonies with a disrupted *Cenpb* allele were obtained from the R1, W9.5, and W9.8 cell lines. Two of these colonies, R1-26 from the R1 line and W-190 from the W9.8 cell line, were retransfected with the IRES(hygro) construct to obtain a Cenpb null cell line. Selection of the transfected cells in neomycin and hygromycin gave rise to one double-targeted colony (out of five resistant colonies screened) designated R1-189N/H from R1-26, and two double-targeted colonies (out of 76 colonies screened) from W-190. All three colonies showed normal cell morphology and apparently normal growth rates. No desired double-targeted event (0 out of 81 colonies) were seen for both W9.8 and R1 when the transfected cells were selected in hygromycin alone, due presumably to a direct replacement of the IRES(neo)-targeted allele with the IRES(hygro) cassette. Furthermore, as with the IRES(neo) construct, a much higher frequency (three out of five colonies for R1-26, and 57 out of 76 colonies for W-190) of the undesired targeting event involving the loss of the D/TAA linker was observed.

The heterozygous R1-26 cell line was injected into C57 bla/6 blastocysts to produce germline chimeras, from which heterozygous (+/− neo) and homozygous (−/− neo) mice carrying the IRES(neo)-targeted allele were produced (Fig. 1 *f*). The double-targeted R1-189N/H cell line was similarly injected into C57 bla/6 blastocysts and, through selective breeding, heterozygous (+/− hygro) and homozygous (−/− hygro) mice carrying the IRES (hygro) allele were generated (data not shown). These mice, together with the various cell lines created above, were subjected to further detailed studies.

Abolition of Cenpb Gene Expression in the Targeted Cell Lines

Cenpb gene disruption was determined by RNA analysis using PCR performed with primers designed across the D/TAA linker region. The results (Fig. 1 *g*) indicated the presence of normal *Cenpb* transcripts in the wild-type (Fig. 1 *g*; lanes *1* and *4*) and heterozygous cell lines (lanes *2* and *5*), but not in the double-targeted R1-189N/H cell line (lanes *3* and *6*). This result suggested that transcription of both copies of the wild-type *Cenpb* alleles in the −/− cell line had been abolished and replaced by that of the targeted alleles. In addition, we wished to determine whether the D/TAA linker had incorporated correctly into the NH_2-terminal centromere DNA-binding domain of the targeted *Cenpb* gene, and that no unforeseen sequence rearrangement undetected by the Southern or RT-PCR analyses had occurred. This was done by purifying and cloning the 199-bp fragment corresponding to the targeted allele (Fig. 1 *g*, lane *6*) and direct sequencing analysis. The results (not shown) confirmed the correct insertion of the D/TAA linker and therefore the stop codons.

Absence of Cenpb Binding on Centromeres by Direct Immunofluorescence Staining

Immunofluorescence staining of metaphase chromosomes was used to detect specific centromere-binding proteins. Fig. 2 shows results obtained with the +/+ R1 and −/− R1-189N/H cell lines; the results for the +/− R1-26 cell line were similar to those of the +/+ R1 cell line, and are not shown. The anti-*Cenpb* monoclonal antibody clearly demonstrated the presence of *Cenpb* on the centromeres of the +/+ cell line, but not on those of the −/− cell line. The intensity of the Cenpb signals in the +/+ cells varied considerably on different chromosomes, reflecting the intrinsic quantitative variation in the amount of *Cenpb* boxes and *Cenpb* binding on different centromeres (Earnshaw et al., 1987). When these cell lines were tested with a CREST antibody and antibodies for Cenpc and CENP-E, uniform staining of the centromere was observed (Fig. 2). Similar results (not shown) were obtained with cells established from the +/+, +/−, and −/− IRES(neo) and IRES(hygro) mice. These data therefore provided direct evidence that the *Cenpb* gene has been disrupted in the −/− neo and −/− hygro knockout mice. They also demonstrated that Cenpb is not essential for centromeric binding of Cenpc and Cenpe and for CREST antibody binding on active centromeres.

Cenpb Null Mice Have Lower Body Weight and Testis Size, but Are Otherwise Developmentally Normal

Cenpb null mice appeared phenotypically normal, and routinely gave normal litter size and the expected Mendelian ratios of offspring, suggesting that Cenpb deficiency

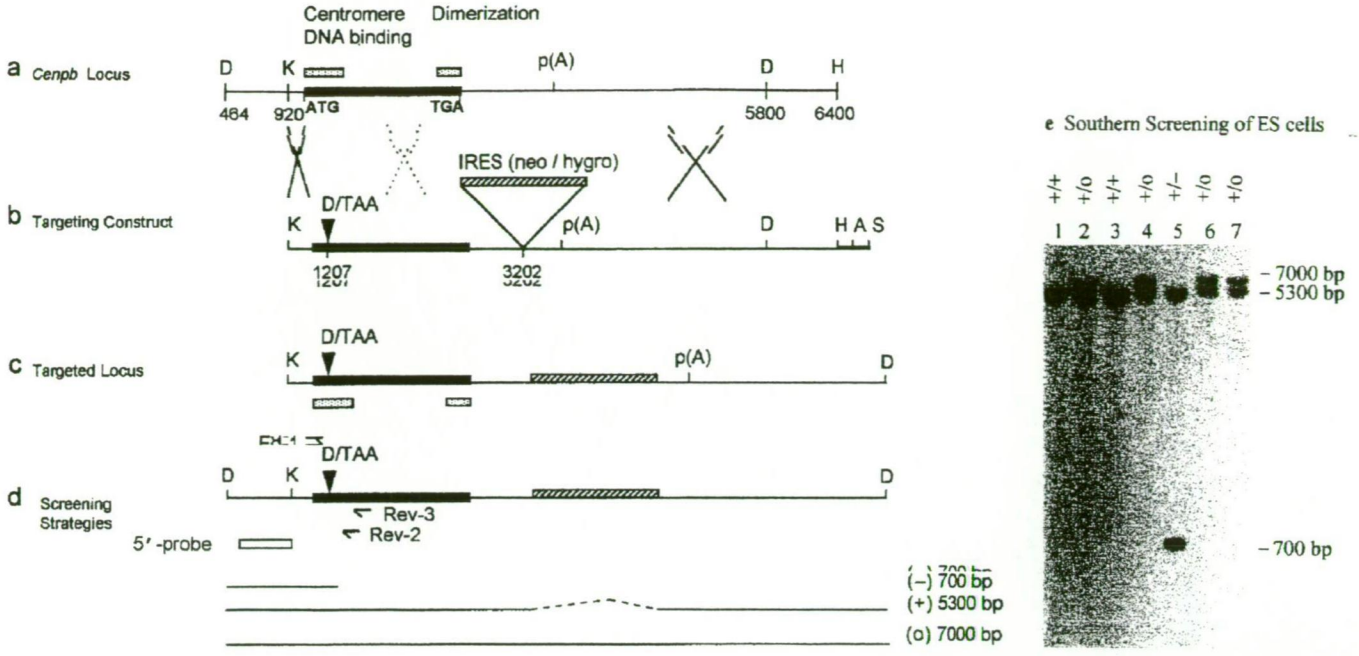

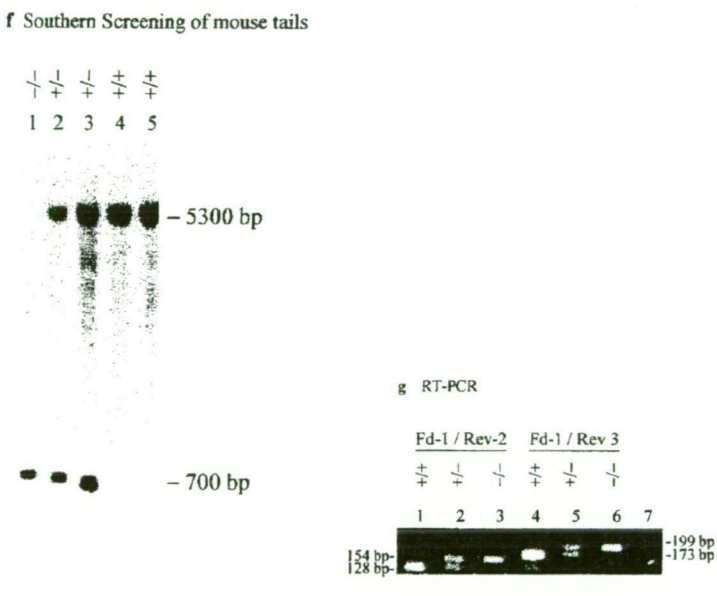

Figure 1. Cenpb targeting construct and screening strategies. (*a*) Intronless wild-type *Cenpb* locus showing the start and stop codons of the 1.8-kb coding region (*solid box*). The positions of the NH_2-terminal 125–amino acid centromere DNA-binding domain and the COOH-terminal 59–amino acid dimerization domain are indicated (*stippled boxes*). Numbers below the line indicate nucleotide positions of the *Cenpb* sequence (EMBL accession no. X55038). (*b*) The IRES(neo) and IRES(hygro) targeting constructs, showing a 5480-bp contiguous KspI/HindIII *Cenpb* fragment that is interrupted by a frame shift-linker (*D/TAA*) containing stop codons and a new DraI site within the centromere DNA-binding domain, and an IRES(neo or hygro) cassette within the 3′ untranslated region. The H-A-S region on the right is vector DNA. Solid crosses denote the preferred regions of homologous recombination that result in the desired gene disruption event shown in *c*, whereas the broken cross indicates an undesired alternative region of recombination which, together with that at the solid-cross region to the right, results in incorporation of the IRES(neo or hygro) cassette, but not the D/TAA linker, generating a targeted event that is not accompanied by a gene disruption. p(A), polyadenylation signal; D, DraI; K, KspI; H, HindIII; A, AatII; S, SspI. (*c*) Correctly targeted *Cenpb* allele. (*d*) Screening strategies for targeted events. In Southern analysis of DraI digests, the 5′-probe (*open box*) detects a wild-type allele (+) of 5,300 bp, a desired targeted gene disruption allele (−) of 700 bp, and an undesired targeted but undisrupted allele (o) of 7,000 bp. Fd-1 and Rev-2/Rev-3 are PCR primers flanking the D/TAA linker region used for mouse tail DNA genotyping and RT-PCR. (*e*) Southern blot screening of transfected ES cells digested with DraI using the 5′-probe. Lane *5* shows a heterozygous colony with the desired gene disruption event. (*f*) Southern blot screening of tail DNA from mouse progeny of a +/− × +/− cross, digested with DraI and probed with the 5′-probe, showing the detection of homozygous *Cenpb* disruption (lane *1*), heterozygous mice (lanes *2* and *3*), and wild-type animals (lanes *4* and *5*). (*g*) RT-PCR of total RNA from +/+ R1, +/− IRES(neo)-targeted R1-26, and −/− IRES(neo) and IRES(hygro) double-targeted R1-189N/H cells using the Fd-1/Rev-2 (lanes *1–3*) and Fd-1/Rev-3 (lanes *4–7*) primer sets. Incorporation of the D/TAA linker in the targeted allele increases the PCR products for both primer sets by 26 bp compared with the wild-type allele. Only the larger band containing the D/TAA linker was detected in the −/− cells (lanes *3* and *6*). Lane *7*, PCR control with no RNA.

did not drastically affect cell division, development, and reproduction of the mice. This phenotype is in stark contrast to that of another mouse model we have recently created with a disruption of *Cenpc*, where null mutants display severe mitotic disarray and die during early embryogenesis (Kalitsis et al., 1998). To determine if *Cenpb* gene disruption has a more subtle effect on growth, we measured the body weight of the IRES(neo) animals over an 8-mo period (Fig. 3). The −/− mice as a group appeared uniform in size at birth, and presented with normal weights at weaning (3 wk), but subsequent weight gain in this group lagged behind those of sex-matched +/+ and +/− animals,

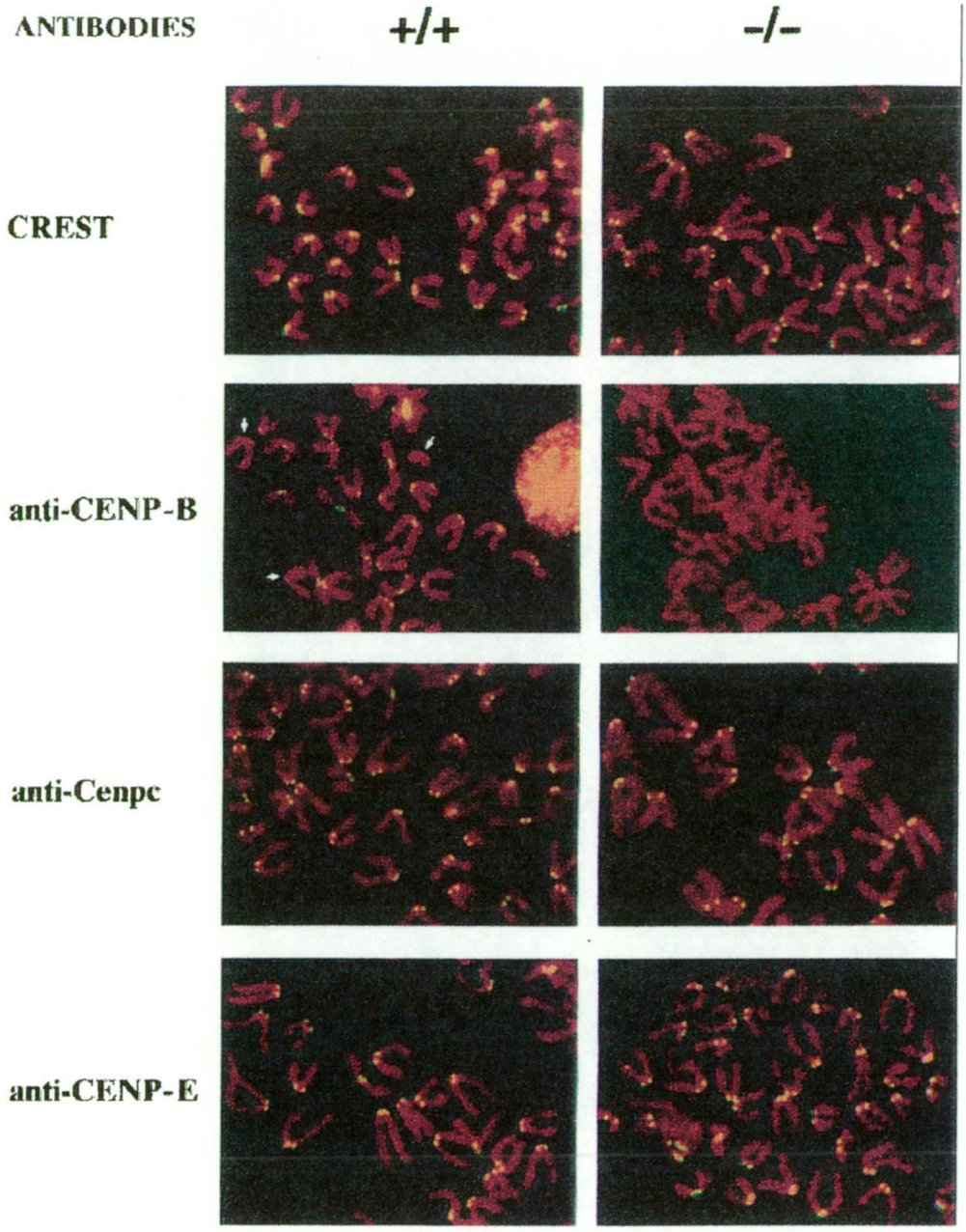

Figure 2. Immunostaining of centromere proteins (*yellow signals*) in +/+ R1 and −/− R1-189N/H cell lines using anticentromere antibodies. Results for the +/− R1-26 cell line were similar to those for the +/+ cell line and are not shown. Uniform signals were observed in all the centromeres in both cell lines when stained with CREST, anti-Cenpc, and anti-CENP-E antibodies. Note differences in the intensity of anti-CENP-B staining on different chromosomes in the +/+ cell line, with some centromeres (*arrows*) showing little or no detectable signals. No Cenpb signal was seen on the centromeres of the −/− cell line, even after maximal enhancement of fluorescence signal (thus the paler background) using computer imaging facility.

with the difference reaching a level of significance ($P < 0.05$) after 22 wk in males and 12 wk in females (see Table I for representative weight data for 26-wk-old animals). When the weight data were collected from the IRES(hygro) animals, similar trends as those obtained for the IRES(neo) mice were seen for the different genotypes in the two sexes (data not shown).

Histological Analysis Reveals No Gross Abnormality

To investigate the reasons for the observed weight difference, various organs from the IRES(neo)-targeted animals were subjected to histological examination. The organs analyzed were stomach, duodenum, descending colon, liver, hairy skin, ear flap, salivary gland, spleen, pancreas, kidney, thymus, brain, lung, adrenal, seminal vesicle, ovary, uterus, and pituitary. When organs from 10-wk- and 6-mo-old male and female −/− mice were directly compared with those derived from age- and sex-matched +/+ and +/− animals, the results indicated no obvious abnormality in any of these organs. During this analysis, the testes of −/− mice were found to be markedly smaller (29%; $P < 0.01$) than those of the wild-type mice (Table I). Follicle-stimulating hormone (FSH) and luteinizing hormone (LH) levels were measured and found to be normal. When the testes of 10-wk-old animals were assessed for sperm content (ASC), a 39.5% reduction ($P = 0.0007$) was seen in the −/− animals ($N = 9$) compared with the +/+ animals ($N = 12$). When the efficiency of meiosis was determined using the more comprehensive stereological analysis on sectioned testicular materials from +/+ ($N = 5$), +/− ($N = 6$), and −/− ($N = 4$) mice, values of 3.9 ± 0.2 (mean ± SEM), 3.8 ± 0.1,

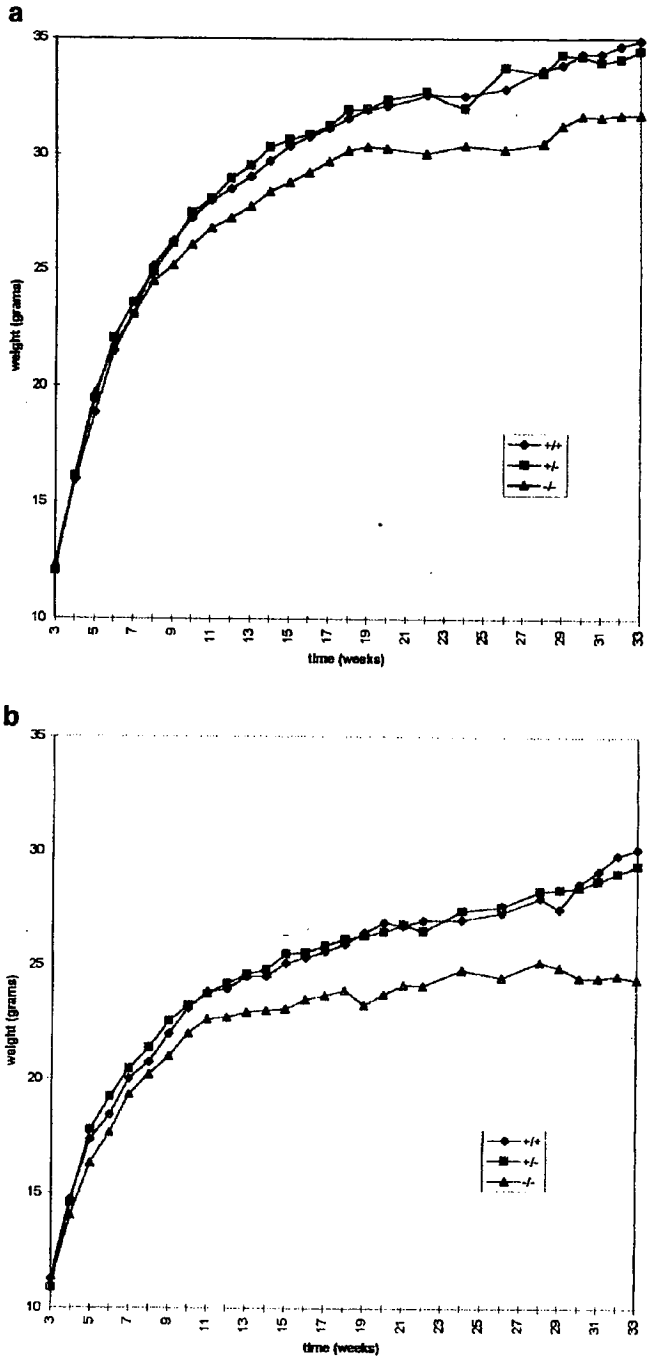

Figure 3. Total body weight of male (*a*) and female (*b*) IRES(neo) mice. The male data were collected from an average of 33, 46, and 19 animals, whereas the female data were from an average of 24, 39, and 17 animals for each time point for the +/+, +/−, and −/− genotypes, respectively. Individual weight value, measured weekly or fortnightly, represents the means of the weights for the total number of animals used at that time point.

and 3.6 ± 0.2, respectively, were obtained, which were not significantly different from the expected 4:1 ratio. Thus, although it appears that reduction in germ cell content is correlated with testicular weight reduction, results of the stereological analysis have revealed no substantial difference in the efficiency of either mitotic or meiotic division.

Table I. Total Body Weight of IRES(neo) Mice at 26 wk.(b) Total Testis Weight of IRES(neo) Mice at 10 wk

	No.	Weight ± SD	*t* test
		g	
(*a*) Male (body)			
+/+	34	32.86 ± 3.58	+/+ vs. +/− (P = 0.2469)
+/−	54	33.75 ± 3.45	+/− vs. −/− (P = 0.0002)
−/−	19	30.25 ± 3.29	+/+ vs. −/− (P = 0.0114)
Female (body)			
+/+	22	27.36 ± 3.79	+/+ vs. +/− (P = 0.7786)
+/−	37	27.62 ± 3.16	+/− vs. −/− (P = 0.0005)
−/−	17	24.45 ± 2.06	+/+ vs. −/− (P = 0.0079)
(*b*) Male (testis)			
+/+	15	0.208 ± 0.029	+/+ vs. +/− (P = 0.27743)
+/−	18	0.195 ± 0.036	+/− vs. −/− (P = 0.00255)
−/−	16	0.154 ± 0.038	+/+ vs. −/− (P = 0.00012)

Karyotyping and Flow Sorting of Cenpb−/− Cells Indicate Normal Meiosis and Mitosis

The chromosomes of the *Cenpb*-disrupted cells were investigated by cytogenetic analysis and flow sorting. For cytogenetic analysis, ES-derived R1-189 N/H −/− cells in culture and spleen and bone marrow cells from 30-wk-old −/− mice (N = 4) were analyzed and compared with the wild-type ES cells and animal. The results indicated a normal karyotype in each case. For flow sorting, 50,000 cells from the spleen, bone marrow, or mitotically and meiotically dividing testis cells were isolated from +/+ (N = 8), +/− (N = 13), and −/− (N = 7) 10-wk-old mice, and +/+ (N = 3), +/− (N = 1), and −/− (N = 8) 30-wk-old mice. Again, no detectable aberration was observed. These results, together with those obtained using the stereological techniques, provide further evidence that Cenpb is not essential for mitosis or meiosis.

Discussion

The question of whether CENP-B is essential for chromosome segregation has been intensely debated in recent years. Conservation of the protein in different mammalian species and in lower eukaryotes and its demonstrated centromere DNA-binding property attest to a significant functional role. However, various cytological observations have hinted at CENP-B not being critical for mitosis, although such evidence are often indirect and open to interpretation. For example, detection of CENP-B on both the active and inactive centromeres of mitotically stable pseudodicentric human chromosomes (Earnshaw et al., 1989; Page et al., 1995; Sullivan and Schwartz, 1995), rather than indicating a lack of functional importance for CENP-B, can be interpreted to mean that additional centromere proteins are necessary to make the inactive centromere fully active. Similarly, the finding that the protein is absent on the Y chromosome in both humans and mouse (Earnshaw et al., 1987) is intriguing but needs to be interpreted in light of the unresolved peculiarity that this observed absence is associated with the only centromere in these genomes that does not undergo sister centromere pairing in meiosis. The absence of CENP-B on various analphoid neocentromeres (Choo, 1997*b*) also does not per se exclude functions for CENP-B (or α-satellite DNA) on normal centromeres

since these neocentromeres may have gained centromere function through some epigenetic modifications (Karpen and Allshire, 1997). Finally, the observation that the α-satellite DNA-containing centromeres of African green monkey lacks binding sites for CENP-B (Goldberg et al., 1996) could be because monkeys have evolved a different and functionally equally important way to compensate for their CENP-B deficiency.

In addition to the uncertainty on mitotic functions, the requirement of CENP-B in meiosis has also not previously been investigated. Such an investigation is especially important in light of recent evidence indicating a specific role of centromeric heterochromatin in meiotic chromosome segregation in *Drosophila* (Dernburg et al., 1996; Karpen et al., 1996), and in view of the fact that CENP-B binds directly to centromeric heterochromatic DNA and is thought to be involved in the higher order organization of this DNA (Yoda et al., 1992; Muro et al., 1992). The production and characterization of Cenpb null mice allows several conclusions regarding the functional significance of this protein in mitosis and meiosis to be drawn. The apparently normal growth and reproductive characteristics of these mice indicate that Cenpb is not essential for either of these cell division processes. This result is confirmed by direct cytogenetic and FACS analyses of chromosomes, which have not detected any karyotypic abnormality in the −/− mice. A closer look at the different stages of male meiosis in these animals has similarly not revealed any obvious defect. The protein also appears not to be required for the structural integrity of the centromere–kinetochore complex since the centromeres of Cenpb-deficient cells continue to show clear association with at least two of the functionally important centromere proteins: Cenpc and Cenpe. The observation that Cenpb is not essential for mitosis or meiosis therefore drastically contrasts the severe phenotypes previously reported for the *cbh+* and *abp1* null yeast strains (Halverson et al., 1997; Lee et al., 1997), suggesting that the functions of these homologues have diverged significantly.

Despite the lack of any detectable mitotic and meiotic phenotype, adult Cenpb null mice are significantly smaller in body weight compared with age- and sex-matched wild-type or heterozygous mice. In addition, the −/− male testes show a pronounced reduction both in weight (by 30%) and in total sperm count (by 39.5%) compared with wild-type animals. Extensive histological analysis of many different organs and direct measurement of FSH and LH hormones have not revealed any abnormality. It is possible that the absence of CENP-B may have a subtle effect on centromere assembly and function, and result in a slight reduction in the rate of progression through one or more phases of the cell cycle, in the efficiency of chromosome capture by microtubules, and/or chromosome movement. Alternatively, a small number of cells beyond our detection ability may not enter mitosis at all, or carry severe chromosomal abnormality, resulting in loss of valuable cells from the cycling cell population sufficiently to cause a significant weight reduction over time. The possibility that the weight phenotype is caused by some as yet unidentified hormonal or metabolic factors cannot be discounted at present.

In formulating any model on the role of CENP-B, the following observations need to be taken into consideration: (*a*) the protein is highly conserved in divergent mammals; (*b*) the protein binds centromeric repetitive DNA via the CENP-B-box motif and possesses dimerization properties that allow the protein to cross-link centromeric repeats (Yoda et al., 1992; Muro et al., 1992); (*c*) CENP-B box and CENP-B protein are not detected on human and mouse Y chromosomes, and are poorly represented on centromeric subdomains of certain human chromosomes (e.g. α13-II, α14-II, and α21-II domains of chromosomes 13, 14, and 21; Trowell et al., 1993; Ikeno et al., 1994; Choo, 1997a); (*d*) the centromeres of African green monkey are composed largely of α-satellite DNA containing few if any binding sites for CENP-B (Goldberg et al., 1996); (*e*) the protein is found on both active and inactive centromeres of dicentric chromosomes (Earnshaw et al., 1989); (*f*) despite the lack of CENP-B binding, human neocentromeres derived from noncentromeric chromosomal regions display full mitotic functions (Voullaire et al., 1993; Depinet et al., 1997; du Sart et al., 1997; Choo, 1997*b*); and (*g*) the protein is neither essential for mitosis nor meiosis in Cenpb knockout mice.

Based on the sequence similarity between CENP-B and certain transposases, Kipling and Warburton (1997) suggested that CENP-B may share the DNA strand cleavage function of transposases and promote nicks adjacent to CENP-B boxes to facilitate the evolution and maintenance of satellite DNA. This model does not, however, take into consideration the dimerization property of CENP-B, offers no direct evidence for the proposed strand cleavage function, and cannot explain the absence of CENP-B on human and mouse Y chromosomes or the paucity of this protein on the α-satellite–containing centromeres of African green monkey and centromeric subdomains of at least some human chromosomes. Here we present a different model that satisfies all the reported observations. Simply stated, we propose that the role of CENP-B is to organize structurally the great abundance of repetitive DNA found in the centromere, with this role neither being exclusive to CENP-B nor directly essential or sufficient for centromere function. Our model further implicates the existence of a functionally related but perhaps lower-affinity protein, arbitrarily designated CENP-Z, that can perform a similar function to CENP-B in its absence (Fig. 4). The proposal of a role for CENP-B in organizing centromeric repeats is based on the biochemical (observation *b* above), cytogenetic (observation *e* above), and, indirectly, evolutionary (observation *a* above) properties of the protein. The suggestion that this role is not exclusive to CENP-B is based on the fact that centromeric repetitive DNAs with little or no CENP-B binding (observations *c*, *d* and *g* above) are nonetheless organized in a way that is compatible with centromere function. The suggestion that CENP-B is neither essential nor sufficient for centromere function is evident from the fact that the protein can be totally absent on centromeres without detrimental effects on chromosome segregation (observations *c*, *d*, *f*, and *g* above), and that its mere presence on some centromeres does not immediately lead to centromere activity (observation *e* above).

A nuclear protein, pJα (Gaff et al., 1994), has previously been described that binds a 9-bp sequence motif, GTG(G/A)AAAAG, that is present as an alternative nucleotide

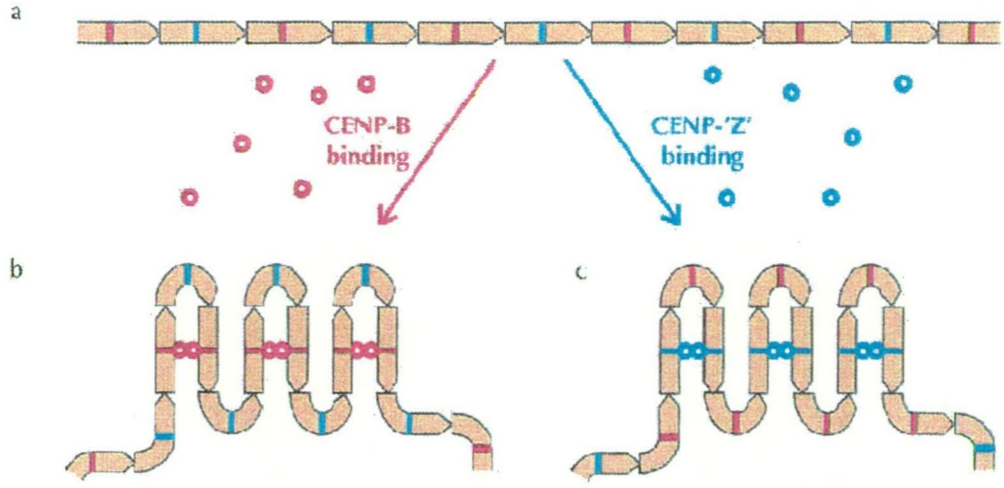

Figure 4. Model depicting the role of CENP-B and its putative functional homolog CENP-Z. (*a*) A centromeric satellite DNA array, showing individual monomers containing either a CENP-B-box (*red bar*) or a CENP-Z-box motif (*blue bar*). (*b*) CENP-B proteins (*red circles*) bind to CENP-B-box motifs and undergo dimerization to cross-link the array into a more stable higher order configuration. This mode of organization is presumably found on chromosomes where CENP-B boxes are prevalent, including the human and mouse autosomes and X chromosomes. (*c*) In the absence of CENP-B-binding, a functionally related protein CENP-Z (*blue circle*) assumes the role of CENP-B to cross-link CENP-Z box–containing monomers. This mode of organization is suggested for the human and mouse Y chromosomes, various CENP-B box-poor centromeric subdomains, and the centromeres of African green monkey and Cenpb null mice.

configuration to the CENP-B-box motif on a significant proportion (~14%) of α-satellite monomers, including those that constitute the centromere of the human Y chromosome and the various CENP-B box-poor human centromeric subdomains (Tyler-Smith and Brown, 1987; Alexandrov et al., 1993; Vissel and Choo, 1992; Romanova et al., 1996). A recent study has further demonstrated that pJα box-containing α-satellite monomers are the primordial DNA from which the CENP-B box-containing monomers arose (Romanova et al., 1996). In preliminary studies, we have detected pJα proteins in the nuclear extracts of the +/+, +/−, and −/− Cenpb knockout mice, and in that of the African green monkey (D.F. Hudson and K.H.A. Choo, unpublished data). In addition, the consensus sequence for the CENP-B box-poor α-satellite DNA of African green monkey has been shown to contain a perfectly conserved pJα-box motif GTGAAAAAG (Yoda et al., 1996). These analyses therefore suggest that pJα may be a suitable candidate for the proposed CENP-Z protein. The availability of the Cenpb null mice should provide an amenable system to allow the further study of the role of Cenpb, as well as investigation of the proposed CENP-Z protein.

We thank L. Robertson, J. Mann, and S. Delaney for STO-Neo^R, W9.5, W9.8, and R1 cell lines, T. Yen, S. Wittingham, and T. Kaye for antibodies, P. Mountford and A. Smith for IRES-neo and IRES-hygro markers, S. Gazeas and R. Breslin for mouse breeding, R. O'Dowd for technical assistance, C.W. Chow for histology, S. Bol and A. Fryga for flow sorting, A. O'Connor for DSP assay, L. Wilton and S. Pompolo for tissue dissection, and Qing Song for stereology. This work was supported by the National Health and Medical Research Council of Australia. KHA Choo is a Senior Associate of the Univeristy of Melbourne and a Principal Research Fellow of the National Health and Medical Research Council of Australia.

Received for publication 12 January 1998 and in revised form 25 February 1998.

References

Alexandrov, I.A., L.I. Medvedev, T.D. Mashkova, L.L. Kisselev, L.Y. Romanova, and Y.B. Yurov. 1993. Definition of a new alpha satellite suprachromosomal family characterized by monomeric organization. *Nucl. Acids Res.* 21:2209–2215.

Bejarano, L.A., and M.M. Valdivia. 1996. Molecular cloning of an intronless gene for the hamster centromere antigen CENP-B. *Biochim. Biophys. Acta.* 1307:21–25.

Bernat, R.L., G.G. Borisy, N.F. Rothfield, and W.C. Earnshaw. 1990. Injection of anticentromere antibodies in interphase disrupts events required for chromosome movement in mitosis. *J. Cell Biol.* 111:1519–1533.

Bernat, R.L., M.R. Delannoy, N.F. Rothfield, and W.C. Earnshaw. 1991. Disruption of centromere assembly during interphase inhibits kinetochore morphogenesis and function in mitosis. *Cell.* 66:1229–1238.

Brenner, S., D. Pepper, M.W. Berns, E. Tan, and B.R. Brinkley. 1981. Kinetochore structure, duplication and distribution in mammalian cells: analysis by human autoantibodies from scleroderma patients. *J. Cell Biol.* 91:95–102.

Brinkley, B.R., I. Ouspenski, and R.P. Zinkowski. 1992. Structure and molecular organization of the centromere-kinetochore complex. *Trends Cell. Biol.* 2:14–21.

Brown, M. 1995. Sequence similarities between the yeast chromosome segregation protein Mif2 and the mammalian centromere protein CENP-C. *Gene.* 160:111–116.

Brown, M.T., L. Goetsch, and L.H. Hartwell. 1993. MIF2 is required for mitotic spindle integrity during anaphase spindle elongation in Saccharomyces cerevisiae. *J. Cell Biol.* 123:387–403.

Buzin, C.H., J.R. Mann, and J. Singer-Sam. 1994. Quantitative RT-PCR assays show Xist RNA levels are low in mouse female adult tissue, embryos and embryoid bodies. *Development.* 120:3529–3536.

Caput, D., B. Beutler, K. Hartog, R. Thayer, S. Brown-Shimer, and A. Cerami. 1986. Identification of a common nucleotide sequence in the 3'-untranslated region of mRNA molecules specifying inflammatory mediators. *Proc. Natl. Acad. Sci. USA.* 83:1670–1674.

Choo, K.H.A. 1997*a*. The Centromere. Oxford University Press, Oxford, United Kingdom. 304 pp.

Choo, K.H.A. 1997*b*. Centromere DNA dynamics: latent centromeres and neocentromere formation. *Am. J. Hum. Genet.* 61:1225–1233.

Choo, K.H.A., B. Vissel, A. Nagy, E. Earle, and P. Kalitsis. 1991. A survey of the genomic distribution of alpha satellite DNA on all human chromosomes and derivation of a new consensus sequence. *Nucl. Acids Res.* 19:1179–1182.

Cooke, C.A., R.L. Bernat, and W.C. Earnshaw. 1990. CENP-B: a major human centromere protein located beneath the kinetochore. *J. Cell Biol.* 110:1475–1488.

Depinet, T.W., J.L. Zackowski, W.C. Earnshaw, S. Kaffe, G.S. Sekhon, R. Stallard, B.A. Sullivan, G.H. Vance, D.L. VanDyke, H.F. Willard, et al. 1997. Characterization of neo-centromeres in marker chromosomes lacking detectable alpha-satellite DNA. *Hum. Mol. Genet.* 6:1195–1204.

Dernburg, A.F., J.W. Sedat, and R.S. Hawley. 1996. Direct evidence of a role of heterochromatin in meiotic chromosome segregation. *Cell.* 86:135–146.

du Sart, D., M.R. Cancilla, E. Earle, J. Mao, R. Saffery, K.M. Tainton, P. Kalitsis, J. Martyn, A.E. Barry, and K.H.A. Choo. 1997. A functional neo-centromere formed through activation of a latent human centromere and consisting of non-alpha-satellite DNA. *Nat. Genet.* 16:144–153.

Earnshaw, W.C., and A.M. MacKay. 1994. Role of nonhistone proteins in the chromosomal events of mitosis. *FASEB J.* 8:947–956.

Earnshaw, W.C., H. Ratrie, and G. Stetten. 1989. Visualization of centromere proteins CENP-B and CENP-C on a stable dicentric chromosome in cytological spreads. *Chromosoma.* 98:1–12.

Earnshaw, W.C., and N. Rothfield. 1985. Identification of a family of human

centromere proteins using autoimmune sera from patients with scleroderma. *Chromosoma.* 91:313–321.
Earnshaw, W.C., K.F. Sullivan, P.S. Machlin, C.A. Cooke, D.A. Kaiser, T.D. Pollard, N.F. Rothfield, and D.W. Cleveland. 1987. Molecular cloning of cDNA for CENP-B, the major human centromere autoantigen. *J. Cell Biol.* 104:817–829.
Fritzler, M.J., and T.D. Kinsella. 1980. The CREST syndrome: a distinct serologic entity with anticentromere antibodies. *Am. J. Med.* 69:520–526.
Fukagawa, T., and W.R.A. Brown. 1997. Efficient conditional mutation of the vertebrate CENP-C gene. *Hum. Mol. Genet.* 6:2301–2308.
Gaff, C., D. du Sart, P. Kalitsis, R. Iannello, A. Nagy, and K.H.A. Choo. 1994. A novel nuclear protein binds centromeric alpha satellite DNA. *Hum. Mol. Genet.* 3:711–716.
Goldberg, I.G., A.F. Sawhney, A.F. Pluta, P.E. Warburton, and W.C. Earnshaw. 1996. Surprising deficiency of CENP-B binding sites in African green monkey alpha satellite DNA: implications for CENP-B function at centromeres. *Mol. Cell. Biol.* 16:5156–5168.
Haaf, T., A.G. Mater, J. Wienberg, and D.C. Ward. 1995. Presence and abundance of CENP-B box sequences in great ape subsets of primate-specific alpha satellite DNA. *J. Mol. Evol.* 41:487–491.
Haaf, T., and D.C. Ward. 1995. Rabl orientation of CENP-B box sequences in *Tupaia belangeri* fibroblasts. *Cytogenet. Cell Genet.* 70:258–262.
Halverson, D., M. Baum, J. Stryker, J. Carbon, and L. Clarke. 1997. A centromere DNA-binding protein from fission yeast affects chromosome segregation and has homology to human CENP-B. *J. Cell Biol.* 136:487–500.
Ikeno, M., H. Masumoto, and T. Okazaki. 1994. Distribution of CENP-B boxes reflected in CREST centromere antigenic sites on long-range alpha-satellite DNA arrays of human chromosome 21. *Hum. Mol. Genet.* 3:1245–1257.
Jeppesen, P., A. Mitchell, B. Turner, and P. Perry. 1992. Antibodies to defined histone epitopes reveal variations in chromatin conformation and underacetylation of centric heterochromatin in human metaphase chromosomes. *Chromosoma.* 101:322–332.
Kalitsis, P., K.J. Fowler, E. Earle, J. Hill, and K.H.A. Choo. 1998. Targeted disruption of mouse centromere protein C gene leads to mitotic disarray and early embryo death. *Proc. Natl. Acad. Sci. USA.* 95:1136–1141.
Karpen, G.H., and R.C. Allshire. 1997. The case for epigenetic effects on centromere identity and function. *Trends Genet.* 13:489–496.
Karpen, G.H., M.-H. Le, and H. Le. 1996. Centric heterochromatin and the efficiency of achiasmate disjunction in *Drosophila* female meiosis. *Science.* 273: 118–273.
Kipling, D., A.R. Mitchell, H. Matsumoto, H.E. Wilson, L. Nicol, and H.J. Cooke. 1995. CENP-B binds a novel centromeric sequence in the Asian mouse *Mus caroli. Mol. Cell. Biol.* 15:4009–4020.
Kipling, D., and P.E. Warburton. 1997. Centromeres, CENP-B and *Tigger* too. *Trends Genet.* 13:141–145.
Kipling, D., H.E. Wilson, A.R. Mitchell, B.A. Taylor, and H.J. Cooke. 1994. Mouse centromere mapping using oligonucleotide probes that detects variants of the minor satellite. *Chromosoma.* 103:46–55.
Kitagawa, K., H. Masumoto, M. Ikeda, and T. Okazki. 1995. Analysis of protein-DNA and protein-protein interactions of centromere protein B (CENP-B) and properties of the DNA-CENP-B complex in the cell cycle. *Mol. Cell. Biol.* 15:1602–1612.
Laursen, H.B., A.L. Jargensen, C. Jones, and A.L. Bak. 1992. Higher rate of evolution of X chromosome alpha-repeat DNA in human than in the great apes. *EMBO J.* 11:2367–2372.
Lee, J., J.A. Huberman, and J. Hurwitz. 1997. Purification and characterization of a CENP-B homologue protein that binds to the centromeric K-type repeat DNA of *Schizosaccharomyces pombe. Proc. Natl. Acad. Sci. USA.* 94: 8427–8432.
Masumoto, H., K. Sugimoto, and T. Okazaki. 1989. Alphoid satellite DNA is tightly associated with centromere antigens in human chromosomes throughout the cell cycle. *Exp. Cell Res.* 181:181–196.
Meluh, P., and D. Koshland. 1995. Evidence that the *MIF2* gene of *Saccharomyces cerevisiae* encodes a centromere protein with homology to the mammalian centromere protein CENP-C. *Mol. Cell. Biol.* 6:793–807.
Moroi, Y., A.L., Hartman, P.K. Nakane, and E.M. Tan. 1981. Distribution of kinetochore (centromere) antigen in mammalian cell nuclei. *J. Cell Biol.* 90: 254–259.
Mullner, E.W., and L.C. Kühn. 1988. A stem-loop in the 3′ untranslated region mediates iron-dependent regulation of transferrin receptor mRNA stability in the cytoplasm. *Cell.* 53:815–825.
Mountford, P., B. Zevnik, A. Duwel, J. Nichols, M. Li, C. Dani, M. Robertson, I. Chambers, and A. Smith. 1994. Dicistronic targeting constructs: Reporters and modifiers of mammalian gene expression. *Proc. Natl. Acad. Sci. USA.* 91:4303–4307.
Muro, Y., H. Masumoto, K. Yoda, N. Nozaki, M. Ohashi, and T. Okazaki. 1992. Centromere protein B assembles human centromeric alpha-satellite DNA at the 17-bp sequence, CENP-B box. *J. Cell Biol.* 116:585–596.
Nagy, A., J. Rossant, R. Nagy, W. Abramow-Newerly, and J.C. Roder. 1993. Derivation of completely cell culture-derived mice from early-passage embryonic stem cells. *Proc. Natl. Acad. Sci. USA.* 90:8424–8428.
Ohashi, H., K. Wakui, K. Ogawa, T. Okano, N. Niikawa, and Y. Fukushima. 1994. A stable acentric marker chromosome: possible existence of an intercalary ancient centromere at distal 8p. *Am. J. Hum. Genet. 55*:1202–1208.
Page, S.L., W.C. Earnshaw, K.H.A. Choo, and L.G. Shaffer. 1995. Further evidence that CENP-C is a necessary component of active centromeres: studies of a dic(X;15) with simultaneous immunofluorescence and FISH. *Hum. Mol. Genet.* 4:289–294.
Palmer, D.K., and R.L. Margolis. 1985. Kinetochore components recognized by human autoantibodies are present on mononucleosomes. *Mol. Cell. Biol.* 5:173–186.
Palmer, D.K., K. O'Day, M.H. Wener, B.S. Andrews, and R.L. Margolis. 1987. A 17-kD centromere protein (CENP-A) copurifies with nucleosome core particles and with histones. *J. Cell Biol.* 104:805–815.
Pietras, D.F., K.L. Bennett, L.D. Siracusa, M. Woodworth-Gutai, V.M. Chapman, K.W. Gross, C. Kane-Haas, and N.D. Hastie. 1983. Construction of a small *Mus musculus* repetitive DNA library: Identification of a new satellite sequence in *Mus musculus. Nucl. Acids Res.* 11:6965–6983.
Pluta, A.F., A.M. Mackay, A.M. Ainsztein, I.G. Goldberg, and W.C. Earnshaw. 1995. The centromere: hub of chromosomal activities. *Science.* 270:1591–1594.
Pluta, A.F., N. Saitoh, I. Goldberg, and W.C. Earnshaw. 1992. Identification of a subdomain of CENP-B that is necessary and sufficient for localization to the human centromere. *J. Cell Biol.* 116:1081–1093.
Rattner, J.B. 1991. The structure of the mammalian centromere. *Bioessays.* 13: 51–56.
Robb, G.W., R.P. Amann, and G.J. Killian. 1978. Daily sperm production and epididymal sperm reserves of pubertal and adult rats. *J. Reprod. Fertil.* 54: 103–107.
Robertson, E.J. 1987. Embryo-derived stem cell lines. *In* Teratocarcinomas and Embryo Stem Cells: A Practical Approach, E.J. Robertson, editor. IRL Press, Oxford, United Kingdom. 71–112.
Romanova, L.Y., G.V. Deriagin, T.D. Mashkova, I.G. Tumeneva, A.R. Mushegian, L.L. Kisselev, and I.A. Alexandrov. 1996. Evidence for selection in evolution of alpha satellite DNA: the central role of CENP-B/pJα binding region. *J. Mol. Biol.* 261:334–340.
Saitoh, H., J. Tomkiel, C.A. Cooke, H. Ratrie III., M. Maurer, N.F. Rothfield, and W.C. Earnshaw. 1992. CENP-C, an autoantigen in scleroderma is a component of the human inner kinetochore plate. *Cell.* 70:115–125.
Seki, N., T. Saito, K. Kitagawa, H. Masumoto, T. Okazaki, and T.A. Horit. 1994. Mapping of the human centromere protein B gene (CENP-B) to chromosome 20p13 by fluorescence in situ hybridization. *Genomics.* 24:187–188.
Simerly, C., R. Balczon, B.R. Brinkley, and G. Schatten. 1990. Microinjected kinetochore antibodies interfere with chromosome movement in meiotic and mitotic mouse oocytes. *J. Cell Biol.* 111:1491–1504.
Stoler, S., K.C. Keith, K.E. Curnick, and M. Fitzgerald-Hayes. 1995. A mutation in *CSE4*, an essential gene encoding a novel chromatin-associated protein in yeast, causes chromosome nondisjunction and cell cycle arrest at mitosis. *Genes Dev.* 9:573–586.
Sullivan, B.A., and S. Schwartz. 1995. Identification of centromeric antigens in dicentric Robertsonian translocations: CENP-C and CENP-E are necessary components of functional centromeres. *Hum. Mol. Genet.* 4:2189–2197.
Sullivan, K.F., and C.A. Glass. 1991. CENP-B is a highly conserved mammalian centromere protein with homology to the helix-loop-helix family of proteins. *Chromosoma.* 100:360–370.
Sullivan, K.F., M. Hechenberger, and K. Masri. 1994. Human CENP-A contains a histone H3 related histone fold domain that is required for targeting to the centromere. *J. Cell Biol.* 127:581–592.
Sugimoto, K., H. Yata, and M. Himemo. 1993. Mapping of the human CENP-B gene to chromosome 20 and the CENP-C gene to chromosome 12 by a rapid cycle DNA amplification procedure. *Genomics.* 17:240–242.
Tomkiel, J., C.A. Cooke, H. Saitoh, R.L. Bernat, and W.C. Earnshaw. 1994. CENP-C is required for maintaining proper kinetochore size and for a timely transition to anaphase. *J. Cell Biol.* 125:531–545.
Trowell, H.E., A. Nagy, B. Vissel, and K.H.A. Choo. 1993. Long-range analyses of the centromeric regions of human chromosomes 13, 14 and 21: identification of a narrow domain containing two key centromeric DNA elements. *Hum. Mol. Genet.* 2:1639–1649.
Tyler-Smith, C., and W.R. Brown. 1987. Structure of the major block of alphoid satellite DNA on the human Y chromosome. *J. Mol. Biol.* 195:457–470.
Vissel, B., and K.H. Choo. 1992. Evolutionary relationships of multiple alpha satellite subfamilies in the centromeres of human chromosomes 13, 14, and 21. *J. Mol. Evol.* 35:137–146.
Volobouev, V., N. Voght, E. Viegas-Pequignot, B. Malfoy, and B. Dutrillaux. 1995. Characterization and chromosomal location of two repeated DNAs in three Gerbillus species. *Chromosoma.* 104:252–259.
Voullaire, L.E., H.R. Slater, V. Petrovic, and K.H.A. Choo. 1993. A functional marker centromere with no detectable alpha-satellite, satellite III, or CENP-B protein: activation of a latent centromere? *Am. J. Hum. Genet.* 52:1153–1163.
Wreford, N.G. 1995. Theory and practice of stereological techniques applied to the estimation of cell number and nuclear volume in the testis. *Microscopy Res. Tech.* 32:423–436.
Wu, Z.A., W-X. Liu, C. Murphy, and J. Gall. 1990. Satellite 1 DNA sequence from genomic DNA of the giant panda *Ailuropoda melanoleuca. Nucl. Acids Res.* 18:1054.
Wilson, R.R., K. Anscough, C. Anderson, M. Baynes, J. Berks, J. Bonfield, M. Burton, T. Connell, J. Copsey, A. Cooper, et al. 1994. 2.2. Mb of contiguous nucleotide sequence from chromosome III of *C. elegans. Nature.* 368:32–38.
Yen, T.J., D.A. Compton, D. Wise, R.P. Zinkowski, B.R. Brinkley, W.C. Earn-

shaw, and D.W. Cleveland. 1991. CENP-E a novel human centromere-associated protein required for progression from metaphase to anaphase. *EMBO J.* 10:1245–1254.

Yen, T.J., G. Li, B.T. Schaar, I. Szilak, and D.W. Cleveland. 1992. CENP-E is a putative kinetochore motor that accumulates just before mitosis. *Nature.* 359:536–539.

Yoda, K., K. Kitagawa, H. Masumoto, Y. Muro, and T. Okazaki 1992. A human centromere protein, CENP-B, has a DNA binding domain containing four potential alpha helices at the NH_2 terminus, which is separable from dimerizing activity. *J. Cell Biol.* 119:1413–1427.

Yoda, K., T. Nakamura, H. Masumoto, N. Suzuki, K. Kitagawa, M. Nakano, A. Shinjo, and T. Okazaki. 1996. Centromere protein B of African green monkey cells: Gene structure, cellular expression, and centromeric localization. *Mol. Cell. Biol.* 16:5169–5177.

PUBLICATION 4

K.J. FOWLER, B.T. KILE, R. SAFFERY, D.V. IRVINE,
D.F. HUDSON, H.E. TROWELL AND K.H.A. CHOO (1998A)

GENETIC MAPPING OF MOUSE CENTROMERE PROTEINS *INCENP* AND *CENPE* GENES.

CYTOGENETICS AND CELL GENETICS, 82: 67-70.

Cytogenet Cell Genet 82:67–70 (1998)

Cytogenetics and Cell Genetics

Genetic mapping of mouse centromere protein (*Incenp* and *Cenpe*) genes

K.J. Fowler, R. Saffery, B.T. Kile, D.V. Irvine, D.F. Hudson, H.E. Trowell, and K.H.A. Choo

The Murdoch Institute, Royal Children's Hospital, Parkville, Victoria (Australia)

Abstract. Inner centromere protein (INCENP) and centromere protein E (CENPE) are two functionally important proteins of the higher eukaryotic centromere. Using a mouse *Incenp* genomic DNA and a mouse *Cenpe* cDNA to analyze recombinant inbred mouse sets, as well as interspecific backcross panels, we have mapped these genes to the proximal regions of mouse Chromosomes 19 and 6, respectively. Comparison of *Cenpe* and human CENPE, which maps to chromosome region 4q24→q25, has further identified a new region of homology between the two species.

The chicken inner centromere protein (INCENP) is a chromosomal "passenger" protein (Earnshaw and Bernat, 1990) that was originally identified with a monoclonal antibody raised against the bulk proteins of a mitotic chromosome scaffold fraction (Cooke et al., 1987). Due to its observed localization at the inner domain of the centromere during metaphase, the protein was thought to have a role in sister chromatid cohesion. At anaphase, the protein leaves the chromosomes and becomes associated with the overlapping microtubules of the central spindle and with the cell cortex at the contractile ring (Earnshaw and Cooke, 1991). Recently, INCENP has been demonstrated to play a major role in the assembly or function of the cleavage furrow during cytokinesis and to be essential for chromosomal congression (Eckley et al., 1997; Mackay et al., 1998).

Like INCENP, centromere protein E (CENPE) was originally identified using a monoclonal antibody raised against a chromosome scaffold fraction (Yen et al., 1991). The protein localizes on mammalian centromeres during prometaphase and throughout metaphase, but diminishes from the chromosomes at anaphase (Yen et al., 1991, 1992; Lombillo et al., 1995). It is the first member of the kinesin-related motor proteins that has been localized to the mammalian centromere, where it has been shown to be present on the surface of the kinetochore that forms part of the fibrous corona (Cooke et al., 1997). The protein is essential for monopolar chromosomes to establish bipolar connections and for chromosomes with connections to both spindle poles to congress and align at the spindle equator (Thrower et al., 1995; Schaar et al., 1997; Wood et al., 1997).

Here, we report the isolation and use of an *Incenp* genomic DNA fragment and *Cenpe* cDNA to map the chromosome positions of the mouse *Incenp* and *Cenpe* genes.

Materials and methods

Incenp probe

To obtain a mouse *Incenp* probe, a chicken cDNA sequence for INCENP (GenBank accession No. Z25420) was used to scan an expressed sequence tag (EST) database using the Basic Local Alignment Search Tool (Blast). Thirty-two EST clones were identified and assembled into two contiguous stretches of DNA representing the 5′ and 3′ end regions of the mouse *Incenp* cDNA, respectively. Confirmation that these two regions were derived from the same cDNA for mouse *Incenp* came from reverse transcriptase PCR (RT-PCR) analysis. Using a pair of oligonucleotides (5′-AAG AAG AGG CGG GTG TCT AAC-3′ derived from EST clone 439746 [GenBank accession No. AA014535] and 5′-GAA GCC TAG ATA AGA GGG TGA-3′ derived from EST clone 354031 [GenBank accession No. W43491]) as primers and total cDNA prepared from mouse embryonic stem cell line (129/1) as template, a single 2.2-kb product (designated RTIN.1) spanning the region between the two clones was obtained. Direct DNA sequencing of this product allowed assembly of a single contiguous mouse *Incenp* cDNA sequence with significant homology to chicken and *Xenopus laevis* (GenBank accession No. U95094; Stukenburg et al., 1997) INCENPs, including a central region of

Supported by the National Health and Medical Research Council of Australia. K.H.A.C. is a Principal Research Fellow of the Council and a Senior Associate of the University of Melbourne.

Received 9 April 1998; revision accepted 15 June 1998.

Request reprints from K.J. Fowler, The Murdoch Institute, Royal Children's Hospital, Flemington Road, Parkville, Victoria 3052 (Australia); telephone: 03-9345-5081; fax: 03-9348-1911; e-mail: fowlerk@cryptic.rch.unimelb.edu.au.

KARGER E-mail karger@karger.ch Fax + 41 61 306 12 34 http://www.karger.com

0301–0171/98/0822–0067$15.00/0

Accessible online at: http://BioMedNet.com/karger

Table 1. Strain distribution pattern for *Incenp* in AKXL RI mice

Progenitor DNA pattern[a]	Series No.										
A	5	6	7	9	12	14	24	25	28	29	37
L	8	13	16	17	19	21	38				

[a] A and L designate the *Pvu*II allelic fragments that are recognized by the *Incenp* probe in the AKR/J and C57L/J progenitor mouse strains, respectively.

Table 2. Linkage of *Incenp* to chromosome 19 markers in AKXL RI mice

Locus	Discordant RI strains/total analyzed	Percentage recombination (cM) (Green, 1981)	95% Confidence limits (cM) (Silver, 1985)
D6Rp19e	1/18	1.5	1.5–11.6
Fosl1	0/17	0.0	0.0–6.9
D19Mit59	0/18	0.0	0.0–6.4
Ltbp2	0/18	0.0	0.0–6.4
Cd98	0/18	0.0	0.0–6.4
Xmmv42	0/18	0.0	0.0–6.4
Cd5	2/18	3.3	0.4–18.1
Fcer1b	3/18	5.6	1.0–27.3

202 amino acids that shares 73% identity and 80% amino acid similarity between mouse and chicken INCENP. Within this region lies a 22 amino acid stretch (corresponding to chicken residues 781–802) that shows 96% identity between mouse, chicken, and *X. laevis* INCENPs. No homology to any other GenBank entries was detected with the mouse *Incenp* sequences. A 5′ *Incenp* EST clone (439746) was purchased from Genome Systems and used as a probe to screen a mouse 129/Sv genomic library (Stratagene). This resulted in the isolation of a positive phage clone, PIN06. A 2.5-kb *Sac*II/*Hin*dIII fragment upstream of the ATG transcription start codon was subcloned from this phage clone into Bluescript II KS+ phagemid (Stratagene) and used as a probe in this study.

Cenpe probe

To obtain a mouse *Cenpe* probe, a BLAST search using the carboxy terminal portion of human CENPE cDNA sequence (GenBank accession No. Z15005) was performed against the EST database. This identified eight mouse cDNA clones that aligned to form two distinct DNA stretches with significant homology to human CENPE (Yen et al., 1992). The first of these regions shows 80% nucleotide identity to human CENPE over 756 bp of DNA, with an internal stretch encoding 25 amino acids that demonstrate 76% identity and 96% similarity to human CENPE (residues 2,261–2,285). The second region (950 bp in size) shows 81% nucleotide identity with human CENPE and contains an internal region of 41 amino acids with 85% identity and 98% similarity (residues 2,591–2,631). Further confirmation that these two regions were derived from a single RNA transcript came from RT-PCR analysis with two oligonucleotides primers (5′-GGA AAG AAG TGC TAC CAG ATC C-3′ and 5′-ATC ATT GAG GTA TCC TGG GC-3′) obtained from the first and second regions, respectively. A single 313-bp product was obtained, confirming the presence of a single cDNA containing the two regions. This internal region shows 77% nucleotide identity with human CENPE, with a random match probability to human CENPE of 1.6×10^{-39} using BLASTN (nucleotide search using BLAST). No significant homology to any other GenBank entries was detected with any of the derived mouse *Cenpe* sequences. One EST clone, designated 570691 (GenBank accession No. AA108598), was purchased from Genome Systems, and a 381-bp *Eco*RI fragment was subcloned from it for use in genomic mapping experiments. Direct sequencing of this subclone shows 80% DNA sequence identity (base pairs 7,403–7,784) and 66% and 81% amino acid identity and similarity, respectively, with human cenpE (residues 2,438–2,564). This region is outside the kinesin-like domains of human cenpE and shows no significant homology to any other mouse cDNA.

Genetic mapping of Incenp and Cenpe

Genomic DNA from progenitor mouse strains, the recombinant inbred (RI) AKXL and AXB mouse sets, as well as Southern blot filters with DNA from The Jackson Laboratory interspecific backcross panel (C57BL/6JEi × SPRET/Ei)F_1 × SPRET/Ei (known as The Jackson BSS; Rowe et al., 1994) were purchased from The Jackson Laboratory, Bar Harbor, ME. Genomic DNA and Southern blots were analyzed as described previously (Fowler et al., 1997).

Data for all known strain distribution patterns (SDPs) of AKXL and AXB RI mouse strains, which date from February 1998, were obtained from the Mouse Genome Database (MGD), Mouse Genome Informatics, The Jackson Laboratory (http://www.informatics.jax.org). Recombination frequencies (r) were calculated using the formula $r = R/(4 - 6R)$, where R is the proportion of discordant strains in the RI set (Green, 1981). The 95% confidence intervals for linkage analysis with RI mice are those tabulated by Silver (1985).

Raw data for The Jackson BSS Panel SDPs were obtained from The Jackson Laboratory (http://www.jax.org/resources/documents/cmdata) and date from March 1998. The Jackson BSS Panel SDP was analyzed using the Map Manager Program (Manly, 1993).

Results

Genetic mapping of Incenp

The 2.5-kb *Sac*II/*Hin*dIII 5′ mouse *Incenp* fragment was used as probe on Southern blots to identify an informative *Pvu*II polymorphism for the *Incenp* locus of AKR/J and C57L/J progenitor RI mouse strains, as well as a *Bgl*II RFLP around the *Incenp* of the C57BL/6J and Spret/Ei mouse strains. The enzyme *Pvu*II revealed two bands at 2.2 and 5.7 kb in the AKR/J mouse strain (designated A) and two bands at 2.2 and 8.6 kb in the C57L/J strain (designated L), whereas *Bgl*II identified fragments of 6.6, 5.0, and 3.5 kb in the Spret/Ei strain and 5.0 and 3.5 kb in the C57BL/6J strain. The *Pvu*II polymorphism was used to genotype DNA from the AKXL mouse set, whereas the *Bgl*II RFLP was used to analyze The Jackson BSS Panel.

The resulting AKXL SDP for *Incenp* is summarized in Table 1. Comparison of the SDP for *Incenp* with those of other markers mapped using these strains indicated that *Incenp* localizes to the proximal region of Chromosome 19. No recombinants (0.0–6.9 cM, 95% limits) were observed between *Fosl1, D19Mit59, Ltbp2, Cd98,* or *Xmmv42* (Table 2).

To further refine the chromosomal position of *Incenp*, the locus was also mapped by the analysis of (C57BL/6JEi × SPRET/Ei)F_1 × SPRET/Ei cross. Inheritance of the homozygous or heterozygous SPRET/Ei 6.6-kb fragment was typed in 94 progeny DNA, and the observed pattern indicated linkage to a large bin of markers on proximal chromosome 19, including *Chk, D19Mit32, D19Mit93,* and *Nofl* (0.0–3.8 cM, 95% limits; Fig. 1a, c). This linkage is consistent with data obtained using the RI mouse strains and extends the data by placing *Incenp* closer to the centromere region of Chromosome 19.

Genetic mapping of Cenpe

The 381-bp *Eco*RI *Cenpe* probe identified *Bam*HI fragments of 4.2 and 3.8 kb in the A/J mouse strain (designated A) and 7.1, 4.2, and 3.8 kb in the C57BL/6J mouse strain (designated B). This probe also identified informative *Bgl*II fragments of 2.8 and 1.8 kb in the SPRET/Ei mouse strain, as well as 8.5, 7.1, and 1.8 kb fragments in the C57BL/6J strain.

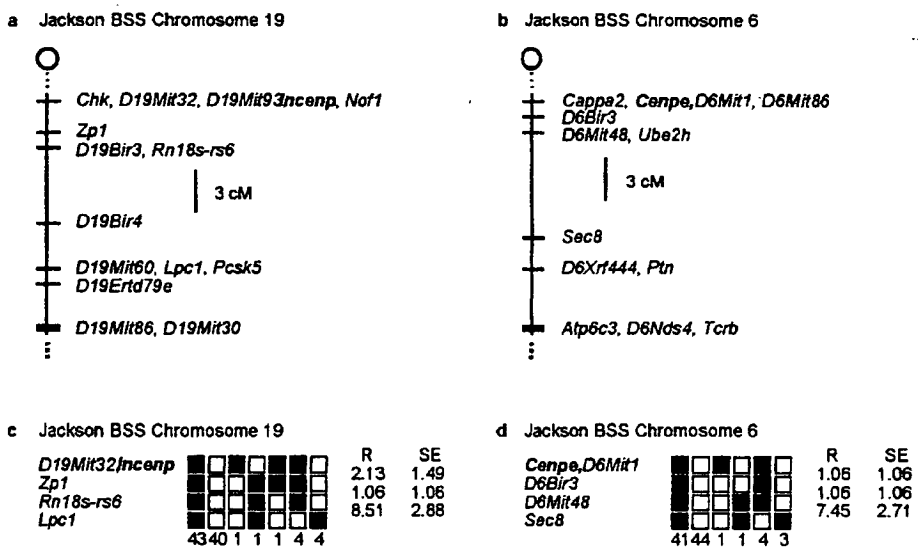

Fig. 1. Map figures (**a**, **b**) and haplotype figures (**c**, **d**) from The Jackson BSS backcross showing the proximal end of mouse Chromosome 19 with loci linked to *Incenp* (**a**) and the proximal end of Chromosome 6 with loci linked to *Cenpe* (**b**). The map is depicted with the centromere toward the top. A 3-cM scale bar is shown to the right of the figure. Loci mapping to the same position are listed in alphabetical order, and not all BSS markers linked to *Incenp* and *Cenpe* are shown in these figures. Missing typings were inferred from the surrounding data where assignment was unambiguous. (**c**, **d**) Haplotype figure from The Jackson BSS backcross showing the proximal end of Chromosome 19 with loci linked to *Incenp* (**c**) and the proximal end of Chromosome 6 with loci linked to *Cenpe* (**d**). Loci in **c** and **d** are listed in order, with the most proximal at the top. The solid boxes represent the C57BL6/Ei allele, and the open boxes the SPRET/Ei allele. The number of animals with each haplotype is given at the bottom of each column of boxes. The percent recombination (R) between adjacent loci is given to the right of the figure, with the standard error (SE) for each R.

The *Bam*HI fragments were used to genotype the AXB RI set (Table 3). No recombinants (0.0–5.0 cM, 95% limits) were observed between *Cenpe*, *D6Mit86*, or *D6Rp2* on proximal Chromosome 6. However, *Cenpe* also displayed linkage (95% limits) to 19 other markers on Chromosome 6 (Table 4). Because some of these markers were quite distal to *D6Mit86* and *D6Rp2* (up to 56 cM, MGD composite map), an independent mapping analysis was performed using The Jackson BSS Panel with the aid of the *Bgl*II polymorphism. The observed SDP for the BSS cross indicated linkage to several markers, including *Cappa2*, *Dlx6*, *D6Mit1*, and *D6Mit86* (0.0–3.8 cM, 95% limits), therefore consolidating the mapping of *Cenpe* to the proximal region on Chromosome 6 (Fig. 1b, d).

Discussion

In comparison with humans, there are at least 14 known loci in the proximal region on mouse Chromosome 19, including genes that display linkage to *Incenp* (*Fosl1*, *Cd5*, and *Fcer1b*; 2–8 cM region, MGD) (Table 1), that have synteny with human chromosome region 11q11→q13 (MGD). This suggests that the human INCENP gene may localize to this region on human chromosome 11; however, the human chromosome positions of the most closely linked genes to *Incenp* (*Chk*, *Nof1*, and *Zp1*; 0.0–0.2 cM region, MGD) (Fig. 1a, c), using The Jackson BSS Panel in this study, are presently unknown.

The mapping of *Cenpe* to mouse Chromosome 6 was somewhat unexpected, given that the human homolog, CENPE, maps to chromosome region 4q24→q25 (Testa et al., 1994). To date, there has been only one other report of homology between mouse Chromosome 6 and human chromosome 4. The human homolog of the *Drosophila* atonal homolog 1 (ATOH1) gene has been assigned to 4q22 (Ben-Arie et al., 1996), whereas

Table 3. Strain distribution pattern for *Cenpe* in AXB RI mice

Progenitor DNA pattern[a]	Series No.											
A	3	4	6	7	8	9	10	12	15	17	21	23
B	1	2	5	11	13	14	18	19	20	24		

[a] A and B designate the *Bam*HI allelic fragments that are recognized by the *Cenpe* probe in the A/J and C57BL/6J progenitor mouse strains, respectively.

Table 4. Linkage of *Cenpe* to chromosome 6 markers in AXB RI mice

Locus	Discordant RI strains/total analyzed	Percentage recombination (cM) (Green, 1981)	95% Confidence limits (cM) (Silver, 1985)
D6Mit86	0/22	0.0	0.0–5.0
D6Rp2	0/22	0.0	0.0–5.0
D6Nds5	0/9	0.0	0.0–17.0
D6Mit50	2/22	2.6	0.3–13.0
D6Mit8	3/22	4.3	0.8–18.3
Met	3/21	4.6	0.8–20.0
D6Mit29	4/22	6.3	1.4–25.4
D6Mit54	4/22	6.3	1.4–25.4
D6Mit25	4/22	6.3	1.4–25.4
Hoxa3	4/21	6.7	1.5–28.2
D6Str1	3/15	7.1	1.2–43.2
D6Mit33	5/22	8.6	2.2–36.0
D6Mit36	5/22	8.6	2.2–36.0
D6Mit65	5/22	8.6	2.2–36.0
lapls2.25	5/22	8.6	2.2–36.0
D6Mit52	5/22	8.6	2.2–36.0
D6Mit61	5/22	8.6	2.2–36.0
D6Mit59	5/22	8.6	2.2–36.0
D6Mit57	5/22	8.6	2.2–36.0
D6Mit14	5/22	8.6	2.2–36.0
Ggc	5/20	10.0	2.5–47.0

Atoh1 maps to the 30.5 cM region on Chromosome 6. The *Atoh1* gene is separated from *Cenpe* by a large segment of approximately 30 cM on Chromosome 6 that has extensive homology to human chromosome 7, encompassing more than 40 genes (MGD). This segment includes six genes that have linkage to *Cenpe* (*Cappa2*, *Dlx6*, *Ggc*, *Met*, *Ptn*, and *Tcrb*), as well as a smaller region that has homology with human chromosome 2. The results of the present analysis have therefore established a new region of homology on mouse proximal Chromosome 6 and the human 4q24→q25 region.

In a previous study, Magnuson and Epstein (1984) reported an embryonic lethal phenotype in *Os* mouse mutants due to a mitotic arrest defect and localized the *Os* locus to Chromosome 8 (42 cM region, MGD). These observations, together with the fact that in the region of CENPE, 15 other genes on human chromosome region 4q23→q35.1 have been shown to share homology with mouse Chromosome 8 (MGD), initially suggested to us the possibility that the *Os* mouse mutant could be a candidate for carrying a mutated *Cenpe* gene. However, the mapping of *Cenpe* to Chromosome 6 in this study has excluded this possibility.

Acknowledgements

We thank Mary Barter and Lucy Rowe, The Jackson Laboratory Backcross DNA Panel Resource, for The BSS backcross map and haplotype figures. We also acknowledge Graham Kay's gift of the 129/1 cell line.

References

Ben-Arie N, McCall AE, Berkman S, Eichele G, Bellen HJ, Zoghbi HY: Evolutionary conservation of sequence and expression of the bHLH protein Atonal suggests a conserved role in neurogenesis. Hum molec Genet 5:1207–1216 (1996).

Cooke CA, Heck MMS, Earnshaw WC: The inner centromere protein (INCENP) antigens: movement from inner centromere to midbody during mitosis. J Cell Biol 105:2053–2067 (1987).

Cooke CA, Schaar B, Yen TJ, Earnshaw WC. Localization of CENP-E in the fibrous corona and outer plate of mammalian kinetochores from prometaphase through anaphase. Chromosoma 106:446–455(1997).

Earnshaw WC, Bernat, RL: Chromosomal passengers: towards an integrated view of mitosis. Chromosoma 100:139–146 (1990).

Earnshaw WC, Cooke CA: Analysis of the distribution of the INCENPs throughout mitosis reveals the existence of a pathway of structural changes in chromosomes during metaphase and early events in cleavage formation. J Cell Sci 98:443–461 (1991).

Eckley DM, Ainsztein AM, Mackay AM, Goldberg IG, Earnshaw WC: Chromosomal proteins and cytokinesis: patterns of cleavage furrow formation and inner centromere protein positioning in mitotic heterokaryons and mid-anaphase cells. J Cell Biol 136:1169–1183 (1997).

Fowler KJ, Newson AJ, MacDonald AC, Kalitsis P, Lyu MS, Kozak, CA, Choo KHA: Chromosomal localization of mouse *Cenpa* gene. Cytogenet Cell Genet 79:298–301 (1997).

Green, MC: Gene mapping, in Foster HL, Small JD, Fox JG (eds): The Mouse in Biomedical Research: History, Genetics, and Wild Mice, Vol 1, pp 105–117 (Academic Press, New York 1981).

Lombillo VA, Nislow C, Yen TJ, Gelfand VI, McIntosh JR: Antibodies to the kinesin motor domain and CENP-E inhibit microtubule depolymerization-dependent motion of chromosomes in vitro. J Cell Biol 128:107–115 (1995).

Mackay AM, Ainsztein AM, Eckley DM, Earnshaw WC: A dominant mutant of inner centromere protein (INCENP), a chromosomal protein, disrupts prometaphase congression and cytokinesis. J Cell Biol 140:991–1002 (1998).

Magnuson T, Epstein CJ: Oligosyndactyly: a lethal mutation in the mouse that results in mitotic arrest very early in development. Cell 38:823–833 (1984).

Manly KF: A Macintosh program for all of our data management. Mammal Genome 4:303–313 (1993).

Rowe LB, Nadeau JH, Turner R, Frankel WN, Letts VA, Eppig JT, Ko MSH, Thurston SJ, Birkenmeier EH: Maps from two interspecific backcross DNA panels available as a community genetic mapping resource. Mammal Genome 5:253–274 (1994).

Schaar BT, Chan GKT, Maddox P, Salmon ED, Yen TJ: CENP-E function at kinetochores is essential for chromosome alignment. J Cell Biol 139:1373–1382 (1997).

Silver J: Confidence limits for estimates of gene linkage based on analysis of recombinant inbred strains. J Hered 76:436–440 (1985).

Stukenburg BT, Lustig KD, McGarry TJ, King RW, Kuang J, Kirschner MW: Systematic identification of mitotic phosphoproteins. Curr Biol 7:338–348 (1997).

Testa JR, Zhou, J-Y, Bell DW, Yen TJ: Chromosomal localization of the genes encoding the kinetochore proteins CENPE and CENPF to human chromosomes 4q24→q25 and 1q32→q41, respectively, by fluorescence in situ hybridization. Genomics 23:691–693 (1994).

Thrower DA, Jordan MA, Schaar BT, Yen TJ, Wilson L: Mitotic HeLa cells contain a CENP-E-associated minus end-directed microtubule motor. EMBO J 14:918–926 (1995).

Wood KW, Sakowics R, Goldstein LS, Cleveland DW: CENP-E is a plus end-directed kinetochore motor required for metaphase chromosome alignment. Cell 91:357–366 (1997).

Yen TJ, Compton DA, Wise D, Zinkowski RP, Brinkley BR, Earnshaw WC, Cleveland DW: CENP-E, a novel human centromere-associated protein required for progression from metaphase to anaphase. EMBO J 10:1245–1254 (1991).

Yen TJ, Li G, Schaar BT, Szilak I, Cleveland DW: CENP-E is a putative kinetochore motor that accumulates just before mitosis. Nature 359:536–539 (1992).

PUBLICATION 5

K.J. FOWLER, R. SAFFERY, D.V. IRVINE, H.E. TROWELL AND K.H.A. CHOO (1998B)

MOUSE CENTROMERE PROTEIN F (*CENPF*) GENE MAPS TO THE DISTAL REGION OF CHROMOSOME 1 USING INTERSPECIFIC BACKCROSS PANEL.

CYTOGENETICS AND CELL GENETICS, 82: 180-181.

Cytogenet Cell Genet 82:180–181 (1998)

Cytogenetics and Cell Genetics

Mouse centromere protein F *(Cenpf)* gene maps to the distal region of Chromosome 1 by interspecific backcross analysis

K.J. Fowler, R. Saffery, D.V. Irvine, H.E. Trowell and K.H.A. Choo

The Murdoch Institute, Royal Children's Hospital, Parkville, Victoria (Australia)

Rationale and significance

Human centromere binding protein F (CENPF) is a 367-kDa nuclear matrix-associated chromosome passenger (Rattner et al., 1993; Liao et al., 1995; Mancini et al., 1996). The protein is uniformly distributed in the cell nucleus during S phase, localizes onto the kinetochore from late G_2/M to metaphase, relocates onto the spindle equator and intracellular bridge during late anaphase and cleavage furrow formation and then is degraded following completion of mitosis. CENPF has been shown to be a valuable proliferation marker for various human tumours (Landberg et al., 1996) and has been mapped to human chromosome 1q32→q41 (Testa et al., 1994). Here we report the use of a mouse genomic fragment to map the chromosome position of mouse *Cenpf*.

Materials and methods

Probe type: 1.4-kb *Hin*dIII genomic fragment of mouse *Cenpf*.

Proof of Authenticity: A 758-bp PCR product corresponding to nucleotides 185 to 942 of the human CENPF sequence (Genbank accession number U19769; Liao et al., 1995) was amplified from human cDNA using primer pairs A (5'-GGA AGA ATG GAA AGA AGG GC-3') and B (5'-TTG ATC GAC TTG GAG TCA CC-3'). Use of this mouse product as a hybridization probe against 129Sv mouse genomic library (Stratagene) allowed the identification of 4 positive phage clones. Restriction enzyme digestion and Southern hybridization analysis of these clones indicated that all were derived from the same, single-copy, genomic region. DNA sequencing analysis in combination with BLAST (Basic Local Alignment Search Tool) searches of these phage clones revealed the presence of four mouse *Cenpf* exons with high homology to human CENPF sequence. Two of these exons showed 77% and 80% identity at the nucleotide sequence level with human CENPF at positions 163–330 and 331–523, respectively. The other two exons were contained within a 1.4-kb *Hin*dIII fragment and showed homologies of 80% and 85% corresponding to nucleotides 524–648 and 649–737, respectively, with human CENPF. Random match probability of these results was calculated as 5.4×10^{-42} using BLASTN (nucleotide search using BLAST), indicating the authenticity of the cloned sequences as mouse *Cenpf*.

Method of mapping: The 1.4-kb *Hin*dIII fragment was used as a probe on Southern blots to identify an informative *Msp*I polymorphism around the *Cenpf* locus of C57BL/6J and Spret/Ei mouse strains. The analysis revealed bands of 4 kb in Spret/Ei and 3.4 kb in the C57BL/6J strain. This polymorphism was used to genotype Southern blot filters with DNA from interspecific backcross panel (C57BL/6JEi × SPRET/Ei) F1 × SPRET/Ei (known as The Jackson BSS panel; Rowe et al., 1994). Progenitor DNA and filters were purchased from The Jackson Laboratory, Bar Harbor, Maine. Genomic DNA and Southern blots were analysed as described previously (Fowler et al., 1997).

Results

Inheritance of the homozygous or heterozygous SPRET/Ei 4-kb fragment was typed in 94 progeny DNA and analysed. The observed pattern indicated linkage to a large bin of markers on the distal region of Chromosome 1, including *D1Bir26* and *D1Mit17* (0.00-3.8 cM, 95% limits; Fig. 1). The mapping of *Cenpf* to the distal region on Chromosome 1 conforms with the expected mouse-human syntenic region, since human CENPF has been localized to chromosome 1q32→q41 (Testa et al., 1994). Beside CENPF, there are in excess of 50 genes that have homology with human chromosome 1q and the distal region of mouse Chromosome 1 (MGD), including the *Apoa2* gene (92.6 cM region, MGD composite map) that was shown to have linkage with *Cenpf* in this study (Fig. 1).

Supported by the NH and MRC of Australia. We thank Mary Barter and Lucy Rowe for the BSS backcross map and haplotype figures.

Received 15 June 1998; manuscript accepted 14 July 1998.

Request reprints from K.J. Fowler, The Murdoch Institute, Royal Children's Hospital, Flemington Road, Parkville, 3052, Victoria (Australia); telephone: 03 9345 5081; fax: 03 9348 1391; email: fowlerk@cryptic.rch.unimelb.edu.au

KARGER

E-mail karger@karger.ch
Fax + 41 61 306 12 34
http://www.karger.com

0301–0171/98/0824–180$17.50/0

Accessible online at:
http://BioMedNet.com/karger

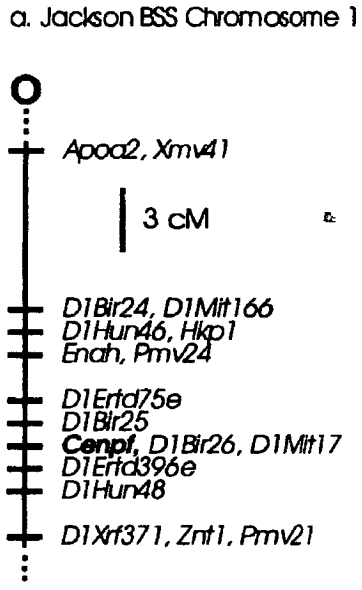

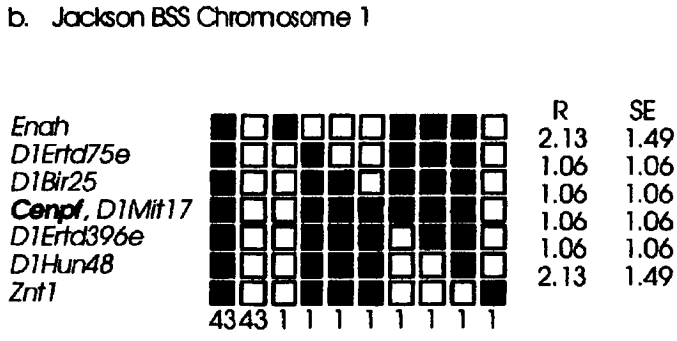

Fig. 1 . Map figure (**a**) and Haplotype figure (**b**) from The Jackson BSS backcross. (**a**) The distal end of Chromosome 1 with loci linked to *Cenpf*. The map is depicted with the centromere toward the top. A 3-cM scale bar is shown to the right of the figure. Loci mapping to the same position are listed in alphabetical order and not all BSS markers linked to *Cenpf* are shown on this figure. Missing typings were inferred from the surrounding data where assignment was unambiguous. Raw data for The Jackson BSS panel strain distribution patterns (SDPs) were obtained from The Jackson Laboratory (http//www.jax.org/resources/documents/cmdata) and date from April 1998. (**b**) Haplotype figure showing the distal end of Chromosome 1 with loci linked to *Cenpf*. Loci are listed in order with the most proximal at the top. The black boxes represent the C57BL6/Ei allele and the white boxes the SPRET/Ei allele. The number of animals with each haplotype is given at the bottom of each column of boxes. The percent recombination (R) and the standard error (SE) for each R value were calculated using the Map Manager Program (Manly, 1993) and are given to the right of the figure. Missing typings were inferred from surrounding data where assignment was unambiguous.

References

Fowler KJ, Newson AJ, MacDonald AC, Kalitsis P, Lyu MS, Kozak CA, Choo KHA: Chromosomal localization of mouse *Cenpa* gene. Cytogenet Cell Genet 79:298–301 (1997).

Landberg G, Erlanson M, Roos G, Tan EM, Casiano CA: Nuclear autoantigen p330d/CENP-F: a marker for cell proliferation in human malignancies. Cytometry 25:90–98 (1996).

Liao H, Winkfein RJ, Mack G, Rattner JB, Yen TJ: CENP-F is a protein of the nuclear matrix that assembles onto kinetochores at late G2 and is rapidly degraded after mitosis. J Cell Biol 130:507–518 (1995).

Mancini MA, He D, Ouspenski II, Brinkley BR: Dynamic continuity of nuclear and mitotic matrix proteins in the cell cycle. J Cell Biochem 62:158–164 (1996).

Manly KF: A Macintosh program for all of our data management. Mammal Genome 4:303–313 (1993).

Rattner JB, Rao A, Fritzler MJ, Valencia DW, Yen TJ. CENP-F is a ca. 400 kDa kinetochore protein that exhibits a cell-cycle dependent localization. Cell Motil Cytoskeleton 26:214–226 (1993).

Rowe LB, Nadeau JH, Turner R, Frankel WN, Letts VA, Epping JT, Ko MSH, Thurston SJ, Birkenmeier EH: Maps from two interspecific backcross DNA panels available as a community genetic mapping resource. Mammal Genome 5:253–274 (1994).

Testa JR, Zhou J-Y, Bell DW, Yen TJ: Chromosomal localization of genes encoding kinetochore proteins CENPE and CENPF to human chromosomes 4q24→q25 and 1q32→q41, respectively, by fluoresence *in situ* hybridization. Genomics 23:691–693 (1994).

PUBLICATION 6

S. M. CUTTS, **K.J. FOWLER**, B.T. KILE, L.L.P. HII, R.A. O'DOWD,
D.F. HUDSON, R. SAFFERY, P. KALITSIS, E. EARLE AND
K.H.A. CHOO (1999)

DEFECTIVE CHROMOSOMAL SEGREGATION, MICROTUBULE BUNDLING, AND NUCLEAR BRIDGING IN INNER CENTROMERE PROTEIN (*INCENP*) GENE-DISRUPTED MICE.

HUMAN MOLECULAR GENETICS,
8: 1145-1155 AND FRONT COVER.

VOLUME 8 NUMBER 7 JULY 1999

Human Molecular Genetics

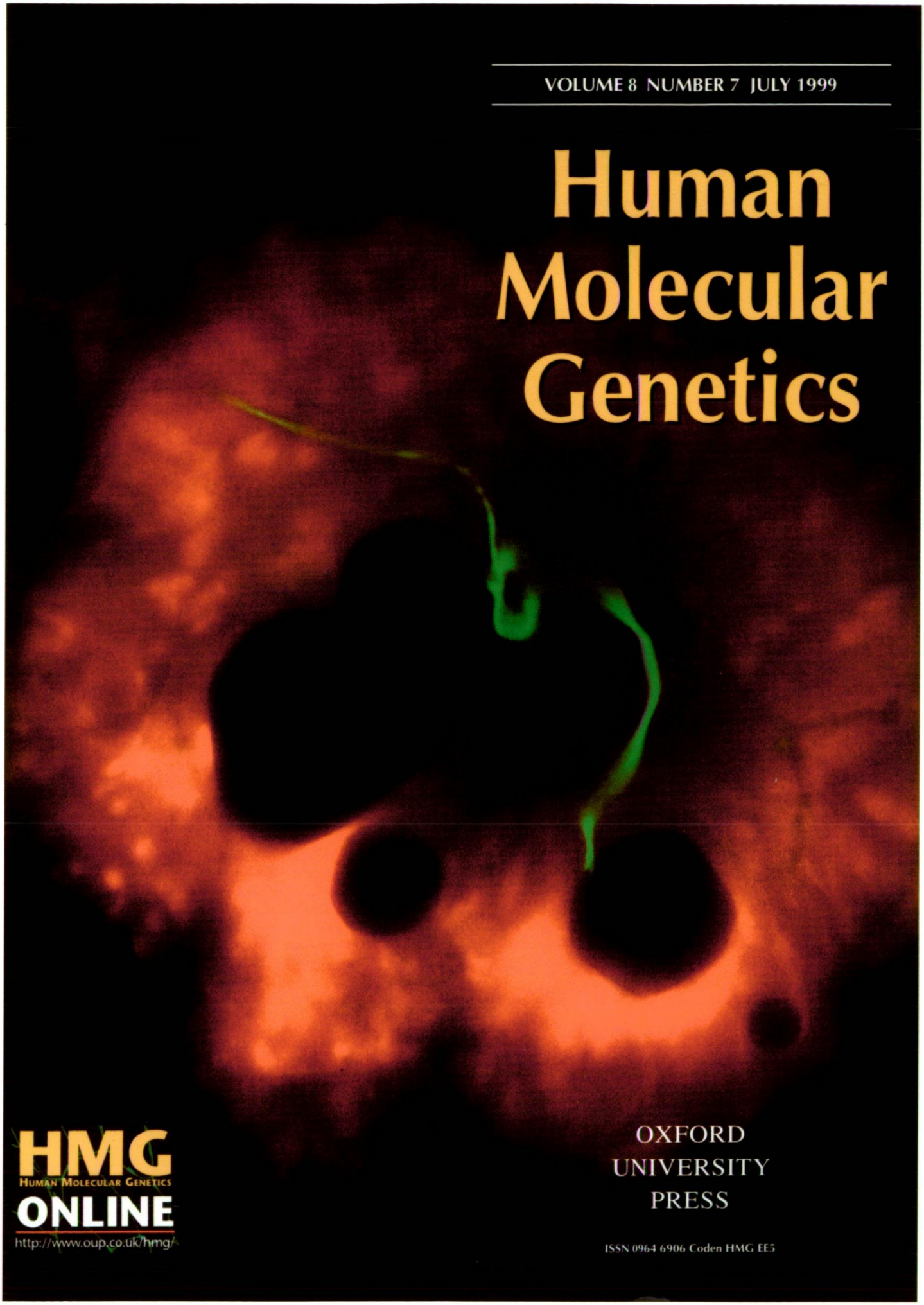

HMG
HUMAN MOLECULAR GENETICS
ONLINE
http://www.oup.co.uk/hmg/

OXFORD
UNIVERSITY
PRESS

ISSN 0964 6906 Coden HMG EE5

Cover: Giant nucleus in *Incenp* null day 3.5 mouse embryo, showing unusual microtubule bundling into a massive spindle 'cord' (Cutts et al, 1999[6]).

Human Molecular Genetics, 1999, Vol. 8, No. 7 1145–1155

ARTICLE

Defective chromosome segregation, microtubule bundling and nuclear bridging in inner centromere protein gene (*Incenp*)-disrupted mice

Suzanne M. Cutts, Kerry J. Fowler, Benjamin T. Kile, Linda L. P. Hii, Rachael A. O'Dowd, Damien F. Hudson, Richard Saffery, Paul Kalitsis, Elizabeth Earle and K. H. A. Choo+

The Murdoch Institute, Royal Children's Hospital, Flemington Road, Parkville 3052, Australia

Received December 14, 1998; Revised and Accepted April 7, 1999

INCENP is a chromosomal passenger protein which relocates from the centromere to thel spindle midzone during the metaphase–anaphase transition, ultimately being discarded in the cell midbody at the completion of cytokinesis. Using homologous recombination, we have generated *Incenp* gene-targeted heterozygous mice that are phenotypically indistinguishable from their wild-type littermates. Intercrossing the heterozygotes results in no live-born homozygous *Incenp*-disrupted progeny, indicating an early lethality. Day 3.5 affected pre-implantation embryos contain large, morphologically abnormal cells that fail to fully develop a blastocoel cavity or thrive *in utero* and in culture. Chromatin and tubulin immunocytochemical stainings of these and day 2.5 affected embryos reveal a high mitotic index, no discernible metaphase or anaphase stages, complete absence of midbodies, micronuclei formation, morphologically irregular macronuclei with large chromosome complements, multipolar mitotic configurations, binucleated cells, internuclear bridges and abnormal spindle bundling. The phenotype is consistent with a defect in the modulation of microtubule dynamics, severely affecting chromosome segregation and resulting in poorly resolved chromatin masses, aberrant karyokinesis and internuclear bridge formation. These latter occurrences could pose a physical barrier blocking cytokinesis.

INTRODUCTION

The centromere is a highly specialized chromosomal structure that is functionally conserved amongst eukaryotes and is essential for accurate meiotic and mitotic segregation of chromosomes. In mammalian cells, two broad groups of centromere-interacting proteins have been described: constitutively binding centromere proteins and passenger or transiently interacting proteins (reviewed in ref. 1). The constitutive proteins include: centromere protein A (CENP-A), which is a histone H3-like structural protein that may function to distinguish centromeric nucleosomes from other chromosomal nucleosomes (2,3); centromere protein B (CENP-B), which interacts directly with α-satellite DNA (4,5); and centromere protein C (CENP-C), which is a component of the inner kinetochore plate that shares homology with the yeast chromosome segregation protein Mif2 (6,7) and appears to be an important and integral structural component of the kinetochore (8).

The term 'passenger proteins' encompasses a broad collection of proteins that localize to the centromere during specific stages of the cell cycle (9). This association may relate to a direct role of the proteins at the centromere or, alternatively, it may simply reflect the role of the centromere as a delivery organelle from which the passenger proteins are distributed to the various final cellular sites of action. Some examples of passenger proteins are: CENP-E, MCAK, Kid and cytoplasmic dynein, which are intimately involved in kinetochore motor function (10–13); CENP-F/mitosin, which associates transiently with the kinetochore, playing an apparent role in kinetochore maturation and signalling pathways for cell division (14–16); and CLiPs, which localize to the inner surface of sister chromatids between kinetochores and are implicated in sister chromatid pairing (17).

The inner centromere proteins (INCENPs) were the founder members of the passenger group of proteins (18). These proteins display a broad localization along chromosomes in the early stages of mitosis but gradually become concentrated at centromeres as the cell cycle progresses into mid metaphase (19). During the metaphase–anaphase transition, INCENPs remain confined to the metaphase plate, associating with stem body material which coats the overlapping antiparallel microtubules of the central spindle, while sister chromatids migrate to the poles. In mid anaphase, a portion of the INCENPs also appears at the cell cortex where the cleavage furrow will later form. During telophase, the proteins are located within the

+To whom correspondence should be addressed. Tel: +61 3 9345 5045; Fax: +61 3 9348 1391; Email: choo@cryptic.rch.unimelb.edu.au

midbody in the intercellular bridge, where they are discarded after cytokinesis (18,19).

The INCENP proteins were originally identified in chicken cells as a doublet consisting of a shorter 96 kDa $INCENP_I$ and a 101 kDa $INCENP_{II}$ polypeptide containing a 38 amino acid insertion that arises through differential splicing of a single primary RNA transcript (20,21). Homologs of INCENP have been isolated in *Xenopus* (22) and mouse (23,24). Analysis of these and the chicken INCENPs (20,21) have revealed complex protein structures containing multiple putative targets for Cdc2 kinase, MAP kinase, *N*-glycosylation, nuclear localization signals and numerous other potential phosphorylation sites. A chicken INCENP cDNA, when expressed in mammalian cells, shows an identical cell cycle distribution to the endogenous protein, suggesting conservation of functional domains between interclass species (21). More recently, overexpression of a truncation mutant of chicken INCENP and a chimeric CENP-B:INCENP protein in mammalian cell culture resulted in dominant-negative characteristics, suggestive of interference with both prometaphase chromosome alignment and completion of cytokinesis (25,26). In the present study, we have investigated the biological importance and functional role of Incenp in mouse. Using homologous recombination, we have specifically disrupted the *Incenp* gene. We describe here the phenotype of such a gene disruption, which provides the first reported knockout of a mammalian chromosomal passenger protein.

RESULTS

Generation of *Incenp* null embryonic stem (ES) cells and mice

The genomic copy number of the mouse *Incenp* gene was determined previously using Southern blot analysis and mouse *Incenp* probes (24). The results indicated a single copy gene with no closely related homologs. Further analysis of *Incenp* mRNA, either by RT–PCR across the differentially spliced region observed in chicken $INCENP_I$ and $INCENP_{II}$ or by northern blot analysis of total RNA from ES cells and a wide range of mouse tissues, has failed to detect alternative forms of *Incenp* mRNA (24). These results suggested that heterozygous gene knockout could be achieved in a single homologous recombination event with our construct. In addition, in separate experiments, we have studied the chromosomal localization of the mouse Incenp protein in 129/1 mouse ES cells by immunocytochemistry using a well-characterized anti-chicken INCENP antibody provided by Dr W.C. Earnshaw (Institute of Cell and Molecular Biology, University of Edinburgh, UK) and obtained a pattern similar to that described previously for chicken cells (data not shown).

For gene targeting, a promoterless IRES/neo^R element was incorporated into the targeting vector to enhance both targeting frequency (by selecting for homologous recombination downstream of the endogenous *Incenp* promoter) and translation of the neomycin gene product (via the internal ribosomal entry site) (27). The construct was further designed to disrupt *Incenp* mRNA translation at amino acid 47, which effectively removed critical downstream regions containing nuclear localizing signals and the chromosome- and microtubule-binding domains (Fig. 1a) (26). That the 47 amino acid N-terminus truncated peptide neither elicited a dominant-negative effect nor was directly functional was clearly demonstrated by the observed phenotypes of the heterozygous and homozygous mice generated (see below).

Upon transfection of the linearized construct, 163 G418-resistant 129/1 ES colonies were analysed. Of these, six demonstrated the correct targeting event (Fig. 1b), corresponding to a frequency of 3.7%. When the construct was electroporated into W9.5 ES cells, 87 G418-resistant colonies were screened, of which four were correctly targeted, yielding a frequency of 4.6%. These targeting frequencies were low compared with the 70–86% seen at the *Oct4* locus (27) and 74% achieved for *Cenpc* gene disruption (28) using a similar strategy. However, the frequencies compared favourably with those obtained with the *Cenpb* (29) and *cytokine DIA/LIF* loci (27). The lower frequency in this case may be due to a lower rate of transcription at the *Incenp* locus, lower accessibility of the chromatin structure at this locus to homologous recombination mechanisms and/or omission of a 600 bp stretch of homology in our targeting vector.

The heterozygous cell lines exhibited normal morphology and growth rates. Injection of these cell lines into C57 BL/6 blastocysts resulted in two germline chimeras originating from the 129/1-derived ES cells. On mating the chimeras with C57 BL/6 mice, heterozygous mice were obtained. Intercrossing these heterozygotes produced 102 phenotypically indistinguishable progeny, of which 73 were found to be heterozygotes and 29 were wild-type (Fig. 1c). The absence of –/– animals indicated embryonic lethality. This was further indicated by the smaller litter size (7.5 ± 1) observed for the +/– × +/– crosses compared with those for +/+ × +/+ (9.6 ± 2.4) and +/+ × +/– (9.5 ± 1.7).

Embryonic lethality occurs before day 8.5

Females from +/– × +/– crosses were killed at day 8.5 post-virginal plug formation and embryos were removed from the uterine implantation sites for genotyping. A total of 23 embryos were obtained, 16 of which were +/– and seven were +/+. This result suggested that lethality of –/– embryos occurred earlier than 8.5 days.

We further investigated the ability of –/– embryos to develop under *in vitro* conditions. Embryos were harvested from the uteri of mothers of +/– × +/– crosses at day 3.5 and placed individually into tissue culture wells. These were observed for 6 days, after which they were harvested for PCR genotyping. Of 35 samples monitored, 31 hatched from the zona pellucida, attached to the culture wells, established two distinct cell types after 3 days of culture (Fig. 2a) and remained healthy throughout the study. Genotyping of these 31 hatched embryos indicated eight to be +/+ and 23 to be +/–. Of the four remaining embryos, three were unable to attach after 3 days of culture; one of these embryos was obviously dead, displaying a dense debri of degraded material, whereas the other two embryos failed to hatch out of the zona pellucida and showed spatial contraction and signs of degeneration within the zona (Fig. 2b). The last embryo (Fig. 2c) had attached after 3 days of culture but was unable to thrive or form the two distinct cell types in comparison with the well-advanced healthy embryos at this stage. These four embryos represented the presumed –/– genotype (see below) and constituted 11% of total embryos. When the experiment was repeated by harvesting embryos from the oviduct as well as the uterus, this frequency increased to 24% (5 of 21), which was closer to the expected

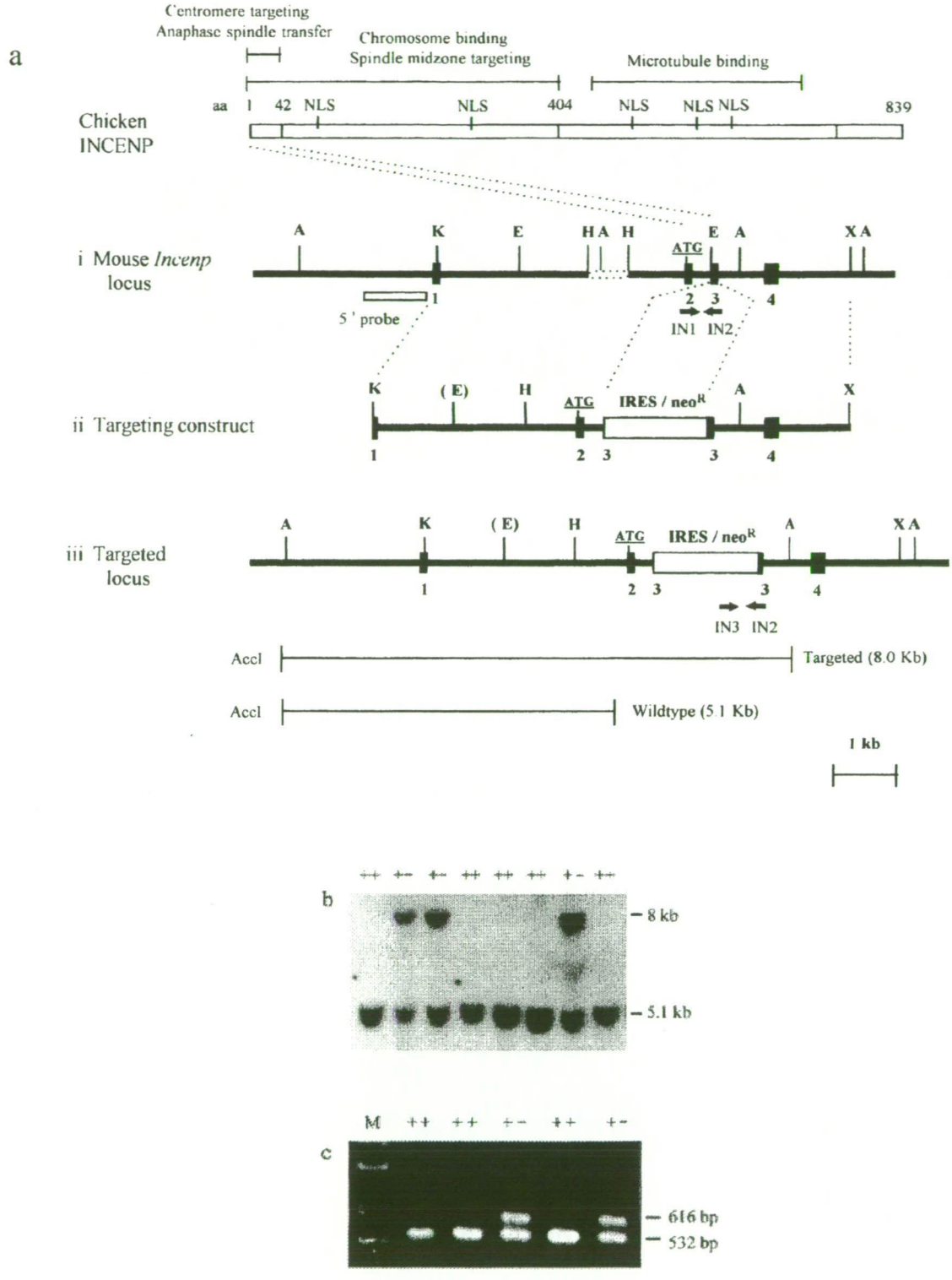

Figure 1. Mouse *Incenp* mapping, targeting construct and screening strategies. (**a**) (i) Mouse *Incenp* locus showing the first 4 exons and the ATG start codon within exon 2. The approximate amino acid positions of the various functional domains and putative nuclear localization signals (NLS) of the chicken INCENP are shown (20,21,26). The stippled box indicates an internal 600 bp *Hin*dIII genomic fragment within intron 2 that has been deleted from the targeting construct. The open box denotes the position of a 5' probe employed in the Southern detection of a targeted event. Restriction sites are: A, *Acc*I; K, *Ksp*I; E, *Eco*RI; H, *Hin*dIII; X, *Xho*I. (ii) Gene targeting construct in which exon 3 has been disrupted by insertion of the IRES/neo^R cassette at the *Eco*RI site. This cloning step required the removal of an *Eco*RI site, shown in parentheses. (iii) Correctly targeted *Incenp* allele showing the expected *Acc*I fragment sizes for targeted and wild-type alleles detected by the 5' probe. IN1, IN2 and IN3 are PCR primers. (**b**) Southern screening of cell lines. Wild-type and targeted bands are 5.1 and 8 kb, respectively [refer to a(iii)]. (**c**) PCR screening of mouse tails. The wild-type (532 bp) and targeted (616 bp) alleles are detected by primers IN1/IN2 and IN2/IN3, respectively. M, 1 kb Plus DNA ladder (Gibco BRL).

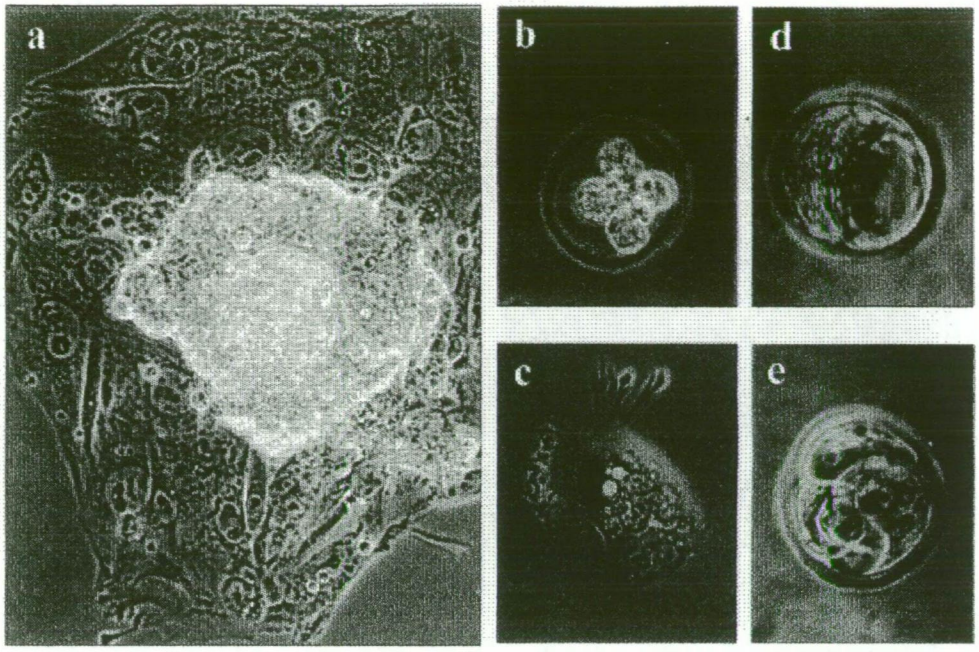

Figure 2. Morphology of day 3.5 and cultured embryos from heterozygous crosses. (**a–c**) Day 3.5 embryos following 3 days of *in vitro* culture, where (a) depicts an embryo which has undergone normal development showing spreading trophoblast cells and inner cell mass, while (b) and (c) depict –/– embryos which have failed to hatch from the zona pellucida or have undergone very rudimentary development, respectively. (**d**) Day 3.5 uncultured normal blastocyst showing formation of the inner cell mass and blastocoel cavity. (**e**) Day 3.5 uncultured –/– embryo showing giant cells and absence of the blastocoel cavity. Magnification ×200.

value, suggesting that affected embryos displayed an increased residence time in the oviduct. In control +/+ × +/+ or +/+ × +/– crosses, of 44 day 3.5 embryos examined, all attached and developed well in culture, although after 6 days some sign of reduced proliferation was observed in five samples. However, as this occurred at a much later stage and clearly differed morphologically from that of presumed –/– embryos, it was assumed to be due to a culturing effect unrelated to the phenotype observed with the presumed –/– embryos.

Cell morphology of day 3.5 embryos

To further ascertain and correlate the phenotype and genotype of day 3.5 –/– embryos, samples were harvested from the uteri and oviducts of heterozygous females from +/– × +/– crosses, individually photographed and subjected to PCR. Due to the low amounts of DNA in these embryos, a modified PCR strategy (Fig. 3a) involving a random preamplification step of the whole genome was employed to enhance the level of template DNA in a linear unbiased manner (30), followed by allele-specific PCR to determine genotype. From a total of 39 embryos, 22 were +/– (56%), nine were +/+ (23%) and eight were –/– (21%) (Fig. 3b). When these genotypes were correlated with the photographic results, the –/– embryos were noticeably the only ones that exhibited abnormal morphology. These embryos consisted of large and non-uniformly sized cells which had failed to develop into inner cell masses and blastocoel cavities (Fig. 2e) compared with their healthy +/+ and +/– counterparts (Fig. 2d). These results clearly establish the presence of –/– embryos at day 3.5 as well as provide evidence for cellular abnormality at this early developmental stage.

Nuclear and chromosomal morphologies of day 3.5 and day 2.5 embryos

To examine the nuclear and chromosomal morphologies of affected embryos, samples from heterozygous crosses were fixed on slides, stained with Giemsa and analysed. Initial studies concentrated on day 3.5 embryos. At this stage, the normal embryos developed into blastocysts, each containing an average of 40–50 cells (inferred from the number of nuclei stained by Giemsa) that exhibited relatively uniform size and healthy morphology. Interphase nuclei were generally also uniform in size and contained 1–3 nucleoli/nucleus (Fig. 4a). Abnormal looking embryos, presumed to be *Incenp*-disrupted, contained nuclei that were both smaller in number (averaging seven per embryo) and much bigger in size (Fig. 4b–d). These embryos contained occasional micronuclei (e.g. Fig. 4d), but the majority of nuclei were significantly (5–10 times) larger than normal. These giant nuclei were often irregular and lobular in morphology and individually carried up to 20 nucleoli. The abnormal embryos comprised 14% (4 of 28) of the embryos studied, which was lower than the expected value since only mouse uteri were flushed for these experiments (see above). When the mitotic index (i.e. percentage of total cells in mitosis) of the affected embryos was determined, this was shown to be 20%, which, as a group, was significantly higher than the 3.9% value obtained for the unaffected embryos, suggesting that mitosis was severely delayed or arrested in the affected embryos.

The mitotic chromosomes of the affected embryos also showed a number of distinct abnormalities (Fig. 4b–d). Most of the chromosomes were highly condensed compared with metaphases of control embryos, although some appeared to be undergoing decondensation or deterioration, as evident from their elongated and/or fragmented morphology (Fig. 4c). A dis-

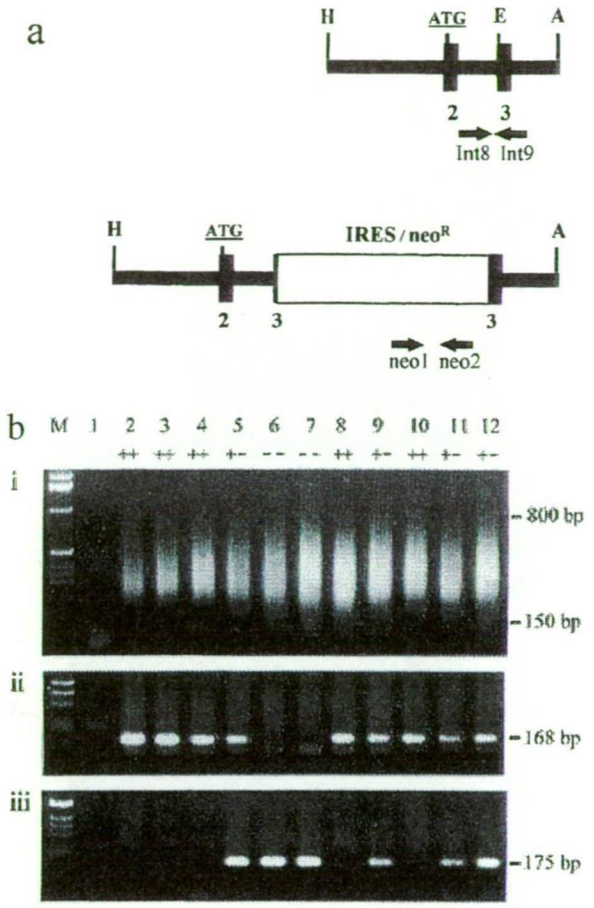

Figure 3. Pre-amplification embryo PCR screening. (**a**) Allele-specific PCR strategy. Lysed embryos were first subjected to whole genome pre-amplification before allele-specific PCR was performed using the primer pair Int8/Int9, which produces a fragment of 168 bp corresponding to the wild-type allele, or the primer pair neo1/neo2, which produces a fragment of 175 bp to depict the targeted allele. (**b**) (i) Whole genome pre-amplification showing DNA products with a size range of ~150–800 bp; (ii) the 168 bp wild-type allele-specific product of Int8/Int9 primers; (iii) the 175 bp targeted allele-specific product of the neo1/neo2 primers. Sample 1, control PCR with buffer only; samples 2–12, different 3.5 day embryos. M, 1 kb DNA ladder (Gibco BRL).

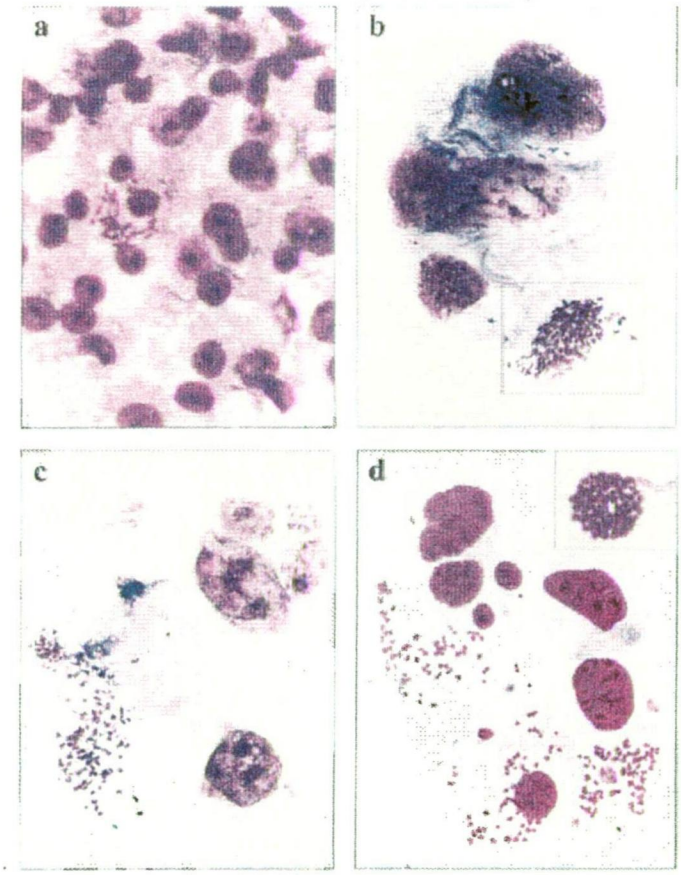

Figure 4. Chromosome and nuclear morphology of Giemsa-stained day 3.5 embryos from +/– × +/– crosses. (**a**) Normal embryo showing relatively uniform nuclear sizes and a normal metaphase. (**b–d**) Individual –/– embryos. Note the presence of micro- and macronuclei, lobular nuclei, mitotic cells with greatly higher than normal chromosome complements (examples are indicated by boxed insets) and macronuclei with large numbers of nucleoli (dark staining nuclear organelles). Magnification ×400.

tinct characteristic of these mitotic chromosomes was their highly disorganized or scattered nature, a feature so predominant that no specific stages of the normal mitosis could be ascribed to most of the affected mitoses. Another outstanding feature was the high prevalence of cells with giant chromosome complements several times that of the normal diploid mouse genome.

The above results indicate that a severe manifestation of Incenp deficiency has occurred in the day 3.5 embryos. To investigate earlier events related to this deficiency, day 2.5 embryos were harvested from heterozygote crosses and analysed. The results clearly indicated expression of the *Incenp* gene-disrupted phenotype in these earlier embryos. Normal embryos contained an average of 16 uniformly sized nuclei (Fig. 5a). Examination of affected embryos, which comprised 21% (9 of 43) of the total embryos analysed, indicated a smaller number of cells per embryo and the presence of nuclei of varying sizes (Fig. 5b–f), including micronuclei, apparently normal sized nuclei and greatly enlarged (up to 10× normal) nuclei that also contained a drastically increased number of nucleoli (see Fig. 5b for some representative examples of each of these events). An unusual feature of these nuclei was the appearance of 'nuclear bridges' in a substantial proportion of the cells (arrows in Fig. 5). Such bridges ranged from a thin band to a much broader region connecting two nuclei, corresponding presumably to different degrees of manifestation of an abnormal process of nuclear reformation. No nuclear bridges were ever observed in the normal embryos, where complete segregation of sister chromatids to the two poles has ensured resolute nuclear reformation around each of the two fully separated sister chromatid complements. As with the day 3.5 embryos, the mitotic chromosomes of day 2.5 embryos were often more condensed, disorganized and present in numbers greater than the usual diploid complement (Fig. 5e).

Tubulin immunocytochemistry of day 2.5 and day 3.5 embryos

Figure 6a shows results for the immunostaining of a normal day 2.5 embryo with anti-β-tubulin antibody. The eight cell embryo contained regular midbodies reminiscent of completed mitotic divisions. In contrast, such midbodies were undetected in nine of nine similarly stained day 2.5 morphologically abnormal,

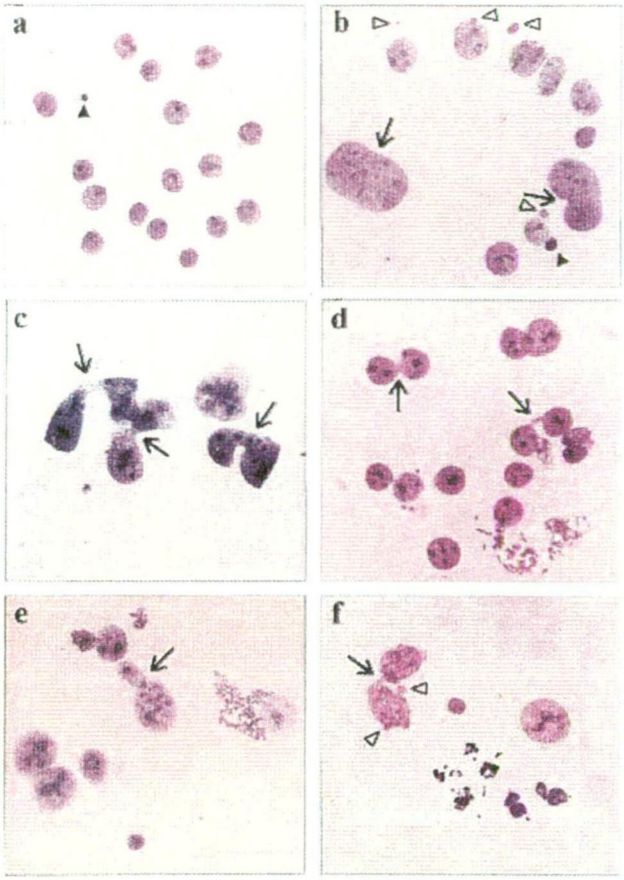

Figure 5. Chromosome and nuclear morphology of Giemsa-stained day 2.5 embryos from +/– × +/– crosses. (**a**) A normal 16 cell embryo showing uniform nuclear structures. (**b–f**) Affected embryos showing micronuclei and nuclei of varying sizes. Arrows point to nuclei with 'bridges'. Open arrowheads show selected examples of micronuclei. Solid arrowheads point to the dark staining polar bodies before they become degraded in subsequent cell divisions. Magnification ×400.

presumed *Incenp* null embryos, suggesting that mitosis failed to reach telophase/cytokinesis, during which spindle midbodies would normally form. Other abnormalities observed in these affected embryos included binucleated cells, irregular cell morphology, reduced cell number, micronuclei and nuclear bridging (Fig. 6b and c). A network of β-tubulin formed around the cells in both the normal and affected embryos.

Figure 7a shows immunostaining results for a normal day 3.5 embryo. The expected midbodies, spindle structures for metaphase/anaphase and cellular microtubule network were detected. Affected embryos at the same developmental stage showed severe abnormalities, including a total absence of midbodies (in 13 of 13 embryos), giant cells with irregular nuclei, micronuclei, multiple (up to 10) spindle poles, large vacuoles and highly abnormal bundling of spindle fibres into giant strands (Fig. 7b–d).

DISCUSSION

Previous studies involving overexpression of truncation mutant proteins in cell culture have suggested roles for INCENP in prometaphase chromosome congression and cytokinesis (26). A significant drawback of these earlier studies is the presence of the endogenous INCENP protein whose effect cannot be unequivocally dissociated from the range of phenotypes observed. Other studies involving microinjection of anticentromere antibodies into cultured cells (31) suffer similar limitations in that the specificity of antibodies and potential steric effects of the antibody–antigen complex may be difficult to ascertain. To minimize these difficulties, we have employed homologous recombination to create an *Incenp* gene knockout in a mouse. Our knockout strategy was designed to produce premature termination of the Incenp protein which, because of the removal of all the putative nuclear localization motifs and essential domains for chromosome and microtubule binding (26), should neither be able to enter the nucleus to interact with the chromosomes and centromeres nor evoke any significant Incenp function. The apparently normal phenotype seen in the heterozygous ES cell lines and mice demonstrates directly that the targeted mutation does not exert a dominant-negative effect. We infer that the severe phenotype seen in the homozygous knockouts must arise from null mutations specifically related to the depletion of Incenp proteins.

Cellular effect of *Incenp* mutation

Analysis of the nuclear details of *Incenp* null embryos enables the likely progression of events underlying the phenotype to be formulated. Incenp deficiency manifests initially in the day 2.5 embryos as a mitotic missegregation problem that results in the lagging of a small number of chromosomes (leading to a few micronuclei), with the bulk of the chromosomes still able to migrate to the poles in anaphase, although aberrant migration will begin to cause an uneven distribution of chromatin at the poles and result in nuclei of varying sizes. During these early events, mitosis proceeds essentially to completion, albeit imperfectly, and results in unambiguous nuclear membrane reformation around each of the two fully separated chromatin masses during telophase, before cytokinesis ensues to achieve cell cleavage. As any potential maternal cytoplasmic protein and/or *Incenp* mRNA and its immediately transcribed products rapidly dwindle after one to two cell divisions (evident from manifestation of a severe phenotype in day 2.5 embryos), chromosomal segregation becomes increasingly aberrant. Sister chromatid masses may still enter into initial polar separation but complete separation to the poles is not achieved. As the chromosomes tether around the spindle midzone, presumably in an unorganized manner (evident from failure to observe metaphase congression or distinct anaphases), progression of mitosis falters and becomes significantly delayed or arrested (evident from increased mitotic index). Eventually, a default telophase (evident from failure of midbody formation) occurs leading to aberrant karyokinesis during which a nuclear membrane reforms around the full chromatin complement and extends across the two poorly or non-separated chromatin masses. Subsequently, cytokinetic furrow formation may be initiated into the extended nuclei or nuclear bridges. Such an attempt becomes increasingly unsuccessful (evident from the giant chromosome complement; discussed below) and leads to large cells with greatly increased nuclear contents.

Two possible explanations may account for a failure in cytokinesis in the *Incenp*-disrupted embryos: the first implicates an underlying direct biochemical cause, while the second involves a physical barrier that prevents cytokinesis. The first possibility

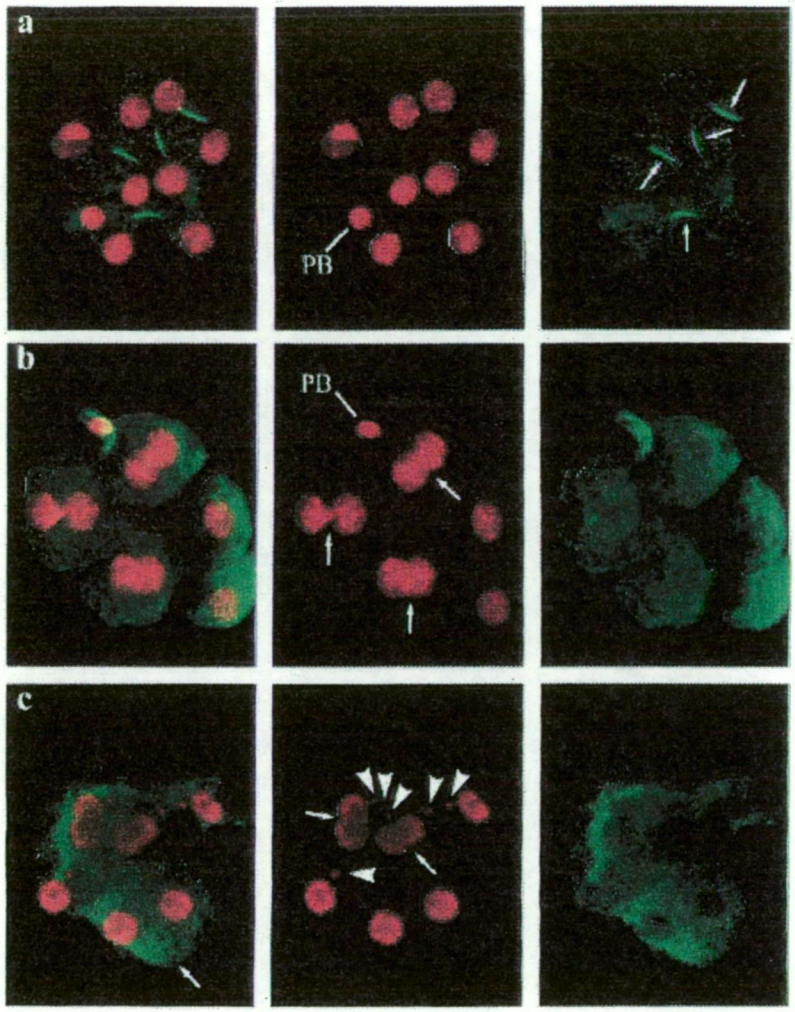

Figure 6. Tubulin immunocytochemistry of day 2.5 embryos from +/– × +/– crosses. (**a**) A normal eight cell embryo showing four midbodies (arrows). (**b**) An affected embryo showing five cells of which the three larger cells were either binucleated or contained nuclear bridges (arrows). (**c**) An affected embryo showing binucleated cells or cells with nuclear bridging (arrows) and micronuclei (arrowheads). (Left) Composite images; (middle) DAPI staining of DNA; (right) β-tubulin staining. PB, polar body. Magnification ×630.

was suggested by Cook *et al.* (19), who proposed a direct involvement of INCENP in cytokinesis. These investigators have demonstrated that the protein is one of the earliest known polypeptides to be present in the presumptive cleavage furrow and that, in addition to the stem body matrix, the protein is closely associated with the cytoplasmic face of the plasma membrane within the cleavage furrow (18). Molecular analysis has demonstrated that INCENP associates with the centromere during metaphase and with the central spindle during anaphase, while overexpressed INCENP binds cytoplasmic microtubules (21). Overexpression of an INCENP truncation mutant that targets to centromeres but lacks the microtubule association region and other C-terminal elements interferes with both prometaphase chromosome alignment and the completion of cytokinesis (26). In addition, cells expressing an artificial chimeric protein in which a truncated INCENP containing the spindle midzone targeting and microtubule-binding domains is tethered to the centromere through a fusion with the centromere-binding motif of the centromere protein CENP-B results in a block in cytokinesis (25). Interestingly, cells expressing such a chimeric protein show no evidence of prometaphase disruption or lagging chromosomes.

In contrast to these studies, our data, unencumbered by the persistence of endogenous normal INCENP or any side-effects that overexpression of mutant or artificial heterologous proteins may have, point to an over-riding primary role of Incenp in proper chromosome segregation. We have demonstrated that deficiency of this protein leads promptly to segregation errors that manifest initially in chromosome lagging (micronuclei formation) but rapidly deteriorates into a catastrophic breakdown in the polar movement of chromatin. This leads to the tethering or stalling of chromatin at the spindle midzone, followed by untimely reformation of an extended nuclear membrane around the full complement of non-separated or poorly separated chromatin, resulting in enlarged nuclei. We propose that these enlarged nuclei and the excessive chromatin material that accumulate across the presumptive cleavage furrow create a physical barrier preventing cytokinesis from proceeding to completion. Using a careful light and electron microscopy study, Mullins and Biesele (32) have reported that where lagging chromatin is trapped in the midbody in the intercellular bridge, cytokinesis proceeds normally until it encounters the chromatin-containing midbody, at which point cytokinesis fails, followed by regres-

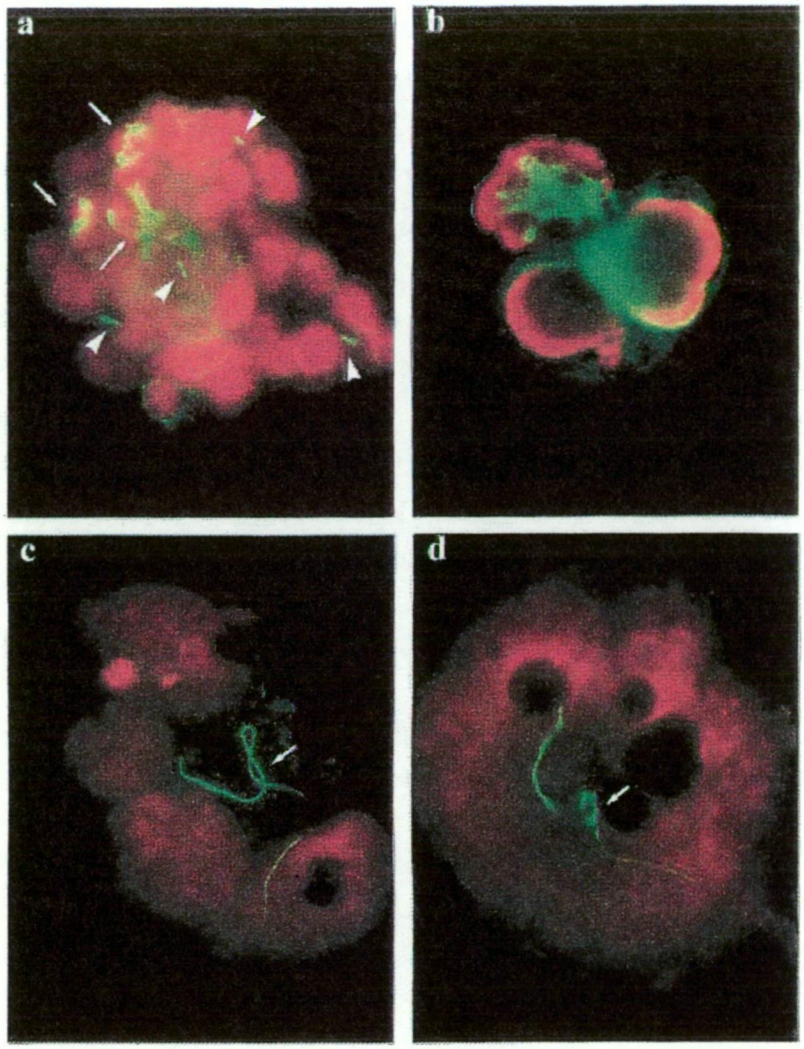

Figure 7. Tubulin immunocytochemistry of day 3.5 embryos from +/– × +/– crosses. (**a**) A normal 32–64 cell embryo showing regular nuclei, metaphase/anaphase spindle structures (arrows) and midbodies (arrowheads). (**b**) An affected embryo with three giant nuclei. Two of the nuclei were in interphase, with one of these nuclei showing an unusually high level of spindle aggregation or bundling around the chromatin material. The third nucleus was in mitosis and showed 8–16 spindle poles with interconnecting fibres; such multiple spindle poles have originated through repeated rounds of failure of the divided centrioles to be distributed to daughter cells due to defective cytokinesis. (**c** and **d**) Two affected embryos showing vacuolation and four highly irregular giant nuclei in (c) and a single 'fused' giant cell/nucleus in (d). A striking feature of these embryos is the presence of a highly extended and continuous tubulin cord (arrow) formed presumably by extensive microtubule bundling and/or elongation; compare the enormous (>20×) size of these giant tubulin cords with the spindle midbody structures shown in (a). Some of the features described for the different embryos in this figure and in Figure 6 may not be immediately apparent from the two-dimensional pictures captured with our CCD camera system but the described features were based on direct microscopic assessment of three-dimensional images. Magnification ×630.

sion of the furrow and the persistence of the midbody. Our observation of a high prevalence of nuclear bridges is consistent with failed and regressed cytokinesis. Furthermore, it appears likely that in our *Incenp*-disrupted cells, a combination of the vast amount of chromatin tethering at the spindle midzone and the reformation of a highly unusual intercellular nuclear structure will constitute a significantly greater barrier to block cytokinesis than that described by Mullins and Biesele (32).

Comparison with *Cenpc* knockout

It is of interest to compare and contrast the phenotype observed for the *Incenp* knockout with that previously described for the embryonically lethal *Cenpc* knockout (28). This comparison highlights a more severe phenotype for the *Incenp* gene knockout, since mitotic problems are already well advanced by day 2.5, while similar staged *Cenpc* knockout embryos still appear relatively normal. Such a phenotypic difference may in part be due to the fact that in addition to the maternal mRNA pool provided by the egg cytoplasm, both the maternal and paternal kinetochores are also likely to contribute to the recycling of the constitutive Cenpc protein through the different cell division cycles. In contrast, the chromosomal passenger Incenp protein is known to be discarded in the cell midbody at the end of cytokinesis during each division cycle (19) and would therefore be rapidly depleted from either the maternal and paternal kinetochores as well as during successive embryonic cell divisions.

In both *Incenp* and *Cenpc* gene disruptions, early mitotic problems result in the formation of micronuclei and provide evidence for errors in anaphase chromosomal segregation in which missegregated or lagging chromosomes become encap-

sulated during the nuclear reformation step in telophase, prior to cytokinesis. The increased mitotic indices in the day 3.5 embryos of *Incenp* and *Cenpc* gene disruptions compared with those of normal embryos indicate that mitotic progression has been delayed or arrested. Again, the delay/arrest phenotype is significantly more severe for Incenp deficiency (mitotic index 20% compared with 3.9% in unaffected embryos) than for a defect in Cenpc (mitotic index 6.9% compared with 3.6% in normal embryos; 28). Mitotic delay or arrest can result from a metaphase checkpoint that serves to delay anaphase onset by monitoring a phosphorylation-dependent signal-generating mechanism at the kinetochore for proper bipolar microtubule attachment and metaphase congression (33). The observed higher mitotic index suggests that *Incenp*-disrupted cells may have a greater difficulty in overcoming this checkpoint control compared with the *Cenpc* mutants and/or that additional mitotic blocks may be in place. Whilst we cannot rule out the possibility of an extended checkpoint arrest in our *Incenp*-disrupted cells, the observed appearance of a high prevalence of cells with large chromosome complements, giant nuclei and highly abnormal nuclear bridges that are not seen in the *Cenpc* knockouts provides a compelling suggestion that additional mitotic blocks may operate (see below). It is also interesting that a noticeably lower prevalence of micronuclei is seen in the *Incenp*-disrupted cells compared with the *Cenpc*-disrupted cells, suggesting that missegregation that results in the lagging of only a small number of chromosomes occurs less frequently in the *Incenp* knockout cells. In addition, the *Incenp*-disrupted embryos show relatively more micronuclei at day 2.5 compared with day 3.5, with the day 3.5 embryos giving a disproportionally higher representation of macronuclei and cells with larger than normal chromosome complements.

Implications for *Incenp* function

It is useful to speculate on the mechanisms responsible for the observed segregation failure in the *Incenp*-disrupted mice. Early manifestation of the mutation in the form of chromosome lagging can result from a possible defect in the kinetochore complex or spindle integrity and function. The former will likely be the case for the *Cenpc*-disrupted mice, since this protein is a constitutive component of the kinetochore, a defect in which is expected to lead to defective microtubule capture or binding, causing improper chromosomal segregation, chromosome lagging and micronuclei formation. The observed distinct differences in the subsequent manifestation of the *Incenp* knockout, on the other hand, suggest that an Incenp defect could specifically affect microtubule dynamics rather than the centromere itself. This suggestion is consistent with the absence of spindle midbody structures and, in particular, the highly aberrant bundling of spindle fibres into gigantic spindle 'cords' in a significant proportion of the severely affected embryos (Fig. 7c and d). Previous studies have also demonstrated the spindle microtubule-binding property of this protein and the relocation of the protein from the centromere onto microtubules at the metaphase plate where spindle fibres overlap during late metaphase/early anaphase (18,19). A defect in microtubule function would not only have an immediate effect on prometaphase movements as proposed previously (26), but could lead to impaired chromatid separation and polar migration of chromosomes during anaphase A. Such a defect could have an even more severe effect on the subsequent step of spindle elongation in anaphase B, during which the distance between the poles is increased. Finally, in addition to our proposed primary role of Incenp in modulating spindle dynamics and chromosomal segregation, the possibility that the protein may have a further downstream biochemical effect on cytokinesis as suggested by earlier dominant-negative mutant studies cannot be ruled out. Alternatively, the observed final relocation of INCENP to the presumptive cleavage furrow structures and the midbody may not reflect any active functional role of INCENP in cytokinesis but rather simply reflect a mode of delivery to a destination for destruction or clearance at the end of each cell cycle. Further studies using our knockout system and other approaches should shed more light on these possibilities.

MATERIALS AND METHODS

Restriction mapping of mouse *Incenp* and construction of targeting vector

A chicken *INCENP* cDNA sequence (GenBank accession no. Z25420) was used to identify a mouse *INCENP* cDNA clone (GenBank accession no. AA014535) (23). A fragment from this clone was used to screen a 129/Sv mouse genomic phage library from which a 14 kb clone designated PIN06 was isolated. Mapping revealed that the clone contained four exons corresponding to the mouse cDNA sequence with the start site for protein translation located within exon 2 [Fig. 1a(i)]. For the construction of a gene targeting vector, a 2.5 kb *Kspl*–HindIII fragment containing a portion of exon 1 was cloned into Bluescript II KS (+). A 3.8 kb *Hin*dIII–*Xho*I fragment containing exons 2–4 was further cloned into the *Hin*dIII site of this construct to form a genomic contig of 6.3 kb. An internal 600 bp *Hin*dIII fragment within intron 2 was deleted from the construct to facilitate subsequent screening. An IRES/neo^R element [obtained from pGT1.8Zin; a gift of Peter Mountford, Monash Medical Centre, Melbourne, Australia (27)] was cloned into the *Eco*RI site present within exon 3 [Fig. 1a(ii)] at a site that was expected to cause a premature termination of Incenp protein synthesis at amino acid 47 following replacement of the wild-type allele.

Generation of targeted ES cells and mice

The targeting vector was linearized at the 5' end by restriction digestion with *Kspl*. The mouse ES cell lines 129/1 and W9.5 were used to generate homologous recombination events. Approximately 10^8 cells were electroporated with 50 μg of linearized construct in each transfection experiment using a single pulse from a Bio-Rad (Hercules, CA) Gene Pulser at 0.8 kV, 3 μFD, ∞ Ω. Cells were plated onto mitomycin C-inactivated STO-neo^R feeder cells (34) in the presence of 10^3 U/ml LIF (AMRAD-Pharmacia, Melbourne, Australia) and selected 24 h later in G418 (Gibco BRL, Gaithersburg, MD) at an active concentration of 300 or 250 μg/ml for 129/1 and W9.5 cells, respectively. Neo^R colonies were grown for 5–8 days before genomic DNA was extracted and digested with *Acc*I. A 1.1 kb *Eco*RI–*Kspl* genomic DNA fragment 5' of the targeting region [Fig. 1a(i)] was used as a probe in Southern blot hybridization to identify correct targeting events [Fig. 1a(iii)].

For chimeric mouse production, W9.5- and 129/1-derived targeted cell lines were microinjected into day 3.5 host

C57BL/6 blastocysts and transferred into pseudopregnant mice following standard methods. Chimeric mice were identified by their coat color and were crossed with C57BL/6 mice to test for germline transmission by heterozygote production. Heterozygous mice were intercrossed to produce homozygous *Incenp*-disrupted mice.

Genotyping of mouse tail DNA

Mouse tail biopsies were taken from 3-week-old animals and lysed overnight in lysis buffer containing 100 mM NaCl, 50 mM Tris, pH 7.5, 10 mM EDTA, 0.5% SDS and 0.2 mg/ml proteinase K. Insoluble materials such as hair and bone were pelleted and the supernatant subjected to one phenol extraction and one chloroform extraction before the DNA was ethanol precipitated and resuspended in TE buffer. An aliquot of 1 µl of this DNA solution was used in a semiduplex PCR strategy as presented in Figure 1a(i and iii), using 1 µM each of the following three primers: IN1 (5'-CCTGGACTTTGTCTGCAATG), IN2 (5'-TGTTAGACACCCGCCTCTTC) and IN3 (5'-CTTCCTCGTGCTTTACGGTATC). Primers IN1 and IN2 gave an expected product of 532 bp for the wild-type allele, while IN2 and IN3 gave an expected 616 bp product for the targeted allele. PCR was performed using Perkin Elmer (Foster City, CA) PCR buffer, 0.05 U/µl Perkin Elmer Taq polymerase, 200 µM dNTPs (Boehringer Mannheim, Mannheim, Germany), 2 mM $MgCl_2$, using 30 cycles at 94°C for 1 min, 58°C for 2 min and 72°C for 2 min.

Genotyping of day 8.5 embryos

Embryos from heterozygote matings were dissected out of their uterine implantation sites into phosphate-buffered saline (PBS) at day 8.5 of gestation. The embryos were rinsed in M2 medium (Sigma, St Louis, MO) and three changes of PBS, incubated in mouse tail lysis buffer at 55°C for 4 h and extracted for DNA as described above. Glycogen was used as an inert carrier in ethanol precipitation to maximize DNA recovery. The DNA was resuspended in 20 µl of TE and 5 µl of this solution was used in the semiduplex PCR strategy described for tail DNA.

Genotyping of day 3.5 and cultured embryos

Heterozygous mouse breeding pairs were examined daily for vaginal plugs. The day of plug formation was defined as day 0.5 of embryonic development. At 3.5 days, female mice were killed and their uterus and oviducts were dissected and flushed with M2 medium. A subset of the embryos was individually placed in 1 ml tissue culture wells in ES cell medium for monitoring development in culture. After 6 days of daily observation, the embryos were washed with PBS, trypsinized, rinsed in PBS and pelleted by centrifugation at 150 *g*. The samples were frozen at –20°C until use in PCR. Cells were resuspended in 15 µl PBS to which was added 15 µl of a lysis solution of 200 mM KOH and 50 mM dithiothreitol. Samples were incubated at 65°C for 10 min followed by addition of 15 µl of a neutralization solution (900 mM Tris, 300 mM KCl, 200 mM HCl). To enhance PCR detection, the extracted DNA was first subjected to a whole genome preamplification step. An aliquot of 45 µl of a master PCR mix was combined with 15 µl of the lysed sample to give the following concentrations of the remaining components: 100 µg/ml gelatin, 2.5 mM $MgCl_2$, 10mM Tris, pH 8.3, 100 µM dNTPs and Taq polymerase. The preamplification PCR was performed by repeated primer extensions using 15 µM of a mixture of 15 base random oligonucleotides as described previously (30).

A second subset of day 3.5 embryos was rinsed twice in M2 medium, photographed and rinsed twice again in PBS, before the embryos were individually placed in thin-walled 0.2 ml PCR tubes (Perkin Elmer) and 5 µl of TE was added. Lysis and whole genome preamplification was carried out in the same reaction tube.

Targeted allele-specific PCR was performed according to the strategy presented in Figure 3a, using 2 µl of preamplification product and the primer pair neo1 (5'-GCAGGATCTCCTGTCATCTCAC) and neo2 (5'-GATCATCCTGATCGACAAGACC), which gave a product of 175 bp. The PCR conditions were 94°C for 1 min, 59°C for 2 min and 72°C for 2 min for 30 cycles. Concentrations of reagents were the same as in the strategy in Figure 1a, except the final concentration of $MgCl_2$ was 1.5 mM. Presence of the wild-type allele was investigated using the primer pair Int8 (5'-GCTGATTTCACAGAGCTTTGG, derived from intron 2 sequence) and Int9 [5'-CATCAGCTCTGGCTCATTGC, derived from exon 3 at nucleotide position 260 of the mouse cDNA (GenBank accession no. AA014535)], which gave a 168 bp product. PCR was performed as described for the neo1/neo2 primer pair except that $MgCl_2$ was present at 2 mM, annealing was at 60°C and 35 cycles were performed.

Embryo morphology studies

Embryos were harvested at day 2.5 or 3.5 as described above, photographed, washed in 0.9% trisodium citrate and transferred to fresh trisodium citrate. After incubation for at least 4 min, embryos were transferred by micropipettes onto clean slides in a minimal volume. Embryos were fixed and spread onto the slides using three floods of methanol:acetic acid (3:1) fixative. Slides were stained in Giemsa solution for 15 min and rinsed for 1 min in PBS. After drying, slides were mounted in DEPEX (Crown Scientific, Melbourne, Australia) and viewed under ×400 magnification under a standard light microscope.

Immunocytochemistry of embryos

Embryos were harvested at day 2.5, rinsed in M2 medium and the zona pellucida was removed using acid Tyrode's solution. Embryos were rinsed again and transferred to ~10 µl of M2 medium in the wells of a Terasaki dish, after which the embryos were transferred to wells containing microtubule stabilizing buffer (buffer M) comprising 25% glycerol, 50 mM imidazole HCl, pH 6.8, 50 mM KCl, 0.5 mM $MgCl_2$, 0.1 mM EDTA, 1 mM EGTA, 1 mM β-mercaptoethanol, 1% Triton X-100 and 0.2 mM phenylmethylsulfonyl flouride (PMSF) (35) for 10 min. They were then removed in a minimal volume of buffer M and placed onto polylysine-coated slides. Attachment of each embryo to a slide was facilitated by gently sweeping the micropipette into the solution and across the surface of the slide to reduce the volume of liquid around the embryo. Embryos were overlayed with a modified buffer M (containing no β-mercaptoethanol, Triton X-100 or PMSF) and were fixed for 10 min at room temperature by the gentle addition of ice-cold methanol. Slides were rinsed in PBS containing 0.1%

Triton X-100 (PBS-TX) and blocked using PBS-TX containing 3 mg/ml BSA (PBS-TX-BSA) for 90 min at 37°C. Mouse monoclonal anti-β-tubulin (Boehringer Mannheim), diluted 1:25 in PBS containing 3 mg/ml BSA (PBS-BSA), was applied and slides incubated at 37°C for 90 min. Slides were then washed three times in PBS-TX-BSA, Texas red-conjugated goat anti-mouse IgG (Jackson Laboratories, West Grove, PA) was applied and slides were incubated and washed as described above. DNA was stained by mounting in Vectashield antifade containing 0.2 μg/μl 4,6'-diamidine-2-phenylindole. Images were captured by a cooled CCD camera fitted to a Zeiss Axioskop fluorescence microscope using ×63 and ×100 objectives and IPlab software.

ACKNOWLEDGEMENTS

We thank G. Kay for the 129/1 cell line, J. Mann for the W9.5 cell line, E. Robertson for STO/Neo^R feeder cells, P. Mountford and A. Smith for the IRES/neo^R marker and S. Gazeas, A. Sylvain and J. Ladhams for mouse breeding. This work was supported by the National Health and Medical Research Council of Australia. K.H.A.C. is a Principal Research Fellow of the NH&MRC.

REFERENCES

1. Choo, K.H.A. (1997) *The Centromere.* Oxford University Press, Oxford, UK.
2. Palmer, D.K., O'Day, K., Wener, M.H., Andrews, B.S. and Margolis, R.L. (1987) A 17-kD centromere protein (CENP-A) copurifies with nucleosome core particles and with histones. *J. Cell Biol.*, **104**, 805–815.
3. Sullivan, K.F., Hechenberger, M. and Masri, K. (1994) Human CENP-A contains a histone H3 related histone fold domain that is required for targeting to the centromere. *J. Cell Biol.*, **127**, 581–592.
4. Earnshaw, W.C. and Rothfield, N. (1985) Identification of a family of human centromere proteins using autoimmune sera from patients with scleroderma. *Chromosoma*, **91**, 313–321.
5. Masumoto, H., Sugimoto, K. and Okazaki, T. (1989) Alphoid satellite DNA is tightly associated with centromere antigens in human chromosomes throughout the cell cycle. *Exp. Cell Res.*, **181**, 181–196.
6. Brown, M. (1995) Sequence similarities between the yeast chromosome segregation protein Mif2 and the mammalian centromere protein CENP-C. *Gene*, **160**, 111–116.
7. Meluh, P. and Koshland, D. (1995) Evidence that the *MIF2* gene of *Saccharomyces cerevisiae* encodes a centromere protein with homology to the mammalian centromere protein CENP-C. *Mol. Cell. Biol.*, **6**, 793–807.
8. Tomkiel, J., Cooke, C.A., Saitoh, H., Bernat, R.L. and Earnshaw, W.C. (1994) CENP-C is required for maintaining proper kinetochore size and for a timely transition to anaphase. *J. Cell Biol.*, **125**, 531–545.
9. Earnshaw, W.C. and Mackay, A.M. (1994) Role of nonhistone proteins in the chromosomal events of mitosis. *FASEB J.*, **8**, 947–956.
10. Yen, T.J., Li, G., Schaar, B.T., Szilak, I. and Cleveland, D.W. (1992) CENP-E is a putative kinetochore motor that accumulates just before mitosis. *Nature*, **359**, 536–539.
11. Holzbaur, E. and Vallee, R. (1994) Dyneins: molecular structure and cellular function. *Annu. Rev. Cell Biol.*, **10**, 339–372.
12. Wordeman, L. and Mitchison, T.J. (1995) Identification and partial characterization of mitotic centromere-associated kinesin, a kinesin-related protein that associates with centromeres during mitosis. *J. Cell Biol.*, **128**, 95–105.
13. Tokai, N., Fujimoto-Nishiyama, A., Toyoshima, Y., Yonemura, S., Tsukita, S., Inoue, J. and Yamamota, T. (1996) Kid, a novel kinesin-like DNA binding protein is localized to chromosomes and the mitotic spindle. *EMBO J.*, **15**, 457–467.
14. Rattner, J.B., Rao, A., Fritzler, M.J., Valencia, D.W. and Yen, T.J. (1993) CENP-F is a ca. 400 kDa kinetochore protein that exhibits a cell-cycle dependent localization. *Cell Motil. Cytoskeleton*, **26**, 214–226.
15. Liao, H., Winkfein, R.J., Mack, G., Rattner, J.B. and Yen, T.J. (1995) Cenp-F is a protein of the nuclear matrix that assembles onto kinetochores at late G2 and is rapidly degraded after mitosis. *J. Cell Biol.*, **130**, 507–518.
16. Zhu, X., Mancini, M.A., Chang, K.H., Liu, C.Y., Chen, C.F., Shan, B., Jones, D., Yang-Feng, T.L. and Lee, W.-H. (1995) Characterisation of a novel 350-kilodalton nuclear phosphoprotein that is specifically involved in mitotic-phase progression. *Mol. Cell. Biol.*, **15**, 5017–5029.
17. Rattner, J.B., Kingwell, B. and Fritzler, M.J. (1988) Detection of distinct structural domains within the primary constriction using autoantibodies. *Chromosoma*, **96**, 360–367.
18. Earnshaw, W.C. and Cooke, C.A. (1991) Analysis of the distribution of the INCENPs throughout mitosis reveals the existence of a pathway of structural changes in the chromosomes during metaphase and early events in cleavage furrow formation. *J. Cell Sci.*, **98**, 443–461.
19. Cooke, C.A., Heck, M.M.S. and Earnshaw, W.C. (1987) The inner centromere protein (INCENP) antigens: movement from inner centromere to midbody during mitosis. *J. Cell Biol.*, **105**, 2053–2067.
20. Mackay, A.M. and Earnshaw, W.C. (1993) The INCENPs: structural and functional analysis of a family of chromosome passenger proteins. *Cold Spring Harbor Symp. Quant. Biol.*, **58**, 697–706.
21. Mackay, A.M., Eckley, D.M., Chue, C. and Earnshaw, W.C. (1993) Molecular analysis of the INCENPs (inner centromere proteins): separate domains are required for association with microtubules during interphase and with the central spindle during anaphase. *J. Cell Biol.*, **123**, 373–385.
22. Stukenberg, P.T., Lustig, K.D., McGarry, T.J., King, R.W., Kuang, J. and Kirschner, M.W. (1997) Systematic identification of mitotic phosphoproteins. *Curr. Biol.*, **7**, 338–348.
23. Fowler, K.J., Saffery, R., Kile, B.T., Irvine, D.V., Hudson, D.F., Trowell, H.E. and Choo, K.H.A. (1998) Genetic mapping of mouse centromere protein (Incenp and cenpe) genes. *Cytogenet. Cell Genet.*, **82**, 67–70.
24. Saffery, R., Irvine D.V., Kile, B.T., Hudson, D.F., Cutts, S.M. and Choo, K.H.A. (1999) Cloning, expression and promoter structure of a mammalian inner centromere protein (INCENP). *Mamm. Genome*, **10**, 415–418.
25. Eckley, D.M., Ainsztein, A.M., Mackay, A.M., Goldberg, I.G. and Earnshaw, W.C. (1997) Chromosomal proteins and cytokinesis: patterns of cleavage furrow formation and inner centromere protein positioning in mitotic heterokaryons and mid-anaphase cells. *J. Cell Biol.*, **136**, 1169–1183.
26. Mackay, A.M., Ainsztein, A.M., Eckley, D.M. and Earnshaw, W.C. (1998) A dominant mutant of inner centromere protein (INCENP), a chromosomal protein, disrupts prometaphase congression and cytokinesis. *J. Cell Biol.*, **140**, 991–1002.
27. Mountford, P., Zevnik, B., Duwel, A., Nichols, J., Li, M., Dani, C., Robertson, M., Chambers, I. and Smith, A. (1994) Dicistronic targeting constructs: reporters and modifiers of mammalian gene expression. *Proc. Natl Acad. Sci. USA*, **91**, 4303–4307.
28. Kalitsis, P., Fowler, K.J., Earle, E., Hill, J. and Choo, K.H.A. (1998) Targeted disruption of mouse centromere protein C gene leads to mitotic disarray and early embryo death. *Proc. Natl Acad. Sci. USA*, **9**, 1136–1141.
29. Hudson, D.F., Fowler, K.J., Earle, E., Saffery, R., Kalitsis, P., Trowell, H., Hill, J., Wreford, N.G., de Kretser, D.M., Cancilla, M.R., Howman, E., Hii, L., Cutts, S.M., Irvine, D.V. and Choo, K.H.A. (1998) Centromere protein B null mice are mitotically and meiotically normal but have lower body and testis weights. *J. Cell Biol.*, **141**, 309–319.
30. Zhang, L., Cui, X., Schmitt, K., Hubert, R., Navidi, W. and Arnheim, N. (1992) Whole genome amplification from a single cell: implications for genetic analysis. *Proc. Natl Acad. Sci. USA*, **89**, 5847–5851.
31. Bernat, R.L., Borisy, G.G., Rothfield, N.F. and Earnshaw, W.C. (1990) Injection of anticentromere antibodies in interphase disrupts events required for chromosome movement at mitosis. *J. Cell Biol.*, **111**, 1519–1533.
32. Mullins, J.M. and Biesele, J.J. (1977) Terminal phase of cytokinesis in D-98S cells. *J. Cell Biol.*, **73**, 672–684.
33. Li, X. and Nicklas, R.B. (1995) Mitotic forces control a cell cycle checkpoint. *Nature*, **373**, 630–632.
34. Robertson, E.J. (1987) Embryo-derived stem cell lines. In Robertson, E.J. (ed.), *Teratocarcinomas and Embryo Stem Cells: A Practical Approach.* IRL Press, Oxford, UK, pp. 71–112.
35. Simerly, C. and Schatten, G. (1993) Techniques for localization of specific molecules in oocytes and embryos. *Methods Enzymol.*, **225**, 516–553.

PUBLICATION 7

K.J. FOWLER, P. KALITSIS AND K.H.A. CHOO (1999)

MOUSE MITOTIC SPINDLE CHECKPOINT (*BUB3*) GENE MAPS TO THE DISTAL REGION OF CHROMOSOME 7 USING INTERSPECIFIC BACKCROSS ANALYSIS.

CYTOGENETICS AND CELL GENETICS, 87: 91-92.

Cytogenet Cell Genet 87:91–92 (1999)

Cytogenetics and Cell Genetics

Mouse mitotic spindle checkpoint *Bub3* gene maps to the distal region of Chromosome 7 by interspecific backcross analysis

K.J. Fowler, P. Kalitsis, and K.H.A. Choo

The Murdoch Institute, Royal Children's Hospital, Parkville, Victoria (Australia)

Rationale and significance

Human mitotic spindle checkpoint BUB3 gene encodes a 37-kDa protein (Taylor et al., 1998) and is a member of the BUB (budding uninhibited by benzimidazole)-family of genes, first identified in *Saccharomyes cerevisiae* (Hyot et al., 1991). BUB3 has been shown to interact with BUB1 in mammalian cells and like BUB1, the protein localises to the kinetochore before chromosome alignment takes place on the mitotic spindle during cell division (Roberts et al., 1994; Basu et al., 1998; Taylor et al., 1998; Martinez-Exposito et al., 1999). Mutations of the BUB1 gene have been identified in colon cancer cell lines that display an altered mitotic checkpoint status as well as chromosome instability phenotype (Cahill et al., 1998). BUB3 has been mapped to human chromosome 10q24 (Seeley et al., 1999) and 10q24→q26 (Cahill et al., 1999). Chromosome deletions in the 10q24 region appear in cancers from a number of tissues suggesting that BUB3 may function as a tumour suppressor gene (Seeley et al., 1999). Here we report the use of a mouse genomic fragment to map the chromosome position of the mouse *Bub3* gene.

Supported by the NH and MRC of Australia. We thank Mary Barter and Lucy Rowe for the BSS backcross map and haplotype figures.

Received 19 July 1999; manuscript accepted 6 August 1999.

Request reprints from K.J. Fowler, The Murdoch Institute, Royal Children's Hospital, Flemington Road, Parkville, 3052, Victoria (Australia); telephone: +613 8341 6299; fax: +613 9348 1391; email: fowlerk@cryptic.rch.unimelb.edu.au

Materials and methods

Probe type: 437-bp genomic fragment of mouse *Bub3*

Proof of Authenticity: A 437-bp genomic fragment was amplified from 129Sv mouse genomic DNA using primer pairs B1 (5′-AGAAACGTTGCTTAGGCGG-3′) and B2 (5′-CTTGAGCCTCATGGAATTGG-3′). Nucleotide positions 1–26 and 282–437 of the PCR fragment are 100% homologous to nucleotides 24–49 and 50–205 of the mouse *Bub3* cDNA sequence (Genbank Accession No. U67327), respectively. The intervening sequence between nucleotide positions 27–281 of the 437-bp genomic fragment is the first intron.

Method of mapping: The 437-bp PCR fragment was used as a probe on Southern blots to identify an informative *Msp*I polymorphism around the Bub3 locus of C57BL/6J and Spret/Ei mouse strains. The enzyme revealed bands of 1.4 kb in Spret/Ei and 3.4 kb in the C57BL/6J strain. This polymorphism was used to genotype Southern blot filters with DNA from interspecific backcross panel (C57BL/6JEi × SPRET/Ei) F1 × SPRET/Ei (known as The Jackson BSS panel) (Rowe et al., 1994). Progenitor DNA and filters were purchased from The Jackson Laboratory, Bar Harbor, Maine. Genomic DNA and Southern blots were analysed as described previously (Fowler et al., 1997).

Results

Inheritance of the homozygous or heterozygous SPRET/Ei 1.4-kb fragment was typed in 94 progeny DNA and analysed. The observed pattern indicated linkage to the *Hmx3* gene and several markers on the distal region of Chromosome 7, including D7Ertd558e and D7Xrf281 (0.00–3.8 cM, 95% limits; Fig. 1). The mapping of *Bub3* to the distal region on Chromosome 7 conforms with the expected mouse/human syntenic region, since human BUB3 has been localised to chromosome 10q24 (Seeley et al., 1999) and 10q24→q26 (Cahill et al., 1999). Beside *Bub3*, there are ten genes that have homology with human chromosome 10q24→q26 and the distal region of mouse Chromosome 7 (MGD), including the *Cyp2e1* gene (68.4 cM region, MGD composite map) that was shown to have linkage with *Bub3* (Fig. 1) in this study.

KARGER

Fax + 41 61 306 12 34
E-mail karger@karger.ch
www.karger.com

0301–0171/99/0872–0091$17.50/0

Accessible online at:
www.karger.com/journals/ccg

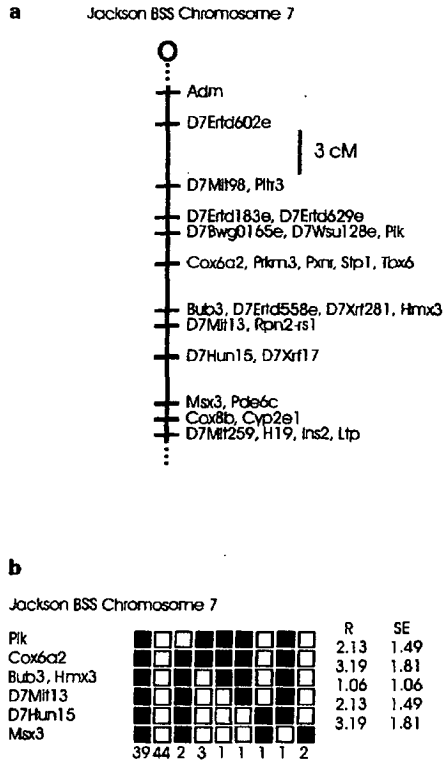

Fig. 1 . Map figure (**a**) and Haplotype figure (**b**) from The Jackson BSS backcross. (**a**) The distal end of Chromosome 7 with loci linked to *Bub3*. The map is depicted with the centromere toward the top. A 3-cM scale bar is shown to the right of the figure. Loci mapping to the same position are listed in alphabetical order and not all BSS markers linked to *Bub3* are shown on this figure. Missing typings were inferred from the surrounding data where assignment was unambiguous. Raw data for The Jackson BSS panel strain distribution patterns (SDPs) were obtained from The Jackson Laboratory (http//www.jax.org/resources/documents/cmdata) and date from July 1999. (**b**) Haplotype figure showing the distal end of Chromosome 7 with loci linked to *Bub3*. Loci are listed in order with the most proximal at the top. The black boxes represent the C57BL6/Ei allele and the white boxes the SPRET/Ei allele. The number of animals with each haplotype is given at the bottom of each column of boxes. The percent recombination (R) and the standard error (SE) for each R value were calculated using the Map Manager Program (Manly 1993) and are given to the right of the figure. Missing typings were inferred from surrounding data where assignment was unambiguous.

References

Basu J, Logarinho E, Herrmann S, Bousbaa H, Li Z, Chan GKT, Yen TJ, Sunkel CE, Goldberg ML: Localization of the *Drosophila* checkpoint control protein Bub3 to the kinetochore requires Bub1 but not Zw10 or Rod. Chromosoma 107:376–385 (1998).

Cahill DP, Lengauer C, Yu J, Riggins GJ, Willson JKV, Markowitz SD, Kinzler KW, Vogelstein B: Mutations of mitotic checkpoint genes in human cancers. Nature 392:300–303 (1998).

Cahill DP, da Costa LT, Carson-Walter EB, Kinzler KW, Vogelstein B, Lengauer C: Characterisation of MAD2B and other mitotic checkpoint spindle genes. Genomics 58:181–187 (1999).

Fowler KJ, Newson AJ, MacDonald AC, Kalitsis P, Lyu MS, Kozak CA, Choo KHA: Chromosomal localization of mouse *Cenpa* gene. Cytogenet Cell Genet 79:298–301 (1997).

Hyot MA, Totis L, Roberts BT: *S. cerevisiae* genes required for cell cycle arrest in response to loss of microtubule function. Cell 66:507–517 (1991).

Manly KF: A Macintosh program for all of our data management. Mammal Genome 4:303–313 (1993).

Martinez-Exposito MJ, Kaplan KB, Copeland J, Sorger PK: Retention of the Bub3 checkpoint protein on lagging chromosomes. Proc natl Acad Sci, USA (in press 1999).

Roberts BT, Farr KA, Hoyt MA: The *Saccharomyces cerevisiae* checkpoint gene BUB1 encodes a novel protein kinase. Mol Cell Biol 14:8282–8291 (1994).

Rowe LB, Nadeau JH, Turner R, Frankel WN, Letts VA, Epping JT, Ko MSH, Thurston SJ, Birkenmeier EH: Maps from two interspecific backcross DNA panels available as a community genetic mapping resource. Mammal Genome 5:253–274 (1994).

Seeley TW, Wang L, Zhen JY: Phosphorylation of human MAD1 by the BUB1 kinase *in vitro*. Biochem biophys Res Comm 257:589–595 (1999).

Taylor SS, Ha E, McKeon F: The human homologue of Bub3 is required for kinetochore localization of Bub1 and a Mad3/Bub1-related protein kinase. J Cell Biol 142:1–11 (1998).

PUBLICATION 8

K.J. FOWLER , D.F. HUDSON, L. SALAMONSEN, S. EDMONDSON, E. EARLE, M.C. SIBSON AND K.H.A. CHOO (2000)

UTERINE DYSFUNCTION AND GENETIC MODIFIERS IN CENTROMERE PROTEIN B-DEFICIENT MICE.

GENOME RESEARCH, 10: 30-41 AND FRONT COVER.

ISSN 1088-9051

January 2000

GENOME RESEARCH

Volume 10 Number 1

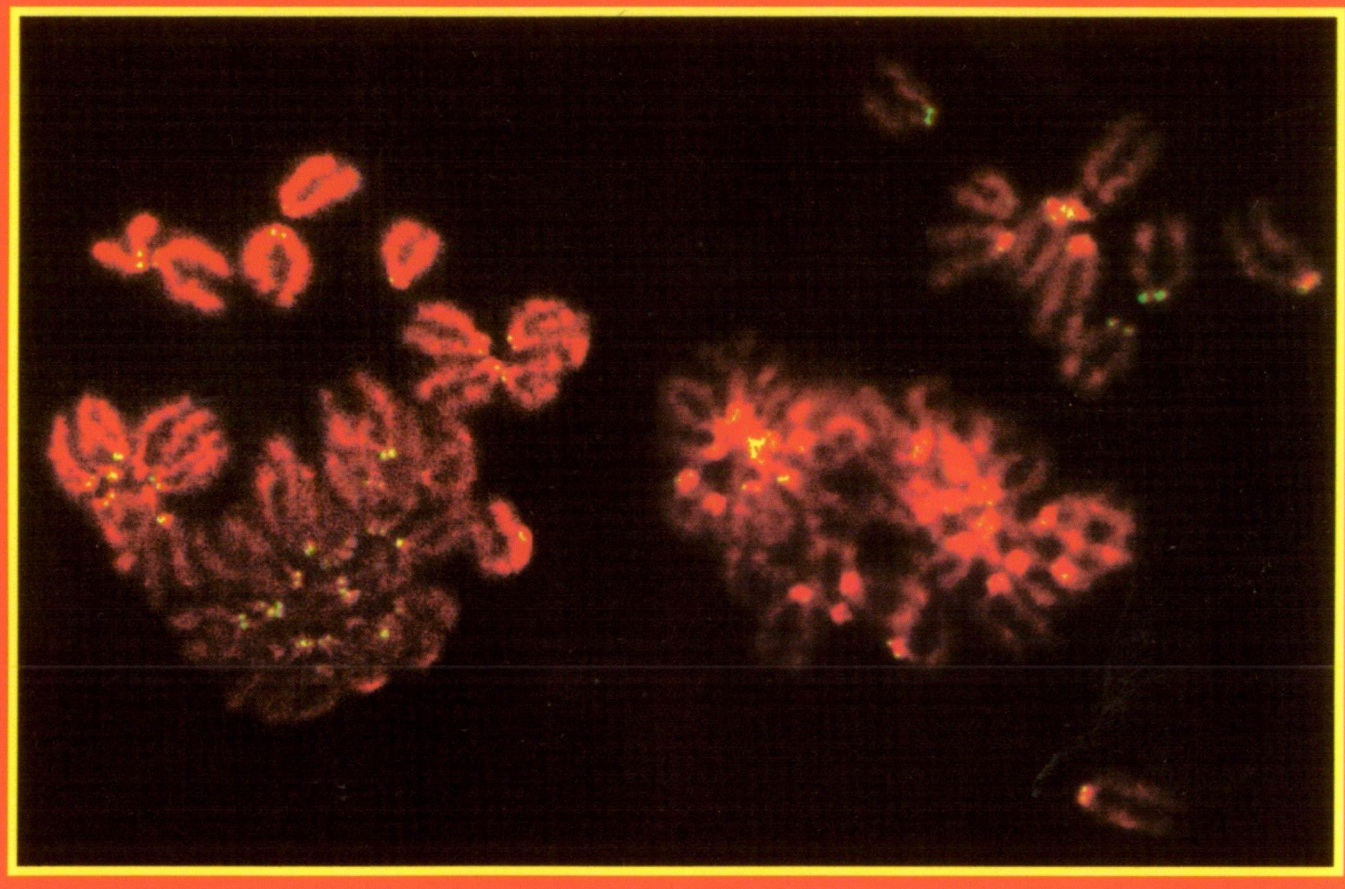

Centromere Protein B-deficient Mice and Uterine Dysfunction ◆ Evolution of Bacterial Replicative Helicase DnaB ◆ Polycystic Kidney Disease Severity Modifiers in Mice ◆ ACAPELLA-1K, A Submicroliter Automated Fluid Handling System ◆ BAC Libraries for Mouse Genome Sequencing

Cold Spring Harbor Laboratory Press

Cover. Immunofluorescence analysis of CENP-B binding on centromeric regions of mouse metaphase chromosomes in wild-type and revertant controls for *Cenpb*-deficient mice studies. The work shows that *Cenpb*-deficient mice have uterine dysfunction and implicates the presence of genetic reproductive modifiers (Fowler et al, 2000[8]).

Uterine Dysfunction and Genetic Modifiers in Centromere Protein B-deficient Mice

Kerry J. Fowler,[1] Damien F. Hudson,[1] Lois A. Salamonsen,[2] Stephanie R. Edmondson,[3] Elizabeth Earle,[1] Mandy C. Sibson,[1] and K.H. Andy Choo[1,4]

[1]*The Murdoch Institute, Royal Children's Hospital, Parkville 3052, Australia;* [2]*Prince Henry's Institute of Medical Research, Clayton 3168, Australia;* [3]*Centre for Hormone Research, Royal Children's Hospital, Parkville 3052, Australia*

Centromere protein B (CENP-B) binds constitutively to mammalian centromere repeat DNA and is highly conserved between humans and mouse. *Cenpb* null mice appear normal but have lower body and testis weights. We demonstrate here that testis-weight reduction is seen in male null mice generated on three different genetic backgrounds (denoted RI, W9.5, and C57), whereas body-weight reduction is dependent on the genetic background as well as the gender of the animals. In addition, *Cenpb* null females show 31%, 33%, and 44% reduced uterine weights on the RI, W9.5, and C57 backgrounds, respectively. Production of "revertant" mice lacking the targeted frameshift mutation but not the other components of the targeting construct corrected these differences, indicating that the observed phenotype is attributable to *Cenpb* gene disruption rather than a neighbouring gene effect induced by the targeting construct. The RI and W9.5 *Cenpb* null females are reproductively competent but show age-dependent reproductive deterioration leading to a complete breakdown at or before 9 months of age. Reproductive dysfunction is much more severe in the C57 background as *Cenpb* null females are totally incompetent or are capable of producing no more than one litter. These results implicate a further genetic modifier effect on female reproductive performance. Histology of the uterus reveals normal myometrium and endometrium but grossly disrupted luminal and glandular epithelium. Tissue in situ hybridization demonstrates high *Cenpb* expression in the uterine epithelium of wild-type animals. This study details the first significant phenotype of *Cenpb* gene disruption and suggests an important role of Cenpb in uterine morphogenesis and function that may have direct implications for human reproductive pathology.

The centromere is essential for proper chromosome movements during mitosis and meiosis. An increasing number of centromere proteins have now been identified but little is known about the precise roles of these proteins, especially in whole animals (Choo 1997a; Craig et al. 1998; Dobie et al. 1999). Recent gene disruption studies in mice have produced null mutations in three different centromere proteins. Mutations in two of these proteins, Cenpc and Incenp, caused early embryonic lethality (Kalitsis et al. 1998; Cutts et al. 1999). The third protein, Cenpb, was nonessential as null mice appeared healthy (Hudson et al. 1998; Kapoor et al. 1998; Perez-Castro et al. 1998) except for lower body and testis weights (Hudson et al. 1998).

The biological role of CENP-B has intrigued researchers for many years. CENP-B is a constitutive and abundant centromere-specific protein, and is highly conserved in mammals (Earnshaw et al. 1987a; Sullivan and Glass 1991; Haaf and Ward 1995; Bejarano and Valdivia 1996; Yoda et al. 1996). The protein shows an overall 96% nucleotide sequence similarity between humans and mouse, with a surprisingly high level (95% and 83%, respectively) of homology even in the 5′ and 3′ untranslated mRNA sequences (Earnshaw et al. 1987b; Sullivan and Glass 1991). The protein binds centromeric human α-satellite and mouse minor satellite DNA via a 17-bp consensus *CENP-B* box motif (Pietras et al. 1983; Rattner 1991). Through its dimerization properties, the protein is thought to be involved in the assembly of the large arrays of centromeric repeats (Muro et al. 1992; Yoda et al. 1992). The presence of this protein on both the active and inactive centromeres of mitotically stable pseudodicentric human chromosomes (Earnshaw et al. 1989; Page et al. 1995; Sullivan and Schwartz 1995) indicates that CENP-B binding is not immediately associated with centromere activity. The absence of this protein on the Y chromosome in humans and mouse (Earnshaw et al. 1987a), on the centromeres of African green monkey (known to be composed largely of α-satellite DNA containing little or no binding sites for CENP-B) (Goldberg et al. 1996), as well as on an increasing number of human marker chromosomes containing analphoid neocentromeres (Voullaire et al. 1993; Choo 1997b; Depinet et al. 1997; du Sart et al. 1997), suggests that the role of this protein is dispensable.

In this study, we have further investigated the

[4]Corresponding author.
E-MAIL CHOO@CRYPTIC.RCH.UNIMELB.EDU.AU; FAX 61-3-9348 1391.

10:30–41 ©2000 by Cold Spring Harbor Laboratory Press ISSN 1054-9803/99 $5.00; www.genome.org

Cenpb null mice and present evidence that the phenotype of these mice was specifically related to *Cenpb* gene disruption, excluding the possibility that the phenotype might have been due to a neighboring gene effect. We describe the influence of the null mutation on body and testis weights in different genetic backgrounds and report a previously unrecognized link between Cenpb deficiency and severe female reproductive dysfunction resulting from abnormality of the uterine epithelium. Our data further indicate a role of genetic modifiers in this reproductive dysfunctional phenotype.

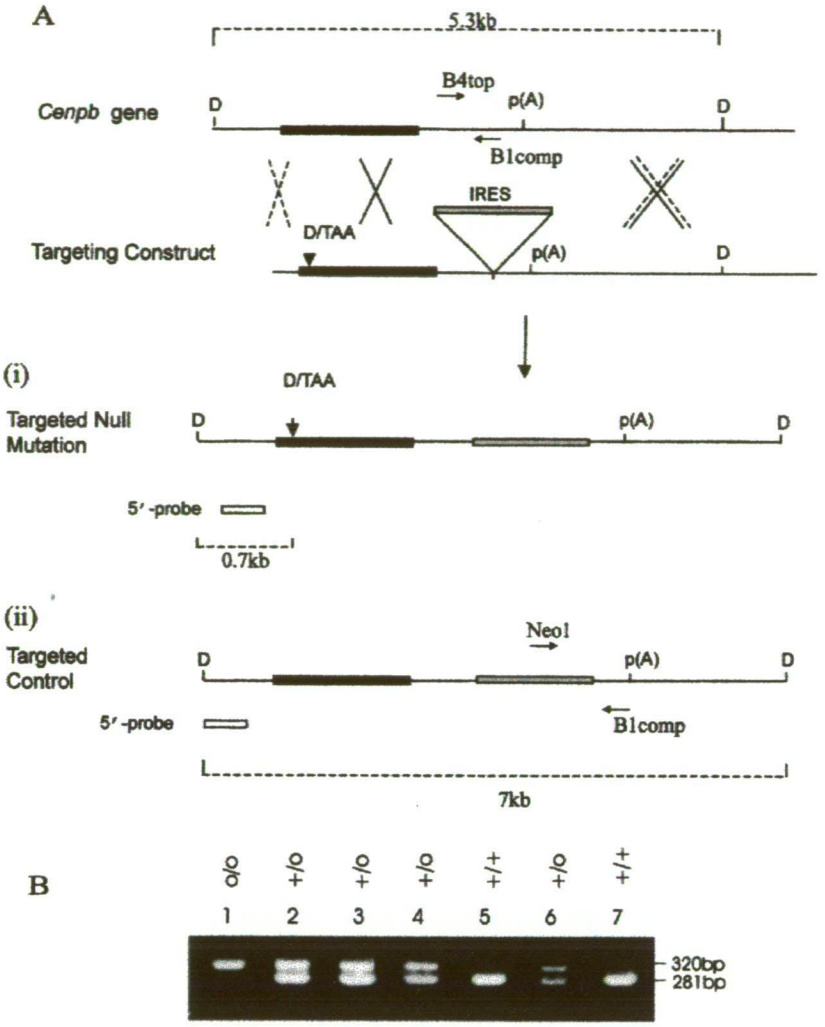

Figure 1 Strategies for production and screening of *Cenpb* disrupted and targeted control mice. (*A*) Intronless wild-type *Cenpb* gene showing the 1.8-kb coding region (solid box) and polyadenylation p(A) site. Recombination at the sites shown by the dotted crosses results in the incorporation of the targeting construct containing a translational frameshift oligonucleotide (D/TAA) at the 5′ coding region and an IRES-selectable marker cassette (shaded box) within the 3′-untranslated region (*i*). This recombination event results in the disruption of the *Cenpb* gene. An alternative recombination event at sites indicated by the solid crosses, one of which is 3′ of the D/TAA frameshift mutation, results in the introduction of the IRES-selectable marker cassette but not the frameshift mutation (*ii*). This targeted allele served as a control for any positional effect the inserted IRES-selectable marker cassette may have on the phenotype of the mice. The *Cenpb* wild-type gene (+), null allele (−), and targeted control allele (o) allele were detected as described previously (Hudson et al. 1998) as 5.3^{-}, 0.7^{-}, and 7-kb bands (broken lines), respectively, by *Dra*I (D) digestion and Southern blot hybridization using a 5′-probe (open box) (see Hudson et al. 1998). Once the heterozygous ES cell lines carrying the + and o alleles were identified, they were used for the production of the targeted control (o/o) mice. Subsequent genotype screening for these mice was based on PCR analysis using primers B4top and B1comp, which gave a 281-bp product for the + allele, and primers Neo1 and B1comp which gave a 320-bp product for the o allele. (*B*) PCR analysis of mouse progeny from a +/o × +/o cross using a combination of the primers B4top, B1comp, and Neo1, showing the +/+ (lanes *5,7*), +/o (lanes *2,3,4,6*), and o/o (lane *1*) genotypes.

RESULTS

Generation of Control Mice Carrying the Targeted Selectable Marker Cassette but not the Frameshift Mutation

To confirm that the phenotype in *Cenpb* null mice was caused by *Cenpb* gene disruption, as distinct from a consequence of the gene targeting event exerting an effect on neighboring genes, we generated mice (designated "targeted control" or o/o mice) carrying the internal ribosome entry site (IRES)–neomycin selectable marker element in the 3′ noncoding region of the *Cenpb* gene but lacking the translational frameshift mutation caused by the 26-mer oligonucleotide designated D/TAA (5′-GTACCTAGGTATACTTTTAAACTGAC-3′) introduced into the 5′ coding region of the *Cenpb* gene in the null mice (Fig. 1A). This linker introduced a *Dra*I site, a frameshift mutation, and three stop codons in all three reading frames, of which TAA was in-frame with Cenpb translation, disrupting not only the critical amino-terminal 125-amino acid centromere DNA-binding domain, but also removing all remaining carboxy-terminal regions including the dimerization domain (Hudson et al. 1998). Heterozygous (+/o) embrionic stem (ES) cell lines carrying the targeted control allele have been produced previously (Hudson et al. 1998). In this study, these cell lines were microinjected into C57BL/6 blastocysts to produce germline chimeras. Through selective breeding, wildtype (+/+), heterozygous (+/o), and homozygous targeted control (o/o) mice were generated and identified by PCR screening (Fig. 1B). The analysis of

128 offspring (generation 2) from 11 heterozygous breeding pairs gave the expected Mendelian ratio of 26 +/+, 73 +/o, and 29 o/o, suggesting no obvious viability bias among the different genotypes.

Figure 2 shows immunofluorescence analysis of fibroblast cell lines derived from +/+ and o/o littermates using an anti-CENP-B monoclonal antibody (Hudson et al. 1998). The results indicated the presence of Cenpb proteins on the centromeres in both the cell lines. The highly variable signals detected on different chromosomes were quite typical for this protein (Hudson et al. 1998). These results therefore established that *Cenpb* gene expression in the o/o animals was normal and had not been noticeably affected by the insertion of the IRES/selectable marker cassette. These animals therefore served as "revertant" controls for the *Cenpb* null mutation.

Body and Testis Weights of *Cenpb* Null Mice on Different Genetic Backgrounds

In a previous study, we generated *Cenpb* null mice that were maintained on a mixed genetic background (Simpson et al. 1997; Hudson et al. 1998). These mice were designated $R1^{-/-}$ here to distinguish them from two new *Cenpb* null mouse strains, $W9.5^{-/-}$ and $C57^{-/-}$, produced on different genetic backgrounds for this study. $W9.5^{-/-}$ was on a mixed but different background to that of $R1^{-/-}$ and represented an independent gene-targeting event to $R1^{-/-}$ (Hudson et al. 1998). $C57^{-/-}$ was a congenic strain (Markel et al. 1997; Simpson et al. 1997) generated by backcrossing the $R1^{+/-}$ mice to C57BL/6 animals for eight generations.

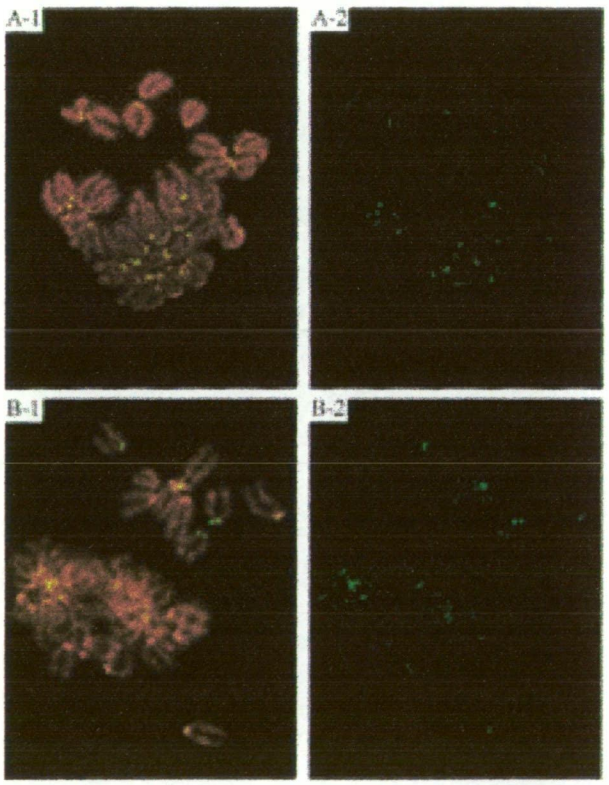

Figure 2 Immunofluorescence analysis of fibroblast cell lines derived from +/+ (*A*) and o/o (*B*) mice. Metaphase chromosomes (DAPI-stained and pseudocolored red) were prepared from fibroblasts cultures of mouse tail tissues and stained with a monoclonal anti-CENP-B antibody (green). (*1*) Merged immunofluorescence signals; (*2*) split image for the anti-CENP-B (green) signals.

We previously described a significant reduction of between 15%–20% in the body weights of 10-week-old adult male and female $R1^{-/-}$ animals up to 33 weeks old (Hudson et al. 1998). We show here that this trend could be extended to much older $R1^{-/-}$ animals of up to 90 to 100 weeks of age (Fig. 3A,B). A similar body weight reduction was observed for the $W9.5^{-/-}$ females (Fig. 3D) but was absent from the $W9.5^{-/-}$ males (Fig. 3C) and the $C57^{-/-}$ animals of both sexes (Fig. 3E,F). When testis weights were determined, a statistically significant, 14%–26% reduction was seen in all three genetic backgrounds (Table 1A). This reduction in testis size did not have any measurable effect on male fertility in animals up to 2 years old. Longevity for the R1 mice [100 weeks of follow-up; hazard ratio of 1.02 ($P = 1.0$) for $-/-$ versus +/+ males ($n = 27$ and $n = 44$, respectively); hazard ratio of 0.79 ($P = 0.7$) for $-/-$ versus +/+ females ($n = 26$ and $n = 28$, respectively)], W9.5, and C57 mice (40 weeks of follow-up) were normal in the different backgrounds.

To further investigate the reasons for the observed body weight reduction, various organs from 4-, 6-, 8-, 10- and 24-week-old, age-matched $R1^{-/-}$ and $R1^{+/+}$ males and females ($n = 4$ for each category) were weighed. The organs included stomach, small and large intestines, liver, salivary gland, spleen, pancreas, kidney, thymus, brain and olfactory bulb, lung, adrenal, heart, testes, epididymis, bulbourethral gland, ovary, uterus, ovarian fat pads, subcutaneous fat pad, and subrenal fat pad. In addition, whole-body compositions were analyzed in 20-week-old $R1^{-/-}$ and $R1^{+/+}$ animals of both sexes in terms of their dry weight, ash weight, moisture, protein, and fat. Nose–rump length was also measured. When the results were expressed as a percentage of fresh body wet weight, no significant difference was seen between the test and control groups for all the measurements, except for the testes (Table 1A) and the uterus (see below). These results suggested that the organs and body composition of the $R1^{-/-}$ animals were overall proportionally smaller than those of the $R1^{+/+}$ animals. Plasma leptin levels [3.7 ± 2.4 ng/ml for the $-/-$ mice ($n = 17$) and 4.6 ± 3.5 ng/ml for the +/+ mice ($n = 21$); $P = 0.358$] were not significantly different between 6-month-old female R1 and W9.5 *Cenpb* null and wild-type animals, suggesting that hypophagia (suppressed food intake)

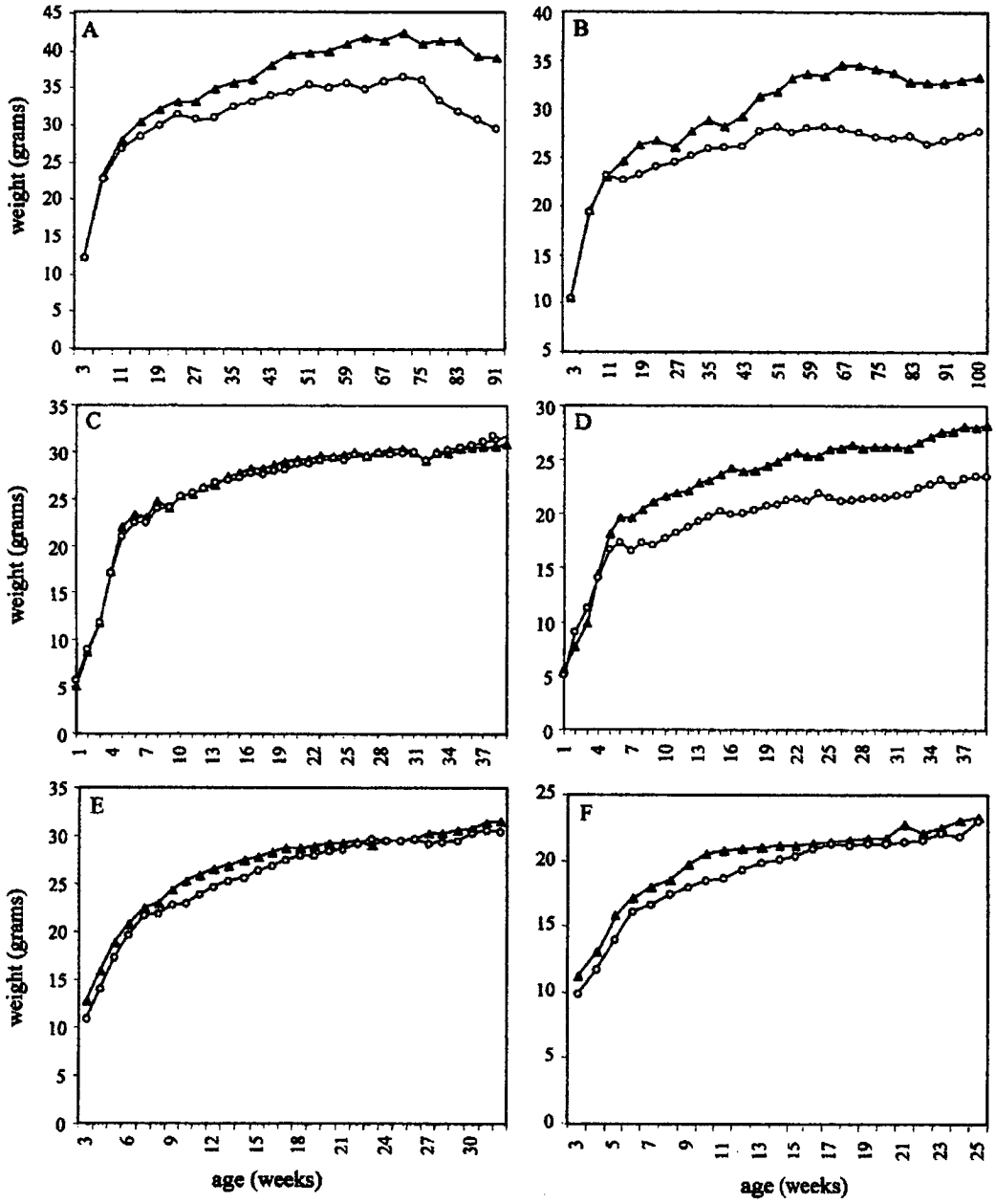

Figure 3 Total body weight of male (*A,C,E*) and female (*B,D,F*) mice in different genetic backgrounds: (*A,B*) RI; (*C,D*)W9.5; and C57 (*E,F*) C57. At least four animals were used for each time point. Age of the animals was determined from birth. (▲) +/+ animals; (○) −/− animals.

was unlikely to be responsible for reduced body weight in the −/− animals.

To determine whether cells deficient in Cenpb have an altered growth rate, we compared the population doubling times of three independently derived −/− ES cell lines (one in R1 and two in W9.5 backgrounds) (Hudson et al. 1998) with those of a +/+ and +/− cell line from each background. No significant difference was observed between the various cell lines over 400 cell divisions (data not shown). Karyotyping of the −/− cell lines at the late doubling passages also revealed no abnormality when compared with +/+ and +/− cells. This suggested that the *Cenpb* null ES cell lines grew normally and that their growth rate, unlike that previously described for the telomerase-deficient ES cells (Niida et al. 1998), did not deteriorate with increasing doubling times over the period tested.

Cenpb Null Mice Showed Reduced Uterus Weights

The uteri of 10-week-old [day 0.5 vaginal plug (VP)]

Table 1. Total Testis, Uterus, and Ovary Weight and Number of Embryos Flushed from the Oviducts of Mice on Different Genetic Backgrounds

Genetic background	Av. weight ± s.d. +/+	−/−	Percent reduction	*t*-test *P*-value
		A. Testis		
R1	208.2 ± 29.4 (n = 15)	154.0 ± 37.6 (n = 16)	26	<0.001
W9.5	191.9 ± 14.3 (n = 6)	156.1 ± 17.1 (n = 7)	19	0.002
C57	186.8 ± 15.3 (n = 13)	159.9 ± 17.9 (n = 12)	14	<0.001
		B. Uterus		
R1	114.9 ± 23.0 (n = 6)	79.7 ± 27.8 (n = 7)	31	0.032
W9.5	122.8 ± 31.7 (n = 9)	82.5 ± 19.0 (n = 5)	33	0.024
C57	94.5 ± 14.3 (n = 10)	52.9 ± 20.1 (n = 7)	44	<0.001
		C. Ovary		
R1	10.4 ± 3.8 (n = 6)	11.2 ± 1.8 (n = 7)	N.R.	0.635
W9.5	8.7 ± 2.1 (n = 9)	8.8 ± 2.4 (n = 5)	N.R.	0.878
C57	7.3 ± 2.2 (n = 10)	8.0 ± 1.8 (n = 7)	N.R.	0.513
		D. No. of embryos		
R1	7.8 ± 5.0 (n = 6)	4.7 ± 3.3 (n = 7)	N.R.	0.198
W9.5	5.9 ± 3.5 (n = 9)	3.4 ± 3.1 (n = 5)	N.R.	0.210
C57	4.9 ± 2.9 (n = 10)	4.6 ± 3.6 (n = 7)	N.R.	0.838

Ten-week-old +/+ and −/− mice were used. Uteri, ovaries, and embryos were collected at day 0.5 of vaginal plug using previously unmated females. Weight is in mg. (N.R.) Not relevant, as *P*-value is insignificant.

previously unmated −/− animals in the R1, W9.5, and C57 backgrounds were weighed and respectively found to be 31%, 33%, and 44%, smaller than those of their corresponding wild-type siblings (Table 1B and Fig. 4A). Table 2A shows the results for the total uterus weights of 8-, 9-, 10-, and 24-week-old previously unmated female R1 mice (day 0.5 VP) as well as the total uterus weights of 4-, 6-, 8-, and 10 week-old C57 mice. No statistically significant difference was observed in the 8-week-old +/+ and −/− R1 animals, with a trend toward a difference emerging at 9 weeks and a significant difference seen at 10 and 24 weeks. Similar trends were observed in the uteri of the W9.5 animals (data not shown). With the C57 null females, however, smaller uteri were observed in −/− animals compared with +/+ mice at a significantly earlier timepoint of 6 weeks (Table 2A). These results indicated a dramatic slowdown in uterine growth during the 8- to 10-week postnatal period for R1 and W9.5 and the 4- to 6-week postnatal period for C57 null mice.

Further Evidence that the *Cenpb* Null Phenotype was Directly Related to *Cenpb* Gene Disruption

The phenotype of the targeted control (o/o) mice was ascertained. At the gross level, these animals were phenotypically indistinguishable from their +/+ wild-type littermates. Table 3 compares the body, testis, and uterus weights of (as well as the ovary weight and number of eggs produced by; see below) these animals. No statistically significant difference was observed between the two genotypes. These results provided evidence that the correction of the frameshift mutation has allowed the o/o animals to revert back to a wild-type phenotype and that the IRES/selectable marker cassette (which was retained in the o/o animals) was not responsible for the phenotype observed in the −/− mice. A corollary of this was that the phenotype seen in our *Cenpb* null mice was a direct consequence of the disruption of the *Cenpb* gene itself.

Compromised Reproduction in *Cenpb* Null Females

When 10-week-old virgin $R1^{-/-}$ females (n = 10) were crossed with stud males in an ongoing breeding program, little difference was observed in the first three to four litters compared with control $R1^{+/+}$ and $R1^{+/-}$ females, indicating normal reproduction in young $R1^{-/-}$ females. A progressive deterioration (see below) in reproductive performance, however, was observed with increasing maternal age until this failed totally in all the $R1^{-/-}$ females by 9 months, when the $R1^{+/-}$ and $R1^{+/+}$ females have continued to be reproductively competent at or long after this age.

Next, we crossed a cohort of $R1^{-/-}$ (n = 3) and $R1^{+/+}$ (n = 4) 9-month-old virgin females with C57BL/6 normal stud males in a breeding program lasting for 7 months. One pregnancy occurred in each of the $R1^{-/-}$ females but the animals sickened because of being overdue and required autopsy (see below). In compari-

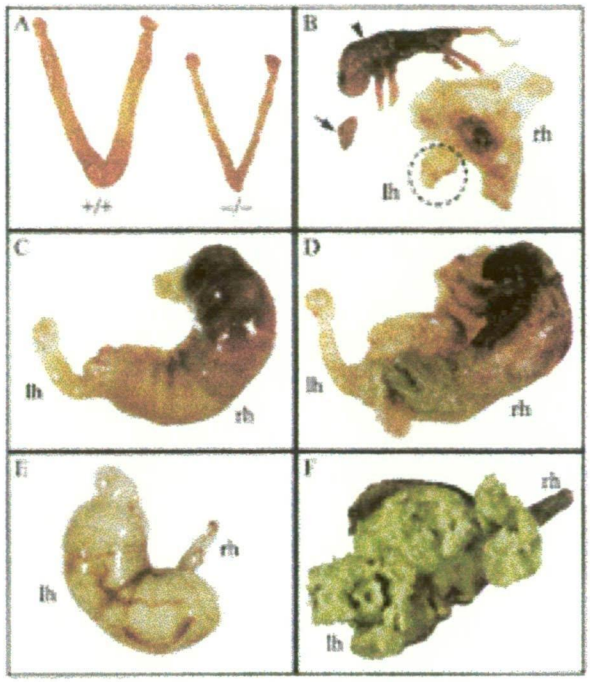

Figure 4 Uterine and pregnancy problems in *Cenpb* null mice. (*A*) Size comparison of uteri from 10-week-old $R1^{+/+}$ and $R1^{-/-}$ mice, showing the left and right uterine horns. The sizes of the ovaries and oviducts attached to these horns were normal in both animals. (*B*) Nine-month-old, 1-week overdue $W9.5^{-/-}$ pregnant female (first pregnancy), showing a full-term dead fetus (arrowhead) attributable to placental necrosis in the right horn (rh) and fetal growth arrest/resorption (arrow) in the left horn (lh; shown in circle). (*C,D*) Twelve-month-old, 10-day-overdue $R1^{-/-}$ pregnant female (fourth pregnancy), showing external and internal views of a necrotic fetus in the right horn, and absence of fetuses in the left horn. (*E,F*) Nine-month-old, 4-day-overdue $R1^{-/-}$ pregnant female (first pregnancy), showing external and internal views of decomposed fetal content in the left horn, and absence of fetuses in the right horn.

son, 20 normal pregnancies occurred in the control group, which resulted in 87 healthy pups over the same period. These results, together with those described above, indicated that the observed reproductive problems were age-related rather than a consequence of prior pregnancies.

A similar reproductive phenotype was seen in 8- to 9-week-old −/− females in the W9.5 background. A cohort of 9-month-old $W9.5^{-/-}$ ($n = 8$) and $W9.5^{+/+}$ ($n = 8$) virgin females was mated with C57BL/6 or ARC SWISS stud males over a 15-week period. Two females in the −/− group achieved a pregnancy but both were distressed because of failure of spontaneous labor at expected delivery date (post maturity) and required autopsy (discussed below). The remaining six −/− animals failed to show any visible sign of pregnancy. In contrast, the +/+ group of animals produced a total of 10 pregnancies that yielded 48 healthy pups over this period.

Compared with the animals in the R1 and W9.5 backgrounds, a significantly more severe reproductive phenotype was apparent in the −/− animals on the C57 congenic background. The reproductive performance of 8- to 15-week-old $C57^{-/-}$ ($n = 5$) females was assessed over a period of 5 months. Pregnancies were observed in all five animals. Only one of these pregnancies went to normal term and birth (four healthy pups); subsequent to this healthy litter, this female failed to become visibly pregnant again. Two of the pregnant females required autopsy because of postmaturity in one case and complication during delivery (dislocated fetal torso entrapped within the birth canal) in the other case. The fourth female had a slow delivery (>24 hr) that resulted in four live and one dead pup; in her second pregnancy, this female sickened because of being overdue and was culled. The fifth animal produced two small litters of two and three well-formed but dead pups at birth; this female has since failed to become pregnant again. Therefore, the five young $C57^{-/-}$ females together gave rise to only eight healthy pups over a 5-month mating period. In stark contrast, 74 healthy pups resulted from a cohort of six, age-matched, control $C57^{+/+}$ females over a shorter mating duration of 3 months. These results suggested that the reproductive fitness of the C57 *Cenpb* null female mice was severely compromised, and to a much greater extent compared with those seen in the R1 and W9.5 *Cenpb* null mice.

Overall, pregnancy problems in the $C57^{-/-}$, $R1^{-/-}$, and $W9.5^{-/-}$ females manifested either as a failure of the animals to become visibly pregnant despite detection of vaginal plug or, as occurred most frequently with mice that did achieve visible pregnancy, the animals sickened because of being overdue (by up to 10 days) or difficulty with delivery. Autopsy of these sickened mice revealed dead fetuses in all cases. Where discernible, fetal development appeared normal (Fig. 4B,D). Causes of fetal death in utero included placental necrosis (Fig. 4B), fetal growth arrest or resorption (Fig. 4B), fetal necrosis (Fig. 4C,D) and decomposition (Fig. 4E,F). Because the progeny of crosses between the −/− females and normal stud males must all have a +/− genotype, the observed fetal problem could not have been related to any possible complication caused by the presence of *Cenpb* null embryos in the litter. Microbacterial tests of necrotic or decomposed tissues revealed profuse growth of a variety of opportunistic bacteria including Flavobacterium, Meningosepticum (water bug), *Haemophilus influenzae* (fecal/genital bug), Gram-negative rods including *Escherichia coli* (gut bug), and Gram-positive cocci.

Normal Ovarian and Hormonal Functions in *Cenpb* Null Females

To further investigate the causes for the compromised

Table 2. Uterus Weight in Female +/+ and −/− R1 and C57 Mice at Different Ages and 17β-Estradiol and Progesterone Levels in R1 Animals

Age (weeks)	+/+	−/−	Percent reduction	*t*-test *P*-value
		A. Uterus		
R1				
8	100.6 ± 29.7 ($n = 8$)	83.3 ± 32.6 ($n = 8$)	N.R.	0.285
9	113.2 ± 34.6 ($n = 6$)	73.9 ± 26.4 ($n = 6$)	35	0.051
10	114.9 ± 23.0 ($n = 6$)	79.7 ± 27.8 ($n = 7$)	31	0.032
24	162.7 ± 50.3 ($n = 7$)	100.0 ± 44.8 ($n = 7$)	39	0.030
C57				
4	8.0 ± 2.9 ($n = 7$)	7.1 ± 1.3 ($n = 3$)	N.R.	0.599
6	82.5 ± 28.2 ($n = 8$)	49.9 ± 5.2 ($n = 7$)	40	0.010
8	98.9 ± 32.5 ($n = 7$)	63.1 ± 8.9 ($n = 5$)	36	0.040
10	94.5 ± 14.3 ($n = 10$)	52.9 ± 20.1 ($n = 7$)	44	<0.001
		B. 17β-Estradiol (R1)		
6	26.0 ± 15.6 ($n = 7$)	19.8 ± 7.2 ($n = 10$)		0.286
8	27.3 ± 14.7 ($n = 6$)	33.3 ± 18.8 ($n = 8$)		0.536
10	33.6 ± 22.1 ($n = 8$)	32.9 ± 11.1 ($n = 12$)		0.927
24	39.8 ± 10.8 ($n = 6$)	42.5 ± 18.2 ($n = 4$)		0.776
		C. Progesterone (R1)		
6	6.2 ± 5.3 ($n = 15$)	11.5 ± 12.4 ($n = 13$)		0.144
8	10.4 ± 12.7 ($n = 5$)	4.0 ± 2.6 ($n = 8$)		0.184
10	4.0 ± 3.8 ($n = 15$)	2.5 ± 3.3 ($n = 5$)		0.533
24	11.7 ± 8.6 ($n = 9$)	6.7 ± 3.5 ($n = 7$)		0.165

Uteri were collected at day 0.5 of vaginal plug except for the prepubertal uteri from 4-week-old virgin C57 mice. Sera were collected from virgin females for measurement of 17β-estradiol (pM/liter) and progesterone (nM/liter) levels. (N.R.) Not relevant, as *P*-value is insignificant.

reproductive phenotype seen in the *Cenpb* null mice, we compared the total ovary weight in previously unmated wild-type and *Cenpb* null littermates at day of vaginal plug. No significant difference was observed for the animals in the R1, W9.5 and C57 background (Table 1C). The ovaries of *Cenpb* null mice on all three genetic backgrounds were able to produce a normal number of fertilized eggs (Table 1D). Direct measurement of the serum 17β-estradiol and progesterone levels in nonmated animals in all three genetic backgrounds also indicated no significant difference between the *Cenpb* null and wild-type animals (Table 2B,C; W9.5 and C57 data not shown). These results suggested that defective egg production or female reproductive hormones were unlikely causes for the observed reproductive problems in the *Cenpb* null female mice.

Defective Uterine Epithelium

We next explored the possibility that a primary defect

Table 3. Total Body and Organ Weight (mg), and Number of Embryos Flushed from the Oviducts of Mice

	Av. weight ± s.d.		*t*-test
	+/+	o/o	*P*-value
Body (grams)			
male	29.5 ± 2.1 ($n = 8$)	29.1 ± 2.5 ($n = 6$)	0.743
female	22.2 ± 1.3 ($n = 6$)	20.9 ± 2.1 ($n = 8$)	0.209
Testis (mg)	207.4 ± 26.4 ($n = 8$)	196.6 ± 30.1 ($n = 6$)	0.485
Uterus (mg)	111.3 ± 32.8 ($n = 6$)	114.2 ± 19.5 ($n = 8$)	0.843
Ovary (mg)	10.7 ± 0.6 ($n = 6$)	11.0 ± 3.7 ($n = 8$)	0.814
No. of embryos	6.7 ± 4.2 ($n = 6$)	6.3 ± 4.8 ($n = 8$)	0.869

Ten-week old +/+ and o/o littermates on W9.5 genetic background were used. Uteri, ovaries, and embryos were collected at day 0.5 of vaginal plug from previously unmated females.

could have occurred in the uterus, affecting its ability to support implantation and/or fetal growth. This was investigated by direct histological examination of the uterine tissues.

Histology of uterine sections indicated no major abnormality in 10-week-old R1$^{-/-}$ mice. In 6- to 9-month-old R1$^{-/-}$ and 10 week-old C57$^{-/-}$ animals, the myometrium and endometrium were relatively normal, but gross abnormality of the epithelium was detected. In the wildtype animals, the tall columnar cells of the uterine luminal epithelium consisted of elongated nuclei that were primarily basally situated (Fig. 5A), whereas the cells of the endometrial glandular epithelium consisted of nuclei that were more ovoid and centrally located (Fig. 5C). In the *Cenpb* null mice, the columnar cell morphology and basal nuclear appearance of the luminal epithelium was severely disrupted and replaced by highly disorganised and apoptotic cells (Fig. 5B). A similar phenotype was also apparent in the epithelium of the endometrial glands (Fig. 5D). Other abnormalities (not shown) included fewer endometrial glands, significantly increased leukocyte infiltration, hemorrhage, ulceration, and infection. It was also evident that the severity of these phenotypes was significantly greater in the C57$^{-/-}$ animals compared with those of the *Cenpb* null animals in the other genetic backgrounds.

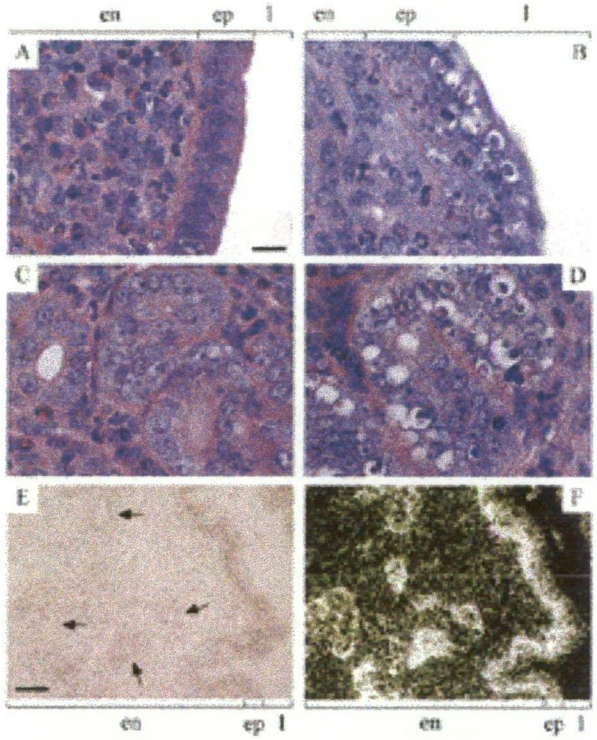

Figure 5 Histology (*A–D*) and in situ hybridization (*E,F*) of uterine sections. (*A,C*) Ten-week-old, hematoxylin-and eosin-stained C57$^{+/+}$ uterus (day 0.5 VP), showing normal morphology of the endometrial epithelium lining the uterine lumen (*A*) and endometrial glands (*C*). (*B,D*) ten-week-old, hematoxylin- and eosin-stained C57$^{-/-}$ uterus (day 0.5 VP), showing highly disorganized and apoptotic (clear) epithelial cells lining the uterine lumen (*B*) and endometrial glands (*D*). Apoptosis of the clear cells (containing condensing chromatin) was confirmed by TUNEL assay (Gavrieli et al. 1992) (data not shown). Scale bar for *A–D*, 20 μm. (*E,F*) Bright-field (hematoxylin-stained) and dark-field views, respectively, of 10-week-old R1$^{+/+}$ uterus hybridized with a ^{35}S-labeled mouse *Cenpb* antisense riboprobe, showing mRNA signals (dark brown grains in E and white grains in F) throughout the endometrium (and the myometrium; not included in picture) with maximal mRNA expression in the epithelial lining of the uterine lumen and endometrial glands (selected examples of which are indicated by arrows). Scale bar for *E* and *F*, 50 μm. (en) Endometrium; (ep) epithelium, (l) uterine lumen.

High *Cenpb* Expression in Uterine Epithelium

In situ hybridization was used to determine the *Cenpb* mRNA expression pattern of the normal uterine tissues. Using a *Cenpb*-specific antisense riboprobe, expression was observed throughout the uterine section. A disproportionately higher level of expression was seen in the epithelial lining of the uterine lumen and endometrial glands compared with the endometrial and myometrial layers (Fig. 5E,F). No significant hybridization was obtained with the *Cenpb* sense control probe in any of these tissues (not shown).

DISCUSSION

Centromere proteins are important components for the proper execution of mitosis and meiosis but relatively little is known about their roles, or the consequences of their defects, in whole animals. The role of Cenpb is particularly intriguing since despite its conservation, cellular abundance, and specificity to the centromere, a number of lines of evidence point to this protein being nonessential for cell division and growth both in tissue culture and in the animal (referenced in Introduction). In a previous study, we demonstrated that *Cenpb* null mice in a mixed (R1) genetic background have a lower body and testis weight but otherwise appear normal (Hudson et al. 1998). Here, we have extended the analysis to mice on two new genetic backgrounds (mixed W9.5 and congenic C57). The results indicate that a reduction in testis weight is also seen in these backgrounds. On the other hand, body-weight reduction is apparent in the W9.5$^{-/-}$ females but not in the W9.5$^{-/-}$ males or the C57$^{-/-}$ males and females. This observation suggests the presence of genetic modifiers (Banbury 1997; Threadgill et al. 1997) that may influence body-weight development in a *Cenpb* null milieu. Furthermore, in the W9.5 genetic background, the modifier effect appears to be gender-dependent. The recognition of these genetic modifier effects offers a possible explanation for the lack of body-weight phenotype in *Cenpb* null mice produced by two other groups on different genetic backgrounds (Kapoor et al. 1998; Perez-Castro et al. 1998). Further

studies setting up a backcross or F_1 intercross (e.g., MacPhee et al. 1995; Rozmahel et al. 1996) with C57 *Cenpb* null mice followed by phenotypic analysis of offspring should enable the identification of the number and chromosomal locations of any likely genetic modifiers that affect *Cenpb* expression.

Our data further indicate that the uteri of 10-week-old −/− animals in all the three genetic backgrounds of R1, W9.5, and C57 were significantly smaller (by 31%, 33%, and 44%, respectively) than their wild-type littermates. It could be argued that our gene targeting strategy, by introducing the IRES/selectable marker cassette into the 3′ noncoding region of the *Cenpb* gene, might have resulted in the observed phenotype in these animals attributable to an inadvertent effect of this cassette on neighboring genes. This possibility, however, now appears unlikely as the newly generated targeted control (o/o) animals, in which the IRES/selectable marker cassette is present but not the frameshift mutation, do not show such a phenotype. It can be inferred from these control studies that the observed phenotype of our *Cenpb* null mice is a direct consequence of a disruption of the *Cenpb* gene.

Evidence is presented that *Cenpb* null females are compromised reproductively. The severity of this abnormality is subjected to the influence of genetic modifiers. This modifier effect is particularly stark when the reproductive performance of the $R1^{-/-}$ females is directly compared with their congenic $C57^{-/-}$ derivatives. In this comparison, although the $R1^{-/-}$ females are reproductively competent (but showing progressive age-dependent deterioration) up to 6–9 months of age, reproduction in the $C57^{-/-}$ females fails totally or is severely affected at an early postpubertal age between 8–10 weeks. At present, it is unclear whether the putative genetic modifiers underlying female reproductive competence and those controlling the body weight are related.

Although our data have indicated a failure of the uteri of the *Cenpb* null mice to reach a normal size, this is unlikely, on its own, to be the major cause of the observed severe reproductive dysfunction. This is evident from the relatively normal reproductive performance of young $R1^{-/-}$ females despite their smaller uteri. Our data point to a disruption in the normal morphogenesis of the uterine epithelial tissue as the likely primary cause. The epithelium is a vital component of the uterus. During pregnancy, this tissue remodels itself to prepare the uterus to become receptive to the developing blastocyst. This remodelling, which is critically dependent on the integrity of the polarised epithelial cell phenotype (Denker 1990; Glasser and Mulholland 1993), provides the embryo with a secure place for nutrition, growth, and differentiation (including the development of a functional placenta) (Denker 1990; Glasser et al. 1991; Giudice 1997). In the reproductively dysfunctional *Cenpb* null mice, the epithelial cells of the uterine lumen and endometrial glands have become grossly disorganized and apoptotic. In particular, the columnar morphology and the basal nuclear positioning of the luminal epithelium have been seriously disrupted. These disruptions are expected to acutely compromise the proper functioning of the uterine epithelium and offer an explanation for the range of pregnancy problems seen in the affected animals.

The mechanism whereby Cenpb deficiency leads to the degeneration of the uterine epithelial cells remains to be determined. It is known that during pregnancy or the periodic oestrus cycle-induced remodelling of the uterus, active mitoses occur especially in the endometrial epithelial layer (Bronson et al. 1996; Kimura et al. 1978). The observed high-expression level of *Cenpb* in the normal uterine epithelial cells is consistent with an important role of this protein in the modulation of the mitotic activities of these cells. We have previously proposed a model whereby the function of Cenpb may be replaced by a functionally redundant protein in the *Cenpb* null mice (Hudson et al. 1998). The present investigation indicates that such a redundant protein if it exists is incapable of fully substituting for the role of Cenpb. Further studies should elucidate what this role may be.

In humans, one-third of normal pregnancies ends in spontaneous abortion, with two-thirds of these occurring before clinical detection of pregnancy (Wilcox et al. 1988). Abnormality in uterine remodelling to make it receptive as well as supportive of the developing blastocyst has been cited as a principal cause of pregnancy wastage (Glasser 1998). Because CENP-B is highly conserved between mouse and humans, it would be of clinical importance to determine whether CENP-B expression is altered in pathological conditions associated with female infertility or aberrant female reproductive performance. In addition, these studies may shed light on conditions like metritis (inflammation of the uterus) and pyometra (uterine infection), which are considerable problems in veterinary medicine without known causal links (Santschi et al. 1995; Dhaliwal et al. 1998; Lawler 1998; Rajala and Grohn 1998; Smith et al. 1999). The observations described in this study have broad implications for understanding uterine morphogenesis, centromere function, as well as human and animal reproductive pathology, and warrant further detailed study.

METHODS

Generation and PCR Screening of *Cenpb* Targeted Control Mice

For chimeric mouse production, W9.5 $^{+/o}$ ES cells (Hudson et al. 1998) were microinjected into C57BL/6 blastocysts, fol-

lowed by breeding of the resulting chimeras to C57BL/6 mice to generate heterozygous progeny (generation 1). Heterozygous (+/o) offspring were bred to obtain wild-type (+/+), +/o, and homozygous (o/o) progeny (generation 2) that were used for subsequent analysis. The W9.5$^{o/o}$ mice have incorporated the IRES-selectable marker cassette but not the 26-mer (D/TAA) translational frameshift oligonucleotide at the 5′ region of the *Cenpb*-coding sequence (Hudson et al. 1998). Targeted W9.5$^{+/o}$ ES cell lines were originally identified by Southern analysis (Hudson et al. 1998) (see Fig. 1). For PCR genotyping of cell line and mouse tail DNA, the following primers were used: B4top (5′-CTTTCCTCCCCATTAGTCCC-3′) and B1comp (5′-ACGCTGTCTTCTTTTAGCC-3′), which gave a 281-bp product for the wild-type (+) allele; or Neo1 (5′-CCTCGTGCTTTACGGTATCG-3′) and B1comp, which gave a 320-bp product for the targeted control (o) allele. PCR conditions were 95°C for 2 min, followed by 35 cycles at 95°C for 30 sec, 60°C for 1 min, and 72°C for 1 min, in a 20-µl volume containing 50–200 ng genomic DNA, 0.66 units of *Taq* polymerase, 200 µM dNTPs, and 200 ng of each primer in dH_2O.

Generation of *Cenpb* Null Mice on Different Genetic Backgrounds

Cenpb null mice were produced previously by microinjecting gene-targeted ES cells derived from the R1 cell line into C57BL/6 blastocysts to obtain chimeras that were subsequently mated to C57BL/6 mice (Hudson et al. 1998). Heterozygous (+/−) offspring (generation 1) were bred to obtain homozygous *Cenpb* null (−/−) mice, +/−, and wild-type (+/+) littermates (generation 2). These mice were maintained on a mixed genetic background of R1 (129/SvJ × 129/Sv-+p+Tyr^{-c} Mgf$^{Sl\text{-}J}$/+) (Simpson et al. 1997) and C57BL/6, in which 129/SvJ has been shown previously to be an impure inbred 129 strain (Threadgill et al. 1997). These animals were designated R1$^{-/-}$ here to distinguish them from *Cenpb* null mice created on two other genetic backgrounds in this study. R1 progeny (generation 2 or 3) from heterozygous brother/sister or cousin matings were used for subsequent analysis.

One of the new mouse strains, denoted W9.5$^{-/-}$, was produced by microinjecting a previously *Cenpb* gene-targeted +/− W9.5 (originally derived from a 129/Sv blastocyst; Buzin et al.1994) ES cell-derived line (Hudson et al. 1998) into C57BL/6 blastocysts to obtain chimeras from which were mated to C57BL/6 mice. Heterozygous progeny (generation 1) were bred to generate homozygous *Cenpb* −/−, +/−, and +/+ littermates (generation 2). The W9.5 mouse strain was maintained on a mixed background of 129/Sv and C57BL/6 by intercrossing W9.5$^{+/-}$ progeny from generation 1 or 2 via brother/sister or cousin matings. The resulting W9.5$^{-/-}$ and W9.5$^{+/+}$ progeny (generation 2 and 3) were used for analysis. The third mouse strain, designated C57$^{-/-}$, was congenic on a C57BL/6 genetic background. This was produced by mating first generation +/− progeny derived from the R1/C57BL/6 chimeras described above to C57BL/6 mice. Heterozygous progeny were backcrossed to C57BL/6 for a further seven generations. At generations 8 and 9, +/− progeny were intercrossed to generate the C57$^{-/-}$ congenic and C57 $^{+/+}$ control mice that were used for analysis in this study.

Immunocytochemistry

Immunofluorescence staining using anti-CENP-B monoclonal antibody was performed as described previously (Hudson et al. 1998) on colcemid-arrested mouse fibroblastic cell lines grown from mouse tail biopsies using the scratch technique (Fowler 1984).

Organ Weighing, Body Composition, Longevity, Reproductive Function, and Hormonal Tests

For organ wet-weight and body-composition determination (Clark and Tarttelin 1976), an average of five age-matched R1$^{-/-}$ and R1$^{+/+}$ animals of each sex were used. Survival/longevity analysis was performed by comparing R1$^{-/-}$ males (n = 27) with R1$^{+/+}$ males (n = 44), and R1$^{-/-}$ females (n = 26) with R1$^{+/+}$ females (n = 28), using Kaplan Meier plot; hazard ratios and significance values were calculated by the Cox proportional hazard regression method (Stata Corp 1997). Reproductive performance of mice was examined by setting up appropriate breeding pairs for mating and observing for vaginal plug (day 0.5 VP). Plugged mice were closely monitored during pregnancy and parturition. Plasma leptin, serum progesterone, and 17β-estradiol evels were measured using Linco Mouse Leptin RIA Kit, Bayer Diagnostics Progesterone Kit, and Sorin 17β-estradiol RIA Kit, respectively.

Histology and Tissue In Situ Hybridization

Tissue preparation, histology, and in situ hybridization were as described previously (Edmondson et al. 1995; Hudson et al. 1998). For in situ hybridization, a 700-bp *Pst*I fragment located at nucleotide positions 1391–2095 of the *Cenpb* sequence (EMBL accession no. X55038) was cloned into Bluescript (Stratagene) in both orientations. The resulting sense and antisense clones were linerized with *Cla*I and riboprobes were labeled with ^{35}S-CTP using T7 polymerase.

ACKNOWLEDGMENTS

We thank S. Gazeas, A. Sylvain and J. Ladhams for care of mice; R. O'Dowd and P. Farmer for technical assistance; R. Wolfe for statistical analysis; A. Thorburn for leptin measurement; B. Leury for body composition determination; C. Print for helpful discussions; C.W. Chow for histological tissue preparation and advice; and the Department of Biochemistry of the Royal Children's Hospital for 17β-estradiol and progesterone assays. This work was approved by the Royal Children's Hospital Animal Ethics Committee and was supported by the National Health and Medical Research Council of Australia. K.H.A.C. is a Principal Research Fellow of the Council.

The publication costs of this article were defrayed in part by payment of page charges. This article must therefore be hereby marked "advertisement" in accordance with 18 USC section 1734 solely to indicate this fact.

REFERENCES

Banbury Conference Consortium. 1997. *Neuron* **19:** 755–759.

Bejarano, L.A. and M.M. Valdivia. 1996. Molecular cloning of an intronless gene for the hamster centromere antigen CENP-B. *Biochim. Biophys. Acta* **1307:** 21–25.

Bronson, F.H., C.P. Dagg, and G.D. Snell. 1966. Reproduction. In *Biology of the laboratory mouse* (ed. E.L. Green), pp. 187–204, McGraw-Hill, New York, NY.

Buzin, C.H., J.R. Mann, and J. Singer-Sam. 1994. Quantitative RT-PCR assays show Xist RNA levels are low in female adult

mouse tissue, embryos and embryoid bodies. *Development* **120:** 3529–3536.

Choo, K.H.A. 1997a. *The centromere.* Oxford University Press, Oxford, UK.

———. 1997b. Centromere DNA dynamics: Latent centromeres and neocentromere formation. *Am. J. Hum. Genet.* **61:** 1225–1233.

Clark, R.G. and M.F. Tarttelin. 1976. An accurate method for the preparation and analysis of the composition of animal tissue. *Physiol. Behav.* **17:** 351–352.

Craig, J.M., W.C. Earnshaw, and P. Vagnarelli. 1998. Mammalian centromere: DNA sequence, protein composition, and role in cell cycle progression. *Exp. Cell Res.* **246:** 249–262.

Cutts, S.M., K.J. Fowler, B.T. Kile, L. Hii, R.A. O'Dowd, D.F. Hudson, R. Saffery, P. Kalitsis, E. Earle, and K.H.A. Choo. 1999. Defective chromosome segregation, microtubule bundling, and nuclear bridging in Inner centromere protein (Incenp) gene-disrupted mice. *Hum. Mol. Genet.* **8:** 1145–1155.

Denker, H.W. 1990. Trophoblast-endometrial interactions at embryo implantation: A cell biological paradox. *Troph. Res.* **4:** 3–29.

Depinet, T.W., J.L. Zackowski, W.C. Earnshaw, S. Kaffe, G.S. Sekhon, R. Stallard, B.A Sullivan, G.H. Vance, D.L. VanDyke, H.F. Willard et al. 1997. Characterization of neo-centromeres in marker chromosomes lacking detectable alpha-satellite DNA. *Hum. Mol. Genet.* **6:** 1195–1204.

Dhaliwal, G.K., C. Wray, and D.E. Noakes. 1998. Uterine bacterial flora and uterine lesions in bitches with cystic endometrial hyperplasia. *Vet. Rec.* **143:** 659–661.

Dobie, K.W., K.L. Hari, K.A. Maggert, and G.H Karpen. 1999. Centromere proteins and chromosome inheritance: a complex affair. *Curr. Opin. Genet. Dev.* **9:** 206–217.

du Sart, D., M.R. Cancilla, E. Earle, J. Mao, R. Saffery, K.M. Tainton, P. Kalitsis, J. Martyn, A.E. Barry, and K.H.A. Choo. 1997. A functional neo-centromere formed through activation of a latent human centromere and consisting of non-alpha-satellite DNA. *Nat. Genet.* **16:** 144–153.

Earnshaw, W.C., P.S. Machlin, B.J Bordwell, N.F. Rothfield, and D.W. Cleveland. 1987a. Analysis of anticentromere autoantibodies using cloned autoantigen CENP-B. *Proc. Natl. Acad. Sci.* **84:** 4979–4983.

Earnshaw, W.C., K.F. Sullivan, P.S. Machlin, C.A. Cooke, D.A. Kaiser, T.D. Pollard, N.F. Rothfield, and D.W. Cleveland. 1987b. Molecular cloning of cDNA for CENP-B, the major human centromere autoantigen. *J. Cell Biol.* **104:** 817–829.

Earnshaw, W.C., H. Ratrie, and G. Stetten. 1989. Visualization of centromere proteins CENP-B and CENP-C on a stable dicentric chromosome in cytological spreads. *Chromosoma* **98:** 1–12.

Edmondson, S.R., G.A. Werther, A. Russell, D. LeRoith, C.T. Roberts, and F. Beck. 1995. Localization of growth hormone receptor/binding protein messenger ribonucleic acid (mRNA) during rat fetal development: Relationship to insulin-like growth factor-I mRNA. *Endocrinology* **136:** 4602–4609.

Fowler, K.J. 1984. Storage of skin biopsies at −70 degrees C for future fibroblast culture. 1984. *J. Clin. Pathol.* **37:** 1191–1193.

Gavrieli, Y., Y. Sherman, and S.A. Ben-Sasson. 1992. Identification of programmed cell death in situ via specific labeling of nuclear DNA fragmentation. *J. Cell Biol.* **119:** 493–501.

Giudice, L.C. 1997. Intimate conversations: The implanting conceptus and its maternal host. *Organ* **VIII:** 48–51.

Glasser, S.R. 1998. The uterus: Idiot savant or Rosetta Stone? *J. Assist. Reprod. Genet.* **15:** 168–173.

Glasser, S.R. and J. Mulholland. 1993 Receptivity is a polarity dependent special function of hormonally regulated uterine epithelial cell. *Microscopy Res. Tech.* **25:** 106–120.

Glasser, S.R., J. Mulholland, J. Julian, and S. Mani. 1991. Blastocyst-endometrial relationships: Reciprocal interactions between uterine epithelial and stromal cells and blastocysts. *Troph. Res.* **5:** 229–280.

Goldberg, I.G., A.F. Sawhney, A.F. Pluta, P.E. Warburton, and W.C. Earnshaw. 1996. Surprising deficiency of CENP-B binding sites in African green monkey alpha satellite DNA: Implications for CENP-B function at centromeres. *Mol. Cell. Biol.* **16:** 5156–5168.

Haaf, T. and D.C. Ward. 1995. Rabl orientation of CENP-B box sequences in *Tupaia belangeri* fibroblasts. *Cytogenet. Cell Genet.* **70:** 258–262.

Hudson, D.F., K.J. Fowler, E. Earle, R. Saffery, P. Kalitsis, H. Trowell, J Hill, N.G. Wreford, D.M. deKretser, M.R. Cancilla, E. Howman, L. Hii, S.M. Cutts, D.V. Irvine, and K.H.A. Choo. 1998. Centromere protein B null mice are mitotically and meiotically normal but have lower body and testis weights. *J. Cell Biol.* **141:** 309–319.

Kalitsis, P., K.J. Fowler, E. Earle, J. Hill, and K.H.A. Choo. 1998. Targeted disruption of mouse centromere protein C gene leads to mitotic disarray and early embryo death. *Proc. Natl. Acad. Sci.* **95:** 1136–1141.

Kapoor, M., R. Montes de Oca Luna,, G. Liu, G. Lozano, C. Cummings, M. Mancini, I. Ouspenski, B.R. Brinkley, and G.S May. 1998. The *cenpB* gene is not essential in mice. *Chromosoma* **107:** 570–576.

Kimura, J., T. Obata, and H. Okada. 1978. Steroidal control mechanism of cell proliferation in mouse uterine epithelium. *Endocrinol. Jpn.* **25:** 7–12.

Lawler, D.F. 1998. Diagnosis and treatment of inflammatory uterine disease in cats. *Vet. Med.* **93:** 750–753.

Markel, P., P. Shu, C. Ebeling, G.A. Carlson, D.L. Nagle, J.S. Smutko, and K.J. Moore. 1997. Theoretical and empirical issues for marker-assisted breeding of congenic mouse strains. *Nat. Genet.* **17:** 280–284.

MacPhee, M., K.P. Chepenik, R.A. Liddell, K.K. Nelson, L.D. Siracusa, and A.M. Buchberg. 1995. The secretory phospholipase A2 gene is a candidate for the Mom1 locus, a major modifier of ApcMin-induced intestinal neoplasia. *Cell* **81:** 957–966.

Muro, Y., H. Masumoto, K. Yoda, N. Nozaki, M. Ohashi, and T. Okazaki. 1992. Centromere protein B assembles human centromeric alpha-satellite DNA at the 17-bp sequence, CENP-B box. *J. Cell Biol.* **116:** 585–596.

Niida, H., T. Matsumoto, H. Satoh, M. Shiwa, Y. Tokutake, Y. Furuichi, and Y. Shinkai. 1998. Severe growth defect in mouse cells lacking the telomerase RNA component. *Nat. Genet.* **19:** 203–206.

Page, S.L., W.C. Earnshaw, K.H.A. Choo, and L.G. Shaffer. 1995. Further evidence that CENP-C is a necessary component of active centromeres: studies of a dic(X;15) with simultaneous immunofluorescence and FISH. *Hum. Mol. Genet.* **4:** 289–294.

Perez-Castro, A.V., F.L. Shamanski, J.J. Meneses, T.L. Lovato, K.G. Vogel, R.K. Moyzis, and R. Pedersen. 1998. Centromeric protein b null mice are viable with no apparent abnormalities. *Dev. Biol.* **201:** 135–143.

Pietras, D., K. Bennett, L. Siracusa., M. Woodworth-Gutai, V. Chapman, K. Gross, C. Kane-Haas, and N. Hastie. 1983. Construction of a small *Mus musculus* repetitive DNA library: Identification of a new satellite sequence in *Mus musculus*. *Nucleic Acids Res.* **11:** 6965–6983.

Rajala, P.J. and Y.T. Grohn. 1998. Effects of dystocia, retained placenta, and metritis on milk yield in dairy cows. *J. Dairy Sci.* **81:** 3172–3181.

Rattner, J.B. 1991. The Structure of the mammalian centromere. *BioEssays* **13:** 51–56.

Rozmahel, R., M. Wilschanski, A. Matin, S. Plyte, M. Oliver, W. Auerbach, A. Moore, J. Forstner, P. Durie, J. Nadeau et al. 1996. Modulation of disease severity in cystic fibrosis transmembrane conductance regulator deficient mice by a secondary genetic factor. *Nat. Genet.* **12:** 280–287.

Santschi, E.M., S.B. Adams, J.T. Robertson, R.M. Bowes, L.A. Mitten, and J.E. Sojka. 1995. Ovariohysterectomy in six mares. *Vet. Surg.* **24:** 165–171.

Simpson, E.M., C.C. Linder, E.E. Sargent, M.T. Davisson, L.E. Mobraaten, and J.J. Sharp. 1997. Genetic variation among 129 substrains and its importance for targeted mutagenesis in mice. *Nature Genet.* **16:** 19–27.

Smith, K.C., T.J. Parkinson, and S.E. Long. 1999. Abbattoir survey of acquired reproductive abnormalities in ewes. *Vet. Rec.* **144:** 491–496.

Stata Corp. 1997. Stata statistical software: Release 5.0, Stata Corp., College Station, TX

Sullivan, B.A. and S. Schwartz. 1995. Identification of centromeric antigens in dicentric Robertsonian translocations: CENP-C and CENP-E are necessary components of functional centromeres. *Hum. Mol. Genet.* **4:** 2189–2197.

Sullivan, K.F. and C.A. Glass. 1991. CENP-B is a highly conserved mammalian centromere protein with homology to the helix-loop-helix family of proteins. *Chromosoma* **100:** 360–370.

Threadgill, D.W., D. Yee, A. Matin, J.H. Nadeau, and T. Magnuson. 1997. Genealogy of the 129 inbred strains: 129/SvJ is a contaminated inbred strain. *Mam. Genome* **8:** 390–393.

Voullaire, L.E., H.R. Slater, V. Petrovic, and K.H.A. Choo. 1993. A functional marker centromere with no detectable alpha-satellite, satellite III, or CENP-B protein: Activation of a latent centromere? *Am. J. Hum. Genet.* **52:** 1153–1163.

Wilcox, A.J., C.R. Weinberg, J.F. O'Connor, D.D. Baird, J.P. Schlatterer, R.E. Canfield, E.G. Armstrong, and B.C. Nisula. 1988. Incidence of early loss of pregnancy. *N. Engl. J. Med.* **319:** 189–194.

Yoda, K., K. Kitagawa, H. Masumoto, Y. Muro, and T. Okazaki. 1992. A human centromere protein, CENP-B, has a DNA binding domain containing four potential α-helices at the NH_2 terminus, which is separable from dimerizing activity. *J. Cell Biol.* **119:** 1413–1427.

Yoda, K., T. Nakamura, H. Masumoto, N. Suzuki, K. Nitagawa, M. Nakano, A. Shinjo, and T. Okazaki. 1996. Centromere protein B of African Green monkey cells: Gene structure, cellular expression, and centromeric localization. *Mol. Cell. Biol.* **16:** 5169–5177.

Received September 7, 1999; accepted in revised form October 26, 1999.

PUBLICATION 9

E.V. HOWMAN, **K.J. FOWLER**, A.J. NEWSON, S. REDWARD,
A.C. MACDONALD, P. KALITSIS AND K.H.A. CHOO (2000)

EARLY DISRUPTION OF CENTROMERIC CHROMATIN ORGANISATION IN CENTROMERE PROTEIN A (*CENPA*) NULL MICE.

PROCEEDINGS OF THE NATIONAL ACADEMY OF SCIENCES USA,
97: 1148-1153.

Early disruption of centromeric chromatin organization in centromere protein A (*Cenpa*) null mice

Emily V. Howman, Kerry J. Fowler, Ainsley J. Newson, Saara Redward, Andrew C. MacDonald, Paul Kalitsis, and K. H. Andy Choo*

The Murdoch Institute, Royal Children's Hospital, Flemington Road, Parkville 3052, Australia

Edited by John A. Carbon, University of California, Santa Barbara, CA, and approved November 23, 1999 (received for review October 5, 1999)

Centromere protein A (Cenpa for mouse, CENP-A for other species) is a histone H3-like protein that is thought to be involved in the nucleosomal packaging of centromeric DNA. Using gene targeting, we have disrupted the mouse *Cenpa* gene and demonstrated that the gene is essential. Heterozygous mice are healthy and fertile whereas null mutants fail to survive beyond 6.5 days postconception. Affected embryos show severe mitotic problems, including micronuclei and macronuclei formation, nuclear bridging and blebbing, and chromatin fragmentation and hypercondensation. Immunofluorescence analysis of interphase cells at day 5.5 reveals complete Cenpa depletion, diffuse Cenpb foci, absence of discrete Cenpc signal on centromeres, and dispersion of Cenpb and Cenpc throughout the nucleus. These results suggest that Cenpa is essential for kinetochore targeting of Cenpc and plays an early role in organizing centromeric chromatin at interphase. The evidence is consistent with the proposal of a critical epigenetic function for CENP-A in marking a chromosomal region for centromere formation.

kinetochore | epigenetic | gene targeting

The centromere is an essential chromosomal component required for the faithful segregation of chromosomes during mitosis and meiosis. The kinetochore is a DNA-protein complex comprising both constitutive proteins that are present at the centromere throughout the cell cycle and transient proteins that are present at various stages (1). Three of the best-studied constitutive proteins are centromere proteins CENP-A, CENP-B, and CENP-C. CENP-A is a 17-kDa histone H3-like protein involved in centromeric nucleosome formation (ref. 2; described below). CENP-B is an 80-kDa protein that binds a 17-bp motif known as the CENP-B box, which is present in human α-satellite and mouse minor satellite DNA (3, 4). Gene knockout analysis of Cenpb in mice indicates that this protein is not essential (5–7), although a decrease in body weight and testis size accompanied protein deficiency (5). CENP-C is a 140-kDa protein that interacts with chromatin at the inner kinetochore plate (8). *In vitro* DNA binding studies suggest that CENP-C may bind to DNA (9). CENP-C null mutation results in embryonic lethality at 3.5 days postconception (pc), with a missegregation phenotype and metaphase arrest (10, 11). Metaphase arrest also is observed after microinjection of anti-CENP-C antibodies at interphase (12). CENP-C shares a region of homology with Mif2, a *Saccharomyces cerevisiae* protein. Mutations in the *MIF2* gene result in defective chromosome segregation and delayed progression through mitosis (13). However, CENP-C alone is not sufficient to induce centromeric formation (14).

A number of transient centromere proteins now have been described (1, 15–19). Of particular relevance to the present study involving the use of the gene targeting technique is the inner CENP (INCENP). This protein localizes to the centromere at early mitosis and is present on the metaphase plate at the metaphase-anaphase transition (20). Gene disruption in mice reveals embryonic lethality at 2.5 days pc, accompanied by enlarged nuclei containing an increased number of nucleoli, nuclear bridging, chromosome condensation, and spindle fiber bundling (21).

The role of CENP-A in centromeric function has yet to be elucidated. CENP-A is a histone-H3 like protein that is conserved in mammals (22, 23) and *S. cerevisiae* (24). The C terminal (residues 48–135) of CENP-A is 62% identical to that of histone H3 and corresponds to the histone fold domain. The histone fold domain consists of three α-helices (HI, HII, and HIII) separated by two β-sheet structures (strand A and strand B) (25) (see Fig. 1). This domain of histone H3 has been shown to be sufficient for nucleosome assembly *in vitro* (26) and *in vivo* (27). There is no similarity seen between the N-termini sequences (residues 1–47) of CENP-A and normal histone H3 (2). Although this divergence initially was thought to provide CENP-A with the centromere targeting property, a histone H3 chimeric protein containing the N terminus of CENP-A and the histone H3 histone fold domain failed to localize to the centromere, indicating that the C-terminal end is responsible for centromere targeting (28). CENP-A synthesis appears to be coupled with centromere replication during mid-S to early G_2 phase, whereas histone H3 expression peaks early in S phase (28). Expression of CENP-A under the histone H3 promoter fails to localize at the centromere (28). These studies suggest that CENP-A is involved in the packaging of centromeric chromatin and that the protein may provide an early epigenetic marker for centromere formation (29).

Only limited functional data are available for CENP-A. Microinjection of antibodies raised against the N terminus of CENP-A into HeLa cells within 3 hr of G_1/S release resulted in interphase arrest (30). Highly condensed nuclei, granular cytoplasm, and loss of cell division capability were observed. Antibody injection in midinterphase did not disrupt mitosis; however, a mitotic lag was observed possibly because of the antibody interfering with microtubule attachment (31). Studies on CSE4p (chromosome segregation protein), an *S. cerevisiae* homolog of CENP-A, have demonstrated the protein to be a component of the core centromere (32). Mutation in CSE4p results in missegregation and cell arrest in mitosis; however, the increase in chromosome loss is slight (33). The arrest phenotype is consistent with a specific cell division block that appears to occur after the mitotic spindle has formed but before the onset of anaphase (33). The arrested cells have a $2n$ DNA content, indicating that DNA replication has taken place before arrest.

This paper was submitted directly (Track II) to the PNAS office.

Abbreviations: ES, embryonic stem; CENP, centromere protein; INCENP, inner CENP; pc, postconception; IRES, internal ribosome-entry site.

*To whom reprint requests should be addressed. E-mail: choo@cryptic.rch.unimelb.edu.au.

The publication costs of this article were defrayed in part by page charge payment. This article must therefore be hereby marked "*advertisement*" in accordance with 18 U.S.C. §1734 solely to indicate this fact.

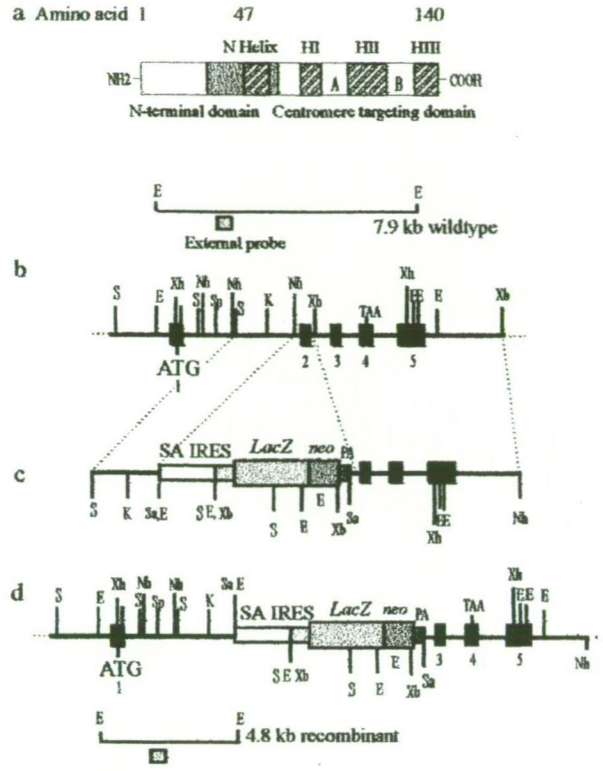

Fig. 1. Targeted disruption of the mouse *Cenpa* gene. (*a*) The mouse Cenpa protein showing the different subdomains, in particular those at the C terminus that are required for centromere targeting. Our targeting construct (see below) was designed to delete amino acids 29–64 (gray box), which will effectively remove the entire centromere-targeting domain. (*b*) A restriction map of the *Cenpa* gene. The exons are denoted by black boxes (23). (*c*) The gene replacement construct, where the selectable marker cassette consists of a splice-acceptor site (SA), a picornaviral IRES, a *lacZ*-neomycin-resistance fusion gene, and a simian virus 40 polyadenylation sequence (PA). (*d*) The *Cenpa* locus after gene disruption. The positions of external probes used in Southern analysis are shown and the expected size fragments are 7.9-kb wild-type allele and a 4.8-kb targeted allele. ATG and TAA are translation start and stop codons, respectively. Restriction enzymes used were *Sac*I (S), *Sal*I (Sa), *Eco*RI (E), *Xba*I (Xb), *Xho*I (Xh), *Kpn*I (K), *Nhe*I (Nh), and *Spe*I (Sp).

To further understand the role of CENP-A in centromere function, we have used the technique of gene targeting by homologous recombination to enable the production of *Cenpa* null mice. Our analysis of *Cenpa* null mutants has enabled us to elucidate the involvement of this protein in mitotic cell division and, in particular, its role in kinetochore assembly.

Methods

Construction of Targeting Vectors. The targeting construct contains 6.4 kb of the *Cenpa* gene (23) and was used to delete exon 2 (amino acids 29–64) and disrupt the protein through the introduction of the selectable marker cassette. Exon 2 was deleted via the flanking *Nhe*I and *Xba*I sites followed by the insertion of a selectable marker cassette isolated from pGT1.8IRES.βgeo, where IRES is the internal ribosome-entry site (34). This construct, when homologously recombined into the mouse *Cenpa* locus, will result in a truncated protein lacking the centromere targeting domain (Fig. 1).

Generation of Targeted Embryonic Stem (ES) Cells and Mice. Mouse ES cells (129/1) were electroporated with 40 μg of linearized construct DNA, grown on STO/Neo^R feeders, and growth-selected by using G418 (21). Resistant colonies were genotyped

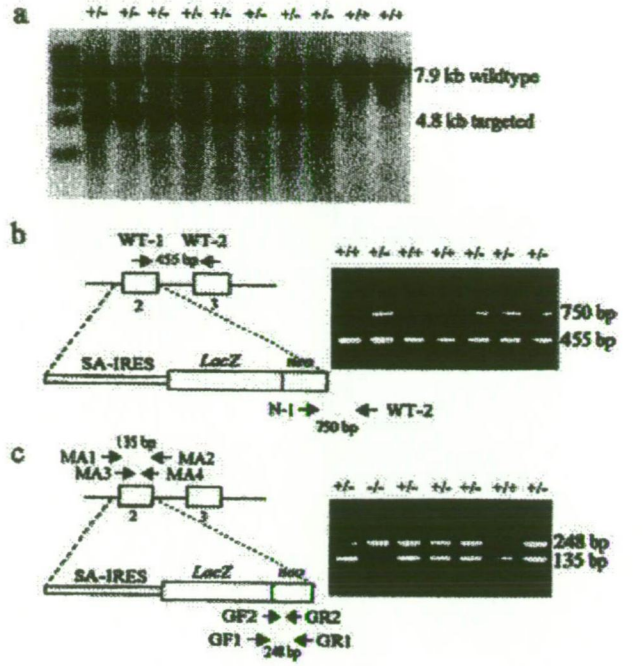

Fig. 2. Southern blotting and PCR genotyping of cell line, tail, and embryo DNA. (*a*) Southern blot analysis of putative targeted ES cell colonies after *Eco*RI digestion and probed with an external probe (see Fig. 1 *b* and *d*). (*b*) PCR analysis of mouse tail DNA showing a wild-type product of 455 bp detected by WT-1 and WT-2 primers, and a targeted product of 750 bp detected by N-1 and WT-2 primers. SA, splice-acceptor site. (*c*) Nested PCR of mouse embryos resulting in a 135-bp wild-type product when using primers MA1, MA2, MA3, and MA4, and a 248-bp targeted product when using primers GF1, GR1, GF2, and GR2.

by Southern blot (Fig. 2*a*). Chimeric mice were produced as described (21). Mice were genotyped by PCR. DNA was extracted from mouse tails as described (21). Primers designed by using GENEWORKS were: WT-1 (5′-TCAGACACTGCGCAGAAGAC); WT-2 (5′-GAGCTTAGGAACTGGCATGG); and N-1 (5′-TTCTATCGCCTTCTTGACGAG) (Fig. 2*b*).

Genotyping of Preimplantation Embryos. Preimplantation embryos were obtained from heterozygous mice. Breeding pairs were examined daily for vaginal plugs (an indicator of 0.5 days gestation) and denoted as 0.5 days pc. A nested PCR protocol was designed and used for the amplification of the 2.5-day embryonic DNA. Embryos were flushed and transferred to PCR tubes in 25 μl of dH_2O. Nest 1a: denaturation at 95°C for 15 min. Nest 1b: addition of 10× buffer (containing 15 mM $MgCl_2$) (Perkin–Elmer), 0.2 mM dNTP, 250 ng of wild-type primers MA1, MA2, and *LacZ*-neomycin primers GF1 and GR1, 1 unit of AmpliTaq DNA Polymerase (Perkin–Elmer) in a final volume of 50 μl. Cycle 1: 95°C for 2 min; 55°C for 3 min; 72°C for 90 sec. Cycles 2–30: 95°C for 60 sec; 57°C for 60 sec, and 72°C for 90 sec. Nest 2: Using 1 μl of the Nest 1b product, add 10× buffer, 0.2 mM dNTP, primers MA3, MA4, GR2, GF2, 1 unit of AmpliTaq, in a final volume of 25 μl. Cycle 1: 95°C, 2 min; 58°C, 60 sec; 72°C, 90 sec. Cycles 2–30: 95°C, 1 min; 58°C, 1 min; 72°C, 90 sec. Oligonucleotide primer sequences were: MA1 (5′-TGGAACTGCAGTCTGGGAAC); MA2 (5′-TCTGTCTTCTGCGCAGTGTC); GF1 (5′-AGTATCGGCGGAATTCCAG); GR1 (5′-GATGTTTCGCTTGGTGGTC); MA3 (5′-CCCAAAGCTCAGAGCAAATTC); MA4 (5′-AGTATGTGGCAGCACAGCAG); GR2 (5′-CCTCGTCCTGCAGTTCATGTCTGGTG); and GF2 (5′-CCATTACCAGTTGGTCTGGTG) (Fig. 2*c*).

Genotyping of Day-8.5 Embryos. Individual embryos were dissected from their implantation site at 8.5 days gestation, washed twice in PBS, and transferred to a microfuge tube. Mouse tail lysis buffer and proteinase K (1 μg/ml) were added and incubated at 50°C for 4 hr. DNA was extracted twice with phenol-chloroform and once with chloroform followed by ethanol precipitation using 1 μl of glycogen. This precipitate was resuspended in 20 μl of Tris-EDTA from which 5 μl was used for each PCR.

Culturing of Mouse Embryos. A culturing protocol was introduced to assess embryo development between 3.5 and 8.5 days pc. Embryos were flushed at 3.5 days and cultured in 15-mm diameter dishes (Nunc) with ES media supplemented with leukemia inhibiting factor (AMRAD, Melbourne, Australia) at 37°C, 5% CO_2. Embryos were photographed daily and harvested at 8.5 days if normal in appearance or earlier if signs of degeneration were apparent. The embryos were rinsed in PBS and treated with 0.25% trypsin for 3–5 min, resulting in detachment of the trophectoderm cells. Micro-glass pipettes were used to collect the cells. The PCR protocol was the same as that used for the 8.5-day embryos (see Fig. 2*c*).

Giemsa Staining of Embryos. Embryos (2.5 and 3.5 days) were placed in M16 media (Sigma) under oil, then transferred to a microwell containing 0.6% trisodium citrate for 4–8 min. Individual embryos were placed on glass slides and fixed in a droplet of methanol/acetic acid (3:1). After two rinses in fixative, the embryos were stained with 10% Giemsa in PBS, pH 6.8 (Gurr), for 10 min, air-dried, and mounted in DPX (BDH) for analysis. To enable morphological analysis of 4.5-, 5.5-, and 6.5-day embryos, embryos were cultured on gelatinized (0.1% gelatin in PBS) coverslips (22 mm × 22 mm) in 35-mm Petri dishes (Nunc). Embryos that failed to attach to the coverslips were harvested and treated in the same manner as the 2.5- and 3.5-day embryos. Embryos were fixed in methanol/acetic acid for 10 min, stained as above, and examined on an Olympus 1×70 microscope/Nikon F-601 camera system.

Mitotic Index Determination. Cultured embryos were either Giemsa-stained (as above) or fixed in 2% paraformaldehyde and mounted in Vectorshield containing 4′,6-diamidino-2-phenylindole (DAPI). DAPI staining of embryos was used to enable mitotic detection in various focal planes. The number of cells undergoing mitosis was calculated as a percentage of the total cell number using both methods.

Immunofluorescence Analysis of Embryos. Embryos were cultured on coverslips, rinsed twice in PBS, fixed for 5 min in 2% paraformaldehyde in PBS, permeabilized with 0.1% Triton X-100 in PBS for 2 min, and rinsed an additional two times in PBS (35). Antibodies were applied to coverslips for 1 hr at 37°C. The coverslips were washed three times for 5 min in 1× KB buffer (10 mM Tris·HCl/15 mM NaCl/0.1% BSA), the secondary antibody was applied for 1 hr and washing was repeated. The coverslips then were rinsed in PBS and stored in PBS at 4°C. Embryos were mounted in 4′,6-diamidino-2-phenylindole. Image analysis was performed by using an Axioskop fluorescence microscope equipped with a 63× objective (Zeiss), a charge-coupled device camera (Photometrics Image Point, Tucson, AZ) and IPLAB software (Signal Analytics, Vienna, VA).

Results

Generation of *Cenpa* Heterozygous Cell Lines and Mice. The CenpaneoR construct (Fig. 1*c*) was transfected into 129/1 ES cells grown on STO/Neo^R feeder cells and placed under G418 selection for 7–10 days. Screening of 48 resistant clones by Southern blot analysis gave 26 positive clones (Fig. 2*a*), indicating a targeting efficiency of 54%. Microinjection of these heterozygous targeted cell lines into blastocysts resulted in four germ-line chimeras. These mice were crossed with C57BL/6 to produce heterozygous mice (Fig. 2*b*).

Table 1. PCR genotyping of embryos at days 2.5 and 8.5 pc, showing the number of embryos and, in brackets, % of total

Genotype	Day 2.5	Day 8.5
+/+	3 (14%)	11 (30%)
+/−	7 (34%)	18 (49%)
−/−	4 (19%)	0
No PCR result	7 (33%)	0
Abortive implantation sites	N.R.	8 (21%)
Total no. of embryos	21	37

N.R., not relevant because embryos have not implanted at day 2.5.

Embryonic Lethality of *Cenpa* Null Offspring Occurs Postimplantation Between Days 3.5 and 8.5 pc. The heterozygous mice were phenotypically normal with no obvious impairment of growth or fertility. Intercrossing of heterozygous mice resulted in a total of 186 progeny of which 63 (34%) were +/+ and 123 (66%) were +/−, indicating embryonic lethality of the homozygous mutant state. Embryonic lethality was also evident from the reduced average litter size of 6.0 ± 2.4 for +/− × +/− crosses (n = 23 litters), compared with 9.1 ± 2.6 and 8.6 ± 3.3 for the +/+ × +/+ (n = 31 litters) and +/− × +/+ (n = 13 litters) crosses, respectively.

To determine the point of *Cenpa* null lethality, embryos at 2.5 and 8.5 days pc were genotyped by nested PCR (Fig. 2*c*). Matings of +/− × +/− yielded 21 embryos at 2.5 days and 37 embryos at 8.5 days. Genotyping by PCR indicated that null mutants were viable (and healthy looking by Giemsa staining; not shown) at 2.5 days (Table 1). The results indicated that the time of embryo death apparently had occurred before 8.5 days because no homozygous mutants were detected. Examination of the uteri of female mice for the 8.5-day embryos revealed eight (21%; Table 1) abortive implantation sites. These abortive sites were either empty or contained remnants of highly degenerate and resorbing embryos. This analysis indicated that the point of embryonic lethality occurred postimplantation between 3.5 and 8.5 days.

Morphological Degeneration of Cultured *Cenpa* Null Embryos at Day 5.5 pc. To further investigate postimplantation development, embryos from +/− × +/− crosses were flushed at 3.5 days and cultured individually. The embryos were photographed daily by phase contrast or stained with Giemsa, and the images were captured for more detailed examination. (In the following discussion, the age of cultured embryo continues to refer to the number of days pc; that is, 3.5 days *in utero* plus days in culture.) At 5.5 days pc (i.e., 2 days in culture), the inner cell mass of a +/+ or +/− embryo was prominent and surrounded by trophectoderm outgrowth after attachment to the coverslip (Fig. 3 *a* and *b*) (the inner cell mass subsequently would give rise to the embryo proper whereas the trophectoderm would form the extra-embryonic tissue). In a number of embryos, degeneration of the inner cell mass and trophectoderm cells was apparent (Fig. 3 *d* and *e*). Rapid degeneration of these embryos continued and, at 6.5 days, a defined inner cell mass was no longer visible, while the trophectoderm cell number also declined dramatically (Fig. 3*f*). The remaining embryos maintained a healthy inner cell mass, trophectoderm growth, and morphology from day 6.5 (Fig. 3*c*) to day 8.5. Healthy embryos were harvested at day 8.5 whereas the degenerating embryos were harvested on day 6.5 for PCR genotyping. The results indicated that all of the day-8.5 embryos were either +/+ or +/−, whereas all of the day-6.5

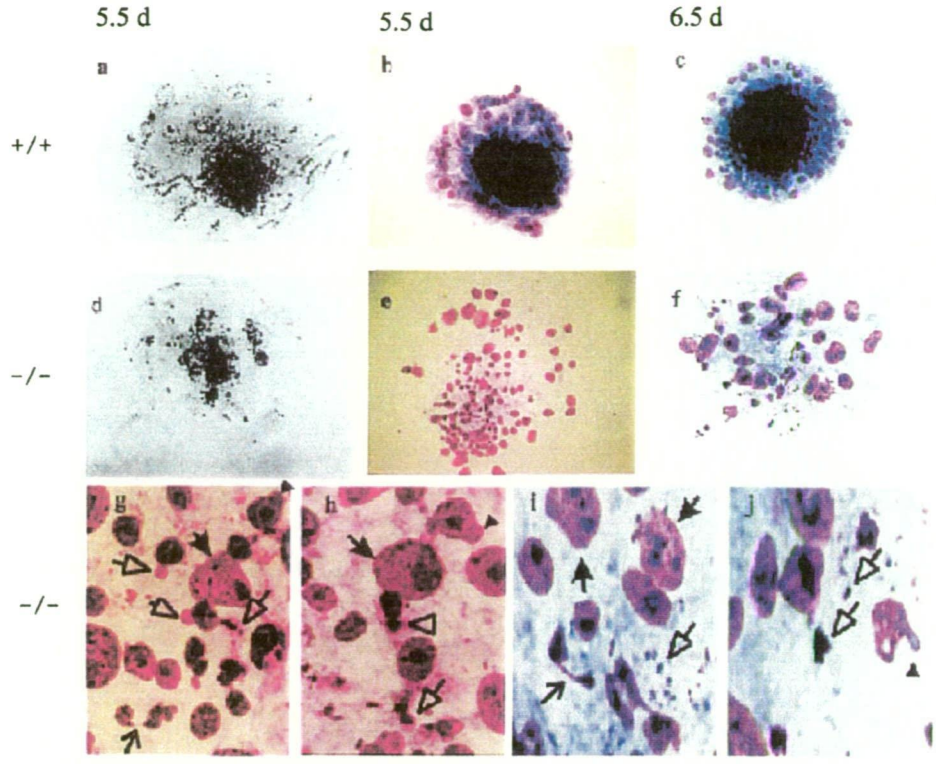

Fig. 3. Phase contrast and Giemsa staining images of day-5.5 and -6.5 embryos. Day-5.5 normal embryo photographed by phase (*a*) or stained with Giemsa (*b*). (*c*) Day-6.5 normal embryo stained with Giemsa. Note the compact, dark inner cell mass and the surrounding trophectoderm outgrowth. Day-5.5 −/− embryo photographed by phase (*d*) or stained with Giemsa (*e*). (*f*) Day-6.5 −/− embryo stained with Giemsa. Note the absence of a defined inner cell mass and the incoherent cells in both the day-5.5 and -6.5 −/− embryos. Magnification for *a–f*: ×150. (*g* and *h*) Close-ups of *e* and (*i* and *j*) close-ups of *f*, showing micronuclei (empty-triangle arrow), macronuclei (filled-triangle arrow), nuclear bridging (open arrow), nuclear blebbing (filled arrowhead), and highly condensed chromatin bodies (empty arrowhead).

degenerating embryos showed a 100% coincidence with the −/− genotype (Table 2).

Chromosomal Missegregation Phenotype. Close examination of the Giemsa-stained, degenerating cultured *Cenpa* null embryos at days 5.5 and 6.5 revealed evidence of a severe chromosomal missegregation phenotype. At day 5.5 (Fig. 3 *e*, *g*, and *h*), a substantial number of micronuclei, formed from lagging chromosomes, was observed. Some macronuclei indicative of enlarged genomic content caused by failure of chromosomes to divide properly were apparent. Chromosomal lagging or polar missegregation also affected normal cytokinesis, resulting in nuclear bridging and blebbing of the nuclear membrane. Chromatin fragmentation and hypercondensation were apparent. Similar mitotic problems were observed in the day-6.5 embryos except for an increased degree of severity (Fig. 3 *f*, *i*, and *j*). At 6.5 days, most of the cells were macronucleated, suggesting that chromosome segregation and normal cytokinesis had come to a halt. When the mitotic indices of day-5.5 cultured embryos were determined, a result of 4.7% for normal embryos (n = 23) and 1.1% for *Cenpa* null embryos (n = 14) was obtained. The chromosomes seen in the null embryos appeared morphologically more condensed and scattered than those of normal embryos, as was previously described for the Cenpc and Incenp null embryos (10, 21) (not shown). Except for an increased background of highly condensed chromatin bodies, no discernible mitotic chromosomes were apparent in the 6.5-day null embryos examined, suggesting cessation of mitosis at this point.

Table 2. Correlation of genotype with morphology of cultured embryos

Genotype	Time of harvest, days	Condition of embryo	No. of embryos (% total)
+/+	8.5	Healthy	9 (26)
+/−	8.5	Healthy	19 (54)
−/−	6.5	Degenerating	5 (15)
No PCR result	6.5	Degenerating	2 (5)
Total no. of embryos			35 (100)

Embryos were flushed from the uterus at day 3.5. Healthy embryos were harvested at day 8.5 (i.e., 5 days in culture), while degenerating embryos were harvested at day 6.5 (i.e., 3.5 days in culture) for nested PCR analysis.

Immunofluorescence Studies. Embryos were analyzed by using antibodies raised against mouse Cenpa (36) or Cenpc (10) or an autoimmune serum (CREST#6) that recognizes human CENP-A and CENP-B (37). Fig. 4 shows typical results obtained on interphase cells in day-5.5 embryos. All three antisera gave strong, discrete signals on the interphase cells of normal embryos (Fig. 4 *a–c*). In the −/− embryos, with the exception of the occasional cell showing weak residual Cenpa staining, most interphases were negative for this antibody (Fig. 4*d*), suggesting a complete or near complete depletion of Cenpa (from maternal cytoplasm) by this stage. The CREST#6 antiserum gave positive signals on the −/− embryos (Fig. 4*e*), but the signals were discernibly different from those seen in the normal embryo in that there was high background staining throughout the nucleus and the enhanced signals on chromatin were unusually diffuse through all focal planes. Because CENP-A was absent from these embryos, the observed CREST#6 signals could be attributed to the staining of CENP-B. When tested with the anti-Cenpc

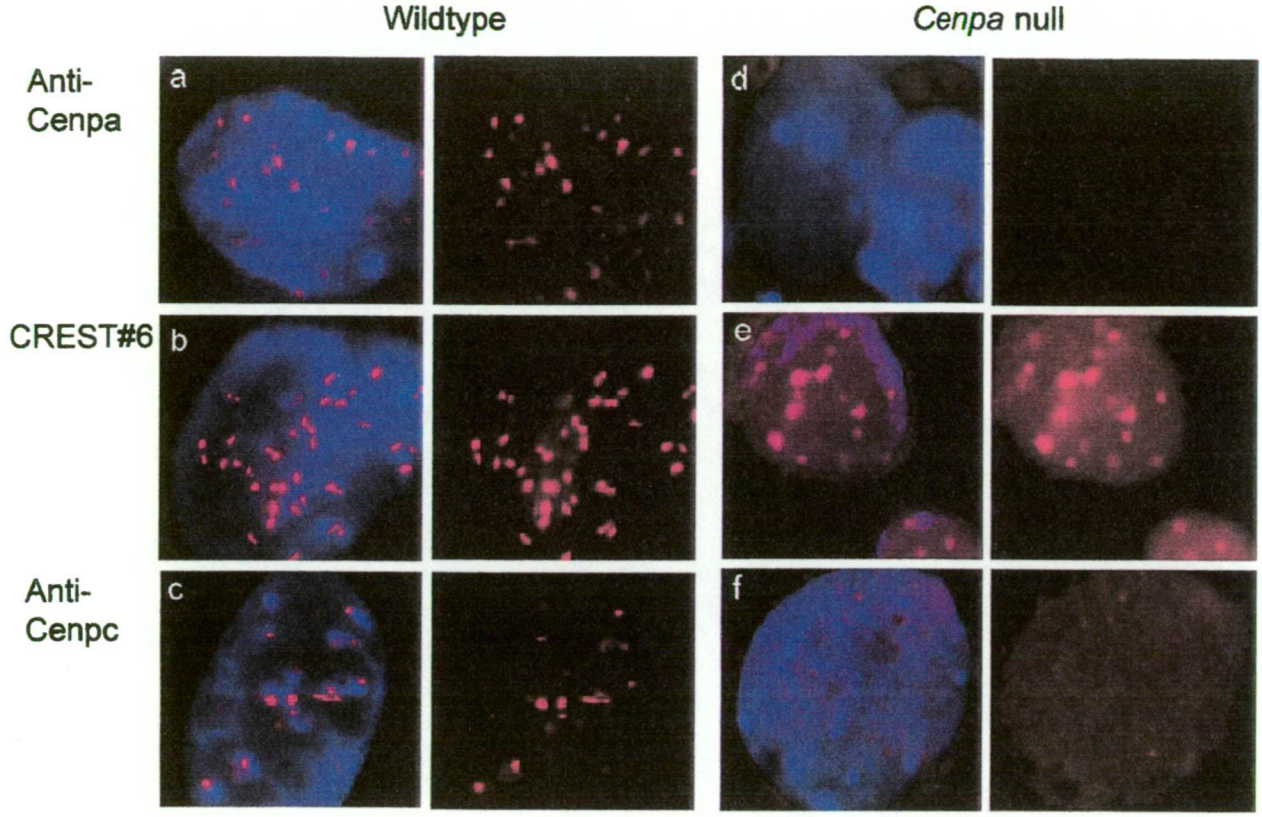

Fig. 4. Immunofluorescence analysis of day-5.5 embryos. (*a–c*) Wild-type interphase cells stained with anti-Cenpa, CREST#6 autoimmune serum, and anti-Cenpc, respectively. (*d–f*) *Cenpa* null interphase cells stained with anti-Cenpa, CREST#6, and anti-Cenpc, respectively. Although these pictures represented the results taken at one focal plane of a three-dimensional interphase cell nucleus, direct microscopic analysis through all the planes indicated only variation in the total number of observable signals but not the morphology of the signals (e.g., the more diffuse spots in *e*, and the higher background signals throughout the nuclei in both *e* and *f* compared with their respective controls). (*Left*) Simultaneous staining of chromatin with 4′,6-diamidino-2-phenylindole (blue) and centromere with anticentromere antibody (red). (*Right*) Split image of *Left* showing anticentromere antibody staining (red) only.

antibody, the prominent and discrete signals seen in normal embryos were undetected in the −/− interphases (Fig. 4*f*). Instead, these interphase cells showed a profuse speckling of Cenpc signals throughout the entire nucleus.

Discussion

Our gene targeting construct was designed to cause a premature translational termination and deletion of the centromere targeting domain of Cenpa. Evidence that complete gene knockout has been achieved comes from the complete absence of immunofluorescence-detectable Cenpa proteins in morphologically degenerating *Cenpa* null embryos. The apparently normal phenotype of the *Cenpa*-targeted heterozygous ES cell line and mice also indicates that our gene disruption strategy does not produce any observable dominant-negative effect.

In previous studies, we reported that targeted gene disruption of the centromere proteins Cenpc and Incenp in mice results in preimplantation embryonic lethality before day 3.5 pc (10, 21). In comparison, expression of a severe phenotype in the *Cenpa* null embryos appears slightly delayed because these embryos are able to implant into the uterus. Embryonic cell division and development up to this stage presumably are sustained by residual maternal cytoplasmic Cenpa protein (the presence of which has been demonstrated in our immunofluorescence experiments on these early embryos; data not shown). The slightly longer survival time for *Cenpa* null embryos could reflect a greater stability of the maternal Cenpa mRNA and/or its translated protein compared with those of Cenpc and Incenp. As the maternal Cenpa becomes depleted at day 5.5 pc, mitotic impairment becomes apparent. Chromosomal missegregation results in the formation of a large number of micronuclei (because of lagging chromosomes), macronuclei (because of nonseparated genomes), and nuclear bridging and blebbing (because of tethering chromosomes affecting cytokinesis). The detection of highly condensed, dark Giemsa-staining bodies reflects shrinking chromatin that prompts speculation of apoptotic cell death (38).

Immunofluorescence analysis has provided insight into the cause of mitotic disarray and the role of Cenpa. Depletion of Cenpa in day-5.5 −/− embryos is accompanied by a significant alteration in Cenpb binding in the interphase cells. Instead of the usual discrete and compact signals, Cenpb binding on interphase chromosomes now becomes more diffuse, suggesting that the local chromatin is no longer as highly condensed as that for a normal interphase centromere (compare Fig. 4 *e* with *a–c*). This disrupted chromatin structure also appears to affect the normal sequestration of Cenpb from the nuclear pool as evident from the increased Cenpb signal seen throughout the nucleus. At present, it is unclear what the role of Cenpb is because the protein appears to be nonessential for normal mitotic and meiotic cell divisions (5–7).

Anti-Cenpc antibody has been used to further investigate whether a structurally normal interphase kinetochore is formed in Cenpa-deficient cells. Cenpc is a good marker for this because the protein is present only on active centromeres (39, 40) and is functionally essential (10). Our results indicate that depletion of Cenpa leads to an absence of discrete Cenpc binding to interphase centromere. As with Cenpb, sequestration of nuclear

Cenpc also becomes impaired, resulting in a diffuse and speckled distribution of the noncentromere-targeted protein throughout the nucleus. The profuse interphase staining seen with both anti-Cenpc and anti-Cenpb antibodies in the $-/-$ embryos also indicates that these proteins are not limiting but are incapable, in the absence of Cenpa, to precipitate kinetochore formation. The observed failure of a structurally normal kinetochore to be properly assembled during interphase provides a suitable explanation for the progressive deterioration of mitotic chromosomal segregation in the *Cenpa* null embryos, leading ultimately to severe mitotic disarray and embryonic cell death.

Recent data suggest that centromere formation does not strictly depend on DNA sequence and that epigenetic factors may be involved (41–43). Such epigenetic factors are assumed to operate at the higher-order organizational level, directly on chromatin structures. The histone H3-like property of CENP-A means that the protein can directly influence centromere-specific chromatin organization at the nucleosomal level, making this protein a suitable candidate for epigenetic regulation. The observation that CENP-A synthesis appears to be coupled with centromere replication (28) has prompted the proposal that through direct incorporation of the protein at the time of DNA replication, a chromosomal region becomes marked for kinetochore assembly (29). A possible role of replication not withstanding, the results of the present study indicate that CENP-A is required for the kinetochore targeting of functionally critical CENP-C and, by virtue of its nucleosomal nature (expected to play a commanding role in establishing the primary level of chromatin packaging before the seeding of other kinetochore proteins such as CENP-C) probably constitutes one of the earliest events in the interphase kinetochore assembly pathway. These properties are consistent with an epigenetic role of CENP-A in marking a chromosomal region for centromere formation. Future studies aimed at understanding the mechanisms that facilitate the recruitment of CENP-A to a potential centromeric site should provide further important insight.

We thank P. Mountford for the IRES-βgeo marker, G. Kay for the 129/1 cell line, E. Robertson for STO/Neo^R feeder cells, S. Gazeas, M. Sibson, A. Sylvain, and J. Ladhams for excellent technical assistance, and E. Earle for helpful discussion. This work was supported by the National Health and Medical Research Council of Australia. K.H.A.C. is a Principal Research Fellow of the Council.

1. Choo, K. H. A. (1997) *The Centromere* (Oxford Univ. Press, Oxford).
2. Sullivan, K., Hechenberger, M. & Masri, K. (1994) *J. Cell Biol.* **127**, 581–592.
3. Pietras, D. F., Bennett, K. L., Siracusa, L. D., Woodworth-Gutai, M., Chapman, V. M., Gross, K. W., Kane-Haas, C. & Hastie, N. D. (1983) *Nucleic Acids Res.* **11**, 6965–6983.
4. Rattner, J. B. (1991) *BioEssays* **13**, 51–56.
5. Hudson, D. F., Fowler, K., Earle, E., Saffery, R., Kalitsis, P., Trowell, H., Hill, J., Wreford, N., de Kretser, D., Cancilla, M., *et al.* (1998) *J. Cell Biol.* **141**, 309–319.
6. Kapoor, M., De Oca Luna, R. M., Liu, G., Lozano, G., Cummings, C., Mancini, M., Ouspenski, I., Brinkley, B. & May, G. (1998) *Chromosoma* **107**, 570–576.
7. Perez-Castro, A., Shamanski, F., Meneses, J., Lovato, T., Vogel, K., Moyzis, R. & Pedersen, R. (1998) *Dev. Biol.* **201**, 135–143.
8. Saitoh, H., Tomkiel, J., Cooke, C., Ratrie, H., Maurer, M., Rothfield, N. F. & Earnshaw, W. C. (1992) *Cell* **70**, 115–125.
9. Yang, C. A., Tomkiel, J., Saitoh, H., Johnson, D. H. & Earnshaw, W. C. (1996) *Mol. Cell Biol.* **16**, 3576–3586.
10. Kalitsis, P., Fowler, K., Earle, E., Hill, J. & Choo, K. H. A. (1998) *Proc. Natl. Acad. Sci. USA* **95**, 1136–1141.
11. Fukagawa, T. & Brown, W. R. A. (1997) *Hum. Mol. Genet.* **6**, 2301–2308.
12. Tomkiel, J. E., Cooke, C. A., Saitoh, H., Bernat, R. L. & Earnshaw, W. C. (1994) *J. Cell Biol.* **125**, 531–545.
13. Brown, M., Goetsch, L. & Hartwell, L. H. (1993) *J. Cell Biol.* **123**, 387–403.
14. Fukagawa, T., Pendon, C., Morris, J. & Brown, W. (1999) *EMBO J.* **18**, 4196–4209.
15. Craig, J. M., Earnshaw, W. C. & Vagnarelli, P. (1998) *Exp. Cell Res.* **246**, 249–262.
16. Rieder, C. L. & Salmon, E. D. (1998) *Trends Cell Biol.* **8**, 310–317.
17. Skibbens, R. V. & Hieter, P. (1998) *Annu. Rev. Genet.* **32**, 307–337.
18. Amon, A. (1999) *Curr. Opin. Genet. Dev.* **9**, 69–75.
19. Dobie, K. W., Hari, K. L., Maggert, K. A. & Karpen, G. H. (1999) *Curr. Opin. Genet. Dev.* **9**, 206–217.
20. Eckley, D. M., Ainsztein, A. M., Mackay, A. M., Goldberg, I. G. & Earnshaw, W. C. (1997) *J. Cell Biol.* **136**, 1169–1183.
21. Cutts, S., Fowler, K., Kile, B., Hii, L., O'Dowd, R., Hudson, D., Saffery, R., Kalitsis, P., Earle, E. & Choo, K. H. A. (1999) *Hum. Mol. Gen.* **8**, 1145–1155.
22. Palmer, D. K., O'Day, K., Trong, H. L., Charbonneau, H. & Margolis, R. L. (1991) *Proc. Natl. Acad. Sci. USA* **88**, 3734–3738.
23. Kalitsis, P., MacDonald, A., Newson, A., Hudson, D. & Choo, K. H. A. (1998) *Genomics* **47**, 108–114.
24. Basrai, M. A. & Hieter, P. (1995) *BioEssays* **17**, 669–672.
25. Arents, G., Burlingame, R. W., Wang, B. C., Love, W. E. & Moudrianakis, E. N. (1991) *Proc. Natl. Acad. Sci. USA* **88**, 10148–52.
26. van Holde, K. E. (1989) *Chromatin* (Springer, New York).
27. Mann, R. K. & Grunstein, M. (1992) *EMBO J.* **11**, 3297–3306.
28. Shelby, R., Vafa, O. & Sullivan, K. (1997) *J. Cell Biol.* **136**, 501–513.
29. Henikoff, S. & Csink, A. K. (1998) *Trends Genet.* **14**, 200–204.
30. Valdivia, M. M., Figueroa, J., Iglesias, C. & Ortiz, M. (1998) *FEBS Lett.* **422**, 5–9.
31. Figueroa, J., Saffrich, R., Ansorge, W. & Valdivia, M. (1998) *Chromosoma* **107**, 397–405.
32. Meluh, P. B., Yang, P., Glowczewski, L., Koshland, D. & Mitchell Smith, M. (1998) *Cell* **94**, 607–613.
33. Stoler, S., Keith, K., Curnick, K. & Fitzgerald-Hayes, M. (1995) *Gene Dev.* **9**, 573–586.
34. Mountford, P., Zevnik, B., Duwel, A., Nichols, J., Li, M., Dani, C., Robertson, M., Chambers, I. & Smith, A. (1994) *Proc. Natl. Acad. Sci. USA* **91**, 4303–4307.
35. Hendzel, M. J., Wei, Y., Mancini, M., Van Hooser, A., Ranalli, T., Brinkey, B., Bazett-Jones, D. & Allis, C. D. (1997) *Chromosoma* **106**, 348–360.
36. Saffery, R., Earle, E., Irvine, D., Kalitsis, P. & Choo, K. H. A. (1999) *Chromosome Res.* **7**, 261–265.
37. du Sart, D., Cancilla, M., Earle, E., Mao, J., Saffery, R., Tainton, K., Kalitsis, P., Martyn, J., Barry, A. & Choo, K. H. A. (1997) *Nat. Genet.* **16**, 144–153.
38. El-Sheraby, A. M. & Hinchliffe, J. R. (1974) *J. Embryol. Exp. Morphol.* **31**, 643–654.
39. Earnshaw, W. C., Ratrie, H. & Stetten, G. (1989) *Chromosoma* **98**, 1–12.
40. Page, S. L., Earnshaw, W. C., Choo, K. H. A. & Shaffer, L. G. (1995) *Hum. Mol. Genet.* **4**, 289–294.
41. Karpen, G. & Allshire, R. (1997) *Trends Genet.* **13**, 489–496.
42. Wiens, G. & Sorger, P. (1998) *Cell* **93**, 313–316.
43. Barry, A., Howman, E. V., Cancilla, M., Saffery, R. & Choo, K. H. A. (1999) *Hum. Mol. Gen.* **8**, 217–227.

PUBLICATION 10

A.W.I. LO, D.F.S. LONGMUIR, **K.J. FOWLER**, P. KALITSIS AND K.H.A. CHOO

(2000)

ASSIGNMENT OF THE CENTROMERE PROTEIN H (*CENPH*) GENE TO MOUSE CHROMOSOME BAND 13D1 BY IN SITU HYBRIDIZATION AND INTERSPECIFIC BACKCROSS ANALYSES.

CYTOGENETICS AND CELL GENETICS,
90: 56-57

Cytogenet Cell Genet 90:56–57 (2000)

Cytogenetics and Cell Genetics

Assignment[1] of the Centromere Protein H *(Cenph)* gene to mouse chromosome band 13D1 by in situ hybridization and interspecific backcross analyses

A.W.I. Lo, D.F.S. Longmuir, K.J. Fowler, P. Kalitsis and K.H.A. Choo

The Murdoch Childrens Research Institute, Royal Children's Hospital, Parkville, Melbourne, Victoria (Australia)

[1] To our knowledge this is the first time this gene has been mapped.

Rationale and significance

The centromere plays an important role in the accurate and coordinated segregation of chromosomes during mitosis and meiosis. In all higher eukaryotes investigated, the normal centromere consists of highly repetitive DNA complexes with proteins forming the kinetochore (reviewed in Choo, 1997). The cDNA of a new member of the constitutive centromere proteins, *Cenph*, was recently cloned from the mouse erythroleukemia cell line SKT6 (Sugata et al., 1999). Its constitutive association with the kinetochore throughout the whole cell cycle and the predicted presence of a coiled-coil region suggests its importance in kinetochore organization and possible interactions with other kinetochore components. Here, we report the mapping of the mouse *Cenph* gene by fluorescence in situ hybridization (FISH) and establishing flanking markers using interspecific backcross analysis.

Materials and methods

Fluorescence in situ hybridization

Two BAC clones, 67A14 and 67A15, containing the 5′ end of the *Cenph* gene were identified by PCR screening of a mouse strain 129/Sv genomic bacterial artificial chromosome (BAC) library (Incyte Genomics Inc.) using the primer pairs HF13 and HR11 (5′-TATTTTCTGTGGCGTTCAAACC-3′ and 5′-AGGCTGATACGGTCCTCGATAC-3′ corresponding to nucleotide positions 62–83 and 183–204 of the *Cenph* cDNA sequence, respectively). These two clones were identical by restriction analysis. The DNA sequence of the PCR product is 100% identical to the corresponding segments of the *Cenph* cDNA sequence. 67A15 was used as probe in FISH on normal mouse metaphase chromosomes derived from embryonal stem cell strain W9.5 as described (DiDonato et al., 1997a). A Chromosome 13–specific point probe (Applied Genetics Laboratories) located at the *D13Mit235* locus (~1 cM) was cohybridized with 67A15.

Probe name: 67A15
Probe type: mouse genomic DNA
Insert size: ~170kb
Vector: pBeloBAC 11
Proof of authenticity: sequencing
Gene reference: Sugata et al., 1999; GenBank/EBI/DDBJ AB017634

Interspecific backcross analysis

Proof of authenticity: Primer pair lahf1 and lahr1 (5′-AAATACAAATCGAGAAGAACAAACAGAAAGAGGA-3′ and 5′-TGCTAAGTAGAGAAGGAGAAAAGAAGACACAACC-3′ corresponding to nucleotide position 600–633 and 1147–1180 of the 3′ end of the *Cenph* cDNA sequence, respectively) amplified ~2.1- and 2.15-kb fragments from the genomic DNA of C57BL/6J and SPRET/Ei, respectively. End-sequencing revealed that the first 86 nucleotides and the last 410 nucleotides of both the PCR products showed >98% homology to the cDNA sequence of *Cenph*. From the limited end-sequences, a polymorphic microsatellite marker consisting of $(CA)_n$ repeats was identified within the intronic region and was used for genotyping. Primer pair Cenph-pA (5′-TGTGCATGTAACTATAGTCCCG-3′) and Cenph-pB (5′-GGAGTTTATTATAGCCAGCCTG-3′), flanking this microsatellite marker, was designed for standard PCR reaction, using AmpliTaq DNA polymerase and the buffer provided (Perkin-Elmer Biosystems, containing 1.5 mM Mg), under the conditions: 94°C 5 min; 30 cycles of 94°C 30 s, 55°C 30 s, 72°C 1 min; 72°C 7 min. This PCR amplified a 251-bp and a 294-bp fragment from C57BL/6J and SPRET/Ei genomic DNA, respectively.

Method of mapping: Genotyping was performed by PCR using the primer pairs Cenph-pA and Cenph-pB for the 3′ end microsatellite marker on the genomic DNA from each of the 94 progenies of the interspecific backcross panels (C57BL/6J × M. spretus)F1 × C57BL/6J, called the Jackson BSB panel, and (C57BL/6JEi × SPRET/Ei)F1 × SPRET/Ei, called the Jackson BSS panel (Rowe et al., 1994). PCR products were analysed by electrophoresis on a 1.2% agarose gel stained with ethidium bromide. The inheritance pattern of each progeny for the C57BL/6J allele and the SPRET/Ei or M. spretus allele was studied according to the presence of the corresponding 251-bp or 294-bp PCR products, respectively. The data was analysed using the program Map Manager QTX version 0.13 (developed by J. Meer, R.H. Cudmore Jr and K.F. Manly, http://mcbio.med.buffalo.edu/mmQTX.html; see Manly, 1993 for reference of an earlier version of the program). Missing typings were inferred from surrounding data where assignment was unambiguous. Raw data from The Jackson Laboratory were obtained from the World Wide Web (http://www.jax.org/resources/document/cmdata) (MGD Accession No. J: 61750).

Supported by MIRS and IPRS of the University of Melbourne (to A.W.I.L.) and NHMRC (to K.H.A.C.) of Australia. We thank Mary Barter of the Jackson Laboratory for assistance in analysing the backcross data.

Received 24 May 2000; manuscript accepted 14 June 2000.

Request reprints from Dr. A.W.I. Lo, The Murdoch Childrens Research Institute, Royal Children's Hospital, Parkville, Victoria 3052 (Australia); telephone: 61-3-8361 6240; fax: 61-3-9348 1391; email: alo@doctor.com

KARGER

Fax + 41 61 306 12 34
E-mail karger@karger.ch
www.karger.com

0301–0171/00/0902–0056$17.50/0

Accessible online at:
www.karger.com/journals/ccg

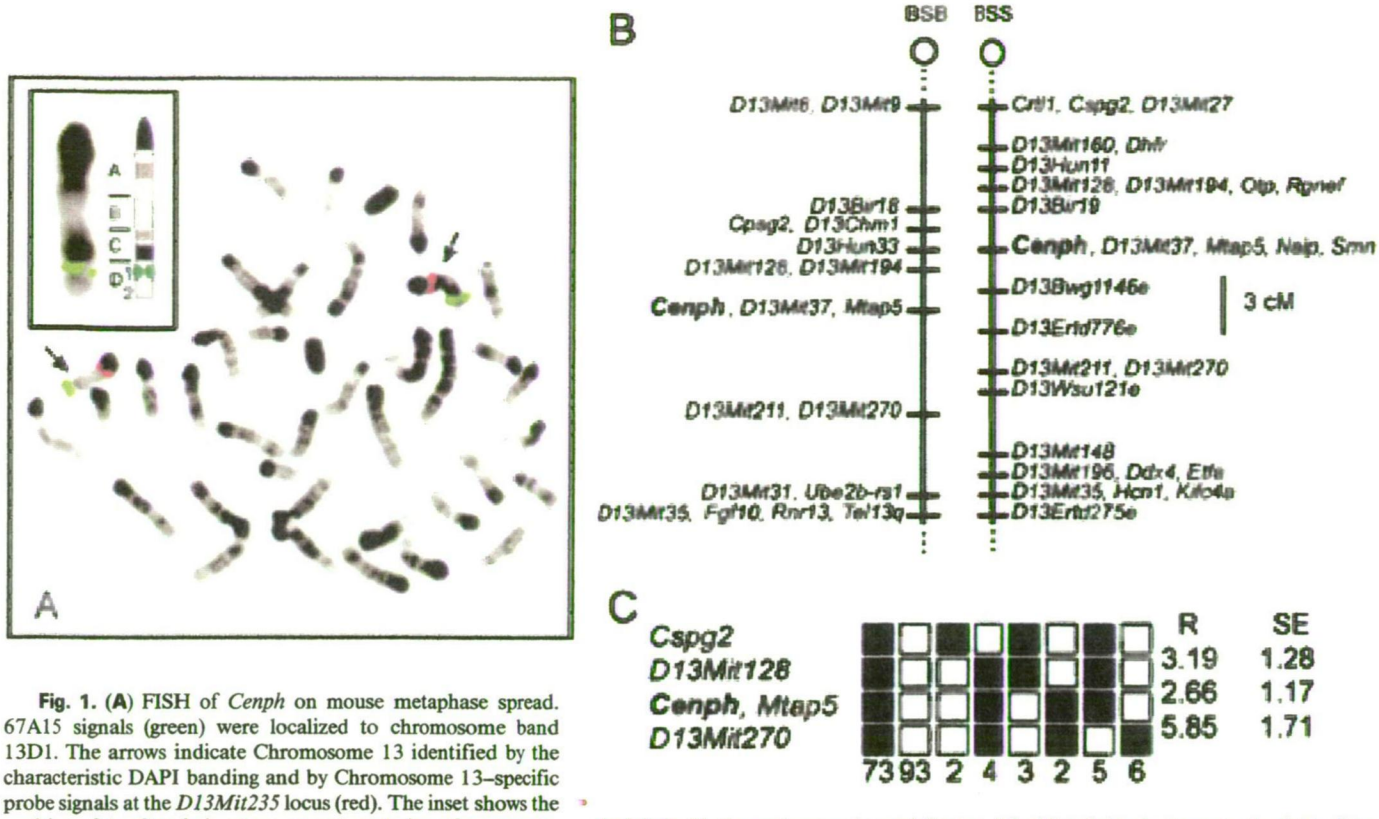

Fig. 1. (**A**) FISH of *Cenph* on mouse metaphase spread. 67A15 signals (green) were localized to chromosome band 13D1. The arrows indicate Chromosome 13 identified by the characteristic DAPI banding and by Chromosome 13–specific probe signals at the *D13Mit235* locus (red). The inset shows the position of the *Cenph* signals on an enlarged view of a representative Chromosome 13 from a different metaphase spread probed with 67A15 (green) aligned with its corresponding ideogram. Images were reversed to show the G-C banding. (**B**) Linkage map of the Jackson BSB and BSS backcrosses showing the part of Chromosome 13 with loci linked to *Cenph*. The Jackson BSB and BSS maps of the distal end of Chromosome 13 are depicted with the centromere toward the top. A 3-cM scale bar is shown to the right of the figure. Loci mapping to the same position are listed in alphabetical order. (**C**) In the combined Jackson BSB and BSS haplotype figure, loci are listed in order with the most proximal at the top. The black boxes represent the C57BL/6J allele and the white boxes the SPRET/Ei allele. The number of animals with each haplotype is given at the bottom of each column of boxes. The percent recombination (R) between adjacent loci is given to the right of the figure with the standard error (SE) for each R.

Results

FISH mapping data (Fig. 1A)

Location: 13D1

Number of cells examined: 100

Number of cells with specific signals: 1 (0), 2 (2), 3 (6), 4 (92) chromatids per cell

Most precise assignment: 13D1

Location of background signals (sites with >2 signals): none observed

Interspecific backcross analyses

The pattern of inheritance of homozygosity and heterozygosity of the C57BL/6J allele and the SPRET/Ei allele were analysed and compared against the known loci in the BSS and BSB backcross panel maps. Close linkage of *Cenph* to the distal region of Chromosome 13 is confirmed in both panels and *Cenph* cosegregates with a number of well-described genes including *Mtap5* (Chakraborti and Kozak, 1992) *Naip* (DiDonato et al., 1997b) and *Smn* (DiDonato et al., 1997a) as shown in Fig. 1B and C. *Cenph* also cosegregates with the following markers, *D13Mit30*, *37*, *70*, and many others (0.0–1.6 cM, at 95% confidence limit).

References

Choo KHA: Centromere (Oxford University Press, Oxford 1997).

Chakraborti A, Kozak CA: Microtubule-associated protein genes (*Mtap-1, Mtap-2* and *Mtap-5*) map to mouse chromosomes 1, 2 and 13. Mouse Genome 90:679–681 (1992).

DiDonato CJ, Chen X-N, Noya D, Korenberg JR, Nadeau JH, Simard LR: Cloning, characterization, and copy number of the murine survival motor neuron gene: Homolog of the spinal muscular atrophy-determining gene. Genome Res 7:339–352 (1997a).

DiDonato CJ, Nadeau JH, Simard LR: The mouse neuronal apoptosis inhibitory protein gene maps to a conserved syntenic region of mouse chromosome 13. Mammal Genome 8:222 (1997b).

Manly KF: A Macintosh program for storage and analysis of experimental genetic mapping data. Mammal Genome 4:303–313 (1993).

Rowe LB, Nadeau JH, Turner R, Frankel WN, Letts VA, Eppig JT, Ko MSH, Thurston SJ, Birkenmeier EH: Maps from two interspecific backcross DNA panels available as a community genetic mapping resource. Mammal Genome 5:253–274 (1994).

Sugata N, Munekata E, Todokoro K: Characterization of a novel kinetochore protein, CENP-H. J biol Chem 274:27343–27346 (1999).

PUBLICATION 11

P. KALITSIS, E. EARLE, **K.J. FOWLER**, AND K.H.A. CHOO (2000)

BUB3 GENE DISRUPTION IN MICE REVEALS ESSENTIAL MITOTIC SPINDLE CHECKPOINT FUNCTION DURING EARLY EMBRYOGENESIS.

GENES AND DEVELOPMENT, 14: 2277-2282

Bub3 gene disruption in mice reveals essential mitotic spindle checkpoint function during early embryogenesis

Paul Kalitsis, Elizabeth Earle, Kerry J. Fowler, and K.H. Andy Choo[1]

Murdoch Children's Research Institute, Royal Children's Hospital, Flemington Road, Parkville 3052, Melbourne, Australia

Bub3 is a conserved component of the mitotic spindle assembly complex. The protein is essential for early development in *Bub3* gene-disrupted mice, evident from their failure to survive beyond day 6.5–7.5 postcoitus (pc). *Bub3* null embryos appear normal up to day 3.5 pc but accumulate mitotic errors from days 4.5–6.5 pc in the form of micronuclei, chromatin bridging, lagging chromosomes, and irregular nuclear morphology. Null embryos treated with a spindle-depolymerising agent fail to arrest in metaphase and show an increase in mitotic disarray. The results confirm Bub3 as a component of the essential spindle checkpoint pathway that operates during early embryogenesis.

Received June 14, 2000; revised version accepted July 25, 2000.

The accurate attachment of chromosomes to the mitotic spindle via the kinetochore is vital for correct segregation of the genetic material into daughter cells. This process is overseen by a feedback-response mechanism, commonly known as the mitotic spindle checkpoint (for review, see Skibbens and Hieter 1998; Amon 1999). If defects are detected in the spindle, mitosis is halted to ensure that chromosomes achieve bipolar alignment before the cell proceeds through to anaphase.

Genetic screens in the budding yeast *Saccharomyces cerevisiae* have identified a series of genes (*BUB1*, *BUB2*, *BUB3*, *MAD1*, *MAD2*, *MAD3*, and *MPS1*) that fail to arrest in response to spindle damage (Hoyt et al. 1991; Li and Murray 1991; Weiss and Winey 1996). In the presence of microtubule-depolymerising drugs, the mutants accumulate severe mitotic errors because of their premature exit into anaphase. Higher eukaryotes contain several functional orthologs of these genes, including Bub1, Bub3, BubR1/Mad3, Mad1, and Mad2 (Chen et al. 1996; Li and Benezra 1996; Taylor and McKeon 1997; Basu et al. 1998; Chen et al. 1998; Taylor et al. 1998; Basu et al. 1999). Mutations and immunodepletion experiments on Bub1, BubR1/Mad3, Mad1, and Mad2 have shown that cells are unable to block at mitosis in response to microtubule-depolymerising agents, resulting in a premature exit into anaphase before the chromosomes have properly aligned (Chen et al. 1996; Li and Benezra 1996; Taylor and McKeon 1997; Cahill et al. 1998; Chen et al. 1998; Gorbsky et al. 1998; Waters et al. 1998; Basu et al. 1999; Chan et al. 1999). In humans, dominant-negative mutations of the Bub1 gene show a chromosomal instability phenotype in colorectal cancer cell lines (Cahill et al. 1998). These cell lines also fail to arrest at metaphase when treated with microtubule-depolymerising drugs.

Bub3 is found in most eukaryotes through evolution (Efimov and Morris 1998; Taylor et al. 1998; Martinez-Exposito et al. 1999). It contains four conserved WD40 repeats that are found in many proteins with diverse functions thought to be involved in protein–protein interactions (Neer et al. 1994). During mitosis, Bub3 appears on kinetochores during prophase, diminishing in quantity by metaphase. When kinetochores are unattached to the spindle, or lagging, the amount of kinetochore-associated Bub3 antigen increases (Martinez-Exposito et al. 1999). In higher eukaryotes, no mutation or depletion studies on Bub3 have been described. In this study, we have performed a genetic disruption of the *Bub3* gene in mouse, using gene-targeting techniques. We describe a lethal phenotype for the gene-disrupted mice and show that Bub3 is an essential component of the mitotic spindle checkpoint pathway that is required for mitotic fidelity.

Results

Disruption of the Bub3 *gene*

To disrupt the mouse *Bub3* gene, a promoterless targeting construct was used to obtain a high level of homologous recombination. The selection cassette, which contained the splice-acceptor/IRES/lacZ-neomycin resistance gene, was used to delete exons 2 and 3 (Fig. 1A). Only the first 65 amino acids of the 326-amino acid Bub3 protein would be correctly translated following gene disruption with the selection cassette. This disruption would result in the loss of three of the four WD40 repeat domains and the Bub1-interacting kinetochore domain and thus was expected to abolish any Bub3 activity at the kinetochore (Taylor et al. 1998). When theconstruct was transfected into two different ES cell lines, 129/1 or W9.5, 20 of 107 (19%) neomycin-resistant cell lines were found to have the desired targeting event (Fig. 1B).

Production of gene-disrupted mice

For the generation of chimeric mice, heterozygous cell lines from the 129/1 and W9.5 embryonic stem (ES) background were injected into C57BL/6 blastocysts. This resulted in independent germ line–transmitting chimeric mice from the 129/1 and W9.5 substrains carrying the targeted allele. The chimeric mice were successfully bred to produce heterozygous animals.

Embryonic lethality of Bub3 gene-disrupted mice

Bub3$^{+/-}$ mice were healthy, fertile, and showed no apparent phenotype due to haplo-insufficiency. PCR geno-

[*Key Words*: Mitotic checkpoint; kinetochore; chromosome missegregation; mouse transgenic]
[1]**Corresponding author.**
E-MAIL choo@cryptic.rch.unimelb.edu.au; FAX 61-3-9348-1391.
Article and publication are at www.genesdev.org/cgi/doi/10.1101/gad.827500.

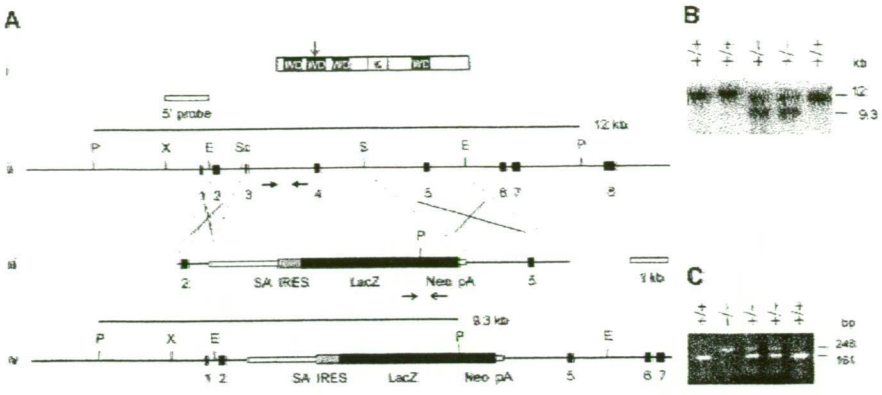

Figure 1. Targeted disruption of the mouse *Bub3* gene. (*A*) Gene disruption construct and restriction maps. (i) Mouse Bub3 protein showing positions of four WD40 motifs (*WD*) and the Bub1-kinetocore-interacting domain (K) (Taylor et al. 1998; Martinez-Exposito et al. 1999). The disruption site is indicated by the vertical arrow. Restriction-enzyme maps for (ii) the *Bub3* gene covering exons 1 to 8, (iii) the neomycin-resistance gene targeting construct, and (iv) the *Bub3* locus following targeted disruption. Black boxes represent exons. The selectable marker cassette contained in the targeting construct consists of a splice acceptor site (SA), a picornaviral internal ribosome-entry site (IRES), a lacZ–neomycin fusion gene (*beta-geo*) and a SV40 polyadenylation sequence (pA). A 1.2-kb *XbaI–EagI* fragment (designated 5′ probe) spanning exon 1 was used in the Southern-screening strategy and detected a 12-kb wild-type *PstI* fragment in the untargeted locus or a 9.3-kb *PstI* fragment in the targeted locus. The positions of the primers for nested PCR genotyping of cultured embryos up to day 3.5 + 4 are shown by the horizontal arrows in (ii) and (iii). Wild type primer pairs include BI3H-BI3I for the first round and BI3J-BI3K for the second round of amplification (closed horizontal arrows in ii), giving a final product of 161 bp for the untargeted allele. Beta-geo primer pairs include GF1–GR1 for first-round synthesis and GF2–GR2 for second-round synthesis (open horizontal arrows in iii), giving a final product of 248 bp for the targeted allele. Crosses denote expected sites of homologous recombination. Abbreviations for restriction enzymes are (E) *EagI*, (P) *PstI*, (Sc) *SacI*, (S) *SalI*, and (X) *XbaI*. (*B*) Southern blot analysis of wild-type and gene-targeted ES cell lines. The sizes of wild-type 12-kb and homologous recombinant 9.3-kb bands are shown. (*C*) Nested PCR analysis of cultured 3.5 + 4 day embryos from heterozygous crosses showing the expected bands for the targeted (248 bp) and untargeted (161 bp) alleles.

type analysis of 91 live-born mice from *Bub3*$^{+/-}$ intercrosses showed 32 wild-type and 59 heterozygote animals with no homozygous mutants detected. The observed wild type:heterozygote:mutant homozygote ratio of ~1:2:0, therefore, suggests an embryonic-lethal phenotype for the null mutant.

To further pinpoint the time of embryonic lethality, day 8.5 embryos from heterozygous crosses were removed from the mice and PCR genotyped. No *Bub3* null embryos were observed out of a sample of 29 embryos, which consisted of eight wild types and 21 heterozygotes. This result suggested that embryonic death occurred prior to day 8.5 pc.

Morphological degeneration of early embryos

For morphological study and the further determination of the time of embryonic lethality, blastocysts were obtained from heterozygous crosses at day 3.5 and cultured in ES cell media. The embryos were monitored and photographed after 2, 3, and 4 days in culture (denoted as days 3.5 + 2, 3.5 + 3, and 3.5 + 4, respectively). At the end of day 3.5 + 4, the embryos were harvested and genotyped using the nested PCR strategy outlined in Figure 1. Of the 32 embryos studied, 10 +/+, 15 +/–, and 7 –/– were obtained (Fig. 1C). All 7 –/– embryos, but not any of the +/+ and +/– embryos, showed a rapidly degenerating phenotype (see below), suggesting a complete correlation between morphological deterioration and the –/– genotype. This result, combined with those for the day 8.5 embryos and the live-born pups, provided evidence that *Bub3*$^{-/-}$ embryos were viable at day 3.5 in utero and persisted in culture up to day 3.5 + 4 but were completely resorbed or proceeded to degenerate beyond experimental detection by the time they reached day 8.5 in utero.

By phase-contrast microscopy, no significant morphological difference was observed between the different genotypes at day 3.5 or 3.5 + 1 (not shown). In both the wild-type and heterozygous embryos, the transition from day 3.5 + 2 to 3.5 + 4 was characterized by an increase in the size of the inner cell mass and the trophectoderm (Fig. 2). This increase was due to the rapidly dividing inner cell mass population, whilst the cells of the outer trophectoderm simply increased in size without undergoing many divisions. In contrast, the inner cell mass of all the *Bub3*$^{-/-}$ embryos were significantly smaller in size and were obviously degenerated by day 3.5 + 3. The trophectoderm, however, appeared morphologically indistinguishable from those of the wild-type and heterozygous littermates throughout the culture period.

Severe mitotic phenotype in null embryos

To further examine the null phenotype, cultured embryos from heterozygous crosses were fixed and then stained with DAPI. Since the results of genotype analysis has indicated a complete concordance between embryo deterioration and the –/– genotype, and because of difficulties associated with PCR genotyping on fixed and stained cells, deteriorating or affected embryos were designated as presumed null mutants without further genotyping in the following studies. At day 3.5, no observable difference in nuclear morphology was detected between the embryos. After one day in culture, eight of 30 embryos exhibited a significantly increased number of micronuclei (Fig. 3B,C), compared to the normal littermate (Fig. 3A). An average of 7.4 micronuclei per affected embryo was scored, compared with a baseline level of 1.1 micronuclei for the unaffected embryos (Tab. 1). Other defects observed in the affected embryos included the occasional chromatin bridge and nuclear blebbing (not shown). No significant difference in the mitotic indices was seen between the normal and affected embryos (Tab. 1).

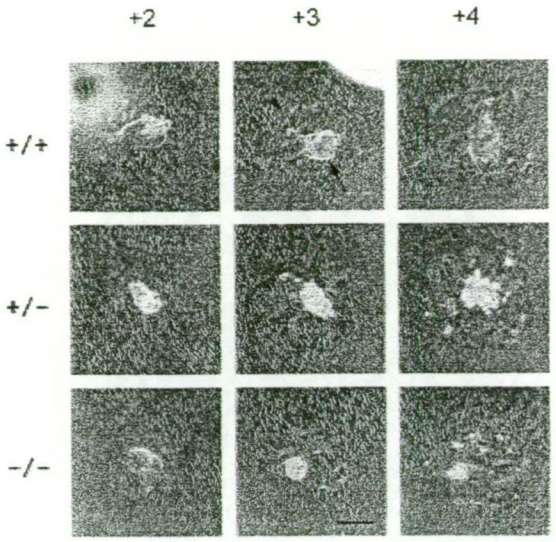

Figure 2. Morphology of cultured blastocyst outgrowths from heterozygous crosses. Cultured wild-type, heterozygous and homozygous embryos were photographed using phase microscopy, from day 3.5 + 2 to +4. The tightly packed inner cell mass is found in the center of all the embryos (arrow), surrounded by the larger, flat cells of the trophectoderm layer (arrowhead). Scale bar represents 200 μm.

At day 3.5 + 2, 12 of 42 embryos were clearly affected, as characterized by an increase in the number of micronuclei, irregular nuclear morphology, and smaller inner cell mass (Fig. 3E,F). When immunofluorescence was performed using a previously described anti-CENP-A and CENP-B antisera (CREST#6) (du Sart et al. 1997) on these embryos, the micronuclei seen in the affected embryos were shown to contain one or more chromosomes, providing evidence that these micronuclei represented lagging chromosomes due to missegregation (Fig. 3J). The average cell number for an affected embryo was 130, which was significantly lower than 200 for a normal day 3.5 + 2 embryo ($P = 0.0047$) (Fig. 3D,E). Thus, while the normal embryos have undergone an approximate doubling in cell number compared to day 3.5 + 1, only a marginal increase of <10% in cell number was seen in the affected embryo over the same culture period (Table 1). The average mitotic index for an affected embryo at day 3.5 + 2 was also noticeably lower than that of a normal embryo at the same stage (3.2% vs. 7.0 %; $P = 1.5 \times 10^{-5}$). These results suggest a slowing down in development at 3.5 + 2 days in the affected group.

At day 3.5 + 3, ten of 37 embryos were abnormal. The abnormalities were more pronounced than those seen in earlier stages and included a greatly reduced cell number, grossly irregular nuclear morphology, chromatin bridging, lagging chromosomes, and the presence of many micronuclei (Fig. 3H,I). At this stage, accurate scoring of the number of cells or mitoses became difficult because of the large highly compacted inner cell mass in the normal embryos and the grossly deteriorated nuclear morphology of the inner cell population of the affected embryos. The approximate cell number for an affected embryo was estimated to be between 50 and 100 compared with the 300–500 cells in an unaffected littermate, suggesting that while the normal embryos continued to actively divide in culture at day 3.5 + 3, cells in the affected embryos had stopped dividing and/or were disintegrating. In addition, while mitoses were clearly visible in the normal embryos, little or no metaphases were observed in the affected embryos by this stage.

Failure of nocodazole to arrest mitosis

To assess whether the observed phenotype was due to the breakdown of a mitotic checkpoint, day 3.5 + 1 embryos from heterozygous crosses were incubated with 2 μM nocodazole for ~5 hrs. This drug depolymerizes and destroys the function of the microtubules. The results indicated that in the presence of nocodazole, mitosis in the normal embryos from heterozygous or control wild-type crosses was severely arrested, as evident from a great increase (by eight–ninefold) in mitotic index from

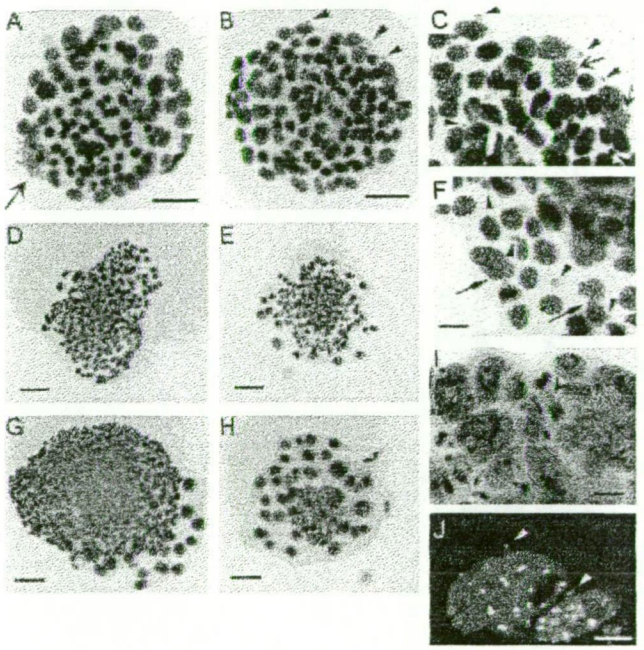

Figure 3. Nuclear morphology of cultured embryos from heterozygous crosses. (*A*) DAPI-stained day 3.5 + 1 normal embryo, showing regular interphase nuclei and metaphase chromosomes (open arrow). (*B,C*) Two different magnifications of a DAPI-stained day 3.5 + 1 affected embryo, showing regular interphase nuclei, metaphase chromosomes (open arrow), and micronuclei (arrowheads). (*D*) A normal embryo at day 3.5 + 2. (*E,F*) Two different magnifications of an affected embryo at day 3.5 + 2, showing greatly reduced cell number, irregular nuclei with blebs (diamond arrows) and many micronuclei (some examples shown by arrowheads). (*G*) A normal day 3.5 + 3 embryo containing over 300 cells, with many metaphases (not shown). (*H,I*) Two different magnifications of a day 3.5 + 3 affected embryo, showing a dramatic reduction in the number of cells and a worsening mitotic phenotype, exhibited by micronuclei, chromatin bridging (closed arrows) and lagging chromosomes (open arrowhead). (*J*) Anticentromere CREST immunofluorescence of day 3.5 + 2 affected embryos, showing positively stained micronuclei (arrowheads). Scale bars, (A–B) 50 μm, (D,E,G,H) 100 μm, (C,F,I) 20 μm, and (J) 10 μm.

Table 1. *Analysis of mitotic phenotype in day 3.5 + 1 untreated or nocodazole-treated embryos from heterozygous crosses*

	+/− cross						+/+ cross
	Untreated			+ Nocodazole			+ Nocodazole
	Normal	Null	*P* value	Normal	Null	*P* value	Normal
No. of embryos	23 (74%)	8 (26%)		21 (78%)	6 (22%)		21 (100%)
No. of cells[a]	110	120	0.12	98	100	0.56	80
Mitotic index[a,b]	2.1	1.6[c]	0.55	19	3[c]	6.1×10^{-6}	17
No. of micronuclei[a]	1.1	7.4[d]	3.6×10^{-7}	1.2	17[d]	3.6×10^{-7}	0.65

In addition to the normal litter mates from the heterozygous crosses, normal embryos from +/+ crosses were used as further controls to ascertain the effects of nocodazole.
[a]Average value per embryo.
[b]Expressed as a percentage of cells in mitosis over total cell number.
[c]$P = 0.071$ for the mitotic indices of untreated versus nocodazole-treated null embryos.
[d]$P = 0.039$ for the number of micronuclei in untreated versus nocodazole-treated null embryos.
P values were derived using the student's t test.

an untreated value of 2.1% to treated values of 19% and 17%, respectively (Table 1; also cf. Fig. 4A with Fig. 3A). In stark contrast to this increase in mitotic index, nocodazole treatment did not result in a significant alteration in the mitotic index of the null embryos (3%) compared to the untreated null embryos (1.6%) (Table 1). However, following the drug treatment, a noticeable deterioration of the mitotic missegregation phenotype was evident from the greatly increased number of micronuclei in the null embryos (from 7.4 micronuclei to 17 micronuclei per embryo before and after treatment) (Table 1; also cf. Fig. 4B with Fig. 3B). Other defects observed were an increase in irregular nuclear morphology, nuclear bridging, and blebbing in the treated null embryos. Control experiments using nocodazole-treated day 3.5 + 1 embryos from wild-type crosses did not result in embryos with a phenotype corresponding to that found in the null embryos (Table 1). This suggests that the effects of this drug seen in the null embryos from the heterozygous crosses were specifically related to the *Bub3*$^{-/-}$ genotype.

Discussion

In order to understand the role of mitotic checkpoint control in mouse development, we have created *Bub3* gene-disrupted mice. Bub3 is part of a protein complex that interacts with the kinetochore before all chromosomes have achieved bipolar attachment to the mitotic spindle. By deleting exons 2 and 3 of the *Bub3* gene, we have interrupted the protein at amino acid No. 65, causing the loss of the Bub1 interaction domain and three of the four WD40 repeat regions (Taylor et al. 1998; Martinez-Exposito et al. 1999). Success in generating a relatively large number of heterozygous knockout ES cell lines indicates that the gene-targeting strategy is efficient and that the growth of heterozygous cells in culture has not been compromised.

Heterozygous Bub3 mice show no apparent abnormalities in development or fertility, showing that one functional copy of the gene is sufficient for normal development. Genotyping of the progeny of heterozygous crosses indicates the absence of *Bub3*$^{-/-}$ pups and suggests an embryonic lethal phenotype. Morphological analysis of embryos grown in culture from the blastocyst stage (day 3.5) demonstrates a dramatic decrease in the size of the inner cell mass of the null embryos from +3 days to +4 days in culture, suggesting that rapid cell divisions have ceased in the mutant embryos by these stages. Closer examination of the embryos from the +/− crosses at the nuclear level reveals mitotic abnormalities in approximately 25% of day 3.5 + 1, 2, and 3 embryos, with no evidence of such abnormalities in any of the progeny of wild-type crosses. Determination of cell number indicates that mitotic division in the null embryos has decreased greatly at day 3.5 + 2 and ceased completely by day 3.5 + 3. By this latter stage, the embryos have accumulated such abundance of mitotic errors, in the form of micronuclei, nuclear bridging, and abnormal nuclear morphology, that cessation of embryo development becomes inevitable. These results show that *Bub3* is essential for normal mitosis and for early embryonic development in the mouse. Such an essential role, therefore, contrasts the phenotype seen in previously reported null mutants of the *BUB3* gene in *S. cerevisiae* and *Aspergillus nidulans* because these mutants are viable, albeit slower in growth relative to the wild type (Hoyt et al. 1991; Efimov and Morris 1998).

When compared to a number of other essential centro-

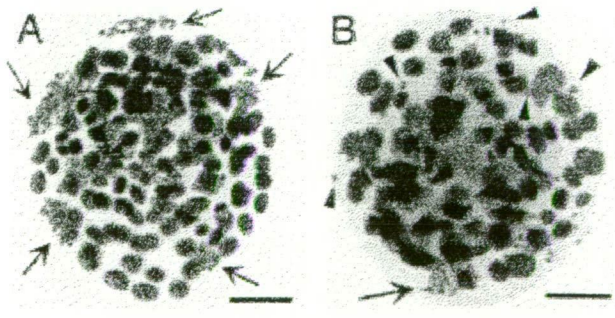

Figure 4. Nocodazole-treated day 3.5+ 1 embryos from heterozygous crosses. (*A*) A normal embryo, showing regular-sized nuclei and many arrested metaphases (some examples indicated by arrows). (*B*) A similarly treated null embryo, showing irregularly sized nuclei, very few metaphases (arrow), and a large number of micronuclei (selected examples shown by arrowheads). Scale bars represent 50 μm.

mere proteins that have recently been disrupted in the mouse, such as Cenpc, Incenp and Cenpa, the *Bub3*$^{-/-}$ mice show a similar phenotype in that the accumulation of severe mitotic errors contribute directly to early lethality (Kalitsis et al. 1998; Cutts et al. 1999; Howman et al. 2000). Closer examination reveals that the *Bub3*$^{-/-}$ embryos appear to survive slightly longer, by two to three days in culture. This may be explained by the fact that a defect in the constitutive centromere proteins Cenpa and Cenpc is expected to immediately disrupt centromere function, leading to a rapid breakdown in kinetochore-microtubule binding and mitotic arrest. Similarly, perturbation of the Incenp protein results in a gross dysfunction in cytokinesis that is expected to have an immediate detrimental effect on mitotic progression. In comparison, a defect in a protein such as Bub3 that plays a checkpoint role (discussed below) may allow mitosis to proceed aberrantly for a slightly greater number of cycles before the accumulation of excessive errors eventually brings it to a halt.

In previous studies on the BUB and MAD genes in yeast and higher eukaryotes, spindle-depolymerizing drugs have been used to assess whether the mutants have a compromised spindle assembly checkpoint. These mutants characteristically fail to arrest in response to mitotic spindle damage, leading to chromosome missegregation. We have used a similar strategy to investigate whether Bub3 functions as a component of a mitotic spindle checkpoint in the developing mouse embryo. Examination of the effect of the spindle-disrupting drug nocodazole on normal embryos indicates that, in the presence of this drug, normal embryos are severely blocked in mitosis, as evident from a large increase in mitotic index, compared to untreated normal embryos. This result suggests that early mouse embryos utilize a mitotic spindle checkpoint mechanism that is sensitive to spindle-depolymerizing drugs, similar to those that have been described in other organisms and somatic cell lines.

To investigate the specific role of Bub3, we studied the effect nocodazole has on the *Bub3* null embryos at day 3.5 + 1, when the total cell number and the extent of mitotic disarray are still sufficiently moderate to allow accurate ascertainment of mitotic indices and micronuclei numbers. At this time point, null embryos that have not been drug treated show clear signs of mitotic errors, as indicated by an approximately sevenfold increase in the number of micronuclei per embryo compared to an untreated normal embryo. However, the relatively unaltered mitotic index in the untreated null embryos compared to the normal embryos indicates that cell division appears to proceed at a normal rate. This mitotic index remains unaffected when the null embryos are challenged with nocodazole, which drastically contrasts with the situation in the normal embryos, in which treatment with the drug precipitates a large rise in mitotic index. This observation indicates that the *Bub3* null embryos are able to escape the block imposed by the mitotic spindle checkpoint pathway that operates upon the normal embryos. A predicted consequence of an escape from such a checkpoint, especially when the mitotic process is seriously compromised by a potent spindle-disrupting drug, is an elevation in the level of mitotic errors. This prediction is supported by the observed significant increase in the number of micronuclei, from 7.4 per untreated null embryo to 17 per nocodazole-treated null embryo. These results are characteristic of mutants that are defective in mitotic spindle checkpoint mechanisms (Hoyt et al. 1991; Li and Murray 1991; Taylor and McKeon 1997; Cahill et al. 1998; Basu et al. 1999), thus lending strong support that mouse Bub3 participates directly in such a checkpoint system.

Genetic and biochemical evidence indicates that Bub3 interacts with other proteins, including Bub1, to form a checkpoint kinase complex (Hoyt et al. 1991; Roberts et al. 1994; Basu et al. 1998; Farr and Hoyt 1998; Taylor et al. 1998; Brady and Hardwick 2000). Since the presence of both Bub3 and Bub1 is required for localization to the kinetochores that have not completely attached to the mitotic spindle, mutations in these two proteins are expected to share a common phenotype. Consistent with this, genetic disruption of the *Drosophila* bub1 gene, which also leads to the depletion of Bub3 at the kinetochore (Basu et al. 1998, 1999), results in embryonic lethality at the larval/pupal transition stage. Cells from these null embryos fail to block in mitosis in response to microtubule-depolymerizing drugs and contain severe mitotic abnormalities (lower mitotic index, premature chromatid separation, lagging chromosomes, and chromatin bridging). Recently, Mad2, another essential component of the MAD/BUB checkpoint complex has been disrupted in the mouse (Dobles et al. 2000). The phenotype of the *Mad2*$^{-/-}$ and *Bub3*$^{-/-}$ embryos share many features. Both mutants show few cells in mitosis beyond day 6.5, contain chromosome segregation errors in the form of lagging chromosomes, and fail to arrest in the presence of nocodazole. Taken together, the results of the above studies in mouse and *Drosophila* clearly indicate that the MAD/BUB complex constitutes a crucial mitotic checkpoint for early embryonic development, and that the mitotic checkpoint pathway is not only conserved at a molecular level but also at the functional level within metazoans.

Materials and methods

Targeting construct

Three BAC clones—195c21, 177c15, and 24e04—were identified in a mouse ES 129 BAC library (Incyte Genomics). DNA pools were screened using PCR with primers, B1 (5′-AGAAACGTTGCTTAGGCGG-3′), and B2 (5′-GAACTCGGAGTACCTTAACC-3′), which spanned exon 1 and 2 of the mouse *Bub3* gene, generating a PCR product size of 437 bp. BAC#177c15 was used for further subcloning. A 12-kb *PstI* genomic fragment containing exons 1 to 7 was cloned into the *PstI* site of pAlter (Promega; Fig. 1A). A 3.1-kb *SacI*/*SalI* fragment spanning exons 3 and 4 was removed and then replaced by a splice-acceptor/IRES/lacZ-neomycin cassette.

Transfections and chimera production

Mouse ES cell culture and manipulations were carried out using standard procedures (Kalitsis et al. 1998). For the creation of heterozygous cell lines, 50 μg of linearized DNA was electroporated at 0.8 kV, 3 μF, ∞ Ω into 5 × 10^7 mouse 129/1 or W9.5 ES cells and selected with 200 μg/ml of G418 (GIBCO BRL). Correctly targeted events were detected using Southern hybridization. A *XbaI*/*EagI* 1.2-kb fragment containing exon 1 was

used as a 5′ external probe in the hybridization assay (Fig. 1A). Genomic DNA was digested with *PstI*, generating a 12-kb wild-type or 9.3-kb targeted band. Targeted ES cell lines were used in the generation of chimeric and heterozygous mice using standard methods (Kalitsis et al. 1998).

Genotyping of mice

Mouse tail DNA was extracted using standard techniques. For PCR genotyping, a duplex strategy was employed using the following primers: BI3G (5′-AGTGAATGACCAAACCTGGG-3′) and BI4F (5′-CAACAGCACACTCTCCAACC-3′) for the wild-type allele (407 bp), and GF2 (5′-CCATTACCAGTTGGTCTGGTG-3′) and GR2 (5′-CCTCGTCCTGCAGTTCATTC-3′) for the targeted allele (248 bp).

Culturing and genotyping of mouse embryos

Embryos were dissected out at day 3.5 and cultured in ES media at 37°C 5% CO_2 for the required duration. After culturing, the DNA was extracted and resuspended in 10 µl of TE. Three µl of the embryo DNA was used in the first round of a nested PCR strategy. The first-round primers BI3H (5′-GATGCCTTTGCGTTCTTAGC-3′) and BI3I (5′-GATTCCAGGAGCAGCATCA-3′) (for the wild-type allele) and GF1 (5′-AGTATCGGCGGAATTCCAG-3′) and GR1 (5′-GATGTTTCGCTTGGTGGTC-3′) (for the targeted allele) were used in a duplex reaction, using the following conditions: first cycle at 95°C for 2 min, 55°C for 3 min, 72°C for 90 sec, and cycles 2–30 at 95°C for 60 sec, 55°C for 60 sec, 72°C for 90 sec, in a final reaction volume of 25 µl. For the second round, 1 µl of the first-round amplified product was used in separate wild-type BI3J (5′-TGTGGCAGGATTTGGAATG-3′) and BI3K (5′-TGTGCTTCTCAGTCCACTCG-3′) and targeted (GF2 and GR2) reactions, producing 161- and 248-bp bands, respectively. The conditions for the second-round amplification were first cycle at 95°C for 2 min, 57°C for 60 sec, 72°C for 90 sec, and cycles 2–30 at 95°C for 60 sec, 59°C for 60 sec, 72°C for 90 sec, in a final reaction volume of 20 µl.

Nuclear staining, immunofluorescence, and statistical analysis

Day 3.5 and 3.5 + 1 embryos were fixed and stained in DAPI, as previously described (Kalitsis et al. 1998). Embryos cultured on coverslips were washed three times in PBS and fixed in 4% paraformaldehyde/PBS for 15 min, followed by 0.1% Triton X-100/PBS for 10 min. The embryos were then rinsed twice in PBS and stained in DAPI and Vectashield (Vector Laboratories). For immunostaining of the kinetochore using the CREST#6 autoimmune serum, day 3.5 + 2 embryos were treated as described previously (Howman et al. 2000). Images were captured using an Axioplan2 microscope (Zeiss), with a Sensys-cooled CCD camera (Photometrics) and processed with IP Lab software (Scanalytics). Statistical analyses were performed using the Student's *t*-test.

Acknowledgments

We thank S. Gazeas, A. Sylvain, J. Ladhams, and P. Rasaratnam for excellent technical assistance; R. Saffery, J. Craig, and D. Magliano for helpful comments; and G. Kay for the 129/1 and J. Mann for the W9.5 ES cell lines. This work was supported by the National Health and Medical Research Council of Australia. K.H.A.C. is a Principal Research Fellow of the council.

The publication costs of this article were defrayed in part by payment of page charges. This article must therefore be hereby marked "advertisement" in accordance with 18 USC section 1734 solely to indicate this fact.

References

Amon, A. 1999. The spindle checkpoint. *Curr. Opin. Genet. Dev.* **9:** 69–75.

Basu, J., Logarinho, E., Herrmann, S., Bousbaa, H., Li, Z., Chan, G.K., Yen, T.J., Sunkel, C.E., and Goldberg, M.L. 1998. Localization of the *Drosophila* checkpoint control protein Bub3 to the kinetochore requires Bub1 but not Zw10 or Rod. *Chromosoma* **107:** 376–385.

Basu, J., Bousbaa, H., Logarinho, E., Li, Z., Williams, B.C., Lopes, C., Sunkel, C.E., and Goldberg, M.L. 1999. Mutations in the essential spindle checkpoint gene bub1 cause chromosome missegregation and fail to block apoptosis in *Drosophila*. *J. Cell. Biol.* **146:** 13–28.

Brady, D.M. and Hardwick, K.G. 2000. Complex formation between Mad1p, Bub1p and Bub3p is crucial for spindle checkpoint function. *Curr. Biol.* **10:** 675–678.

Cahill, D.P., Lengauer, C., Yu, J., Riggins, G.J., Willson, J.K., Markowitz, S.D., Kinzler, K.W., and Vogelstein, B. 1998. Mutations of mitotic checkpoint genes in human cancers. *Nature* **392:** 300–303.

Chan, G.K., Jablonski, S.A., Sudakin, V., Hittle, J.C., and Yen, T.J. 1999. Human BUBR1 is a mitotic checkpoint kinase that monitors CENP-E functions at kinetochores and binds the cyclosome/APC. *J. Cell. Biol.* **146:** 941–954.

Chen, R.H., Waters, J.C., Salmon, E.D., and Murray, A.W. 1996. Association of spindle assembly checkpoint component XMAD2 with unattached kinetochores. *Science* **274:** 242–246.

Chen, R.H., Shevchenko, A., Mann, M., and Murray, A.W. 1998. Spindle checkpoint protein Xmad1 recruits Xmad2 to unattached kinetochores. *J. Cell. Biol.* **143:** 283–295.

Cutts, S.M., Fowler, K.J., Kile, B.T., Hii, L.L., O'Dowd, R.A., Hudson, D.F., Saffery, R., Kalitsis, P., Earle, E., and Choo, K.H.A. 1999. Defective chromosome segregation, microtubule bundling and nuclear bridging in inner centromere protein gene (Incenp)-disrupted mice. *Hum. Mol. Genet.* **8:** 1145–1155.

Dobles, M., Liberal, V., Scott, M.L., Benezra, R., and Sorger, P.K. 2000. Chromosome missegregation and apoptosis in mice lacking the mitotic checkpoint protein Mad2. *Cell* **101:** 635–645.

du Sart, D., Cancilla, M.R., Earle, E., Mao, J., Saffery, R., Tainton, K.M., Kalitsis, P., Martyn, J., Barry, A.E., and Choo, K.H.A. 1997. A functional neo-centromere formed through activation of a latent human centromere and consisting of non-alpha-satellite DNA. *Nature Genet.* **16:** 144–153.

Efimov, V.P. and Morris, N.R. 1998. A screen for dynein synthetic lethals in *Aspergillus nidulans* identifies spindle assembly checkpoint genes and other genes involved in mitosis. *Genetics* **149:** 101–116.

Farr, K.A. and Hoyt, M.A. 1998. Bub1p kinase activates the *Saccharomyces cerevisiae* spindle assembly checkpoint. *Mol. Cell. Biol.* **18:** 2738–2747.

Gorbsky, G.J., Chen, R.H., and Murray, A.W. 1998. Microinjection of antibody to Mad2 protein into mammalian cells in mitosis induces premature anaphase. *J. Cell. Biol.* **141:** 1193–1205.

Howman, E.V., Fowler, K.J., Newson, A.J., Redward, S., MacDonald, A.C., Kalitsis, P., and Choo, K.H.A. 2000. Early disruption of centromeric chromatin organization in centromere protein A (Cenpa) null mice. *Proc. Natl. Acad. Sci. USA* **97:** 1148–1153.

Hoyt, M.A., Totis, L., and Roberts, B.T. 1991. *S. cerevisiae* genes required for cell cycle arrest in response to loss of microtubule function. *Cell* **66:** 507–17.

Kalitsis, P., Fowler, K.J., Earle, E., Hill, J., and Choo, K.H.A. 1998. Targeted disruption of mouse centromere protein C gene leads to mitotic disarray and early embryo death. *Proc. Natl. Acad. Sci. USA* **95:** 1136–1141.

Li, R. and Murray, A.W. 1991. Feedback control of mitosis in budding yeast. *Cell* **66:** 519–531.

Li, Y. and Benezra, R. 1996. Identification of a human mitotic checkpoint gene: hsMAD2. *Science* **274:** 246–248.

Martinez-Exposito, M.J., Kaplan, K.B., Copeland, J., and Sorger, P.K. 1999. Retention of the BUB3 checkpoint protein on lagging chromosomes. *Proc. Natl. Acad. Sci. USA* **96:** 8493–8498.

Neer, E.J., Schmidt, C.J., Nambudripad, R., and Smith, T.F. 1994. The ancient regulatory-protein family of WD-repeat proteins. *Nature* **371:** 297–300.

Roberts, B.T., Farr, K.A., and Hoyt, M.A. 1994. The *Saccharomyces cerevisiae* checkpoint gene BUB1 encodes a novel protein kinase. *Mol. Cell. Biol.* **14:** 8282–8291.

Skibbens, R.V. and Hieter, P. 1998. Kinetochores and the checkpoint mechanism that monitors for defects in the chromosome segregation machinery. *Annu. Rev. Genet.* **32:** 307–337.

Taylor, S.S. and McKeon, F. 1997. Kinetochore localization of murine Bub1 is required for normal mitotic timing and checkpoint response to spindle damage. *Cell* **89:** 727–735.

Taylor, S.S., Ha, E., and McKeon, F. 1998. The human homologue of Bub3 is required for kinetochore localization of Bub1 and a Mad3/Bub1-related protein kinase. *J. Cell. Biol.* **142:** 1–11.

Waters, J.C., Chen, R.H., Murray, A.W., and Salmon, E.D. 1998. Localization of Mad2 to kinetochores depends on microtubule attachment, not tension. *J. Cell. Biol.* **141:** 1181–1191.

Weiss, E. and Winey, M. 1996. The *Saccharomyces cerevisiae* spindle pole body duplication gene MPS1 is part of a mitotic checkpoint. *J. Cell. Biol.* **132:** 111–123.Amon, A. 1999. The spindle checkpoint. *Curr. Opin. Genet. Dev.* **9:** 69–75.

PUBLICATION 12

A.G. UREN, L. WONG, M. PAKUSCH, **K.J. FOWLER**, F.J. BURROWS,
D.L. VAUX AND K.H.A. CHOO

(2000)

SURVIVIN AND THE INNER CENTROMERE PROTEIN INCENP SHOW CELL-CYCLE LOCALIZATION AND GENE KNOCKOUT PHENOTYPE.

CURRENT BIOLOGY, 10: 1319-1328

Survivin and the inner centromere protein INCENP show similar cell-cycle localization and gene knockout phenotype

Anthony G. Uren*†, Lee Wong†‡, Miha Pakusch*, Kerry J. Fowler‡, Francis J. Burrows§, David L. Vaux* and K.H. Andy Choo‡

Background: Survivin is a mammalian protein that carries a motif typical of the inhibitor of apoptosis (IAP) proteins, first identified in baculoviruses. Although baculoviral IAP proteins regulate cell death, the yeast Survivin homolog Bir1 is involved in cell division. To determine the function of Survivin in mammals, we analyzed the pattern of localization of Survivin protein during the cell cycle, and deleted its gene by homologous recombination in mice.

Results: In human cells, Survivin appeared first on centromeres bound to a novel para-polar axis during prophase/metaphase, relocated to the spindle midzone during anaphase/telophase, and disappeared at the end of telophase. In the mouse, Survivin was required for mitosis during development. Null embryos showed disrupted microtubule formation, became polyploid, and failed to survive beyond 4.5 days post coitum. This phenotype, and the cell-cycle localization of Survivin, resembled closely those of INCENP. Because the yeast homolog of INCENP, Sli15, regulates the Aurora kinase homolog Ipl1p, and the yeast Survivin homolog Bir1 binds to Ndc10p, a substrate of Ipl1p, yeast Survivin, INCENP and Aurora homologs function in concert during cell division.

Conclusions: In vertebrates, Survivin and INCENP have related roles in mitosis, coordinating events such as microtubule organization, cleavage-furrow formation and cytokinesis. Like their yeast homologs Bir1 and Sli15, they may also act together with the Aurora kinase.

Addresses: *The Walter and Eliza Hall Institute of Medical Research, Post Office Royal Melbourne Hospital, Victoria 3050, Australia. ‡The Murdoch Childrens Research Institute, Royal Childrens Hospital, Flemington Road, Parkville, Victoria, 3052, Australia. §Idun Pharmaceuticals, 11085 North Torrey Pines Road, La Jolla, California 92037, USA.

Correspondence: David L. Vaux
E-mail: vaux@wehi.edu.au

†A.G.U. and L.W. contributed equally to this work.

Received: **21 August 2000**
Revised: **7 September 2000**
Accepted: **7 September 2000**

Published: **10 October 2000**

Current Biology 2000, 10:1319–1328

0960-9822/00/$ – see front matter

Background

Inhibitor of apoptosis (IAP) proteins were first identified as baculoviral products that could inhibit the defensive apoptotic response of infected insect cells. Subsequently, a number of cellular IAP homologs were found in diverse organisms including vertebrates, insects, nematodes and yeasts. All of these proteins bear one to three zinc-binding motifs termed baculoviral IAP repeats (BIRs) [1–3]. Biochemical and genetic evidence indicates that some IAPs—such as MIHA/XIAP/hILP, MIHB/c-IAP-1/hIAP2, MIHC/cIAP-2/hIAP1 [4–7] and *Drosophila* DIAP1 [8,9]—are able to inhibit caspase-mediated apoptosis directly or indirectly (reviewed in [10]). In contrast, IAPs from *Caenorhabditis elegans* and the yeasts *Schizosaccharomyces pombe* and *Saccharomyces cerevisiae* do not appear to be caspase inhibitors, but seem to function during cell division. For example, *C. elegans* zygotes lacking BIR-1 fail to undergo cytokinesis, *S. pombe bir1* mutants have defects in spindle elongation, and Bir1p from *S. cerevisiae* associates with kinetochore proteins [11–15].

The kinetochore is a DNA–protein complex that assembles on the centromere and is required for attachment of microtubules during mitosis. Some mammalian centromere-interacting proteins (such as CENP-A, CENP-B and CENP-C) associate constitutively, whereas others (such as CENP-E, CENP-F and the inner centromere protein INCENP), collectively known as chromosome passenger proteins, localize transiently to the centromere during specific stages of the cell cycle (reviewed in [16]). As the cell cycle progresses into metaphase, INCENP becomes concentrated at centromeres. During the metaphase–anaphase transition, INCENP remains confined to the equator while the sister chromatids migrate to the poles. During telophase, it is located in the midbodies at the intercellular bridge, and is degraded after cytokinesis [17,18]. The timing of expression and distribution of INCENP resembles that of Aurora1, a member of the Aurora/Ipl1p family of serine threonine kinases ([19], reviewed in [20]). Furthermore, overexpression of kinase-inactivated Aurora1 disrupts cleavage-furrow formation, resulting in a failure of cytokinesis similar to that caused by deletion or expression of a dominant-negative INCENP [21–23]. Therefore, INCENP and Aurora1 may have related roles during mitosis.

Survivin is a mammalian protein that has a single BIR [24]. Structurally, it resembles more closely the BIR-containing proteins from yeasts and *C. elegans* [2] than it does the IAPs that control apoptosis. Survivin expression is regulated during the cell cycle [25,26], and inhibition of

Survivin has been associated with cell-cycle defects [27]. Because the BIR-containing proteins from *S. pombe*, *S. cerevisiae* and *C. elegans* all have roles in cell division [11,12,15], Survivin may have a similar function. Here, we raised antibodies against Survivin and analyzed its pattern of expression during the cell cycle. To determine the requirement for Survivin in normal cells, we deleted its gene by homologous recombination in mice. The phenotype of the *survivin* null mouse embryos, and the pattern of Survivin staining, are consistent with a role as a chromosome passenger protein that functions during mitosis.

Results

Localization of Survivin during the cell cycle

We determined the distribution of Survivin during the cell cycle using cultured HeLa cells. Initial immunofluorescence staining using the anti-Survivin antibody TO65 revealed strong punctate signals on condensed chromatin that were suggestive of specific association of Survivin with chromosomal structures (data not shown). This prompted us to compare the localization of Survivin with that of the centromeric α-satellite DNA-binding protein CENP-B, using the monoclonal antibody 2D-7. As expected for a constitutive centromere protein, CENP-B was detected as discrete spots on centromeres throughout the cell cycle (Figure 1a). No Survivin was detectable in the interphase cells. A low level was detected at early prophase, during which no specific localization to the centromere was apparent. In late prophase, nuclear staining became intense, with foci of Survivin now colocalizing with CENP-B. As the cells progressed into metaphase, Survivin became prominently concentrated on centromeres, as shown by strong colocalization with CENP-B. At anaphase, while CENP-B moved with the separating sister chromatin masses to the poles, Survivin remained at the midzone where the metaphase plate once was. During telophase, Survivin was found on the midbody between the daughter cells, and after telophase it was degraded.

In view of previous studies indicating the close association of Survivin with the microtubules [26,27], we compared the cell-cycle distribution profiles of Survivin and microtubules, using a monoclonal anti-β-tubulin antibody (Figure 1b). No significant colocalization was observed between interphase and metaphase. During early anaphase, some Survivin began to relocate onto the microtubules at the spindle midzone. By late anaphase and telophase, Survivin colocalized with the concentrated intercellular microtubule bundles that formed the midbody. This distribution profile is characteristic of the chromosome passenger class of proteins.

We were also interested to know whether disrupting the integrity of microtubules had any effect on the localization

Figure 1

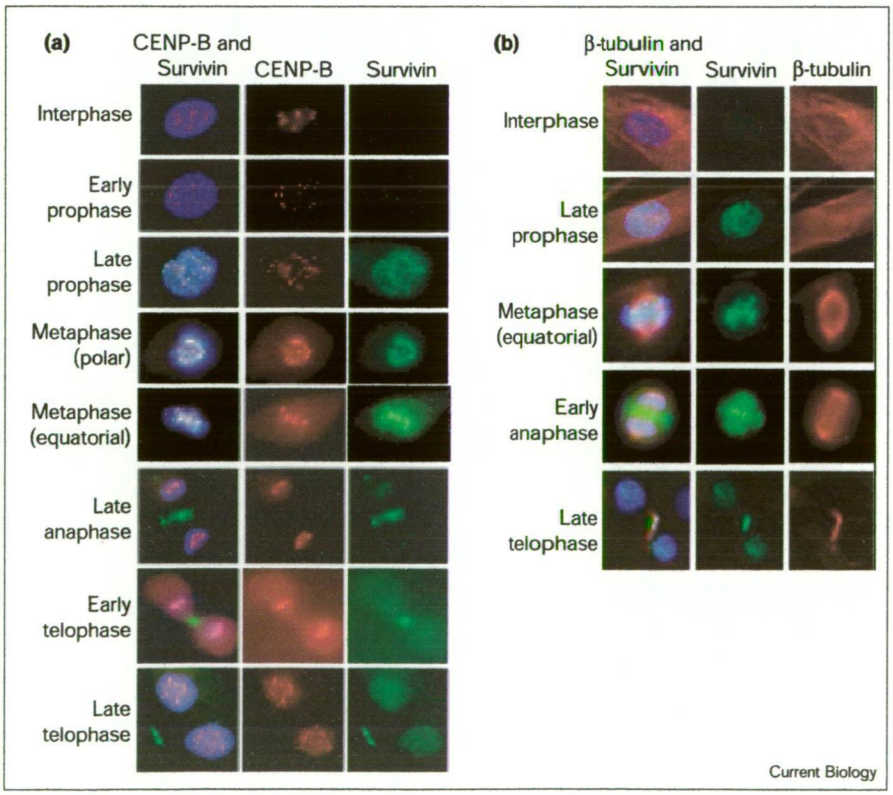

Cell-cycle distribution of Survivin, CENP-B and β-tubulin. **(a)** Simultaneous immunofluorescence staining for Survivin (green) and CENP-B (red) in HeLa cells grown on coverslips and analyzed at different cell-cycle stages. Two different views of metaphase cells are shown, one from the pole (presenting a 'rosette' configuration), the other from the side (showing chromosomal congression on the equatorial plate). Left panels, combined CENP-B and Survivin immunofluorescence; the chromatin was stained with 4,6-diamidino-2-phenylindole (DAPI, blue). Middle and right panels, CENP-B and Survivin staining, respectively. **(b)** Simultaneous immunofluorescence staining for Survivin (green) and β-tubulin (red) during different cell-cycle stages of HeLa cells grown on coverslips.

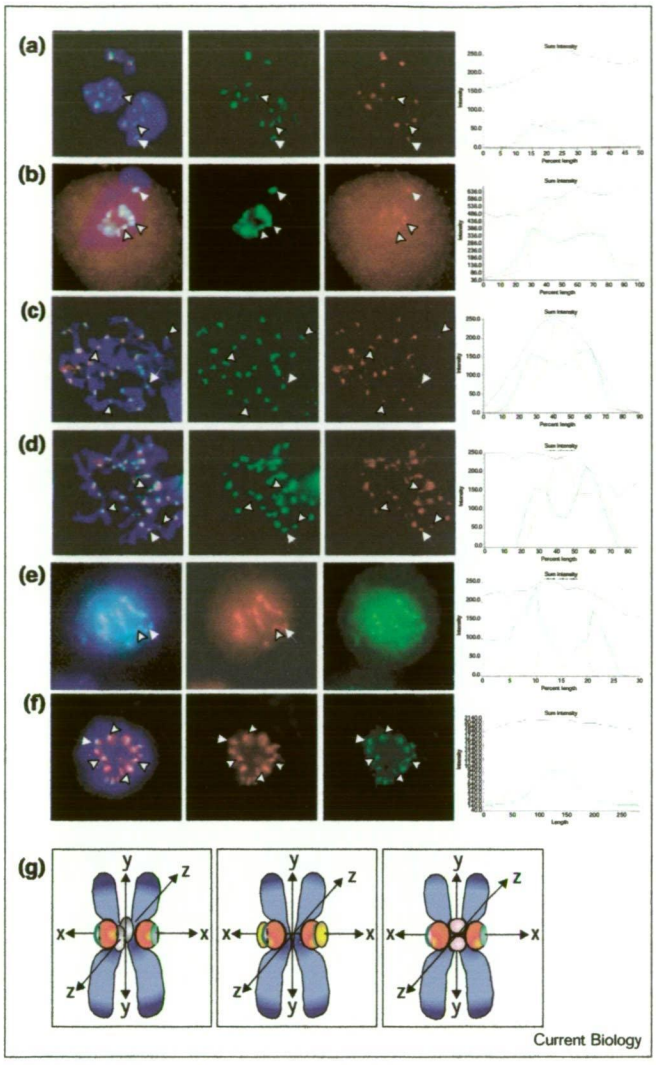

Figure 2

Immunofluorescence analysis of Survivin and various centromere-binding proteins. **(a–d)** Dual-color immunofluorescence analysis using CREST#6 (green) and anti-Survivin antibody (red). Metaphase chromosomes were prepared from HeLa cells treated with (a) nocodazole, (b,d) taxol, or (c) colcemid. The cells in (a,b) were cultured on coverslips directly, whereas the cells in (c,d) were spun onto a slide by cytocentrifugation (which gave better spreading of metaphases). First column, combined immunofluorescence images in which the chromatin was stained with DAPI (blue). The green and red signals are shown individually in the second and third columns, respectively. Note that CREST#6 and Survivin both bound to the centromere to give doublet signals. Nevertheless, whereas the paired signals for CREST#6 were generally similar in intensity when viewed on the same focal plane, the Survivin doublet signals (some examples shown by arrowheads) were apparent only when viewed on different focal planes (not shown). Fourth column, multi-color scanning of the centromere (arrowed) along the trans-polar axis. 'Length' indicates position along the trans-polar axis, and 'intensity' indicates the fluorescence signal. Both are in arbitrary units. The colors of the different curves correspond to those of the images shown in the first three columns. **(e,f)** Dual-color immunofluorescence analysis using (e) CREST#6 (red) and anti-CENP-E antibody (green), or (f) CREST#6 (red) and anti-INCENP antibody (green). Metaphase chromosomes were prepared from HeLa cells grown on a coverslip in normal culture media. The arrows and arrowheads point to examples of centromeres showing trans-polar binding of the CENP-E signal in (e), or para-polar association of the INCENP signal in (f). The examples indicated by the arrows were used to derive the multi-color scanning profile shown in the fourth column. **(g)** Models for the different subregional topographic distribution of centromere proteins along three possible axes: the x- or trans-polar axis, which connects the midpoints of the two opposite-facing kinetochore discs; the y- or longitudinal axis, which runs parallel to the long axis of the chromosome, between the kinetochore discs; and the z- or para-polar axis, which bisects between the kinetochore discs perpendicular to both the x and y axes. Left panel, alignment of CREST#6 antigen doublet signal at the kinetochore discs (green, CENP-A binding) and inner centromere heterochromatin (red, CENP-B binding) along the trans-polar (x) axis, and the Survivin and INCENP doublet signals (gray) at a midpoint between the sister chromatids along the para-polar (z) axis. Sister chromatids are shown in blue. Middle panel, as in the left panel except yellow signals represent binding of CENP-E and CENP-F to the outer edges of the kinetochore discs or corona regions along a common trans-polar (x) axis. Right panel, previously described binding of INCENP (pink) along the y axis [41] or throughout the heterochromatic region (red) beneath the kinetochore discs (green) along the x axis [42,43] (see Discussion).

of Survivin at the centromere. For this analysis, HeLa cells were cultured in the presence of taxol (a microtubule-stabilizing agent), or nocodazole or colcemid (microtubule-destabilizing agents). We also compared cells that had been grown directly on coverslips with cells that were spread onto slides by cytocentrifugation, a procedure that disrupts microtubules mechanically. In each case, strong colocalization of Survivin with the CREST#6 antibodies (anti-CENP-A and anti-CENP-B antibodies) on metaphase chromosomes was observed (Figure 2a–d). Therefore, binding of Survivin to the centromere did not depend on the integrity of the microtubules.

Survivin binds to the centromere on a different axis to the kinetochore axis

Earlier studies have described the binding patterns of more than 20 different proteins on the metaphase centromere (for example, [28,29]). Although the distance between the paired signals for these proteins on the two chromatids varies slightly depending on whether binding is at the inner centromere region, on the kinetochore, or at the outer kinetochore region, the evenness of the doublet signal intensity indicates that antigen binding occurs along the same axis (designated as the trans-polar or x axis) joining the two kinetochore discs. This pattern was typical for staining with the CREST#6 antiserum, shown in Figure 2a–f.

Even though Survivin also bound to the metaphase centromeres to give doublet signals, the two Survivin spots were not in the same focal plane. Furthermore, Survivin was generally present at the midpoint of the CREST#6 doublet signals, as evident from direct immunofluorescence visualization and from multi-color electronic scanning of centromere staining (Figure 2a–d). Survivin was located along an axis (denoted here as the para-polar or z axis) that perpendicularly bisects both the trans-polar x axis

and the longitudinal y axis that runs parallel to the long axis of the chromosome, between the kinetochore discs (see Figure 2g). Similar results were obtained in cells that had not been drug-treated, and in cells grown directly on coverslips or centrifuged onto slides, suggesting that the observed para-polar alignment was not an artifact of microtubule inhibition or cytocentrifugation (Figure 2 and data not shown). For comparison, we examined the staining patterns for three other chromosomal passenger proteins (CENP-E, CENP-F and INCENP). The results indicated that CENP-E bound typically as a doublet of even intensity along the same trans-polar axis as that for the CREST#6 signals, although the distance between the doublet spots for CENP-E was noticeably greater than that for CREST#6, suggesting that CENP-E binding occurred external to the regions occupied by CENP-A and CENP-B (Figure 2e). The results for CENP-F (previously shown to interact with CENP-E [30]) were identical to those for CENP-E (data not shown), whereas INCENP binding was detected along the same para-polar axis as that seen for Survivin (Figure 2f). The relative subregional centromeric distribution profiles for CENP-A/CENP-B, Survivin, INCENP, CENP-E and CENP-F are illustrated in Figure 2g.

Cloning and characterization of the mouse *survivin* locus and deletion of the gene

To determine the requirement for Survivin in mouse embryos, we deleted the gene by homologous recombination. The human and mouse *survivin* transcripts encode proteins of 142 and 140 amino acids, respectively [24,25]. We obtained both human and mouse *survivin* cDNA clones from the IMAGE consortium [31] and sequenced them (accession numbers AF077349 and AF077350). The human *survivin* gene has previously been reported to have significant similarity to the EPR-1 cDNA in its antisense orientation, suggesting a common origin for both loci [32,33]. There is, however, no similarity to the EPR-1 open reading frame or any other protein in the opposite orientation of the mouse *survivin* transcript. Thus, it appeared that deletion of the mouse *survivin* locus should not affect expression of EPR-1, if indeed it exists [34]. A mouse *survivin* cDNA was used to screen a mouse genomic library. Multiple independent lambda phage clones were isolated and mapped by restriction enzyme digestion, and 9 kb of the longest clone was sequenced, spanning the region encoding the whole of the mouse *survivin* transcript (accession number AF077351; Figure 3).

Figure 3

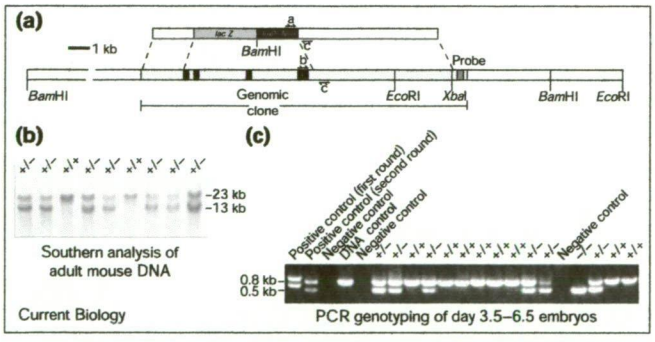

Deletion of the *survivin* gene by homologous recombination. **(a)** The gene targeting construct replaced a genomic fragment bearing all four exons (labeled 1–4) of *survivin* with a cassette encoding β-galactosidase in-frame after the ATG. A probe 3′ to the region recombined was used to type mutated embryonic stem (ES) cells by Southern blot analysis. **(b)** The same probe was hybridized to *Bam*HI-digested tail DNA from adult mice and detected a 23 kb wild-type allele and a 13 kb targeted allele. **(c)** Day 3.5–6.5 embryos from heterozygous intercrosses were typed by PCR using nested primers (denoted a, b and c), which generated a 0.8 kb wild-type product and a 0.5 kb targeted product. The positive controls were tail DNA from heterozygous and wild-type mice, and the negative controls contained no DNA.

A vector for targeted disruption of *survivin* was designed that replaced all sequences except those encoding the first four amino acids of the *survivin* open reading frame with the *lacZ* gene. The 5′ and 3′ arms of the vector were 2 and 6.5 kb in length, respectively, and the selectable marker was a neomycin cassette flanked by *loxP* sites. This construct was electroporated into the C57Bl/6-derived Bruce 4 ES cell line. Clones with homologous integrations of the vector were identified by Southern hybridization with a probe external to the vector (Figure 3) and used to generate chimeras that passed the mutation through the germ line. Of the first 39 pups born from mating of heterozygous parents, Southern analysis of tail DNA revealed 13 were wild type and 26 were heterozygous. No homozygous *survivin* mutant mice were found, or have been identified to date, demonstrating that loss of the *survivin* gene caused embryonic lethality. The ratio of wild-type to heterozygous mice indicated that loss of one copy of the *survivin* gene was unlikely to cause developmental defects.

Developmental lethality of *survivin* null embryos

Embryos from heterozygous intercrosses were flushed on day 2.5 post coitum and their development observed in culture. Of a total of 96 embryos collected, 73 showed normal development, whereas 23 developed abnormally. When the embryos were collected for genotyping by PCR on day 6.5, a complete correlation between embryos showing a deteriorating phenotype and the *survivin*$^{-/-}$ genotype was observed, indicating that 24% of the total embryos were homozygous mutants. This suggests that there were no significant losses of the *survivin*$^{-/-}$ embryos before day 2.5.

The onset of morphological deterioration was variable amongst the *survivin*$^{-/-}$ embryos. In most of the embryos, degeneration was apparent at day 2.5 (Figure 4b). Of the remaining *survivin*$^{-/-}$ embryos, the morphology was indistinguishable from the *survivin*$^{+/+}$ and *survivin*$^{+/-}$ embryos up to day 4.5, during which blastocysts containing an inner

Figure 4

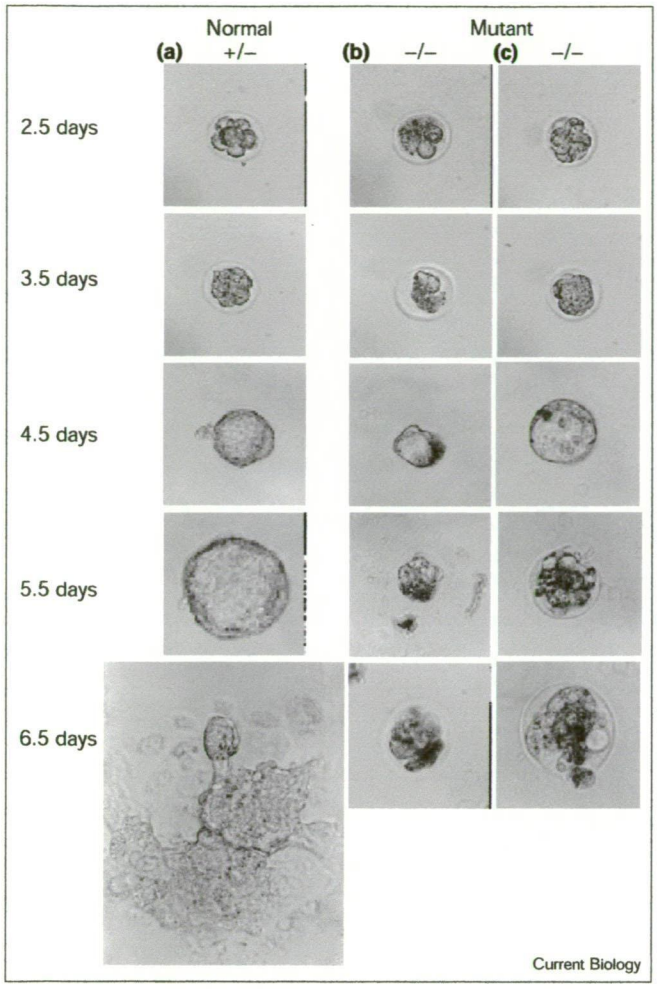

Morphology of normal and *survivin* null embryos. Embryos were collected at day 2.5 post coitum and cultured *in vitro* up to day 6.5. **(a)** The normal embryo, subsequently confirmed by PCR genotyping to be *survivin*$^{+/-}$, developed an inner cell mass, a blastocoel cavity, and hatched out of the zona pellucida by day 4.5, forming an expanded inner cell mass and surrounding trophoblast cells by day 6.5. The *survivin*$^{-/-}$ embryo in **(b)** showed deterioration of a number of the blastomeres at day 2.5, but managed to continue developing further, albeit aberrantly. The *survivin*$^{-/-}$ embryo in **(c)** showed a seemingly healthy morphology up till 4.5 days. By day 5.5, both *survivin*$^{-/-}$ embryos showed gross cellular degeneration, absence of distinct inner cell mass, blastocoel cavity, or trophoblasts, and the formation of giant cells. Magnification ×200, phase contrast microscopy.

cell mass and blastocoel cavity were formed (Figure 4c). However, by days 5.5 and 6.5, all *survivin*$^{-/-}$ embryos were grossly abnormal and showed deteriorated cell masses and giant cells, whereas the *survivin*$^{+/+}$ and *survivin*$^{+/-}$ embryos had gone on to form a compact inner cell mass and spreading trophoblast cells. Furthermore, the *survivin*$^{-/-}$ embryos never hatched out of their zona pellucida over the study period, whereas hatching occurred around day 4.5 for all of the wild-type and heterozygous embryos.

Table 1

Number of nuclei.

Days	+/+ or +/–	–/–*	*p* value
2.5	11.2 ± 3.2 (*n* = 11)	8.0 ± 2.4 (*n* = 7)	0.051
3.5	40.4 ± 3.3 (*n* = 18)	19.6 ± 6.1 (*n* = 9)	< 0.001
4.5	76.2 ± 9.7 (*n* = 6)	23.25 ± 9.9 (*n* = 8)	< 0.001
5.5	232.5 ± 22.3 (*n* = 6)	13.4 ± 2.7 (*n* = 9)	< 0.001

The number of nuclei were determined in embryos from heterozygous intercrosses at day 2.5 of development *in utero* or following culture (days 3.5–5.5); *n*, number of embryos analyzed. *Micronuclei were not included.

Formation of giant nuclei in *survivin* null embryos

Day 2.5 *post coitum* embryos from heterozygous intercrosses were collected and either analyzed immediately or cultured for up to 3 days before fixing on slides and staining with DAPI so that the number of nuclei and their morphology could be ascertained. At day 2.5, the number of nuclei in the *survivin*$^{-/-}$ embryos was marginally fewer than those in the *survivin*$^{+/+}$ or *survivin*$^{+/-}$ embryos (Table 1). Nuclear morphology appeared normal in some of the *survivin*$^{-/-}$ embryos, but in most the nuclei were irregular and varied in size (Figure 5). At day 3.5, the *survivin*$^{-/-}$ embryos contained only about half as many nuclei as the *survivin*$^{+/-}$ and *survivin*$^{+/+}$ embryos, and micronuclei, irregular nuclei, and some large nuclei were apparent. Day 4.5 *survivin*$^{-/-}$ embryos contained on average less than a third of the number of nuclei found in the corresponding *survivin*$^{+/+}$ or *survivin*$^{+/-}$ embryos. Micronuclei and irregular macronuclei with bridging or lobular morphology indicative of incomplete nuclear fission occurred. By day 5.5, an average of only 13 nuclei were present in each *survivin*$^{-/-}$ embryo, compared with more than 200 in the *survivin*$^{+/+}$ or *survivin*$^{+/-}$ embryos. Most of these nuclei were much bigger than normal, and had highly irregular morphology, with pronounced bridging and blebbing.

Survivin deficiency leads to altered microtubule organization

Embryos at different stages of development were stained with anti-β-tubulin antibody to visualize the integrity of the microtubules (Figure 6). Normal embryos showed the expected mitotic spindle structures, midbodies and extensive network of cellular microtubules at all stages. From day 2.5 onwards, *survivin*$^{-/-}$ embryos consistently showed very little or no detectable mitotic spindle organization and midbodies. As the *survivin*$^{-/-}$ phenotype developed, an increasing number of binucleated and multinucleated cells, as well as cells with grossly enlarged and morphologically irregular nuclei were observed. The extensive and fibrous network of tubulin staining seen in normal embryos was progressively replaced by a more diffuse and patchy staining, with an increasing propensity for the tubulin molecules to bundle into highly concentrated strands in the later stages of development.

Figure 5

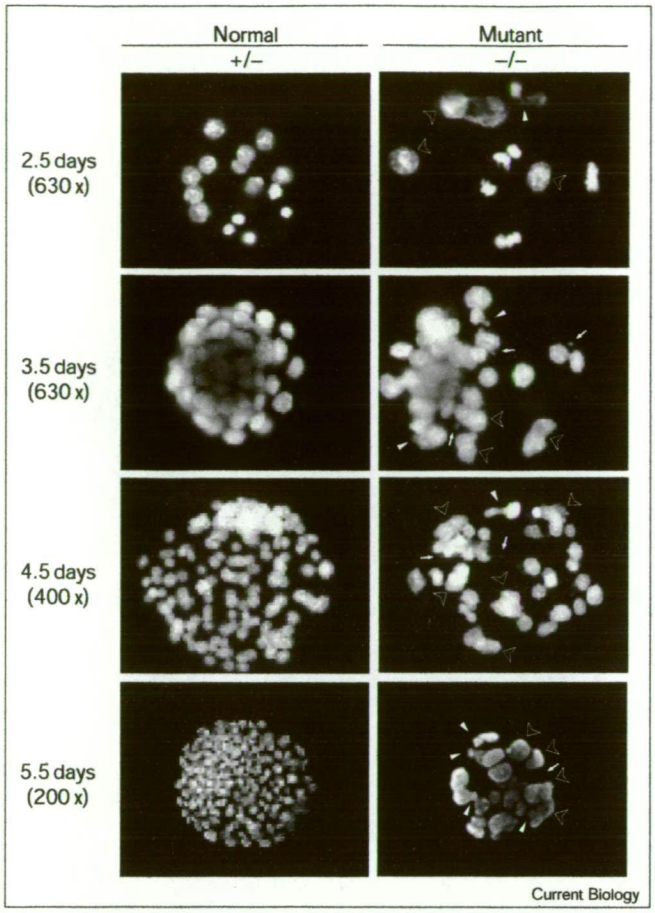

Nuclear morphology of DAPI-stained embryos cultured at day 2.5 post coitum. Examples of micronuclei (arrows), macronuclei (open arrowheads) and nuclei showing bridging or blebbing (filled arrowheads) are shown. The numbers in brackets indicate the different magnifications used.

Figure 6

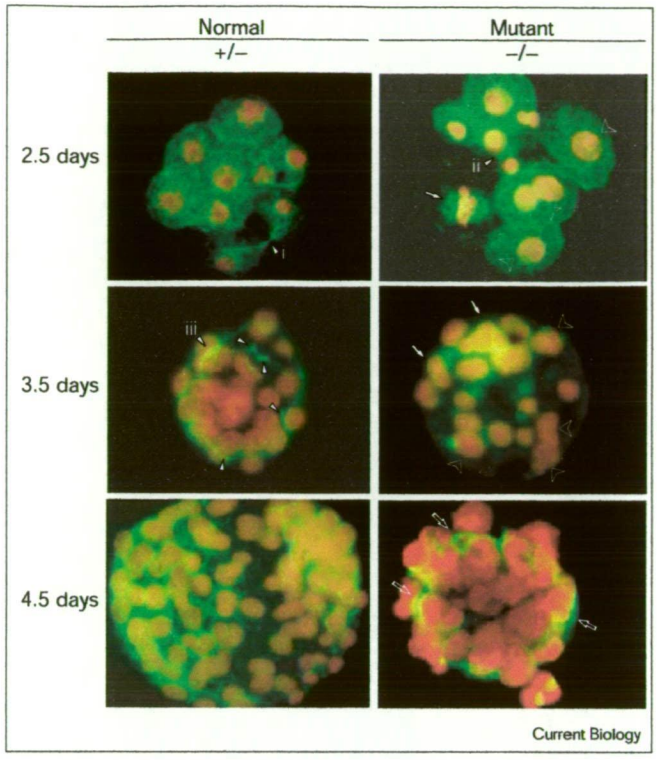

Immunofluorescence analysis of tubulin localization in embryos at different developmental stages. In the normal embryo at day 2.5, a dividing cell (denoted i) is seen at the telophase stage, showing a well-organized midbody, whereas no discernible midbodies were detected in the *survivin*$^{-/-}$ embryos at day 2.5 (denoted ii). At day 3.5, the normal dividing cell (denoted by iii) shows a proper microtubule spindle, but this was not seen in *survivin*$^{-/-}$ embryos at day 3.5. Examples are shown of midbodies in the day 2.5 and 3.5 normal embryos (solid arrowheads; not shown for the day 4.5 mutant embryo as most of the nuclei were large), and binucleated or multinucleated cells (solid arrow), and highly bundled microtubule spindle cords in the day 4.5 mutant embryo (open arrows). Magnification ×630.

Discussion

Survivin is a new member of the family of centromere-binding passenger proteins

In agreement with earlier studies showing expression of this gene in the G2/M phase of the cell cycle [25,26], immunofluorescence analysis showed that Survivin is undetectable at interphase but first appears in the nucleus in early prophase. Maximal expression was seen in late prophase, during which the protein was present throughout the nucleus. Binding to the centromere first occurred at this stage and strengthened into metaphase, with a concomitant reduction in the intensity of the nuclear staining, suggesting a relocation of Survivin onto the maturing centromere. As the sister chromatids moved apart during anaphase, Survivin dissociated from the centromere and tethered at the spindle midzone, where it subsequently formed a midbody to be degraded at telophase. Thus, the cell-cycle distribution pattern for Survivin corresponded to those of the chromosome passenger proteins (reviewed in [16,35]). Previous studies have suggested that the distribution of Survivin is closely associated with microtubules [26,36]. Treatment of cells with three different microtubule-inhibiting agents (taxol, nocodazole and colcemid), or mechanical disruption of microtubules by cytocentrifugation, had no major effect on the centromere localization of Survivin. This observation suggests that the cell-cycle distribution of Survivin, in particular its relocation to the centromere during metaphase, is not dependent on the integrity of the mitotic microtubules.

Survivin and INCENP bind to the centromere on a novel para-polar axis

Immunofluorescence showed the two constitutive centromere proteins CENP-A and CENP-B, as well as two of the chromosome passenger proteins CENP-E and CENP-F,

to bind along the trans-polar axis containing the kinetochore plates. Along this axis, CENP-E and CENP-F bound external to the positions occupied by CENP-A and CENP-B. These results are consistent with those of previous studies demonstrating localization of CENP-A, CENP-B, and CENP-E/CENP-F at the kinetochore domain, inner centromere domain, and fibrous corona domain, respectively [37–40].

In chicken cells INCENP has been localized either as a doublet between the sister chromatids on an axis parallel to the longitudinal axis of the chromosome (y-axis; Figure 2g) [41], or throughout the heterochromatin beneath the kinetochore (Figure 2g) [42,43]. In contrast, in human HeLa cells we found both INCENP and Survivin bound along a para-polar z-axis that perpendicularly bisects the longitudinal y-axis and the trans-polar x-axis. The reason for the discrepancy is unclear, but could be related to differences between vertebrate classes, or the sensitivity and resolution of the techniques used.

The pattern of localization we observed suggests that the chromosome passenger class of centromere proteins can be subdivided into two subgroups depending on whether they reside along the trans-polar axis or the para-polar axis. The trans-polar orientation would allow the organization of the structural proteins (and their interacting DNA) into configurations (the kinetochore discs) such that their active faces will point toward the spindle poles to provide opposite attachment sites for microtubules. This orientation would also facilitate the functioning of proteins, such as the molecular motor CENP-E [44,45], whose activity may depend on direct, end-on interactions with the kinetochore-associated microtubules to effect chromosome movement [46]. The para-polar orientation would favor roles such as sister chromatid cohesion, side-on centromere interaction with microtubules, or provides a depot to facilitate the relocation of proteins onto microtubules for downstream functions, such as regulation of microtubule activity and cell cleavage.

Survivin disruption results in microtubule bundling and impaired cytokinesis resembling that of INCENP null mice

The onset of an abnormal phenotype with *survivin* gene disruption varied slightly amongst the embryos, with some embryos exhibiting normal morphology until day 4.5 *post coitum*, while others showed deterioration as early as day 2.5. Irrespective of the time of onset, all null embryos became grossly affected by day 5.5. Early signs of embryo deterioration included degenerating blastomeres, micronuclei formation, variable nuclear sizes, irregular nuclear morphology and multinucleation. These aberrations were characteristic of an underlying defect in mitosis. As the phenotype progressed, cells ceased to complete mitosis, with the decreasing number of normal cells rapidly replaced by a small number of giant cells with large and morphologically unusual nuclei. Tubulin staining revealed the absence of normal mitotic spindle structures and intercellular midbodies, with reduced microtubule networks around the cells, and bundling of microtubules. Thus, the observed phenotype was very similar to that previously described for the INCENP null mouse embryos [22]. In both cases, the phenotype was consistent with a defect affecting microtubule organization and/or cytokinesis.

Figure 7

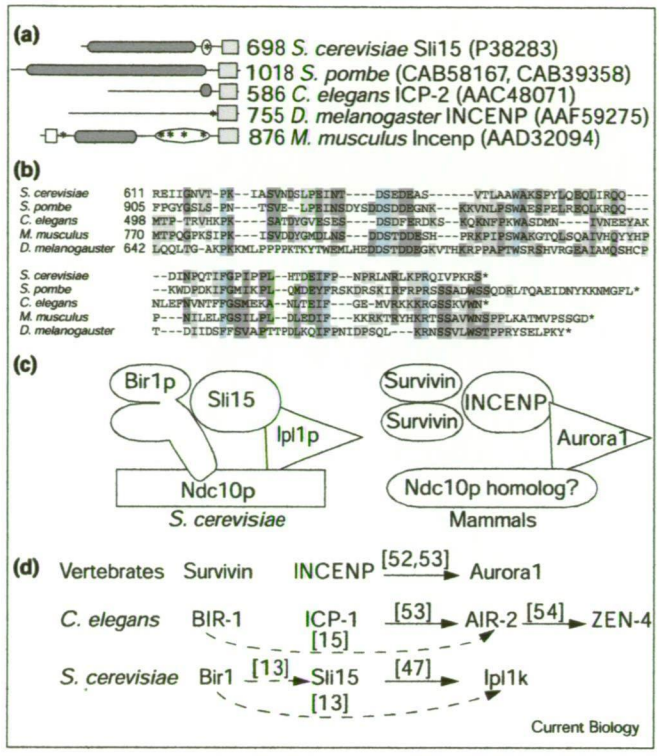

Like Survivin and Bir1, INCENP and Sli15 appear to be homologs with conserved functions. **(a)** Proteins bearing an INCENP box (light gray box) can be found in organisms ranging from yeasts to vertebrates. Asterisks, putative nuclear localization signals; dark gray ovals, regions resembling neurofilaments; white box, a region of INCENP shared by vertebrate homologs and required for centromere targeting [23]; white ovals, predicted coiled-coil domains of INCENP and Sli15. The respective sequence database accession numbers are indicated in parentheses. **(b)** Comparison of INCENP box sequences, with universally conserved residues highlighted in blue and less well-conserved residues in shades of gray. **(c)** Relationship of a BIR-containing protein (Bir1p), INCENP protein (Sli15) and Aurora homolog (Ipl1p) to the centromere-binding protein Ndc10p in *S. cerevisiae* is shown on the left. Bir1p binds to Ndc10p through its carboxy-terminal half, rather than through its BIRs, which are in the amino-terminal region. Hypothetical relationship of the corresponding homologous mammalian proteins (Survivin, INCENP and Aurora1) is shown on the right. **(d)** Survivin, INCENP and Aurora1 and their homologs have been observed to interact with each other directly or indirectly in a hierarchy that often determines their localization. Arrows with reference numbers indicate interactions that have been shown to be direct (solid arrows) or may be indirect (dashed arrows).

Relationship between Survivin, INCENP, Aurora kinase and Ndc10p

A number of observations suggest that Survivin and INCENP may have related roles in mitotic cell division. Both are members of the chromosome passenger class of proteins with very similar cell-cycle expression, distribution pattern and gene knockout phenotype ([22,42] and this study). On metaphase chromosomes, Survivin and INCENP both bind to the para-polar axis of the centromere, as distinct from binding along the trans-polar axis that typifies most of the other centromere proteins. Furthermore, the functions of these proteins appear to be highly conserved, because yeasts have homologs of both Survivin [2] and INCENP (Figure 7a,b) that are also involved in chromosome segregation. Mutation of Bir1p, the closest homolog of Survivin in *S. cerevisiae*, causes a chromosome-loss phenotype [13] and, although homologs of INCENP have not yet been described in invertebrates, proteins that share a similar carboxy-terminal motif to that of INCENP, here dubbed the 'INCENP box', can be found in the mouse, *Drosophila*, *C. elegans*, *S. pombe* and *S. cerevisiae* (Figure 7a,b). Significantly, there is a single INCENP-box-bearing protein in *S. cerevisiae*, termed Sli15, which, like INCENP, associates with the spindle and is required for proper chromosome segregation [47].

It is interesting to note that the *S. cerevisiae* homologs of both proteins interact directly or indirectly with the same protein, the serine threonine kinase Ipl1p. Thus, Sli15 binds and may regulate Ipl1p in yeast [47], and Bir1p binds the Ipl1p substrate Ndc10p, a key component of the *S. cerevisiae* kinetochore [13,48,49]. Furthermore, there is also a functional correlation, because mutation of IPL1, like SLI15 and BIR1, causes chromosome missegregation [50]. The association of these proteins is likely to be evolutionarily conserved because interference with *bir-1* in *C. elegans* causes defects in cytokinesis similar to those in which *air-2*, the gene for an Ipl1p-like kinase, is inhibited [11,51], and AIR-2 does not localize to centromeres in the absence of BIR-1 [15].

The mammalian homologs of Ipl1p are the Aurora kinases (reviewed in [20]). Intriguingly, expression of mutant proteins and immunohistochemistry has shown that, in mammalian cells, Aurora1 and INCENP demonstrate similar cell-cycle distribution profiles and have related roles in mitosis [19,21–23]. Thus, it appears that Survivin, INCENP and Aurora1 are part of a mechanism governing chromosome segregation and cytokinesis that has been conserved from the yeasts to mammals (Figure 7c). This model is strongly supported by evidence in papers made available to us after submission of this manuscript showing that INCENP and Aurora1 bind to each other directly, and INCENP is required for Aurora1 localization to centromeres and the central spindle [52]. Furthermore, in *C. elegans*, the INCENP homolog ICP-1 is able to bind the Aurora1 homolog AIR-2 [53]. AIR-2 is in turn required for localization of the kinesin-like protein ZEN-4/CeMKLP1 to the spindle midzone [54]. In *C. elegans*, AIR-2 requires the Survivin homolog BIR-1 for its localization [15], but it remains to be seen whether in mammals (or *C. elegans*) Survivin interacts directly with INCENP or Aurora1, or indirectly, as in the yeast *S. cerevisiae* (Figure 7d).

Two groups of BIR-bearing proteins

Structural and functional considerations suggest that there are two classes of BIR-bearing proteins. Members of one class, which includes Survivin, are primarily involved in cell division, and members of the other are primarily involved in the control of apoptosis. The yeasts and *C. elegans* appear to encode only the former class, whereas other organisms such as *Drosophila* and mammals have proteins of both classes. Perhaps, during metazoan evolution, there was duplication of the gene encoding the primordial BIR-containing protein, which functions in cell division, and because this protein had an intrinsic affinity for caspases the second class of specifically anti-apoptotic BIR-containing proteins developed.

It has previously been shown that expression of Survivin is higher in cancers than in normal tissues [24]. Expression of Survivin during mitosis may explain this correlation as tumor cells have a higher mitotic index than cells in normal adult tissues. It has been proposed that Survivin may contribute to oncogenesis through inhibition of apoptosis, but the cell-cycle role of Survivin raises several additional possibilities. Inappropriate Survivin expression may induce chromosome instability, leading to oncogenic changes in ploidy. Alternatively, Survivin expression may induce inappropriate proliferation in cancer cells, or may simply be required for quiescent cells to escape their normal proliferative restraints. Whatever the function of Survivin in tumor cells, the absence of its expression in most normal adult tissues warrants further investigation of this protein as a target for novel anti-cancer therapeutics.

Conclusions

In *S. cerevisiae*, the proteins Bir1, Sli15 and Ipl1p interact with each other either directly or through the kinetochore protein Ndc10p. Furthermore, yeast mutant for these genes display similar defects in chromosome segregation and cytokinesis. The mammalian homologs of these proteins — Survivin, INCENP and Aurora1 — have similar expression patterns and localization. These observations, and the similar phenotypes of mouse embryos lacking Survivin or INCENP, suggest that the primary role of these proteins is to regulate chromosome segregation and cytokinesis, and they are likely to function in concert with the kinase Aurora1.

Materials and methods

Gene targeting and genotyping of mice

A mouse *survivin* cDNA clone was used to screen a mouse genomic library (strain 129Sv). Multiple independent lambda phage clones

were isolated and mapped by restriction-enzyme digestion; 9 kb of the longest clone was sequenced, encompassing the region encoding the entirety of the mouse *survivin* cDNAs. The targeting vector for *survivin* was electroporated into Bruce 4 (C57Bl/6) ES cells [55], which were then selected in G418-containing medium. Genomic DNA isolated from G418-resistant colonies was digested with *Bam*HI and analyzed by Southern hybridization using a PCR-generated 250 bp fragment 3′ of the homologous regions as a probe. Chimeric mice were generated from a correctly targeted mutant ES cell line (as described in [56]), and high-percentage chimeras were bred to C57Bl/6, and offspring from these crosses were genotyped by Southern hybridization to confirm germ-line transmission of the targeted allele. Mice were maintained on a C57Bl/6 background. Subsequent genotyping of mice was performed by PCR using the following primers: 5′ wild-type primer, 5′-GCAAAGGAGACCAACAACAAGC-3′; 5′ knockout primer, 5′-GGATTAGATAAATGCCTGCTCT-3′; 3′ primer, 5′-CAGCTCTG-CATCATTTAGTGCA-3′. These primers gave products of 0.9 kb for the wild-type allele and 0.6 kb for the mutant allele. Embryos were genotyped by a nested PCR strategy using the above primers for first round reactions and the following primers in the second round of PCR: 5′ wild-type primer, 5′-GGACCTGAGTGACATGCCAC-3′; 5′ knockout primer, 5′-GGCCAGCTCATTCCTCCCA-3′; 3′ primer, 5′-GGTCCTCCTCAATGCAATCAA-3′. The second-round primers gave products of 0.8 kb for the wild-type allele and 0.5 kb for the mutant allele. The reactions contained 1× PCR reaction buffer with $MgCl_2$ (Boehringer Mannheim), 800 μM dNTPs, 800 nM each primer and Taq polymerase (Boehringer Mannheim).

Embryo harvesting, culturing and morphological studies

Mouse breeding pairs were monitored daily for vaginal plugs (day 0.5 of embryonic development). Plugged mice were culled at day 2.5 or day 3.5 post coitum. The uterus and oviducts were dissected and flushed with M2 media. The embryos obtained were used for direct morphological studies, culturing and/or PCR genotyping. For direct morphological studies, day 2.5 and day 3.5 embryos were placed in M16 media (Sigma) under oil, transferred to microwells containing PHEM buffer (45 mM Pipes, 45 mM Hepes, both adjusted to pH 6.7, 10 mM EGTA, 5 mM $MgCl_2$, 1 mM PMSF, 0.7% Triton X-100) for 4–8 min at 37°C, before the embryos were placed individually on glass slides and fixed in a droplet of methanol. After two rinses in fixative, the embryos were stained and mounted in Vectashield antifade mounting medium (Vector Laboratories) containing 20 μg/ml DAPI. For the morphological study of days 4.5, 5.5 and 6.5 embryos, embryos were cultured on gelatinized (0.1% gelatin in PBS) coverslips (22 mm × 22 mm) in 35 mm Petri dishes (Nunc) with ES cell media supplemented with LIF and β-mercaptoethanol at 37°C, 5% CO_2 and photographed daily. The embryos were harvested by rinsing in PBS and treating with 0.25% trypsin for 3–5 min to detach the trophectoderm cells. Microglass pipettes were used to collect the cells. Harvested embryos were used for PCR genotyping or fixed in methanol/acetic acid for 10 min followed by staining as above and analysis on an Olympus 1X70 microscope/Nikon F-601 camera.

Immunofluorescence analysis

HeLa cells used for immunofluorescence analysis were either harvested and cytospun onto a slide or were cultured directly on a coverslip. Cytospun cells or cells grown on coverslips were fixed and processed for immunocytochemistry as described previously [57]. In some experiments, cells were treated with microtubule-inhibiting drugs before harvesting as follows: Taxol (PacliTaxel; Sigma) or nocodazole (Sigma) was added to the culture at 10 μM concentration for 2 h at 37°C. Colcemid (Gibco) was used at 0.1 μM for 1 h at 37°C. Immunohistochemistry was performed essentially as described previously [22]. The rabbit anti-Survivin antibody TO65 was raised against a peptide (sequence APTLPPAWQPFLKDHRI) derived from residues 3–19 at the amino terminus of human Survivin. The peptide was derivatized with an amino-terminal cysteine residue, coupled to keyhole limpet hemocyanin and rabbits were immunized five times (Alpha Diagnostics). The anti-Survivin antibody was affinity purified on the immunizing peptide on a SulfoLink column (Pierce) with elution in 100 mM glycine pH 2.5, according to manufacturer's instructions. The titer and specificity of the antibody was determined and confirmed by ELISA against the immunizing peptide and western blotting of Survivin-transfected cells, which clearly demonstrated specific immunostaining of the Survivin band (data not shown). CREST#6 was an autoimmune serum that detected CENP-A and CENP-B [57]. CENP-B detection used a monoclonal antibody 2D-7 [58]. Rabbit anti-chicken INCENP antibody was the generous gift of W.C. Earnshaw (University of Edinburgh, UK), and rabbit anti-CENP-E and anti-CENP-F antibodies were kindly provided by T.J. Yen (Fox Chase Cancer Center, Philadelphia). Mouse monoclonal anti-β-tubulin antibody (Boehringer) was used diluted 1:25 in PBS containing 3 mg/ml BSA (PBS-BSA).

Acknowledgements

We thank F. Köntgen and L. Barnett for ES cell work; W.C. Earnshaw and T.J. Yen for antibodies; E. Earle, A. Lo, S. Chan and H. Sim for helpful discussions and assistance with graphics. This work was partly funded by grants from NHMRC, AusIndustry, the Anti-Cancer Council of Victoria and AMRAD. D.L.V. is a Scholar of the Leukemia and Lymphoma Society.

References

1. Crook NE, Clem RJ, Miller LK: **An apoptosis inhibiting baculovirus gene with a zinc finger like motif.** *J Virol* 1993, **67**:2168-2174.
2. Uren AG, Coulson EJ, Vaux DL: **Conservation of baculovirus inhibitor of apoptosis repeat proteins BIRps in viruses, nematodes, vertebrates and yeasts.** *Trends Biochem Sci* 1998, **23**:159-162.
3. Hinds MG, Norton RS, Vaux DL, Day CL: **Solution structure of a baculoviral inhibitor of apoptosis IAP repeat.** *Nat Struct Biol* 1999, **6**:648-651.
4. Uren AG, Pakusch M, Hawkins CJ, Puls KL, Vaux DL: **Cloning and expression of apoptosis inhibitory protein homologs that function to inhibit apoptosis and/or bind tumor necrosis factor receptor-associated factors.** *Proc Natl Acad Sci USA* 1996, **93**:4974-4978.
5. Liston P, Roy N, Tamai K, Lefebvre C, Baird S, Chertonhorvat G, *et al.*: **Suppression of apoptosis in mammalian cells by NAIP and a related family of IAP genes.** *Nature* 1996, **379**:349-353.
6. Duckett CS, Nava VE, Gedrich RW, Clem RJ, Vandongen JL, Gilfillan MC, *et al.*: **A conserved family of cellular genes related to the baculovirus IAP gene and encoding apoptosis inhibitors.** *EMBO J* 1996, **15**:2685-2694.
7. Rothe M, Pan MG, Henzel WJ, Ayres TM, Goeddel DV: **The TNFR2-TRAF signaling complex contains two novel proteins related to baculoviral-inhibitor of apoptosis proteins.** *Cell* 1995, **83**:1243-1252.
8. Hay BA, Wassarman DA, Rubin GM: ***Drosophila* homologs of baculovirus inhibitor of apoptosis proteins function to block cell death.** *Cell* 1995, **83**:1253-1262.
9. Meier P, Silke J, Leevers SJ, Evan GI: **The *Drosophila* caspase DRONC is regulated by DIAP1.** *EMBO J* 2000, **19**:598-611.
10. Deveraux QL, Reed JC: **IAP family proteins - suppressors of apoptosis.** *Genes Dev* 1999, **13**:239-252.
11. Fraser AG, James C, Evan GI, Hengartner MO: ***Caenorhabditis elegans* inhibitor of apoptosis protein IAP homologue BIR-1 plays a conserved role in cytokinesis.** *Curr Biol* 1999, **9**:292-301.
12. Uren AG, Beilharz T, O'Connell MJ, Bugg SJ, van Driel R, Vaux DL, Lithgow T: **Role for yeast inhibitor of apoptosis IAP-like proteins in cell division.** *Proc Natl Acad Sci USA* 1999, **96**:10170-10175.
13. Yoon HJ, Carbon J: **Participation of Bir1p, a member of the inhibitor of apoptosis family, in yeast chromosome segregation events.** *Proc Natl Acad Sci USA* 1999, **96**:13208-13213.
14. Rajagopalan S, Balasubramanian MK: ***S. pombe* Pbh1p: an inhibitor of apoptosis domain containing protein is essential for chromosome segregation.** *FEBS Lett* 1999, **460**:187-190.
15. Speliotes EK, Uren AG, Vaux DL, Horvitz HR: **The survivin-like *C. elegans* BIR-1 protein acts with the aurora-like kinase AIR-2 to control chromosome behavior and spindle midzone organization.** *Mol Cell* 2000, **6**:211-223.
16. Choo KHA: *The Centromere.* Oxford: Oxford University Press; 1997
17. Ainsztein AM, Kandels-Lewis SE, Mackay AM, Earnshaw WC: **INCENP centromere and spindle targeting: identification of essential conserved motifs and involvement of heterochromatin protein HP1.** *J Cell Biol* 1998, **143**:1763-1774.

18. Mackay AM, Earnshaw WC: **The INCENPs — structural and functional analysis of a family of chromosome passenger proteins.** *Cold Spring Harb Symp Quant Biol* 1993, **58**:697-706.
19. Martineau-Thuillier S, Andreassen PR, Margolis RL: **Colocalization of TD-60 and INCENP throughout G2 and mitosis: evidence for their possible interaction in signalling cytokinesis.** *Chromosoma* 1998, **107**:461-470.
20. Bischoff JR, Plowman GD: **The Aurora/Ipl1p kinase family: regulators of chromosome segregation and cytokinesis.** *Trends Cell Biol* 1999, **9**:454-459.
21. Terada Y, Tatsuka M, Suzuki F, Yasuda Y, Fujita S, Otsu M: **Aim-1 — a mammalian midbody-associated protein required for cytokinesis.** *EMBO J* 1998, **17**:667-676.
22. Cutts SM, Fowler KJ, Kile BT, Hii LLP, O'Dowd RA, Hudson DF, *et al.*: **Defective chromosome segregation, microtubule bundling and nuclear bridging in inner centromere protein gene *Incenp*-disrupted mice.** *Hum Mol Genet* 1999, **8**:1145-1155.
23. Mackay AM, Ainsztein AM, Eckley DM, Earnshaw WC: **A dominant mutant of inner centromere protein INCENP, a chromosomal protein, disrupts prometaphase congression and cytokinesis.** *J Cell Biol* 1998, **140**:991-1002.
24. Ambrosini G, Adida C, Altieri DC: **A novel anti-apoptosis gene, survivin, expressed in cancer and lymphoma.** *Nat Med* 1997, **3**:917-921.
25. Kobayashi K, Hatano M, Otaki M, Ogasawara T, Tokuhisa T: **Expression of a murine homologue of the inhibitor of apoptosis protein is related to cell proliferation.** *Proc Natl Acad Sci USA* 1999, **96**:1457-1462.
26. Li FZ, Ambrosini G, Chu EY, Plescia J, Tognin S, Marchisio PC, Altieri DC: **Control of apoptosis and mitotic spindle checkpoint by survivin.** *Nature* 1998, **396**:580-584.
27. Li FZ, Ackermann EJ, Bennett CF, Rothermel AL, Plescia J, Tognin S, *et al.*: **Pleiotropic cell-division defects and apoptosis induced by interference with survivin function.** *Nat Cell Biol* 1999, **1**:461-466.
28. Saffery R, Irvine DV, Griffiths B, Kalitsis P, Wordeman L, Choo KHA: **Human centromeres and neocentromeres show identical distribution patterns of > 20 functionally important kinetochore-associated proteins.** *Hum Mol Genet* 2000 **9**:175-185.
29. Earle E, Saxena A, MacDonald A, Hudson DF, Shaffer LG, Saffery R, *et al.*: **PolyADP-ribose polymerase at active centromeres and neocentromeres at metaphase.** *Hum Mol Genet* 2000, **9**:187-194.
30. Chan GKT, Schaar BT, Yen TJ: **Characterization of the kinetochore binding domain of CENP-E reveals interactions with the kinetochore proteins CENP-F and Hbubr1.** *J Cell Biol* 1998, **143**:49-63.
31. Lennon G, Auffray C, Polymeropoulos M, Soares MB: **The Image Consortium — an integrated molecular analysis of genomes and their expression.** *Genomics* 1996, 33:151-152.
32. Altieri DC: **Molecular cloning of effector cell protease receptor-1, a novel cell surface receptor for the protease factor Xa.** *J Biol Chem* 1994, **269**:3139-3142.
33. Ambrosini G, Adida C, Sirugo G, Altieri DC: **Induction of apoptosis and inhibition of cell proliferation by survivin gene targeting.** *J Biol Chem* 1998, **273**:11177-11182.
34. Zaman GJR, Conway EM: **The elusive factor Xa receptor: failure to detect transcripts that correspond to the published sequence of EPR-1.** *Blood* 2000, **96**:145-148.
35. Craig JM, Earnshaw WC, Vagnarelli P: **Mammalian centromeres: DNA sequence, protein composition, and role in cell cycle progression.** *Exp Cell Res* 1999, **246**:249-262.
36. Li FZ, Altieri DC: **The cancer antiapoptosis mouse survivin gene: Characterization of locus and transcriptional requirements of basal and cell cycle-dependent expression.** *Cancer Res* 1999, **59**:3143-3151.
37. Cooke CA, Bernat RL, Earnshaw WC: **CENP-B: a major human centromere protein located beneath the kinetochore.** *J Cell Biol* 1990, **110**:1475-1488.
38. Cooke CA, Schaar B, Yen TJ, Earnshaw WC: **Localization of CENP-E in the fibrous corona and outer plate of mammalian kinetochores from prometaphase through anaphase.** *Chromosoma* 1997, **106**:446-455.
39. Rattner JB, Rao A, Fritzler MJ, Valencia DW, Yen TJ: **CENP-F is a *Ca* 400 kDa kinetochore protein that exhibits a cell-cycle dependent localization.** *Cell Motil Cytoskel* 1993, **26**:214-226.
40. Warburton PE, Cooke CA, Bourassa S, Vafa O, Sullivan BA, Stetten G, *et al.*: **Immunolocalization of CENP-A suggests a distinct nucleosome structure at the inner kinetochore plate of active centromeres.** *Curr Biol* 1997, **7**:901-904.
41. Cooke CA, Heck MM, Earnshaw WC: **The inner centromere protein INCENP antigens: movement from inner centromere to midbody during mitosis.** *J Cell Biol* 1987, **105**:2053-2067.
42. Earnshaw WC, Cooke CA: **Analysis of the distribution of the INCENPs throughout mitosis reveals the existence of a pathway of structural changes in the chromosomes during metaphase and early events in cleavage furrow formation.** *J Cell Sci* 1991, **98**:443-461.
43. Eckley DM, Ainsztein AM, Mackay AM, Goldberg IG, Earnshaw WC: **Chromosomal proteins and cytokinesis: patterns of cleavage furrow formation and inner centromere protein positioning in mitotic heterokaryons and mid-anaphase cells.** *J Cell Biol* 1997, **136**:1169-1183.
44. Yen TJ, Li G, Schaar BT, Szilak I, Cleveland DW: **CENP-E is a putative kinetochore motor that accumulates just before mitosis.** *Nature* 1992, **359**:536-539.
45. Thrower DA, Jordan MA, Schaar BT, Yen TJ, Wilson L: **Mitotic HeLa cells contain a CENP-E-associated minus end-directed microtubule motor.** *EMBO J* 1995, **14**:918-926.
46. Rieder CL, Salmon ED: **The vertebrate cell kinetochore and its roles during mitosis.** *Trends Cell Biol* 1998, **8**:310-318.
47. Kim JH, Kang JS, Chan CSM: **Sli15 associates with the Ip11 protein kinase to promote proper chromosome segregation in *Saccharomyces cerevisiae*.** *J Cell Biol* 1999, **145**:1381-1394.
48. Biggins S, Severin FF, Bhalla N, Sassoon I, Hyman AA, Murray AW: **The conserved protein kinase Ipl1 regulates microtubule binding to kinetochores in budding yeast.** *Genes Dev* 1999, **13**:532-544.
49. Sassoon I, Severin FF, Andrews PD, Taba MR, Kaplan KB, Ashford AJ, *et al.*: **Regulation of *Saccharomyces cerevisiae* kinetochores by the type 1 phosphatase Glc7p.** *Genes Dev* 1999, **13**:545-555.
50. Tung HYL, Wang WF, Chan CSM: **Regulation of chromosome segregation by Glc8p, a structural homolog of mammalian inhibitor 2 that functions as both an activator and an inhibitor of yeast protein phosphatase 1.** *Mol Cell Biol* 1995, **15**:6064-6074.
51. Schumacher JM, Golden A, Donovan PJ: **AIR-2: an Aurora/Ipl1-related protein kinase associated with chromosomes and midbody microtubules is required for polar body extrusion and cytokinesis in *Caenorhabditis elegans* embryos.** *J Cell Biol* 1998, **143**:1635-1646.
52. Adams RR, Wheatley SP, Gouldsworthy AM, Kandels-Lewis SE, Carmena M, Smythe C, *et al.*: **INCENP binds the Aurora-related kinase AIRK2 and is required to target it to chromosomes, the central spindle and cleavage furrow.** *Curr Biol* 2000, **10**:1075-1078.
53. Kaitna S, Mendoza M, Jantsch-Plunger V, Glotzer M: **Incenp and an Aurora-like kinase form a complex essential for chromosome segregation and efficient completion of cytokinesis.** *Curr Biol* 2000, **10**:1172-1181.
54. Severson AF, Hamill DR, Carter JC, Schumacher J, Bowerman B: **The Aurora-related kinase AIR-2 recruits ZEN-4/CeMKLP1 to the mitotic spindle at metaphase and is required for cytokinesis.** *Curr Biol* 2000, **10**:1162-1171.
55. Kontgen F, Suss G, Stewart C, Steinmetz M, Bluethmann H: **Targeted disruption of the MHC Class-II A gene in C57Bl/6 mice.** *Int Immunol* 1993, **5**:957-964.
56. Barnett L, Koentgen F: *Gene Knockout Protocols.* Totowa, NJ: Humana; 1998.
57. du Sart D, Cancilla MR, Earle E, Mao JI, Saffery R, Tainton KM, *et al.*: **A functional neo-centromere formed through activation of a latent human centromere and consisting of non-α-satellite DNA.** *Nat Genet* 1997, **16**:144-153.
58. Hudson DF, Fowler KJ, Earle E, Saffery R, Kalitsis P, Trowell H, *et al.*: **Centromere protein B null mice are mitotically and meiotically normal but have lower body and testis weights.** *J Cell Biol* 1998, **141**:309-319.

References

A. Abbott (2000)
Drive for more genomes threatens mouse sequence.
Nature, 405: 602-603.

R.R. Adams, S.P. Wheatley, A.M. Gouldsworthy, S.E. Kandels-Lewis, M. Carmena, C. Smythe, D.L. Gerloff and W.C. Earnshaw (2000)
INCENP binds to the Aurora-related kinae AIRK2 and is required to target it to chromosomes, the central spindle and cleavage furrow.

C. Adida, P.L. Crotty, J. McGrath, D. Berrebi, J. Diebold and D.C. Altieri (1998)
Developmentally regulated expression of the novel cancer anti-apoptosis gene survivin in human and mouse differentiation.
Am J Pathol, 152: 43-49.

A.M. Ainsztein, S.E. Kandels-Lewis, A.M. Mackay and W.C. Earnshaw (1998)
INCENP centromere and spindle targeting: Identification of essential conserved motifs and involvement of heterochromatin protein HP1.
J Cell Biol, 143: 1763-1774.

B. Alberts, D. Bray, J. Lewis, M. Raff, K. Roberts and J. D. Watson (1994a)
The mechanics of cell division *In* Molecular Biology of the Cell.
3rd Edition; Garland Publishing Inc, New York pp 911-946.

B. Alberts, D. Bray, J. Lewis, M. Raff, K. Roberts and J. D. Watson (1994b)
Germ cells and fertilization *In* Molecular Biology of the Cell.
3rd Edition; Garland Publishing Inc, New York p 1020.

B. Alberts, D. Bray, J. Lewis, M. Raff, K. Roberts and J. D. Watson (1994c)
The cell nucleus *In* Molecular Biology of the Cell.
3rd Edition; Garland Publishing Inc, New York p 342.

B. Alberts, D. Bray, J. Lewis, M. Raff, K. Roberts and J. D. Watson (1994d)
Recombinant DNA technology *In* Molecular Biology of the Cell.
3rd Edition; Garland Publishing Inc, New York pp 321-322.

B. Alberts, D. Bray, J. Lewis, M. Raff, K. Roberts and J. D. Watson (1994e)
The cytoskeleton *In* Molecular Biology of the Cell.
3rd Edition; Garland Publishing Inc, New York p 803.

L. Aragon-Alcaide, T. Miller, T. Schwarzacher, S. Reader and G. Moore (1996)
A cereal centromeric sequence.
Chromosoma, 105: 261-268.

J.J. Babon, M. McKenzie, R.G. Cotton (1999)
Mutation detection using fluorescent enzyme mismatch cleavage with T4 endonuclease VII.
Electrophoresis, 20: 1162-1167.

Banbury Conference Consortium (1997)
Neuron, 19: 755-759.

O. Barbosa-Cisneros, S. Fraire-Velazquez, J. Moreno and R. Herrera-Esparza (1997)
CENP-B autoantigen is a conserved protein from humans to higher plants: identification of the aminoterminal domain in Phaseolus vulgaris.
Rev Rhum Engl Ed, 64: 368-374.

A.E. Barry, E.V. Howman, M.R. Cancilla, R. Saffery and K.H.A. Choo (1999)
Sequence analysis of an 80 kb human neocentromere.
Hum Mol Genet, 8: 217-227.

J. Basu, E. Logarinho, S. Herrmann, H. Bousbaa, Z. Li , G.K. Chan, T.J. Yen, C.E. Sunkel and M.L. Goldberg (1998)
Localization of the Drosophila checkpoint control protein Bub3 to the kinetochore requires Bub1 but not Zw10 or Rod.
Chromosoma, 107: 376-385.

M. Baum and L. Clarke (2000)
Fission yeast homologs of human CENP-B have redundant functions affecting cell growth and chromosome segregation.
Mol and Cell Biol, 20: 2852-2864.

M.A. Bedell, N.A. Jenkins and N.G. Copeland (1997)
Mouse models of human disease. Part I: Techniques and resources for genetic analysis in mice.
Genes and Dev,11: 1-10.

N. Ben-Arie, A.E. McCall, S. Berkman, G. Eichele, H.J. Bellen and H.Y. Zoghbi (1996)
Evolutionary conservation of sequence and expression of the bHLH protein Atonal suggests a conserved role in neurogenesis.
Hum Mol Genet, 5: 1207-1216.

R.L. Bernat, G.G. Borisy, N.F.Rothfield and W.C. Earnshaw (1990)
Injection of anticentromere antibodies in interphase disrupts events required for chromosomal movement at mitosis.
J Cell Biol, 111: 1519-1533.

R.L. Bernat, M.R. Delannoy, N.F.Rothfield and W.C. Earnshaw (1991)
Disruption of centromere assembly during interphase inhibits kinetochore morphogenesis and function in mitosis.
Cell, 66: 1229-1238.

J.R. Bischoff and G.D. Plowman (1999)
The Aurora/Ipl1p kinase family: regulators of chromosome segregation and cytokinesis.
Trends in Cell Biol, 9: 454-459.

E. H. Blackburn and C.W. Grieder (1995)
Telomeres.
Cold Spring Harbor Laboratory Press; Cold Spring Harbor, New York.

S. Bowman, D. Lawson, D. Basham, D. Brown, T. Chillingworth, C.M. Churcher, A. Craig, R.M. Davies, K. Devlin, T. Feltwell, S. Gentles, R. Gwilliam, N. Hamlin, D. Harris, S. Holroyd, T. Hornsby, P. Horrocks, K. Jagels, B. Jassal, S. Kyes, J. McLean, S. Moule, K. Mungall, L. Murphy, K. Oliver, M.A. Quail, M.-A. Rajandream, S. Rutter, J. Skelton, R. Squares, S. Squares, J.E. Sulston, S. Whitehead, J.R. Woodward, C. Newbold and B.G. Barrell (1999)

The complete nucleotide sequence of chromosome 3 of Plasmodium falciparum.
Nature, 400: 532-538.

W.R.A. Brown, P.J. Mee and M.H. Shen (2000)
Artificial chromosomes: ideal vectors?
TibTech, 18: 218-223.

B.R. Brinkley, I. Ouspenski and R.P. Zinkowski (1992)
Structure and molecular organization of the centromere-kinetochore complex.
Trends in Cell Biol, 2: 15-21.

B.J. Buchwitz, K. Ahmad, L.L. Moore, M.B. Roth and S. Henikoff (1999)
A histone-H3-like protein in *C.elegans*.
Nature, 401: 547-548.

D.P. Cahill, C. Lengauer, J. Yu, G.J. Riggins, J.K.V. Willson, S.D. Markowitz, K.W. Kinzler and B. Vogelstein (1998)
Mutations of mitotic checkpoint genes in human cancers.
Nature, 392: 300-303.

D.P. Cahill, L.T da Costa, E.B. Carson-Walter, K.W. Kinzler, B. Vogelstein and C. Lengauer (1999)
Characterisation of MAD2B and other mitotic checkpoint spindle genes.
Genomics, 58: 181-187.

E.B. Cambareri, R. Aisner and J. Carbon (1998)
Structure of the chromosome VII centromere region in Neurospora crassa: degenerate transposons and simple repeats.
Mol Cell Biol, 18: 5465-5477.

G.A. Carlson, C. Ebeling, M. Torchia, D. Westaway and S.B. Prusiner (1993)
Delimiting the location of the scrapie prion incubation time gene on chromosome 2 of the mouse.
Genetics, 133: 979-988.

G.K. Chan, B.T. Schaar and T.J. Yen (1998)
Characterization of the kinetochore binding domain of CENP-E reveals interactions with the kinetochore proteins CENP-F and hBUBR1.
J Cell Biol, 143: 49-63.

L. Chantalat, D.A. Skoufias, J.P. Kleman, B. Jung, O. Dideberg and R.L. Margolis (2000)
Crystal structure of human survivin reveals a bow tie-shaped dimer with two unusual alpha-helical extensions.
Mol Cell, 6: 183-189.

K.H.A. Choo (1997a)
The Centromere.
Oxford University Press, Oxford.

K.H.A. Choo (1997b)
Centromere DNA dynamics: latent centromeres and neocentromere formation.
Amer Soc Hum Gen, 6: 1225-1233.

K.H.A. Choo (1998a)
Turning on the centromere.
Nat Genet, 18: 3-4.

K.H.A. Choo (1998b)
Why is the centromere so cold?
Genet Res, 8: 81-82.

D.O. Co, A.H. Borowski, J.D. Leung, J. van der Kaa, S. Hengst, G.J. Platenburg, F.R. Pieper, C. F. Perez, F.R. Jirik and J.I. Drayer (2000)
Generation of transgenic mice and germline transmission of a mammalian artificial chromosome introduced into embryos by pronuclear microinjection.
Chrom Res, 8: 183-191.

C.A. Cooke, M.M. Heck and W.C. Earnshaw (1987)
The inner centromere protein (INCENP) antigens: movement from inner centromere to midbody during mitosis.
J Cell Biol, 105: 2053-2067.

C.A. Cooke, R.L. Bernat and W.C. Earnshaw (1990)
CENP-B: A major human centromere protein located beneath the kinetochore.
J Cell Biol, 110: 1475-1488.

C.A. Cooke, B. Schaar, T.J. Yen and W.C. Earnshaw (1997)
Localization of CENP-E in the fibrous corona and outer plate of mammalian kinetochores from prometaphase through anaphase.
Chromosoma, 106: 446-455.

G.P. Copenhaver, K. Nickel, T. Kuromori, M-I. Benito, S. Kaul, X. Lin, M. Bevan, G. Murphy, B. Harris, L. D. Parnell, W. R. McCombie, R. A. Martienssen, M. Marra and D. Preuss (1999)
Genetic definition and sequence analysis of *Arabidopsis* centromeres.
Science, 286: 2468-2474.

J.M. Craig, W.C. Earnshaw and P. Vagnarelli (1999)
Mammalian centromeres: DNA sequence, protein composition, and role in cell cycle progression.
Exp Cell Res, 246: 249-262
V.J. Cristofalo (2000)

A DNA chip off the old block.
Nat Med, 6: 507.

A.K. Csink and S. Henikoff (1998)
Something from nothing: the evolution and utility of satellite repeats.
Trends Genet, 14: 200-204.

S.M. Cutts, K.J. Fowler, B.T. Kile, L.L.P. Hii, R.A. O'Dowd, D.F. Hudson,
R. Saffery, P. Kalitsis, E. Earle and K.H.A. Choo (1999)
Defective chromosomal segregation, microtubule bundling, and nuclear bridging in
Inner centromere protein (*Incenp*) gene-disrupted mice.
Hum Mol Genet, 8:1145-1155 and front cover.

T.M. Dechiara, E.J. Robertson and A. Efstratiadis (1991)
Parental imprinting of the mouse insulin-like growth factor II gene.
Cell, 64: 849-859.

Q.L. Deveraux and J.C. Reed (1999)
IAP family of proteins - suppressors of apoptosis.
Genes and Dev, 13: 239-252.

G.K. Dhaliwal, C. Wray and D.E. Noakes (1998)
Uterine flora and uterine lesions in bitches with cystic endometrial hyperplasia
(pyometra).
Vet Rec, 143: 659-661.

M. Dobles, V. Liberal, M.L. Scott, R. Benezra and P.K. Sorger (2000)
Chromosome missegregation and apoptosis in mice lacking the mitotic checkpoint
protein Mad2.
Cell, 101: 635-645.

D. du Sart, M.R. Cancilla, E. Earle, J. Mao, R. Saffery, K.M. Tainton, P. Kalitsis, J. Martyn, A.E. Barry and K.H.A. Choo (1997)
A functional neo-centromere formed through activation of a latent human centromere and consisting of non-alpha-satellite DNA.
Nat Genet, 16:144-153.

W.C. Earnshaw and N. Rothfield (1985)
Identification of a family of human centromere proteins using autoimmune sera from patients with scleroderma.
Chromosoma, 91: 313-321.

W.C. Earnshaw, K.F. Sullivan, P.S. Machlin, C.A. Cooke, D.A Kaiser, T.D. Pollard, N.F. Rothfield and D.W. Cleveland (1987)
Molecular cloning of cDNA for CENP-B, the major human centromere autoantigen.
J Cell Biol, 104: 817-829.

W.C. Earnshaw, H. Ratrie and G. Stetten (1989)
Visualization of centromere proteins CENP-B and CENP-C on a stable dicentric chromosome in cytological spreads.
Chromosoma, 98: 1-12.

W.C. Earnshaw and C.A. Cooke (1991)
Analysis of the distribution of the INCENPs throughout mitosis reveals the existence of a pathway of structural changes in chromosomes during metaphase and early events in cleavage formation.
J Cell Sci, 98: 443-461.

W.C. Earnshaw and J.E. Tomkiel (1992)
Centromere and kinetochore structure.
Curr Opin Cell Biol, 4: 86-93.

D.M. Eckley, A.M. Ainsztein, A.M. Mackay, I.G. Goldberg and W.C. Earnshaw (1997)
Chromosomal proteins and cytokinesis: patterns of cleavage furrow formation and inner centromere protein positioning in mitotic heterokaryons and mid-anaphase cells.
J Cell Biol, 136: 1169-1183.

V.P. Efimov and N.R. Morris (1998)
A screen for dynein synthetic lethals in *Aspergillus nidulans* identifies spindle assembly checkpoint genes and other genes involved in mitosis.
Genetics, 149: 101-106.

J.T. Eppig and J.H. Nadeau (1995)
Comparative maps: the mammalian jigsaw puzzle.
Curr Opin Genet Dev, 5: 709-716.

J. Figueroa, R. Saffrich, W. Ansorge and M. Valdivia (1998)
Microinjection of antibodies to centromere protein CENP-A arrest cells in interphase but does not prevent mitosis.
Chromosoma, 107: 397-405.

K.J. Fowler, W.M. Clouston, R.E.K. Fournier and B.A. Evans (1991)
The relaxin gene is located on chromosome 19 in the mouse.
FEBS Lett, 292: 183-186.

K.J. Fowler, G.B. Mann and A.R. Dunn (1993)
Linkage of the murine Transforming Growth Factor alpha gene with *Igk*, *Ly-2* and *Fabpl* on chromosome 6.
Genomics, 16: 82-784.

K.J. Fowler, F. Walker, W. Alexander, M.L. Hibbs, E.C. Nice, R.M. Bohmer, G.B. Mann, C. Thumwood, R. Maglitto, J..A. Danks, R. Chetty, A.W. Burgess and A.R. Dunn (1995)
A mutation in the epidermal growth factor receptor in *waved-2* mice has a profound effect on receptor biochemistry resulting in impaired lactation.
Proc Natl Acad Sci USA, 92: 1465-1469.

K.J. Fowler, A.J. Newson, A.C. MacDonald, P. Kalitsis, M.S. Lyu, C.A. Kozak and K.H.A. Choo (1997)
Chromosomal localization of mouse *Cenpa* gene.
Cytogenet and Cell Genet, 79: 298-301.

K.J. Fowler, R. Saffery, B.T. Kile, D.V. Irvine, D.F. Hudson, H.E. Trowell and K.H.A. Choo (1998a)
Genetic mapping of mouse centromere proteins *Incenp* and *Cenpe* genes.
Cytogenet and Cell Genet, 82: 67-70.

K.J. Fowler, R. Saffery, D.V. Irvine, H.E. Trowell and K.H.A. Choo (1998b)
Mouse centromere protein F (*Cenpf*) gene maps to the distal region of Chromosome 1 using interspecific backcross panel.
Cytogenet and Cell Genet, 82: 180-181.

K.J. Fowler, P. Kalitsis and K.H.A. Choo (1999)
Mouse mitotic spindle checkpoint (*Bub3*) gene maps to the distal region of Chromosome 7 using interspecific backcross analysis.
Cytogenet and Cell Genet, 87: 91-92.

K.J. Fowler, D.F. Hudson, L. Salamonsen, S. Edmondson, E. Earle, M.C. Sibson and K.H.A. Choo (2000)
Uterine dysfunction and genetic modifiers in Centromere protein B-deficient mice.
Genome Res, 10: 30-41 and front cover.

A.G. Fraser, C. James, G.I. Evan and M.O. Hengartner (1999)
Caenorhabditis elegans inhibitor of apoptosis protein (IAP) homologue BIR-1 plays a conserved role in cytokinesis.
Curr Biol, 9: 292-301.

T. Fukagawa and W.R. Brown (1997)
Efficient conditional mutation of the vertebrate CENP-C gene.
Hum Mol Genet, 6: 301-2308.

Y. Gavrieli, Y. Sherman and S.A. Ben-Sasson (1992)
Identification of programmed cell death in situ specific labeling of nuclear fragmentation.
J Cell Biol, 119: 493-501.

S.R. Glasser and S. M^{c}Cormack (1981)
Separated cell types as analytical tools in the study of decidualization and implantation *In* Cellular and Molecular Aspects of Implantation. *Eds* S.R. Glasser and D.W. Bullock.
Plenum Press, New York pp 217-239.

S.R. Glasser and J. Julian (1986)
Intermediate filament protein as a marker of uterine stromal cell decidualization. Biol of Reprod, 35: 463-474.

I.G. Goldberg, H. Sawhney, A.F. Pluta, P.E. Warburton, and W.C. Earnshaw (1996)
Surprising deficiency of CENP-B binding sites in African green monkey alpha-satellite DNA: implications for CENP-B function at centromeres.
Mol Cell Biol, 169: 5156-5168.

F. Golden and M.D. Lemonick (2000)
The race is over.
Time, 26: 57-61.

A. Gossler and J. Zachgo (1993)
Gene targeting vectors for mammalian cells *In* Gene Targeting. A Practical Approach. *Ed* A.L. Joyner.
Oxford University Press, Oxford, New York, Tokyo pp 181-227.

T. Goto and T. Kinoshita (1999)
Maternal transcripts of mitotic checkpoint gene, Xbub3, are accumulated in the animal blastomeres of Xenopus early embryo.
DNA Cell Biol, 18: 227-234.

M.C. Green (1981)
Gene mapping *In* The Mouse in Biomedical Research. History, Genetics, and Wild Mice. Vol 1, *Eds* H.L. Foster, J.D. Small and J.G. Fox.
Academic Press, New York pp 105-117.

J.G. Hacia (1999)
Resequencing and mutational analysis using oligonucleotide microarrays.
Nat Genet Supplement, 21: 42-47.

A. Hammes and A. Schedl (2000)
Generation of transgenic mice from plasmids, BACs and YACs *In* Mouse Genetics and Transgenics. A Practical Approach. *Eds* I.J. Jackson and C.M. Abbott.
Oxford University Press, Oxford, New York, Tokyo pp 217-245.

P. Hasty and A. Bradley (1993)
Gene targeting vectors for mammalian cells *In* Gene Targeting. A Practical Approach. *Ed* A.L. Joyner.
Oxford University Press, Oxford, New York, Tokyo pp 1-32.

D. He, C. Zeng, K. Woods, L. Zhong, D. Turner, R.K. Busch, B.R. Brinkley and H. Busch (1998)
CENP-G: a new centromeric protein that is associated with the α-1 satellite DNA subfamily.
Chromosoma, 107: 189-197.

C. Holm (1994)
Coming undone: how to untangle a chromosome.
Cell, 77: 955-957.

E.V. Howman (2000)
The neocentromere and centromere protein A (CENP-A).
PhD thesis, University of Melbourne.

E.V. Howman, K.J. Fowler, A.J. Newson, S. Redward, A.C. MacDonald, P. Kalitsis and K.H.A. Choo (2000)
Early disruption of centromeric chromatin organisation in centromere protein A (*Cenpa*) null mice.
Proc Natl Acad Sci USA, 97: 1148-1153.

D.F. Hudson (1998)
Gene disruption and functional characterisation of mouse centromere protein B.
PhD thesis, University of Melbourne.

D.F. Hudson, K.J. Fowler, E. Earle, R. Saffery, P. Kalitsis, H. Trowell, J. Hill, N.G. Wreford, D.M. deKretser, M.R. Cancilla, E. Howman, L. Hii, S.M. Cutts, D.V. Irvine, and K.H.A. Choo (1998)
Centromere protein B null mice are mitotically and meiotically normal but have lower body and testis weights.
J Cell Biol, 141: 309-319.

M.A. Hyot, L. Totis and B.T. Roberts (1991)
S. cerevisiae genes required for cell cycle arrest in response to loss of microtubule function.
Cell, 66: 507-517.

A.L. Jacobs, G.L. Decker, S.R. Glasser, J. Julian and D.D. Carson (1990)
Vectorial secretion of prostaglandins by polarized rodent uterine epithelial cells.
Endocrinology, 126: 2175-2136.

A.L. Joyner (1993)
Gene Targeting. A Practical Approach.
Oxford University Press, Oxford, New York, Tokyo.

P. Kalitsis (1998)
Structural and functional studies of mouse centromere protein C.
PhD thesis, University of Melbourne.

P. Kalitsis, K.J. Fowler, E. Earle, J. Hill, and K.H.A. Choo (1998a)
Targeted disruption of mouse centromere protein C leads to mitotic disarray and early embryo death.
Proc Natl Acad Sci USA, 95: 1136-1141.

P. Kalitsis, A.C. McDonald, A.J. Newson, D.F. Hudson and K.H.A. Choo (1998b)
Gene structure and sequence analysis of mouse centromere proteins A and C.
Genomics, 47: 108-114.

P. Kalitsis, E. Earle, K.J. Fowler, and K.H.A. Choo (2000)
Bub3 gene disruption in mice reveals essential mitotic spindle checkpoint function during early embryogenesis.
Genes and Dev, 14: 2277-2282.

T. Kanda, K.F. Sullivan and G.M. Wahl (1998)
Histone-GFP fusion protein enables sensitive analysis of chromosome dynamics in living mammalian cells.
Curr Biol, 8: 377-385.

M. Kapoor, R. Montes de Oca Luna, G. Liu, G. Lozano, C. Cummings, M. Mancini, I. Ouspenski, B.R. Brinkley and G.S. May (1998)
The cenpB gene is not essential in mice.
Chromosoma, 107: 570-576.

G.H. Karpen and R.G. Allshire (1997)
The case for epigenetic effects on centromeric identity and function.
Trends Genet, 13: 489-496.

B. Kile (1997)
Cloning and targeted disruption of the gene for mouse centromere protein Incenp.
BSc Honours thesis, University of Melbourne.

D. Kipling, A.R. Mitchell, H. Masumoto, H.E. Wilson, L. Nicol and H.J. Cooke (1995)
CENP-B binds a novel centromeric sequence in the asian mouse *Mus caroli.*
Mol Cell Biol, 15: 4009-4020.

D. Kipling and P.E. Warburton (1997)
Centromeres, CENP-B and *Tigger* too.
Trends Genet, 13: 141-144.

C.A. Kozak (1996)
Retroviral and cancer-related genes *In* Genetic variants and strains of the laboratory mouse. Vol 2, 3rd Edition, *Eds* M.F. Lyon, S. Rastan and S.D.M. Brown.
Oxford University Press, Oxford, New York, Tokyo pp 855-879.

T.K. Kwon, A.L. Hawkins, C.A. Grifin and E. Gabrielson (2000)
Assignment of BUB3 to human chromosome band 10q26 by in situ hybridisation.
Cytogenet and Cell Genet, 88: 202-203.

E.C. LaCasse, S. Baird, R.G. Korneluk and A.E. MacKenzie (1998)
The inhibitors of apoptosis (IAPs) and their emerging role in cancer.
Oncogene, 17: 3247-3249.

G. Landberg, M. Erlanson, G. Roos, E.M. Tan and C.A. Casiano (1996)
CENP-F: a marker for cell proliferation in human malignancies.
Cytometry, 25: 90-98.

L. Lanini and F. McKeon (1995)
Domains required for CENP-C assembly at the knetochore.
Mol Cell Biol, 6: 1049-1059.

D.F. Lawler (1998)
Diagnosis and treatment of inflammatory uterine disease in cats.
Vet Med, 93: 750-753.

H.W. Lee, M.A. Blasco, G.J. Gottlieb, J.W. Horner 2nd, C.W. Greider and R.A. DePinho (1998)
Essential role of mouse telomerase in highly proliferative organs.
Nature, 392: 569-574.

F. Li, G. Ambrosini, E.Y. Chu, J. Piescia, S. Tognin, P.C. Marchisio and D.C. Altieri (1998)
Control of apoptosis and mitotic checkpoint by survivin.
Nature, 396: 580-584.

F. Li, E.J. Ackermann, C.F. Bennett, A.L. Rothermel, J. Piescia, S. Tognin, A. Villa, P.C. Marchisio and D.C. Altieri (1999)
Pleiotrophic cell-division defects and apoptosis induced by interference with survivin.
Nat Cell Biol, 1: 461-466.

F. Li and D.C. Altieri (1999)
The cancer antiapoptosis mouse survivin gene: characterization of locus and transcriptional requirements of basal and cell cycle-dependent expression.
Can Res, 13: 3143-3151.

H. Liao, R.J. Winkfein, G. Mack, J.B. Rattner and T.J. Yen (1995)
CENP-F is a protein of the nuclear matrix that assembles onto kinetochores at late G2 and is rapidly degraded after mitosis.
J Cell Biol, 130: 507-518.

G.J. Lieschke, D. Grail, G. Hodgson, D. Metcalf, E. Stanley, C. Cheers, K.J. Fowler, S. Basu, Yi F. Zhan and A.R. Dunn (1994)
Mice lacking granulocyte colony-stimulating factor have chronic neutropenia, granulocyte and macrophage progenitor cell deficiency and impaired neutrophil mobilization.
Blood, 84: 1737-1746.

Q. Liu, S. Guntuku, X.S. Cui, S. Matsuoka, D. Cortez, K. Tamai, G. Luo, S. Carattini-Rivera, F. DeMayo, A. Bradley, L.A. Donehower and S.J. Elledge (2000)
Chk1 is an essential kinase that is regulated by Atr and required for the G(2)/M DNA damage checkpoint.
Genes Dev, 14: 1448-1459.

A.W.I. Lo, D.F.S. Longmuir, K.J. Fowler, P. Kalitsis and K.H.A. Choo (2000)
Assignment of the centromere protein H (*Cenph*) gene to mouse chromosome band 13D1 by in situ hybridization and interspecific backcross analyses.
Cytogenet and Cell Genet, 90: 56-57.

B. Lomax, S. Tang, E. Separovic, D. Phillips, E. Hillard, T. Thomson and D.K. Kalousek (2000)
Comparative genomic hybridisation in combination with flow cytometry improves results of cytogenetic analysis of spontaneous abortions.
Am J Hum Genet, 66: 1516-1521.

V.A. Lombillo, C. Nislow, T.J. Yen, V.I. Gelfand and J.R. McIntosh (1995)
Antibodies to the kinesin motor domain and CENP-E inhibit microtubule depolymerization-dependent motion of chromosomes in vitro.
J Cell Biol, 128: 107-115.

D.H. Ly, D.J. Lockhart, R.A. Lerner and P.G. Schultz (2000)
Mitotic misregulation and human aging.
Science, 287: 2486-2492.

A.M. Mackay, D.M. Eckley, C. Chue and W.C. Earnshaw (1993)
Molecular analysis of the INCENPs (inner centromere proteins): Separate domains are required for association with microtubules during interphase and with the central spindle during anaphase.
J Cell Biol, 123: 373-385.

A.M. Mackay, A.M. Ainsztein, D.M. Eckley and W.C. Earnshaw (1998)
A dominant mutant of inner centromere protein (INCENP), a chromosomal protein, disrupts prometaphase congression and cytokinesis.
J Cell Biol, 140: 991-1002.

T. Magnuson and C.J. Epstein (1984)
Oligiosyndactyly: a lethal mutation in the mouse that results in mitotic arrest at very early in development.
Cell, 38: 823-833.

M.A. Mancini, D. He, I.I. Ouspenski and R.R. Brinkley (1996)
Dynamic continuity of nuclear and mitotic matrix proteins in the cell cycle.
J Cell Biochem, 62: 158-164.

T. Maney, L.M. Ginkel, A.W. Hunter and L. Wordeman (1999)
The kinetochore of higher eucaryotes: a molecular view.
Internat Rev Cytol, 194: 67-131.

K.F. Manly (1993)
A Macintosh program for all of our data management.
Mammal Gen, 4: 303-313.

G.B. Mann, K.J. Fowler, A. Gabriel, E. Nice, L.Williams and A.R. Dunn (1993)
Mice with a null mutation of the TGF alpha gene have abnormal skin architecture, wavy hair and curly whiskers and often develop corneal inflammation.
Cell, 73: 249-261 and front cover.

S.L. Mansour, K.R. Thomas and M.R. Capecchi (1988)
Disruption of the proto-oncogene *int-2* in mouse embryo-derived stem cells: a general strategy for targeting mutations to non-selectable genes.
Nature, 336: 348-352.

S. Martineau-Thuillier, P.R. Andreassen and R.L. Margolis (1998)
Colocalization of TD-60 and INCENP throughout the G2 and mitosis: evidence for their possible interaction in signalling cytokinesis.
Chromosoma, 107: 461-470.

M.J. Martinez-Exposito, K.B. Kaplan, J. Copeland and P.K. Sorger (1999)
Retention of the BUB3 checkpoint protein on lagging chromosomes.
Proc Natl Acad Sci USA, 96: 8493-8498.

L.K. Miller (1999)
An exegsis of IAPs: salvation and surprises from BIR motifs.
Trends Cell Biol, 9: 323-328.

P. Mountford, B. Zevnik, A. Dowel, J. Nichols, M. Li, C. Dani, M. Robertson, I. Chambers and A. Smith (1994)
Dicistronic targeting constructs: reporters and modifiers of mammalian gene expression.
Proc Natl Acad Sci USA, 91: 4303-4307.

Mouse Facts Database (accessed July, 2000)
Available at: http://www.informatics.jax.org/mgihome/other/mouse_facts1.shtml.

Mouse Genome Sequencing (accessed September, 2000)
Available at: http://www.ncbi.nim.nih.gov/genome/seq/MmHome.html.

Y. Moroi, C. Peebles, M.J. Fritzler, J. Steigerwald, E.M. Tan (1980)
Autoantibody to centromere (kinetochore) in scleroderma sera.
Proc Natl Acad Sci USA, 77: 1627-31.

A.R. Moser, W.F. Dove, K.A. Roth and J.I. Gordon (1992)
The Min (multiple intestinal neoplasia) mutation: its effect on gut epithelial cell differentiation and interaction with a modifier system.
J Cell Biol, 116: 1517-1526.

S.W. Muchmore, J. Chen, C. Jakob, D. Zakula, E.D. Matayoshi, W. Wu, H. Zhang, F. Li, S.C. Ng and D.C. Altieri (2000)
Crystal structure and mutagenic analysis of the inhibitor-of-apoptosis protein survivin.
Mol Cell, 6: 173-182.

U. Muller (1999)
Ten years of gene targeting: targeted mouse mutants, from vector design to phenotype analysis.
Mech of Dev, 82: 3-21.

L.C. McCarthy, J. Terrett, M.E. Davis, C.J. Knights, A.L. Smith, R. Critcher, K.Schmitt, J. Hudson, N.K Spurr and P.N. Goodfellow (1997)
A first-generation whole genome-radiation hybrid map spanning the mouse genome.
Genome Res, 7: 1153-1161.

A.C. MacDonald (1996)
A structural and functional analysis of centromere proteins A and C.
BSc Honours thesis, University of Melbourne.

S. McKay, E. Thomson and H. Cooke (1994)
Sequence homologies and linkage group conservation of the human and mouse *Cenpc* genes.
Genomics, 22: 36-40.

K. Nagaki, H. Tsujimoto and T. Sasakuma (1998)
A novel repetitive sequence of sugar cane, SCEN family, locating on centromeric regions.
Chrom Res, 6: 295-302.

K. Nasmyth, J-M. Peters and F. Uhlmann (2000)
Splitting the chromosome: cutting the ties that bind sister chromatids.
Science, 188: 1379-1384.

E.J. Neer, C.J. Schmidt, R. Nambudripad and T.F. Smith (1994)
The ancient regulatory-protein family of WD-repeat proteins.
Nature, 371: 297-300.

A.J. Newson (1997)
A structural and functional analysis of the mouse centromere protein A gene, encoding a conserved histone H3-like domain.
BSc Honours/LLB thesis, University of Melbourne.

H. Niida, T. Matsumoto, H. Satoh, M. Shiwa, Y. Tokutake, Y. Furuichi and Y. Shinkai (1998)
Severe growth defect in mouse cells lacking the telomerase RNA component.
Nat Genet, 19: 203-206.

S. Nomoto, N. Haruki , T. Takahashi, A. Masuda, T. Koshikawa, Y. Fujii and H. Osada (1999)
Search for in vivo somatic mutations in the mitotic checkpoint gene, hMAD1, in human lung cancers.
Oncogene, 18: 7180-7183.

E.N. Olson, H.-H. Arnpold, P.W.J. Rigby and B.J. Wold (1996)
Know your neighbours: Three phenotypes in null mutants of the myogenic bHLH gene MRF4.
Cell, 85: 1-4.

Online Journals and Impact Factors Database (accessed September 2000)
Available at: http//:www.med.rug.nl/mdl/journal.html.

A. Orimo, S. Inoue, O. Minowa, N. Tominaga, Y. Tomioka, M. Sato, J. Kuno, H. Hiroi, Y. Shimizu, M. Suzuki, T. Noda and M. Muramatsu (1999)
Underdeveloped uterus and reduced estrogen responsiveness in mice with disruption of the estrogen-responsive finger protein gene, which is a direct target of estrogen receptor alpha.
Proc Natl Acad Sci USA, 96: 12027-12032

S.L. Page, W.C. Earnshaw, K.H.A. Choo and L.G. Shaffer (1995)
Further evidence that CENP-C is a necessary component of active centromeres: Studies of a dic(X; 15) with a simultaneous immunofluorescence and FISH.
Hum Mol Genet, 4: 289-294.

K. Paigen (1995)
A miracle enough: the power of mice.
Nat Med, 3: 215-220.

A. Pellicer, C. Rubio, F. Vidal, Y. Minguez, C. Gimenez, J. Egozcue, J. Remohi and C. Simon (1998)
In vitro fertilisation plus preimplantation genetic diagnosis in patients with recurrent miscarriage: an analysis of chromosome abnormalities in human preimplantation embryos.
Fertil Steril, 71: 1033-1039.

A.V. Perez-Castro, F.L. Shamanski, J.J. Meneses, T.L. Lovato, K.G. Vogel, R.K. Moyzis and R. Pedersen (1998)
Centromeric protein b null mice are viable with no apparent abnormalities.
Dev Biol, 201: 135-143.

C.M. Pfarr, M. Coue, P.M. Grisom, T.S. Hays, M.E. Porter and J.R. McIntosh (1990)
Cytoplasmic dynein is localized to kinetochores during mitosis.
Nature, 345: 263-265.

A.L. Pidoux and R.C. Allshire (2000)
Centromeres: getting a grip of chromosomes.
Curr Opin Cell Biol, 12:308-319.

A. Plagge, G. Kelsey and N.D. Allen (2000)
Directed mutagenesis in embryonic stem cells *In* Mouse Genetics and Transgenics.
A Practical Approach. *Eds* I.J. Jackson and C.M. Abbott.
Oxford University Press; Oxford, New York pp 247-284.

A.F. Pluta, A.M. Mackay, A.M. Ainsztein, I.G. Goldberg and W.C. Earnshaw (1995)
The centromere: the hub of chromosomal activities.
Science, 270: 1591-1594.

A.F. Pluta and W.C. Earnshaw (1996)
Specific interaction between human kinetochore protein CENP-C and a nucleolar transcriptional regulator.
J Cell Biol, 271: 18767-18774.

A.F. Pluta, W.C. Earnshaw and I.G. Goldberg (1998)
Interphase-specific association of intrinsic centromere protein CENP-C with Hdaxx, a death domain-binding protein implicated in Fas-mediated cell death.
J Cell Sci, 111: 2029-2041.

C. Poirier, A. Laloutte, V.C Folletta, D.R. Cohen and J.L. Guenet (1997)
The gene encoding the Fos-related antigen 2 (*Fosl2*) maps to mouse Chromosome 5.
Mammal Gen, 8: 223.

PubMed (accessed September, 2000)
Available at: http://www.ncbi.nlm.nih.gov:80/entrez/journals/loftext_noprov.html.

A. Purohit, S.H. Tynan, R. Vallee and S.J. Doxsey (1999)
Direct interaction of pericentrin with cytoplasmic dynein light intermediate chain contributes to mitotic spindle organization.
J Cell Biol, 147: 481-492.

M.B. Qumsiyeh, K.-R. Kim, M.N. Ahmed and W. Bradford (2000)
Cytogenetics and mechanisms of spontaneous abortions: increased apoptosis and decreased cell proliferation in chromosomally abnormal villi.
Cytogenet Cell Genet, 88: 230-235.

J.B. Rattner (1991)
The structure of the mammalian centromere.
BioEssays, 13: 51-56.

J.B. Rattner, A. Rao, M.J. Fritzler, D.W. Valencia and T.J. Yen (1993)
CENP-F is a .ca 400 kDa kinetochore protein that exhibits a cell-cycle dependent localization.
Cell Motil and Cytoskel, 26: 214-226.

S. Redward (1998)
Functional analysis of mouse centromere protein CENP-A.
BSc Honours, University of Melbourne.

J.C. Reed and S.I. Reed (1999)
Survivin' cell-separation anxiety.
Nat Cell Biol, 1: E199-E200.

C.L. Rieder and R.W. Cole (1998)
Entry into mitosis in vertebrate somatic cells is guarded by a chromosome damage checkpoint that reverses the cell cycle when triggered during early but not late prophase.
J Cell Biol, 142: 1013-1022.

L.R. Robb, R. Li, L. Hartley, H.H. Nandurkar, F. Koentgen and C.G. Begley (1998)
Infertility in female mice lacking the receptor for interleukin 11 is due to a defective uterine response to implantation.
Nat Med, 4: 303-308.

B.T. Roberts, K.A. Farr and M.A. Hoyt (1994)
The *Saccharomyces cerevisiae* checkpoint gene BUB1 encodes a novel protein kinase.
Mol Cell Biol, 14: 8282-8291.

E.J. Robertson (1987)
Embryo-derived stem cell lines *In* Teratocarcinomas and embryonic stem cells.
A practical approach.
IRL Press; Oxford, Washington DC pp 71-112.

L. Rowe, M. Barter, J. Naggert and J. Eppig (1999)
Cross-referencing the T31 whole genome radiation hybrid data to the high quality recombination map of the mouse.
Abstract B12, 13th International Mouse Genome Conference, Philadelphia.

R. Rozmahel, M. Wilschanski, A. Matin, S. Plyte, M. Oliver, W. Auerbach, A. Moore, J. Forstner, P. Durie, J. Nadeau, C. Bear and L.C. Tsui (1996)
Modulation of disease severity in cystic fibrosis transmembrane conductance regulator deficient mice by a secondary genetic factor (published erratum appears in Nat Genet 1996; 13: 129).
Nat Genet, 12: 280-287.

R. Saffery, D.V. Irvine, B.T. Kile, D.F. Hudson, S.M. Cutts and K.H.A. Choo (1999a)
Cloning, expression, and promoter structure of a mammalian Inner Centromere Protein (INCENP).
Mammal Gen, 10: 415-418.

R. Saffery, E. Earle, D.V. Irvine, P. Kalitsis and K.H.A. Choo (1999b)
Conservation of centromere proteins in vertebrates.
Chrom Res, 7:261-265.

R. Saffery, D.V. Irvine, B. Griffiths, P. Kalitsis, L. Wordeman and K.H.A. Choo (2000)
Human centromeres and neocentromeres show identical distribution patterns of >20 functionally important kinetochore-associated proteins.
Hum Mol Genet, 9: 175-185.

E.M. Santschi, S.B. Adams, J.T. Robertson, R.M. DeBowes, L.A. Mitten and J.E. Sojka (1995)
Ovariohysterectomy in six mares.
Vet Surg, 24: 165-167.

B.T. Schaar, G.K.T. Chan, P. Maddox, E.D. Salmon, T.Y. Yen (1997)
CENP-E function at kinetochores is essential for chromosome alignment.
J Cell Biol, 139: 1373-1382.

T.W. Seeley, L. Wang and J.Y. Zhen (1999)
Phosphorylation of human MAD1 by the BUB1 kinase *in vitro*.
Biochem Biophys Res Comm, 257: 589-595.

N. Seiki, T. Saito, K. Kitagawa, H. Masumoto, T. Okazaki and T.A. Hori (1994)
Mapping of the human centromere protein B gene (CENPB) to chromosome 20p13 by fluorescence in situ hybridization.
Genomics, 24: 187-188.

M. H. Shen, P.J. Mee, J. Nichols, J. Yang, F. Brook, R.L. Gardiner, A.G. Smith and W.R. Brown (2000)
A structurally defined mini-chromosome vector for the mouse germ line.
Curr Biol, 10: 31-34.

C.J. Sher (1996)
Cancer cell cycles.
Science, 274: 1672-1677.

Y. Shi (2000)
Survivin structure: crystal unclear.
Nat Struct Biol, 7: 620-623.

M. Sibilia and E.F. Wagner (1995)
Strain-dependent epithelial defects in mice lacking the EGF receptor.
Science, 269: 234-238.

J. Silver (1985)
Confidence limits for estimates of gene linkage based on analysis of recombinant inbred strains.
J Heredity, 76: 436-440.

L.M. Silver (1995)
Mouse Genetics. Concepts and Applications.
Oxford University Press, New York, Oxford.

A. Sivak (1982)
Chemical carcinogenesis *In* The Mouse in Biomedical Research. Experimental Biology and Oncology. Vol 4, *Eds* H.L. Foster, J.D. Small and J.G. Fox.
Academic Press, New York pp 342-349.

H.R. Slater, S. Nouri, E. Earle, W.I. Lo, L.G. Hale and K.H.A. Choo (1999)
Neocentromere formation in a stable ring 1p32-p36.1 chromosome.
J Med Gen, 36: 914-918.

E.K. Speliotes, A.Uren, D. Vaux and H.R. Horvitz (2000)
The survivin-like *C. elegans* BIR-1 acts with the Aurora-like kinase AIR-2 to affect chromosomes and the spindle midzone.
Mol Cell, 6: 211-223 and front cover.

E.R. Steuer, L. Wordeman, T.A. Schroer and M.P. Sheetz (1990)
Localization of cytoplasmic dynein to mitotic spindles and kinetochores.
Nature, 345: 266-268.

C.L. Stewart, P. Kasper, L.J. Brunet, H. Bhatt, I. Gadi, F. Kontgen and
S. J. Abbondanzo (1992)
Blastocyst implantation depends on maternal expression of leukaemia inhibitory factor.
Nature, 359: 76-79.

S. Stoler, K.C. Keith, K.E. Curnick and M. Fitzgerald-Hayes (1995)
A mutation in *CSE4*, an essential gene encoding a novel chromatin-associated protein in yeast, causes chromosome nondisjunction and cell cycle arrest at mitosis.
Genes Dev, 9: 573-586.

B. T. Stukenburg, K.D. Lustig, T.J. McGarry, R.W. King, J. Kuang and
M.W. Kirschner (1997)
Systematic identification of mitotic phosphoproteins.
Curr Biol, 140: 338-348.

N. Sugata, E. Munekata and K.Todokoro (1999)
Characterization of a novel kinetochore protein, CENP-H.
J Biol Chem, 274: 27343-27346.

K.F. Sullivan and C.A. Glass (1991)
CENP-B is a highly conserved mammalian centromere protein with homology to the helix-loop-helix family of proteins.
Chromosoma, 100: 360-370.

K.F. Sullivan, M. Hechenberger and K. Masri (1994)
Human CENP-A contains a histone H3 related histone fold domain that is required for targeting to the centromere.
J Cell Biol, 127: 581-592.

C.E. Sunkel and P.A. Coelho (1995)
The elusive centromere: sequence diversion and functional conservation.
Curr Opin Genet Dev, 5: 756-767.

H. Takai, K.Tominaga, N. Motoyama, Y.A. Minamishima, H. Nagahama, T. Tsukiyama, K. Ikeda, K. Nakayama, M. Nakanishi and Ki. Nakayama (2000) Aberrant cell cycle checkpoint function and early embryonic death in Chk1(-/-) mice. Genes Dev, 14: 1439-1447.

K. Tanaka, Y. Matsuda, J.S. Masangkay, C.D. Solis, R.V. Anunciado and T. Namikawa (1999)
Characterisation and chromosomal distribution of satellite DNA sequences of the water buffalo (Bubalis bubalis).
J Hered, 90: 418-422.

B.A. Taylor (2000)
Mapping phenotypic trait loci *In* Mouse Genetics and Transgenics. A Practical Approach. *Eds* I.J. Jackson and C.M. Abbott.
Oxford University Press, Oxford, New York pp 87-120.

S.S. Taylor, E. Ha and F. McKeon (1998)
The human homologue of Bub3 is required for kinetochore localization of Bub1 and a Mad3/Bub1-related protein kinase.
J Cell Biol, 142: 1-11.

J.R. Testa, J-Y. Zhou, D.W. Bell and T.J. Yen (1994)
Chromosomal localization of the genes encoding the kinetochore proteins CENPE and CENPF to human chromosomes 4q24-q25 and 1q32-q41, respectively, by fluorescence in situ hybridization.
Genomics, 23: 691-693.

The Chipping Forecast (1999)
Supplement to Nat Genet, 21: 1-60.

D.W. Threadgill, A.A. Dlugosz, L.A. Hansen, T. Tennenbaum, U. Lichti, D. Yee, C. LaMantia, T. Mourton, K. Herrup, R.C. Harris, J.A. Barnard, S.H. Yuspa, R.J. Coffey and T. Magnuson (1995)
Targeted disruption of mouse EGF receptor: effect of genetic background on mutant phenotype.
Science, 269: 230-234.

D.A. Thrower, M.A. Jordan, B.T. Schaar, T.J. Yen and L. Wilson (1995)
Mitotic HeLa cells contain a CENP-E-associated minus end-directed microtubule motor.
EMBO J, 14: 918-926.

J.E. Tomkiel, C.A. Cooke, H. Saitah, R.L. Bernat and W.C. Earnshaw (1994)
CENP-C is required for maintaining kinetochore size and for a timely transistion to anaphase.
J Cell Biol, 125: 531-545.

M. Toth, J. Grimsby, G. Buzsaki and G.P. Donovan (1995; 1996)
Epileptic seizures caused by inactivation of a novel gene, *jerky*, related to centromere binding protein-B in transgenic mice (published erratum appears in Nat Genet 1996; 12: 110).
Nat Genet, 11: 71-75.

C. Tyler-Smith and H.F. Willard (1993)
Mammalian chromosome structure.
Curr Opin Genet and Dev, 3: 390-397.

C. Tyler-Smith and G. Floridia (2000)
Many paths to the top of the mountain: diverse evoluntionary solutions to centromere structure.
Cell, 102: 5-8.

A.G. Uren, T. Beilharz, M.J. O'Connell, S.J. Bugg, R. van Driel, D.L. Vaux, T. Lithgow (1999)
Role for yeast inhibitor of apoptosis (IAP)-like proteins in cell division.
Proc Natl Acad Sci USA, 96: 10170-10175.

A.G. Uren, L. Wong, M. Pakusch, K.J. Fowler, F.J. Burrows, D.L. Vaux and K.H.A. Choo (2000)
Survivin localises to the centromere, and *Survivin* gene-disrupted mice show a mitotic defect resembling the *Incenp* null phenotype.
Curr Biol, 10: 1319-1328.

A.A. Van Hooser, M.A. Mancini, C.D. Allis, K.F. Sullivan and B.R. Brinkley (1999)
The mammalian centromere: structural domains and the attenuation of chromatin modeling.
The FASEB J, 13: S216-S220.

M.A. Verdecia, H. Huang, E. Dutil, D.A Kaiser, T. Hunter and J.P. Noel (2000)
Structure of the human anti-apoptotic protein survivin reveals a dimeric arrangement.
Nat Struct Biol, 7: 602-608

L.E. Voullaire, H.R. Slater, V. Petrovic and K.H. Choo (1993)
A functional neocentromere with no detectable alpha-satellite, satellite III, or CENP-B protein: activation of a latent centromere?
Am J Hum Genet, 52: 1153-1163.

L. Voullaire, R. Saffery, J. Davies, E. Earle, P. Kalitsis, H. Slater, D.V. Irvine and K.H.A. Choo (1999a)
Trisomy 20p resulting from inverted duplication and neocentromere formation.
Am J Med Gen, 85: 403-408.

L. Voullaire, L. Wilton, H. Slater and R. Williamson (1999b)
Detection of aneuploidy in single cells using comparative genomic hybridization.
Prenat Diagn, 19: 846-851.

L. Voullaire, H. Slater, R. Williamson and L. Wilton (2000)
Chromosome analysis of blastomeres from human embryos by using comparative genomic hybridization.
Hum Genet, 106: 210-217.

P.E. Warburton, C. Cooke, S. Bourassa, O. Vafa, B.A. Sullivan, G. Stetten, G. Gimelli, D. Warburton, C. Tyler-Smith, K.F. Sullivan, G.G. Poirier and W.C. Earnshaw (1997)
Immunolocalization of CENP-A suggests a distinct nucleosome structure at the kinetochore plate of active centromeres.
Curr Biol, 7: 901-904.

R. Weide, J. Hontelez, A. van Kammen, M. Koornneef and P. Zabel (1998)
Paracentromeric sequences on tomato chromosome 6 show homology to human satellite III and to mammalian CENP-B binding box.
Mol General Genet, 259: 190-197.

D. Wells, J.K. Sherlock, A.H. Handyside and J.D. Delhantly (1999)
Detailed chromosomal and molecular genetic analysis of single cells by whole genome amplification and comparative genomic hybridisation.
Nuc Acids Res, 27: 1214-1218.

A.J. Wilcox, C.R. Weinberg, J.F. O'Connor, D.D. Baird, J.P. Schlatterer, R.E. Canfield, E.G. Armstrong and B.C. Nisula (1988)
Incidence of early loss of pregnancy.
N Engl J Med, 319: 189-194.

H.F. Willard (1998)
Centromeres: the missing link in the development of human artificial chromosomes.
Curr Opin Genet Dev, 8: 219-225.

B.C. Williams, T.D. Murphy, M.L. Goldberg and G.H. Karpen (1998)
Neocentromere activity of structurally acentric mini-chromosomes in *Drosophila*.
Nat Genet, 18: 30-37.

K.W. Wood, R. Sakowics, L.S. Goldstein and D.W. Cleveland (1997)
CENP-E is a plus end-directed kinetochore motor required for metaphase chromosome alignment.
Cell, 91: 357-366.

C. H. Yang, J. Tomkiel, H. Saitoh, D.H. Johnson and W.C. Earnshaw (1996)
Identification of overlapping DNA-binding and centromere-targeting domains in the human kinetochore protein CENP-C.
Mol Cell Biol, 16: 3576-3586.

X. Yao, A. Abrieu, Y. Zheng, K.F. Sullivan and D.W. Cleveland (2000)
CENP-E forms a link between attachment of spindle microtubules to kinetochores and to the mitotic checkpoint.
Nat Cell Biol, 2: 484-491.

T.J. Yen, D.A. Compton, D. Wise, R.P. Zinkowski, B.R. Brinkley, W.C. Earnshaw and D.W. Cleveland (1991)
CENP-E, a novel human centromere-associated protein required for progression from metaphase to anaphase.
EMBO J, 10: 1245-1254.

T.J. Yen, G. Li, B.T. Schaar, I. SzilakI and D.W. Cleveland (1992)
CENP-E is a putative kinetochore motor that accumulates just before mitosis.
Nature, 359: 536-539.

K.K. Yoda, H. Kitagawa, Y. Maumoto, Y. Muro and T. Okazaki (1992)
A human centromere protein, CENP-B, has DNA binding domain containing four potential alpha helices at the NH_2-terminus, which separable from dimerization activity.
J Cell Biol, 119: 1413-1427.

J.K. Yucel, J.D. Marszalek, J.R. McIntosh, L.S. Goldstein, D.W. Cleveland and A.V. Philp (2000)
CENP-meta, an essential kinetochore kinesin required for the maintenance of metaphase chromosome alignment in *Drosophila*.
J Cell Biol, 150:1-12.

J. Zielenski, M. Corey, R. Rozmahel, D. Markiewicz, I. Aznarez, T. Casals, S. Larriba, B. Mercier, G.R. Cutting, A. Krebsova , M. Macek Jr, E. Langfelder-Schwind, B.C. Marshall, J. DeCelie-GermanaJ, M. Claustres, A. Palacio, J. Bal, A. Nowakowska, C. Ferec, X. Estivill, P. Durie and L.C. Tsui (1999)
Detection of a cystic fibrosis modifier locus for meconium ileus on human chromosome 19q13.
Nat Genet, 22: 128-129.